JGRG28

The 28th Workshop on General Relativity and Gravitation in Japan – JGRG28
Tachikawa Memorial Hall, Rikkyo University
5-9 November 2018

Volume I

Proceedings of the 28th Workshop on General Relativity and Gravitation in Japan

November 5th–9th 2018
Tachikawa Memorial Hall, Rikkyo University,
3-34-1 Nishi-Ikebukuro, Toshima, Tokyo, Japan

Volume I

Workshop Information
Oral Presentations: Day 1, 2

JGRG : http://www-tap.scphys.kyoto-u.ac.jp/jgrg/index.html

Contents

Preface

Since the first direct detection of gravitational waves in September 2015, the LIGO and also later Virgo detectors have observed 11 events until the end of 2018. These events correspond to the mergers of binary black holes of tens of solar masses except for a single event corresponding to the merger of binary neutron stars. The LIGO, Virgo and other detectors including KAGRA in Kamioka, Japan are expected to observe much more events with higher accuracy and higher resolution in the near future so that we can study various aspects of sciences based on improved statistical significance. Gravitational waves are now playing a crucial role not only in astronomy and astrophysics but also in cosmology, gravitational theories and many other fields of physics. In such an extremely stimulating and historical year, it is our great pleasure to have hosted the 28th workshop on general relativity and gravitation in Japan (JGRG28). The workshop was held at Tachikawa Memorial Hall on Ikebukuro campus of Rikkyo University from the 5th to the 9th of November 2018.

Rikkyo University is a private university in Ikebukuro, Tokyo. It started as Rikkyo School in 1874 in Tsukiji, Tokyo and has been located in Ikebukuro since 1918. It has 11 faculties and 20,000 undergraduate students and is a member of Tokyo 6 universities. Its College of Science was founded in 1949 and has the longest history among those in private universities in Japan.

We invited outstanding lecturers, who are very active in the theoretical and observational research fields, including Bernard J. Carr (Queen Mary University of London), Jonathan R. Gair (University of Edinburgh), Mark B. Hindmarsh (University of Sussex), David F. Mota (Institute for Theoretical Physics, University of Oslo), José M. M. Senovilla (University of Basque Country UPV/EHU), Alexei A. Starobinsky (Landau Institute for Theoretical Physics, Moscow), Hirotaka Takahashi (Nagaoka University of Technology), Jean-Philippe Uzan (Institut d'Astrophysique de Paris), and Vincent Vennin (Paris U. VII, APC). Besides these 9 invited talks, 76 contribution talks and 54 poster presentations were given. The total number of participants was 220 including 25 participants from abroad.

The workshop was co-hosted by College of Science, Rikkyo University and Research Center for Measurement in Advanced Science, Rikkyo University. The workshop was supported by MEXT Grant-in-Aid for Scientific Research on Innovative Areas "New developments of gravity theory research in gravitational wave physics", JP17H06359, PI: Shinji Mukohyama, "Inflationary Universe", 15H05888, PI: Misao Sasaki, and MEXT-Supported Program for the Strategic Research Foundation at Private Universities, 2014-2017 (S1411024), PI: Shunji Kitamoto. The Local Orginizing Committee includes Tomohiro Harada (Rikkyo U.) [Chair], Takashi Hiramatsu (Rikkyo U.), Takahisa Igata (Rikkyo U.), Tsutomu Kobayashi (Rikkyo U.), Takafumi Kokubu (Rikkyo U.), Kazufumi Takahashi (Rikkyo U.), and Shuichiro Yokoyama (Rikkyo U.).

We would like to thank all the participants for their paticipation in and important contributions to the JGRG28.

Tomohiro Harada (on behalf of the JGRG28 LOC)

Presentation Award

The JGRG presentation award program was established at the occasion of JGRG22 in 2012. This year, we are pleased to announce the following six winners of the Outstanding Presentation Award for their excellent presentations at JGRG28. The winners were selected by the selection committee consisting of the JGRG28 SOC based on ballots of the participants.

Haruka Suzuki (Waseda University)
"The Effect of Kozai-Lidov Mechanism on the Period Shift of the Binary Neutron Stars by Gravitational Waves" (Oral)

Keigo Shimada (Waseda University)
"Inflation in Metric-Affine Gravity" (Oral)

Masato Nozawa (YITP, Kyoto University
"On the uniqueness theorems of static black holes" (Oral)

Shi Pi (Kavli IPMU)
"Gravitational Waves Induced by non-Gaussian Scalar Perturbations" (Oral)

Priti Gupta (Waseda University)
"Gravitational Waves and Chaos" (Poster)

Takahisa Igata (Rikkyo University)
"Bright edge of a near extremal Kerr black hole shadow" (Poster)

Participant list

Samir Hussein Abuzaid	Egypt
Satoshi Akagi	Japan
Shingo Akama	Japan
Yuji Akita	Japan
Kensuke Akita	Japan
Katsuki Aoki	Japan
Arata Aoki	Japan
Hideki Asada	Japan
Masroor C Pookkillath	Japan
Bernard John Carr	UK
Takeshi Chiba	Japan
Fabio Chibana	Japan
Kutay Arinc Cokluk	Turkey
Antonio De Felice	Japan
Rajesh Kumar Dubey	India
Naoya Era	Japan
Filip Ficek	Poland
Antonino Flachi	Japan
Kohei Fujikura	Japan
Hiei Fukuda	Japan
Hayato Fukunaga	Japan
Yu Furuya	Japan
Jonathan Gair	UK
Xian Gao	China
Priti Gupta	Japan
Yuki Hagihara	Japan
Tomohiro Harada	Japan
Takuya Hasegawa	Japan
Soichiro Hashiba	Japan
Kota Hayashi	Japan
Minxi He	Japan
Hector Hernandez	Mexico
Yoshiaki Himemoto	Japan
Mark Hindmarsh	UK
Takashi Hiramatsu	Japan
Koichi Hirano	Japan
Shin'ichi Hirano	Japan
Yuta Hiranuma	Japan
Takahisa Igata	Japan
Daisuke Iikawa	Japan
Keisuke Inomata	Japan
Akihiro Ishibashi	Japan
Hideki Ishihara	Japan
Asuka Ito	Japan
Aya Iyonaga	Japan
Keisuke Izumi	Japan
Sanjay Jhingan	Japan
Takuma Kajihara	Japan
Chao Kang	China
Sugumi Kanno	Japan
Masumi Kasai	Japan
Takuya Katagiri	Japan
Ryo Kato	Japan
Yushi Kawamoto	Japan
Masahiro Kawasaki	Japan
Anton Khirnov	Czech
Jafar Khodagholizadeh	Iran
Suro Kim	Japan
Yuto Kimura	Japan
Masashi Kimura	Portugal
Rampei Kimura	Japan
Shunichiro Kinoshita	Japan
Naoya Kitajima	Japan
Hiroyuki Kitamoto	Taiwan
Tomotaka Kitamura	Japan
Tsutomu Kobayashi	Japan
Yoh Kobayashi	Japan
Shinpei Kobayashi	Japan
Yasutaka Koga	Japan
Tatsuhiko Koike	Japan
Takahiro Koike	Japan
Takafumi Kokubu	Japan
Ryunosuke Kotaki	Japan
Yashmitha Kumaran	India
Masashi Kuniyasu	Japan
Yasunari Kurita	Japan
Kei Kusumi	Japan
Kei-ichi Maeda	Japan
Emi Masaki	Japan
Akira Matsumura	Japan
Satsuki Matsuno	Japan
Yamato Matsuo	Japan
Anupam Mazumdar	Netherlands
Yuta Michimura	Japan

Masato Minamitsuji	Portugal
Yosuke Mishima	Japan
Shoichiro Miyashita	Japan
Daiki Miyata	Japan
Atsushi Miyauchi	Japan
Shuntaro Mizuno	Japan
Yuko Mori	Japan
Taisaku Mori	Japan
Yoshiyuki Morisawa	Japan
David F. Mota	Norway
Hayato Motohashi	Japan
Shinji Mukohyama	Japan
Jiro Murata	Japan
Keiju Murata	Japan
Shigehiro Nagataki	Japan
Yuya Nakamura	Japan
Kouji Nakamura	Japan
Tomohiro Nakamura	Japan
Shintaro Nakamura	Japan
Yuki Nakamura	Japan
Takashi Nakamura	Japan
Ken-ichi Nakao	Japan
Keisuke Nakashi	Japan
Hiromasa Nakatsuka	Japan
Yasusada Nambu	Japan
Tatsuya Narikawa	Japan
Chiaki Nasu	Japan
Andrea Nerozzi	Portugal
Vu Hoang Nguyen	Vietnam
Yuki Niiyama	Japan
Kazuya Nishimura	Japan
Atsushi Nishizawa	Japan
Sousuke Noda	Japan
Masato Nozawa	Japan
Ippei Obata	Japan
Kota Ogasawara	Japan
Tatsuya Ogawa	Japan
Hiromu Ogawa	Japan
Takayuki Ohgami	Japan
Kazumasa Okabayashi	Japan
So Okano	Japan
Michele Oliosi	Japan
Hidetoshi Omiya	Japan
Toshiaki Ono	Japan
Ken-ichi Oohara	Japan
Sirachak Panpanich	Thailand
Shi Pi	Japan
Naeem Ahmad Pundeer	India
L. N. Rieger	USA
Kazutaka Sadohara	Japan
Norichika Sago	Japan
Hiromi Saida	Japan
Kaishu Saito	Japan
Ryo Saito	Japan
Arisa Sano	Japan
Yukinori Sasagawa	Japan
Misao Sasaki	Japan
Tadashi Sasaki	Japan
Shinataro Sato	Japan
Toyokazu Sekiguchi	Japan
Mikito Sekine	Japan
JosÃľ MartÃŋn Senovilla	Spain
Naoki Seto	Japan
Osamu Seto	Japan
Muhammad Sharif	Pakistan
Swarnim Shashank	Japan
Hiroyuki Shibaguchi	Japan
Masaru Shibata	Germany
Keigo Shimada	Japan
Masahiro Shimano	Japan
Hisaaki Shinkai	Japan
Masashi Shinoda	Japan
Kiyoshi Shiraishi	Japan
Tetsuya Shiromizu	Japan
Jiro Soda	Japan
Hajime Sotani	Japan
Alexei A. Starobinsky	Russia
Satoru Sugimoto	Japan
Naonori Sugiyama	Japan
Hideaki Suzuki	Japan
Haruka Suzuki	Japan
Yuichiro Tada	Japan
Hideyuki Tagoshi	Japan
Hiroaki Tahara	Japan

Kanna Takagi	Japan
Kazufumi Takahashi	Japan
Hirotaka Takahashi	Japan
Kazuma Takahashi	Japan
Tomo Takahashi	Japan
Kentaro Takami	Japan
Hiroki Takeda	Japan
Norihiro Tanahashi	Japan
Takahiro Tanaka	Japan
Kazuma Tani	Japan
Junsei Tokuda	Japan
Yoshimune Tomikawa	Japan
Keitaro Tomikawa	Japan
Shinya Tomizawa	Japan
Takashi Torii	Japan
Shinji Tsujikawa	Japan
Takuma Tsukamoto	Japan
Naoki Tsukamoto	Japan
Nami Uchikata	Japan
Kodai Ueda	Japan
Shu Ueda	Japan
Jean-Philippe Uzan	France
Vincent Vennin	France
Yuki Watanabe	Japan
Yukinobu Watanabe	Japan
Yota Watanabe	Japan
Satoshi Watanabe	Japan
Marcus Christian Werner	Japan
Yi-Peng Wu	Japan
Kei Yamada	Japan
Masahide Yamaguchi	Japan
Kazuhiro Yamamoto	Japan
Takahiro Yamamoto	Japan
Daisuke Yamauchi	Japan
Zhi-Bang Yao	China
Mai Yashiki	Japan
Akihiro Yatabe	Japan
Shuichiro Yokoyama	Japan
Jun'ichi Yokoyama	Japan
Chulmoon Yoo	Japan
Shin'ichirou Yoshida	Japan
Daiske Yoshida	Japan
Hirotaka Yoshino	Japan

Programme

	5 Nov (Mon)	6 Nov (Tue)	7 Nov (Wed)	8 Nov (Thu)	9 Nov (Fri)	
9:00	registration	c:J.Yokoyama: Invited talk 3 Prof. David F. Mota; Session 2A1	c: H.Tagoshi: Invited talk 5 Prof. Jonathan Gair; Session 3A1	c: T.Harada: Invited talk 6 Prof. Bernard John Carr; Session 4A1	c:S.Mukohyama: Invited talk 8 Prof. Alexei A. Starobinsky; Invited talk 9 Prof. Jean-Philippe Uzan	9:00
10:00	Opening (T. Harada); c: T.Tanaka: Invited talk 1 Prof. Hirotaka Takahashi	Coffee & Posters; c: Y.Nambu: Session 2A2	Short talk B; Coffee & Posters	Coffee & Posters; c: K.Nakao: Session 4A2	Coffee; c: H.Asada: Session 5A	10:00
11:00	Session 1A		c:K.Oohara: Session 3A2			11:00
12:00	Lunch	Lunch	Lunch	Group photo; Lunch	Awards; Closing (K-i.Maeda)	12:00
13:00						13:00
14:00	c: M.Sasaki: Invited talk 2 Prof. Mark B. Hindmarsh; Session 1P1	c: T.Shiromizu: Invited talk 4 Prof. José M.M. Senovilla; Session 2P1	c: M.Yamaguchi: Session 3P1	c: S.Kanno: Invited talk 7 Prof. Vincent Vennin; Session 4P1		14:00
15:00	Short talk A; Coffee & Posters	Coffee & Posters	Coffee & Posters	Coffee & Posters		15:00
16:00	c: K.Yamamoto: Session 1P2	c: T.Chiba: Session 2P2	c: M.Shibata: Session 3P2	c: H.Ishihara: Session 4P2		16:00
17:00						17:00
18:00			Banquet at Main Dining Hall			18:00
19:00				SOC meeting		19:00
20:00						20:00

Monday 5th November
Invited lecture 10:15–11:00

[Chair: Takahiro Tanaka]

Hirotaka Takahashi
Nagaoka University of Technology

“Status of KAGRA and KAGRA data analysis (tentative)”
(40+10 min.)

[JGRG28 (2018) 110501]

Status of KAGRA and KAGRA data analysis

Hirotaka Takahashi*
on behalf of the KAGRA collaboration
*Nagaoka University of Technology

KAGRA Project

- 3km laser interferometer
- Underground site
- Cryogenic mirror

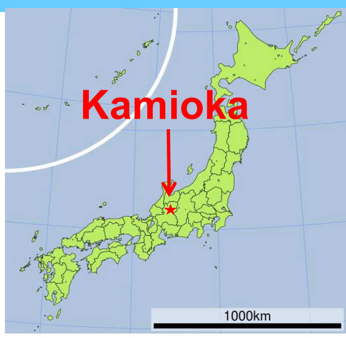

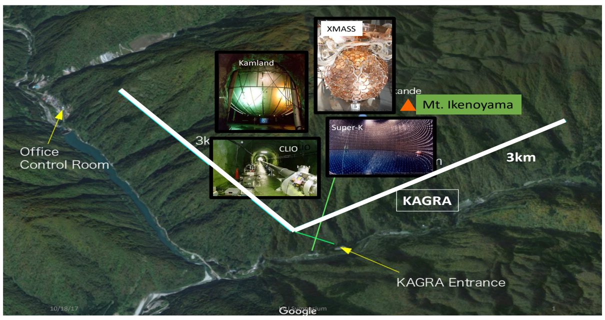

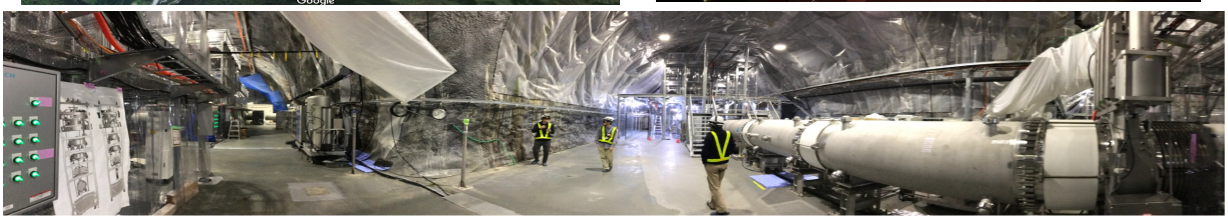

KAGRA Collaboration

- Host Institute: ICRR, University of Tokyo
- Cooperative institutes: NAOJ, KEK, and many universities.
- Over 385 collaborators (June 2018)

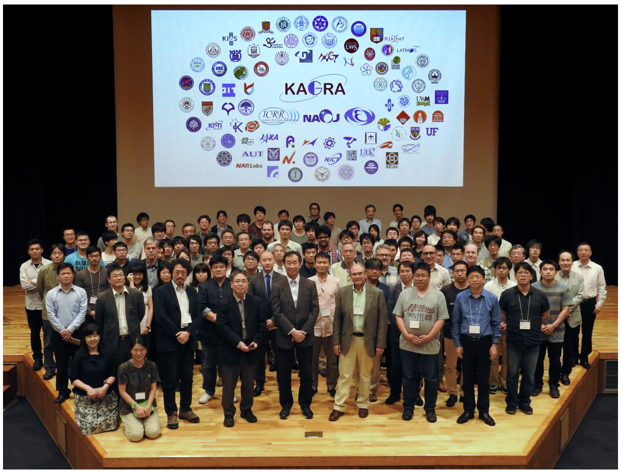

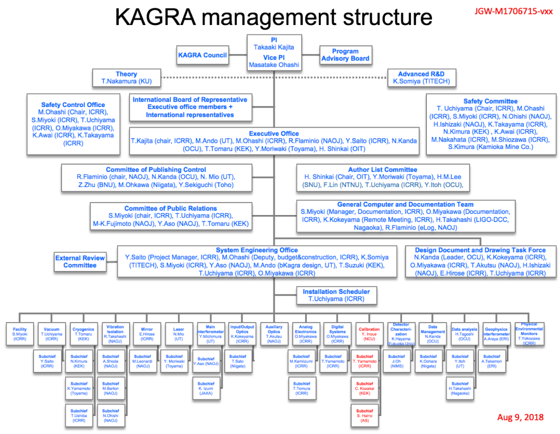

F2F meeting @ OCU, May 2018

Brief history of KAGRA

- June 2010: KAGRA was funded by MEXT
- 2011: Tunnel excavation postponed for 1 year due to the earthquake
- May 2012: Started the tunnel excavation
- March 2014: Finished the tunnel
- Nov. 2015: Laboratory area mostly done

History and Roadmap of KAGRA

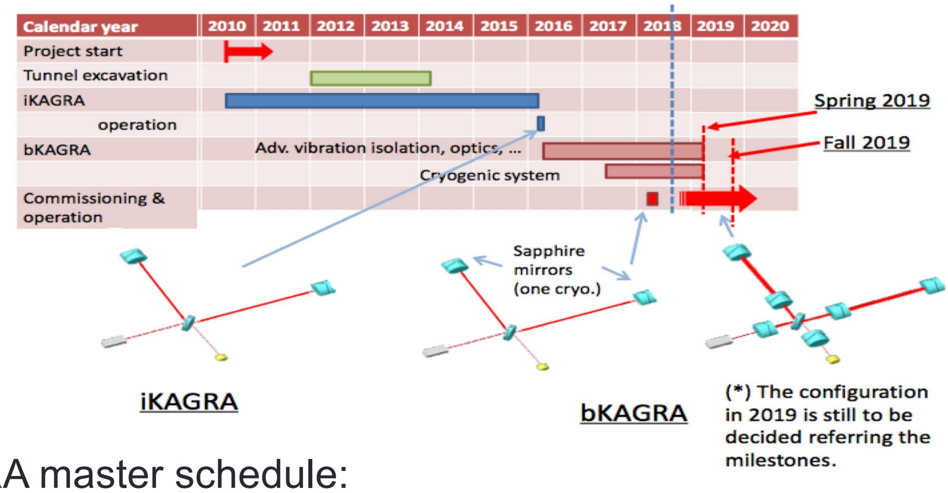

KAGRA master schedule:

- **iKAGRA** (- Mar 2016): Room Temperature Michelson Interferometer
- **bKAGRA phase-1** (- May 2018): Cryogenic Michelson Interferometer
- **bKAGRA phase-2** (- 2019): Cryogenic FPM/RSE Interferometer (full configuration)
- **bKAGRA phase-3** (2019 -): Commissioning and Observation run

長岡技術科学大学 Nagaoka University of Technology

initial KAGRA (iKAGRA) test run (1)

KAGRA Collaboration, PTEP 013F01-1-23 (2018).

- March 25 - 31 and April 12 - 25, 2016

Main purpose:

Demonstration of 3km interferometer operation

Configuration:

- 3 km Michelson at room temperature
- Low power laser
- Simplified suspension
- At air pressure

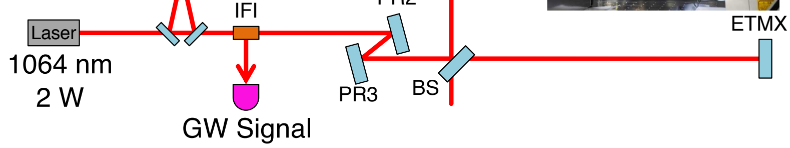

iKAGRA test run (2)

KAGRA Collaboration, PTEP 013F01-1-23 (2018).

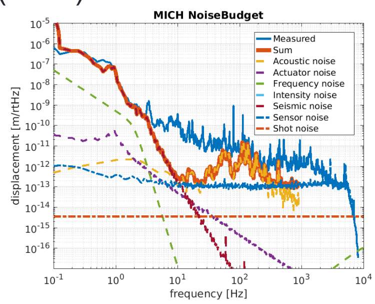

Sensitivity and duty cycle:

- Typical sensitivity: 3 x 10^{-15} $Hz^{-1/2}$
  – 6 x 10^{-16} $Hz^{-1/2}$ @ 100Hz
- Continuous operation with duty cycle : 85 – 90%

Data transfer and data analysis:

- Stable online data transfer to permanent data storage site (ICRR-Kashiwa)
  (K. Sakai et al., 電子情報通信学会論文誌 B, Vol.J101-B No.9, pp.818-827 (2018).)
- Hardware signal injection test was performed
- CBC: Matched filter analysis (for 1-3 Msun)
- Continuous wave: F-statistic analysis
  for 62 known pulars
- Burst: Excess power analysis (all sky search,
  targeted search for GRB events)

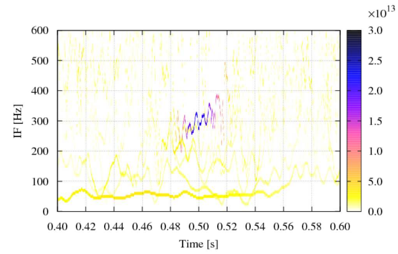

e.g. Analysis result of hardware injection signal
from Ueki-kun's Master Thesis

KAGRA
長岡技術科学大学
Nagaoka University of Technology

baseline KAGRA (bKAGRA)

Final goal : Operation of full configuration KAGRA with good sensitivity

- **bKAGRA phase-1** (- May 2018): Cryogenic Michelson Interferometer
- **bKAGRA phase-2** (- 2019): Cryogenic FPM/RSE Interferometer (full configuration)
- **bKAGRA phase-3** (2019 -): Commissioning and Observation run

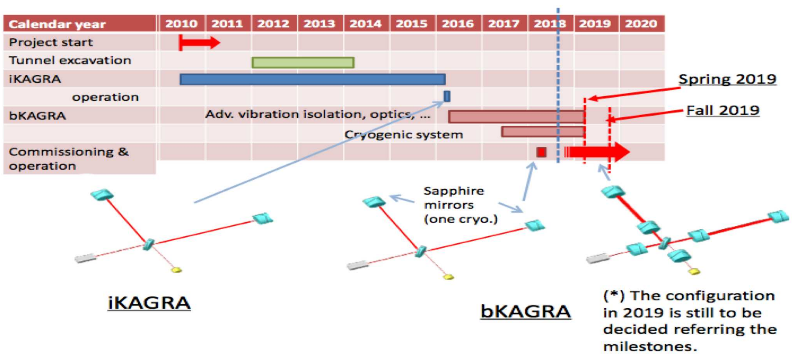

KAGRA
長岡技術科学大学
Nagaoka University of Technology

bKAGRA phase-1 test run (1)

bKAGRA phase-1 test run: April 28 – May 6, 2018.

- Michelson IF with Cryogenic mirrors.
- One end mirror cooled down ~18 K.

- Many tests for the interferometer, calibration, GW waveform injection, data transfer and analysis pipeline etc.
- Analysis of the injection signal is going on.

	4/28	4/29	4/30	5/1	5/2	5/3	5/4	5/5	5/6	5/7
Day (9:00-17:00)	OLG measurements	Type-A Yend TRF	BS TRF	Type-A Xend TRF	Noise injection Center	Noise injection YEND	Schnupp Assymmetry & IFO noise budget	Noise injection XEND	CRY Extra EXP. 1 & 2	Phase 2
Night (17:00-9:00)	OLG measurements	Type-A Yend TRF	CW injection	Type-A Xend TRF	CBC injection	CBC injection	Schnupp Assymmetry & IFO noise budget	OLG measurements	CRY Extra EXP. 1 & 2	
Parallel	Data transfer, Pipeline tests, GIF									

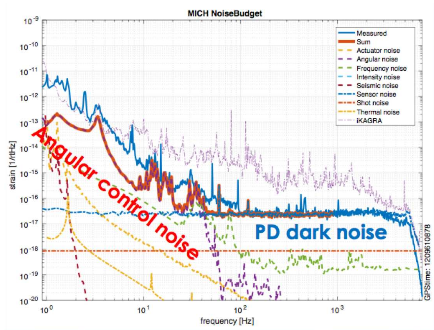

bKAGRA phase-1 test run (2)

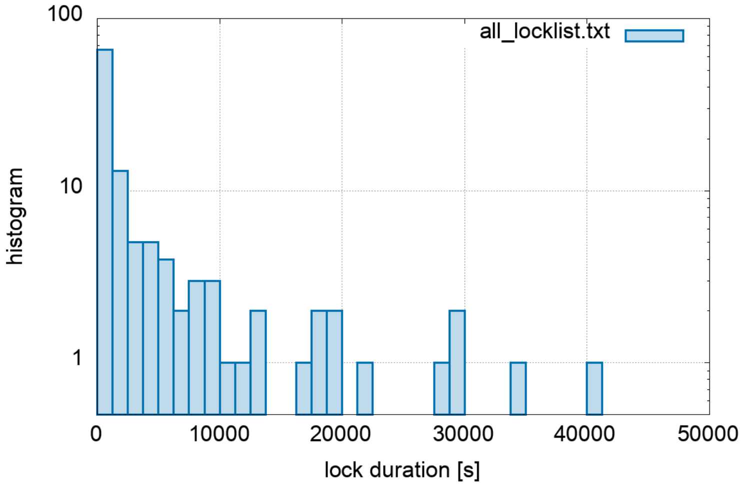

- The maximum of the lock duration was 40721 seconds ~ 11.3 hours.

Example of activity during bKAGRA phase-1 test run (1)

Hardware injection test

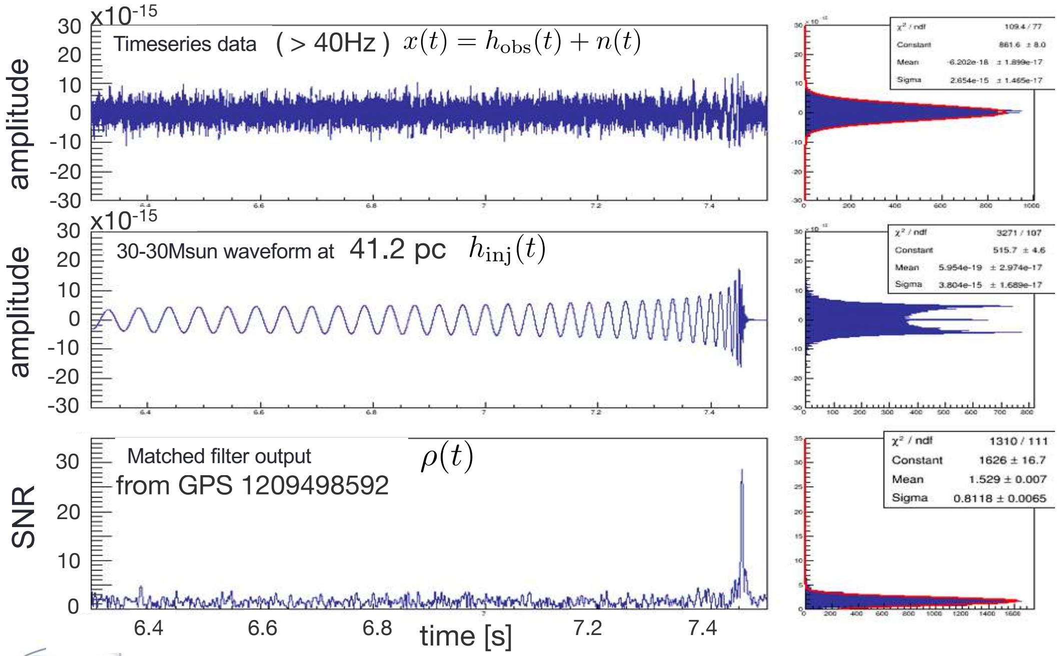

KAGRA

長岡技術科学大学 Nagaoka University of Technology

Example of activity during bKAGRA phase-1 test run (2)

Summary plots of the data transfer system

- to check status of data transfer system easily.

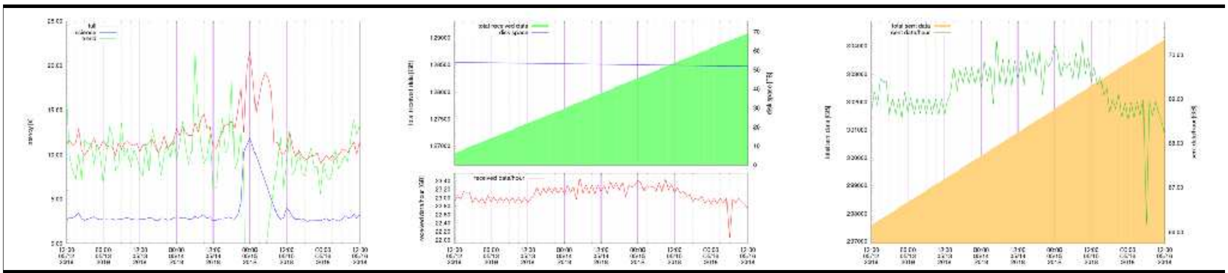

✓ the latency of data transfer

✓ amounts of received/sent data to/from a server and the remaining space of disk

- Useful for checking the transfer system during the phase-I operation.

KAGRA

長岡技術科学大学 Nagaoka University of Technology

Example of activity during bKAGRA phase-1 test run (3)

Monitor of Frame Data

- We prepared a monitor system of the latest frame data on DMG data transfer.
- The latest data will be displayed and updated automatically.
- This system is installed in Kamioka and OCU server. It will be also installed in Kashiwa server.

monitor example

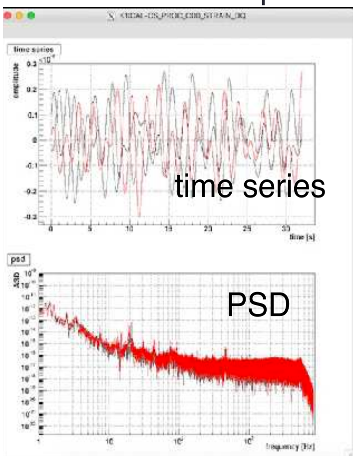

In KAGRA control room

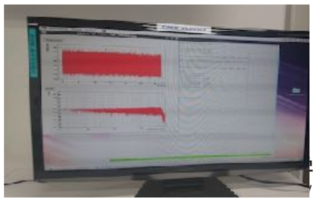

We are planning to provide the GUI application.

KAGRA

baseline KAGRA (bKAGRA)

Final goal : Operation of full configuration KAGRA with good sensitivity

- **bKAGRA phase-1** (- May 2018): Cryogenic Michelson Interferometer
- **bKAGRA phase-2** (- 2019): Cryogenic FPM/RSE Interferometer (full configuration)
- **bKAGRA phase-3** (2019 -): Commissioning and Observation run

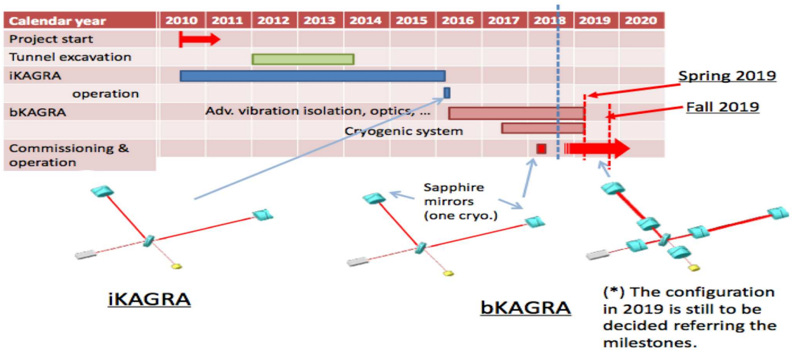

KAGRA

長岡技術科学大学 Nagaoka University of Technology

Sapphire mirrors

- All 4 sapphire mirrors are ready to install.
- 3 of them have been installed.
- These are suspended by Type-A suspension and Cryo-Payload.

- Two mirrors cooled down to 20K.

The Nikkei (Japan Economical Newspaper)

International

日本經濟新聞
2018年8月30日（木）

2018.8.21

トップ　経済・政治　ビジネス　マーケット　テクノロジー　国際・アジア　スポーツ

速報　朝刊・夕刊

重力波望遠鏡「かぐら」、心臓部の鏡を公開　東大

科学＆新技術

2018/8/21 12:53

保存　共有　印刷　その他

東京大学宇宙線研究所などが来冬の本格稼働を目指す重力波望遠鏡「かぐら」の心臓部となる４枚の人工サファイアの鏡が完成、最後の４枚目が東大柏キャンパス（千葉県柏市）で21日に公開された。かぐらは神岡鉱山（岐阜県飛騨市）の地下にある。１辺３キロのＬ字形の真空パイプ内でレーザー光を往復させ、重力波による空間の非常にわずかなゆがみを超高精度で検出する。

同規模の重力波望遠鏡が米欧に３台あるが、かぐらは先進的な技術を導入している。中核となるのがレーザー光を反射させるサファイア鏡。極低温に冷やすことで、観測の邪魔になる鏡の熱による変動を抑える。

鏡はいずれも直径22センチ、厚さ15センチの平たい円筒形で重さは23キログラム。公開された鏡を含む２枚はレーザー光を反射させると同時に透過させる役割も担い、サファイア結晶により高い性能が求められる。東大宇宙線研が国内の結晶メーカーの信光社（横浜市）と共同開発した。

画像の拡大

東大柏キャンパスで21日公開された重力波望遠鏡「かぐら」の鏡

かぐらと欧米の望遠鏡が連携すれば、重力波がどの方向から到来しているのか、より高い精度で迅速に突き止められる。重力波で宇宙を探る天文学の新分野の一段の発展が期待されている。東大宇宙線研の大橋正健教授は「早ければ来年10月にも国際共同観測に参加したい」と話している。

Installation of Mirrors and Cryo-Payload

Type A suspension

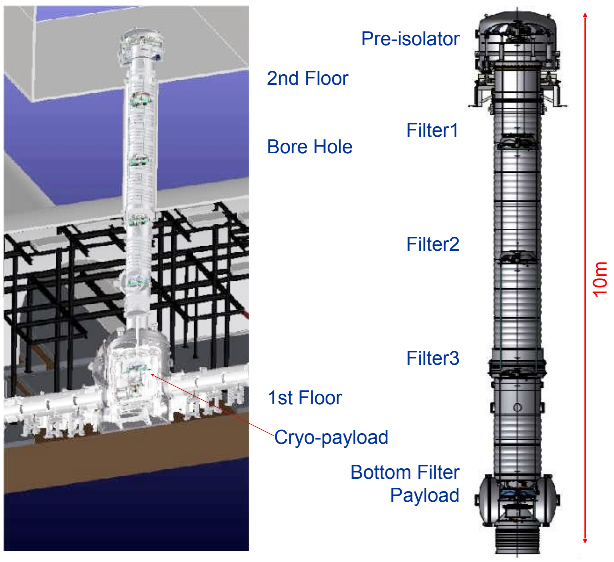

Cryo-Payload

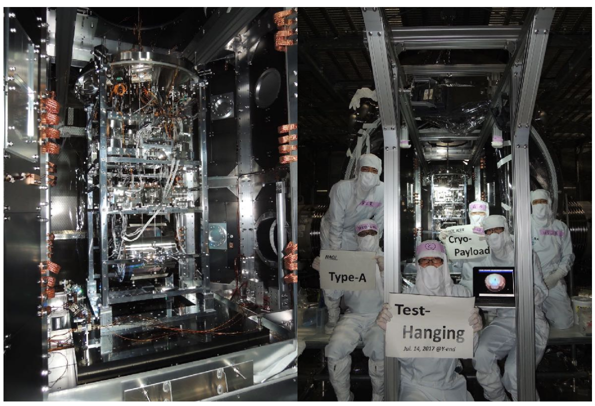

Calibration

Photon calibrator is preparing for Phase-2 and after.

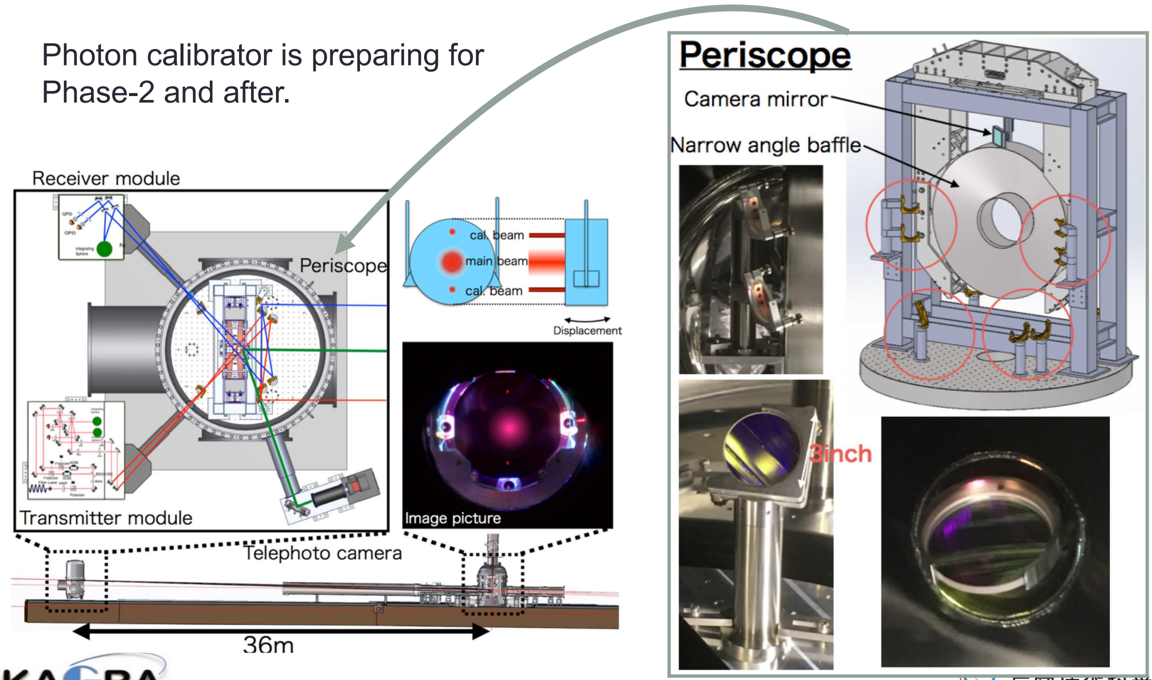

Data sharing with LIGO and Virgo

Bulk data sharing

- preparing LDR (LIGO Data Replicator) protocol.

Low latency h(t)

- 4sec frame is also preparing.
- We achieved the shared memory **connection with LIGO/Virgo in June, 2018.**

(Thanks for the support by LIGO/Virgo colleagues.)

- KAGRA calibration group is now installing low latency h(t) generator.

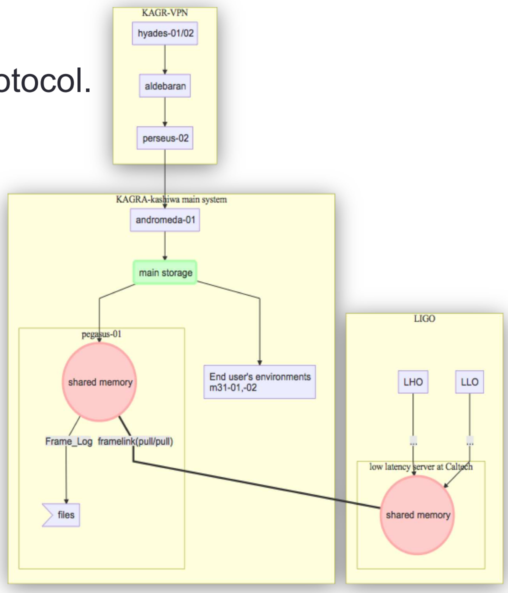

Technical items for the data sharing will be fully ready soon.

LIGO/Virgo joint observation plan

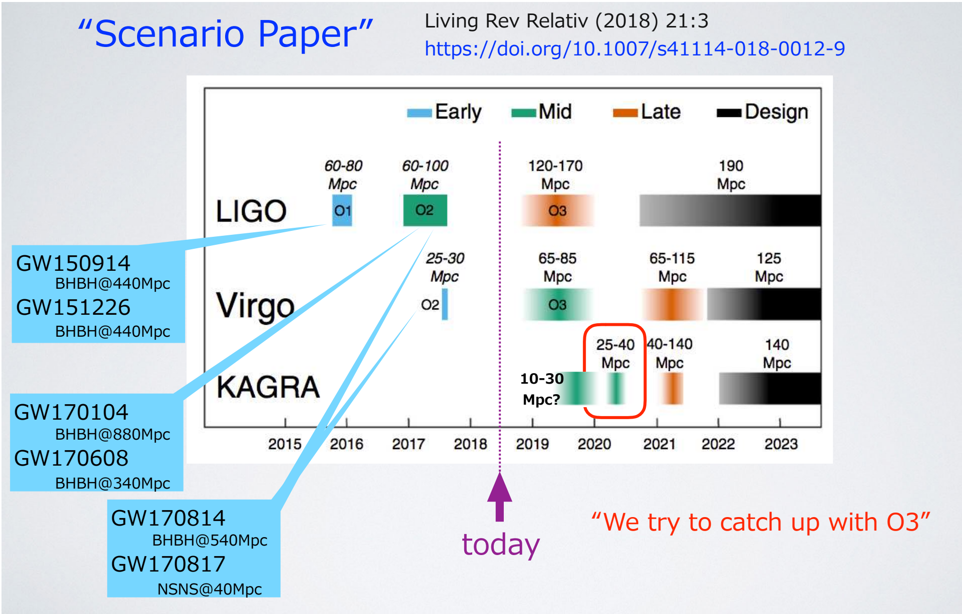

KAGRA

長岡技術科学大学
Nagaoka University of Technology

Installation and commissioning toward phase-2 and phase-3

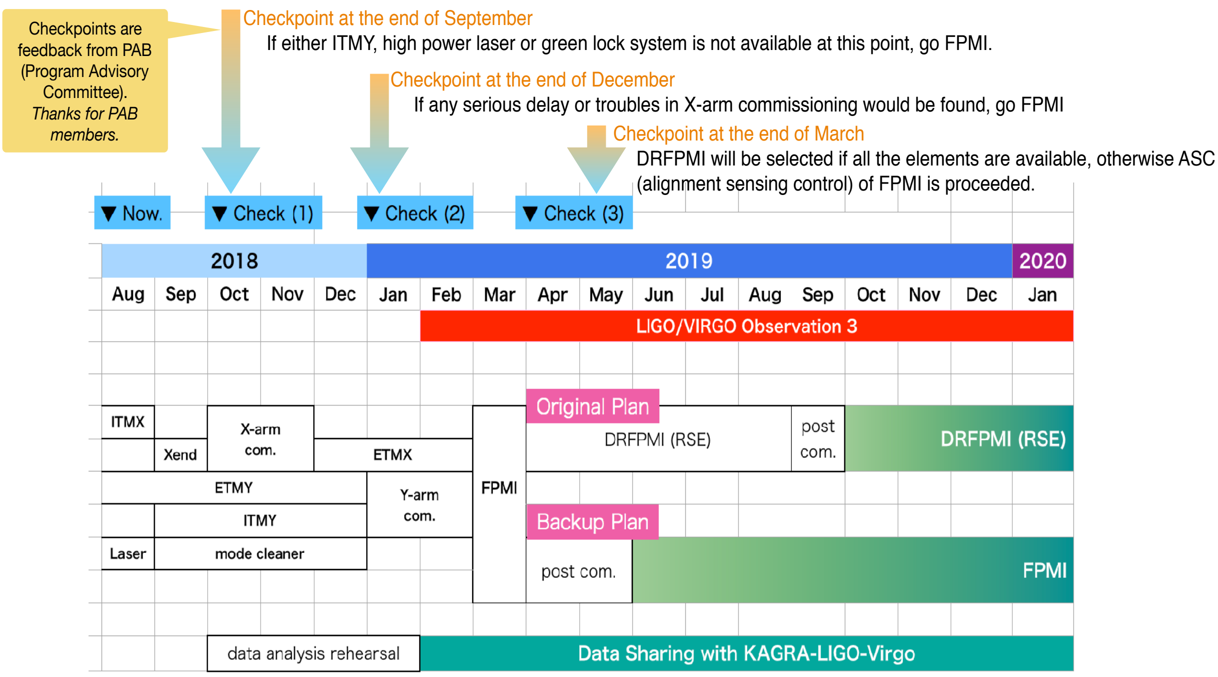

Steps toward O3. We have two plans: RSE or FPMI. We anyway will join the observation no later than October 2019.

Data Analysis Activities

	Projects
GW search pipeline	CBC (KAGALI)
	CBC (gstlal-inspiral)
	Burst
	CW
	Radiometry
	CBC (GPU acceralation)
	Cosmic string
PE pipeline	CBC MCMC (KAGALI)
	CBC Nested Samping

	Projects
KAGALI	KAGALI Management
Phase-1	Analysis of HW injection data
Development of analysis method, Analysis of LV open data, etc	CBC-PE (BNS tidal)
	EOB waveforms
	QNM analysis
	Auto Regressive model
	HHT
	NHA
Others	Commissioning tools
	$\boxed{\text{Sensitivity Threshold for O3}}$

KAGRA

長岡技術科学大学 Nagaoka University of Technology

On the KAGRA's sensitivity threshold at O3

by Tagoshi-san, Haino-san, Narikawa-san and Morisaki-san

- Installation of KAGRA is ongoing
- We want to perform an observation run during the period of LIGO/Virgo O3 run, and want to join the international network of LIGO/Virgo.

- How much improvement on the measurement accuracy of CBC signals
  - we would have for various possible sensitivities of KAGRA during O3 period.
  - In this talk:
    - ✓ We show some results for source localization accuracy evaluated by Fisher matrix.
    - ✓ We show the case when KAGRA's sensitivity is 10Mpc as BNS range.

(The possibility of 10Mpc sensitivity was first pointed out by Kipp Cannon.)

KAGRA

長岡技術科学大学 Nagaoka University of Technology

Noise Curves

Enomoto-san and Michimura-san made 3 noise curves of KAGRA with BNS range of 1.3Mpc, 9.6Mpc, and 42Mpc.
We interpolate these curves to obtain noise curves for other ranges.
For LIGO/Virgo, LIGO: 120Mpc, Virgo 60Mpc (taken from arXiv:1304.0670v6) (Living Reviews in Relativity; 21:3; 2018)

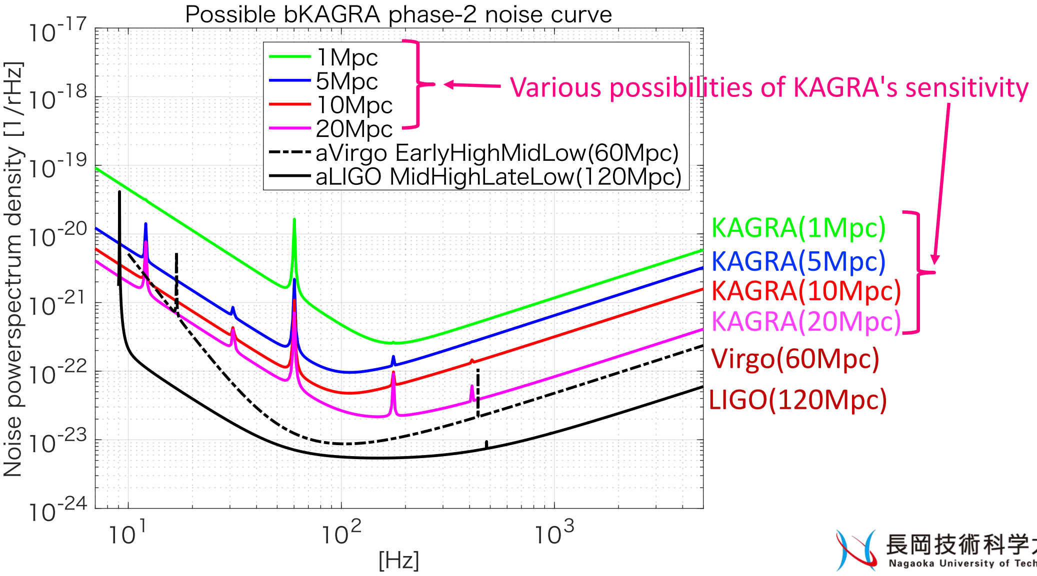

Setup

Source

Binary Neutron stars at 40Mpc (like GW170817)
Uniform distribution for sky location, inclination, polarization
5000 realizations

Sensitivity

BNS range (average observable distance with SNR=8):
KAGRA: 10Mpc
LIGO: 120Mpc (MidHighLateLow)
Virgo: 60Mpc (EarlyHighMidLow)

Method

Fisher matrix

Source localization accuracy (1)

LHV

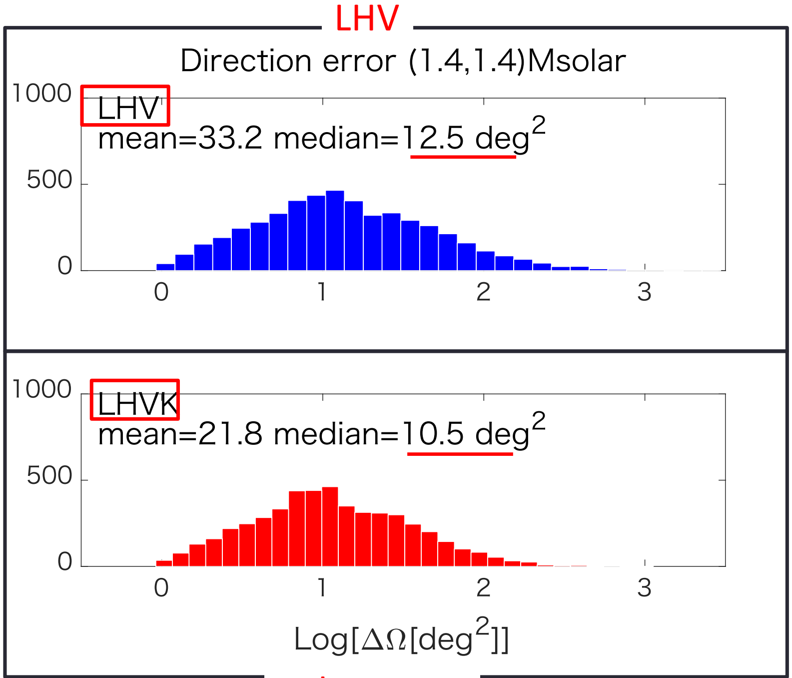

4 detectors

Source localization accuracy (2)

All cases

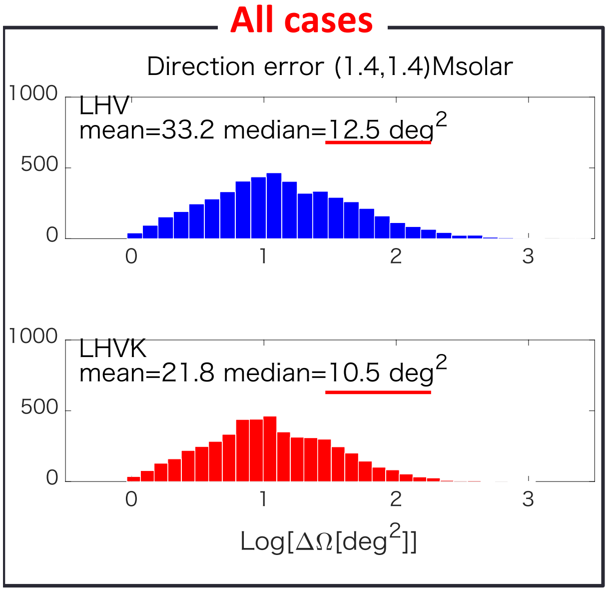

Only ρ_{KAGRA} > 2 cases

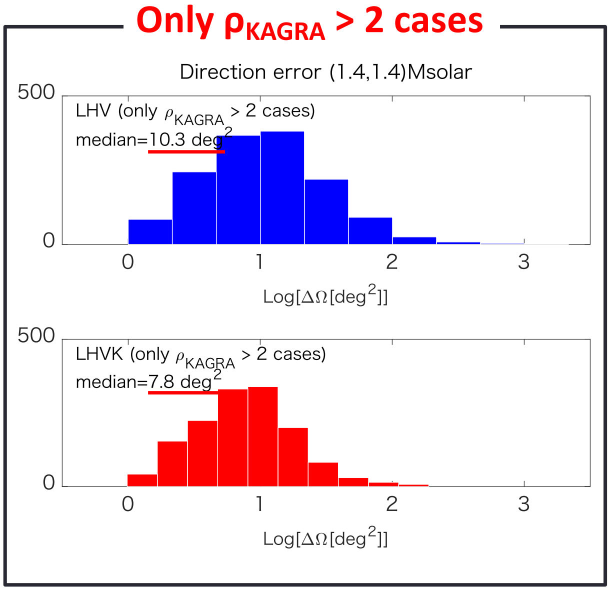

$$\frac{\Delta\Omega_{LHV}}{\Delta\Omega_{LHVK}} = \frac{10.5}{12.5} = 0.84$$

$$\frac{\Delta\Omega_{LHV}|_{\rho\geq 2}}{\Delta\Omega_{LHVK}|_{\rho\geq 2}} = \frac{7.8}{10.3} = 0.76$$

Source localization accuracy (3)

3 detectors including KAGRA

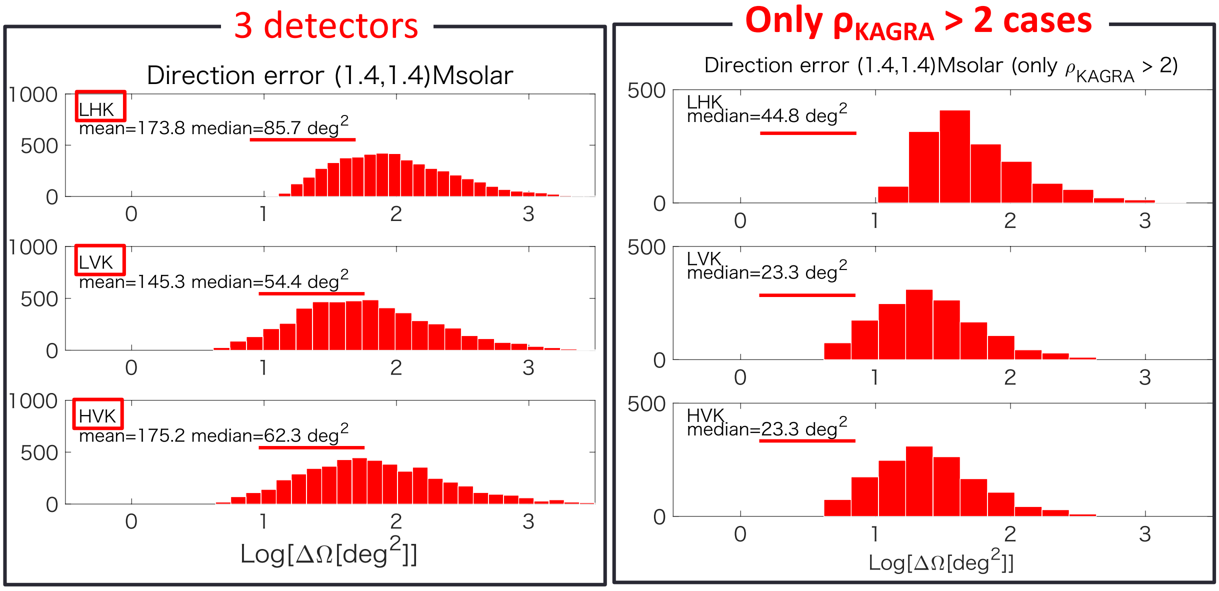

GW170817 case: ΔΩ ~ 30 deg^2

Fraction of number of events with ρ_{KAGRA} > 2

Source: BNS (1.4, 1.4) Msolar at 40Mpc

BNS Range [Mpc]	20	15	10	9	8	7	6	5
Fraction of ρ_{KAGRA} > 2 for 40Mpc source	71.8%	54.7%	28.5%	21.0%	14.6%	9.4%	4%	0.8%
Horizon distance with SNR=2 [Mpc]	180	135	90	81	72	63	54	45

KAGRA sensitivity : 10Mpc (for BNS range)

28.5 % are ρ_{KAGRA} > 2

On the KAGRA's sensitivity threshold at O3

- If BNS range of KAGRA is 10Mpc, for BNS sources at 40Mpc, the median of the source localization accuracy for the LHVK case is about 10% better than that of LHV.
- If BNS range of KAGRA is 10Mpc, about 28% of events can be detected by KAGRA with SNR > 2. In these cases, the improvement of the localization accuracy from LHV to LHVK becomes larger (about 24%).
- Above results are derived with Fisher matrix. We did not explain in this talk Nested sampling code produces slightly different results quantitatively, but overall feature is similar to that of Fisher matrix.
- For some limited number of specific cases, the results are confirmed by LALInference.
- Based on these results, in the KAGRA's collaboration meeting, we agreed that we want to realize the sensitivity of at least 10 Mpc for BNS range.
- If that sensitivity is realized, we would be able to contribute to the improvement of localization accuracy slightly even if the improvement is not very large.

Data Analysis Activities

	Projects
GW search pipeline	CBC (KAGALI)
	CBC (gstlal-inspiral)
	Burst
	CW
	Radiometry
	CBC (GPU acceralation)
	Cosmic string
PE pipeline	CBC MCMC (KAGALI)
	CBC Nested Samping

	Projects
KAGALI	KAGALI Management
Phase-1	Analysis of HW injection data
Development of analysis method, Analysis of LV open data, etc	CBC-PE (BNS tidal)
	EOB waveforms
	QNM analysis
	Auto Regressive model
	HHT
	NHA
Others	Commissioning tools
	Sensitivity Threshold for O3

QNM Analysis

Mock data challenge for finding ringdown gravitational waves

Hiroyuki Nakano,[1,*] Tatsuya Narikawa,[2,3,†] Ken'ichi Ohara,[4,‡] Kazuki Sakai,[5,§] Hisa-aki Shinkai,[6,¶] Hirotaka Takahashi,[7,8,**] Takahiro Tanaka,[3,††] Nami Uchikata,[2,4,‡‡] Shun Yamamoto,[6] and Takahiro Yamamoto[3,§§]

modified ringdown signals from GR with LIGO detector's noise

1. Standard Matched-filtering method
2. Improved Matched-filtering method
3. Hilbert-Huang transformation method
4. Auto-Regressive method
5. Neural network method

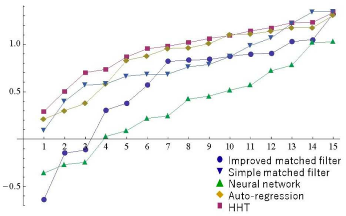

FIG. 1: Real part for Set A

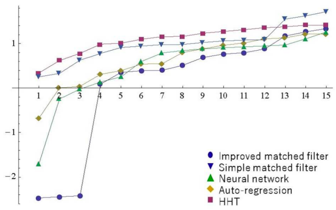

FIG. 3: Imaginary part for Set A

PA21:Tanaka-san's poster

Data Analysis Activities

	Projects
GW search pipeline	CBC (KAGALI)
	CBC (gstlal-inspiral)
	Burst
	CW
	Radiometry
	CBC (GPU acceralation)
	Cosmic string
PE pipeline	CBC MCMC (KAGALI)
	CBC Nested Samping

	Projects
KAGALI	KAGALI Management
Phase-1	Analysis of HW injection data
Development of analysis method, Analysis of LV open data, etc	CBC-PE (BNS tidal)
	EOB waveforms
	QNM analysis
	Auto Regressive model
	HHT
	NHA
Others	Commissioning tools
	Sensitivity Threshold for O3

Analysis of GWs from Core Collapse Supernovae with Hilbert-Huang Transform

- We consider gravitational waves from core collapse supernovae obtained by 3D numerical simulation (T. Kuroda, K. Kotake, and T. Takiwaki, ApJ, **827**, L14 (2016)).

- This is one of the waveform and its time-frequency map made with the short-time Fourier transform.

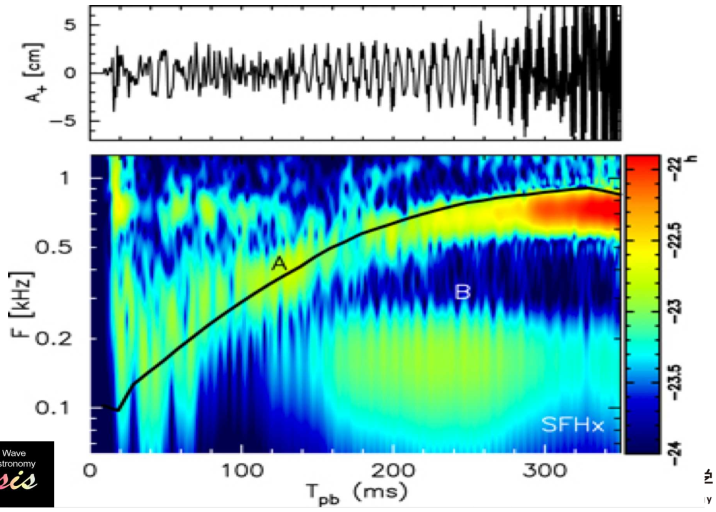

Analysis of GWs from Core Collapse Supernovae with Hilbert-Huang Transform

- There are mainly two components in the time-frequency map;
  - ✓The high-frequency component (A) is originated from the g-mode oscillation of the proto-neutron star.
  - ✓The low-frequency one (B) is considered to be associated with the standing accretion shock instability (SASI) activities.

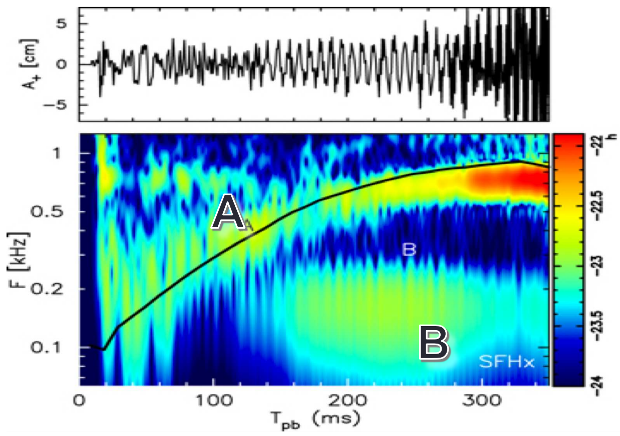

長岡技術科学大学
Nagaoka University of Technology

Analysis of GWs from Core Collapse Supernovae with Hilbert-Huang Transform

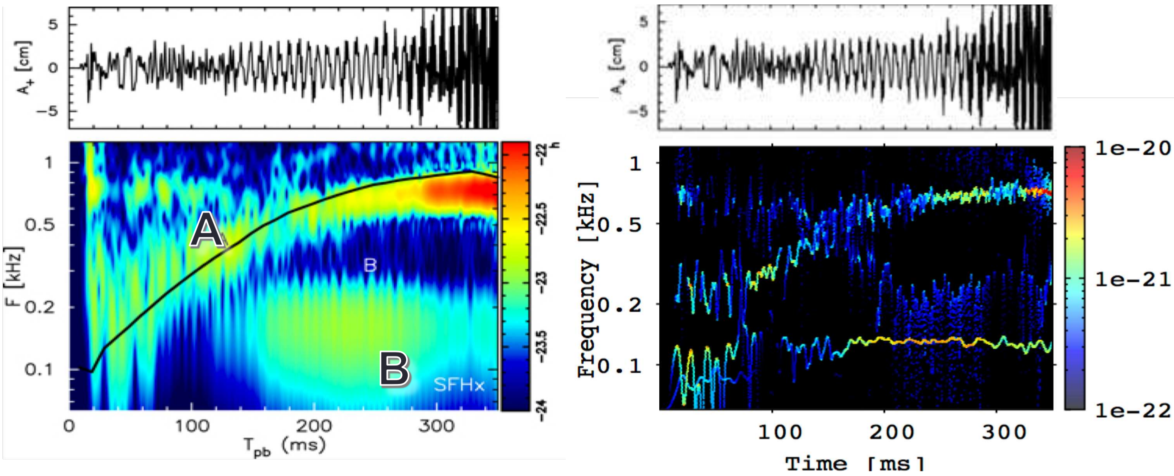

The detailed discussion can be found in Hiranuma-kun's poster (PA3) and Watanabe-kun’s poster (PB5)

KAGRA Genesis 長岡技術科学大学 Nagaoka University of Technology

Re-organize data analysis group in KAGRA

- We reorganized the data analysis group in KAGRA.
- Data analysis group moves under the KSC (KAGRA Scientific Congress).
- Working groups are organized **as corresponding to LV data analysis groups** for near future cooperation.

New organization structure of KAGRA

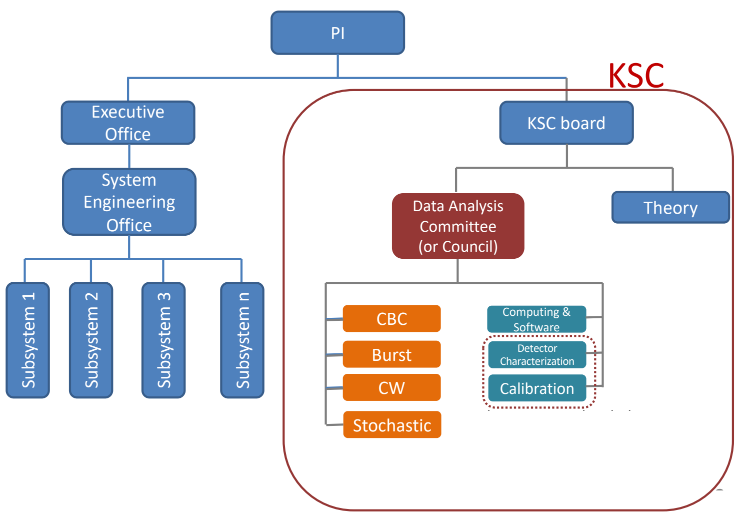

KAGRA 長岡技術科学大学 Nagaoka University of Technology

Data analysis related talks

Monday, November 5

11:00 – 12:15 Session 1A

[T1*] Nami Uchikata *Niigata University*
Analysis of echoes by a new template
[T2*] Takahiro Yamamoto *Kyoto University*
Analysis of Ringdown Gravitational Wave by Neural Network
[T3*] Hiroki Takeda *University of Tokyo*
Polarization test of gravitational waves from compact binary coalescences
[T4*] Haruka Suzuki *Waseda University*
The Effect of Kozai-Lidov Mechanism on the Period Shift of the Binary Neutron Stars by Gravitational Waves
[T5*] Asuka Ito *Kobe University*
A strategy for detecting the bispectrum of stochastic gravitational waves

Wednesday, November 7

9:00 – 9:45 Invited Talk 5 (Chair: H. Tagoshi)

Jonathan Gair *University of Edinburgh*
Science with the Laser Interferometer Space Antenna

Summary

- **KAGRA achieved phase-1 test run in this April-May.**
  3km Michelson Interferometer with cryogenic mirrors.

- **KAGRA is under the installation and commissioning for phase-2.**
  In 2019, KAGRA would like to join O3 with full configuration.

  KAGRA master schedule:
  - iKAGRA (- Mar 2016): Room Temperature Michelson Interferometer
  - bKAGRA phase-1 (- May 2018): Cryogenic Michelson Interferometer
  - bKAGRA phase-2 (- 2019): Cryogenic FPM/RSE Interferometer (full configuration)
  - bKAGRA phase-3 (2019 -): Commissioning and Observation run

Session S1A 11:00–12:15

[Chair: Takahiro Tanaka]

Nami Uchikata

Niigata University

“Analysis of echoes by a new template”

(10+5 min.)

[JGRG28 (2018) 110502]

Analysis of echoes by a new template

Nami Uchikata (Niigata Univ.)

Takahiro Tanaka (Kyoto Univ.),
Hiroyuki Nakano (Ryukoku Univ.), Tatsuya Narikawa (Kyoto Univ.),
Norichika Sago (Kyushu Univ.), and Hideyuki Tagoshi (ICRR)

Exotic Compact Objects

Five binary black hole merger events were detected by LIGO and Virgo.
These events are consistent with black holes but do not exclude
exotic compact objects.

⬇

Theoretical compact object models alternative to black holes
Ex) Boson stars, gravastars, wormholes

As compact as black holes, but do not possess the event horizon.
Cannot distinguish from black holes by electromagnetic observations.

How to distinguish ECOs from black holes?

- Gravitational waves
  - Quadrupole moment (rotation Q, tidal force Λ)
    Black holes: $Q = 1, \Lambda = 0$ (dimensionless)
  - Oscillation modes
    Black holes: quasinormal modes
  - "Echoes" after mergers
    (Cardoso et al . (2016))

- Tentative evidence of echoes from LIGO events was reported by Abedi et al. (2017)

Cardoso et al. (2016)

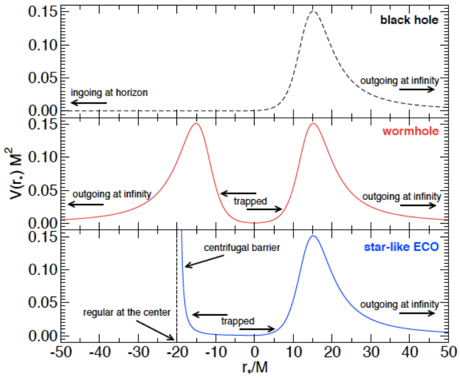

Gravitational wave echoes from binary black hole mergers

Abedi et al. (2017)

- Reflection membrane near the event horizon produced by quantum effects.

- Merger-ringdown waveform will be iteratively reflected.

- Observable as "echoes".

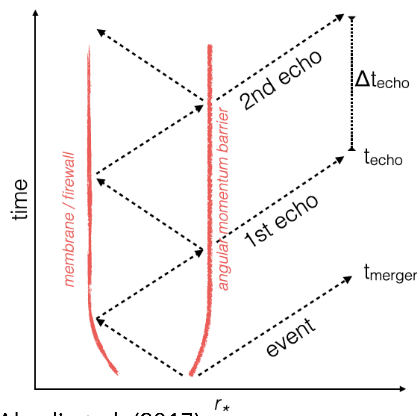

Abedi et al. (2017)

Evidence of echoes?

Abedi et al. (2017)

- Tentative evidence 2.5σ significance level. 32 seconds data were used.

(GW150914, GW151226, LVT151012)

Westerweck et al. (2018) (AEI group)

- Re-analyse echo-signals using the same template as Abedi et al..

(GW150914, GW151226, LVT151012, GW170104)

- Using 4096 seconds of data for background estimation, the significance level decreases.

Templates of echoes

Abedi et al. (2017)

$$h_{MR}(t) = \Theta(t_0) h_{IMR}(t)$$

seed waveform

$$\tilde{h}(f) = \sum_{n=1}^{N} \gamma^{n-1} (-1)^n \tilde{h}_{MR}(f)\, e^{-2\pi i f \Delta t_{echo}(n-1)}$$

<u>Parameters</u>

Cutoff parameter: t_0

Reflection rate: γ ⇦ Less physical?

Interval of echoes: Δt_{echo}

(Can be determined theoretically.)

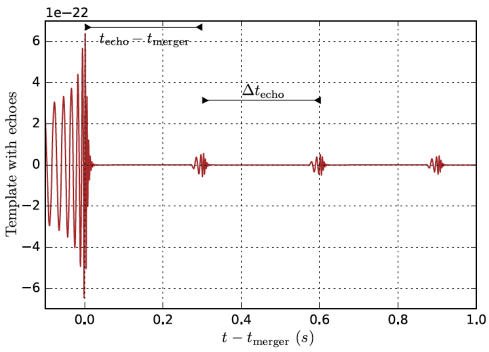

Abedi et al. (2017)

Modification of template

- Spacetime outside the membrane is exactly Kerr spacetime.
- Reflection rate can be obtained by solving linear perturbation of Kerr spacetime. (Nakano et al. 2017)
- In this study, we reanalyze echo signals by new templates whose reflection rate depends on frequency.

New echo templates

Nakano et al. (2017)

reflection rate

$$\tilde{h}(f) = \sum_{n=1}^{N} [\boxed{R_f(a, M, f)}]^{n-1} (-1)^n \tilde{h}_{MR}(f)\, e^{-2\pi i f \Delta t_{echo}(n-1)}$$

seed waveform

<u>Parameters</u>

(Cutoff parameter: t_0)

Black hole spin and mass: (a, M)

Interval of echoes: Δt_{echo}

Method of analysis 1

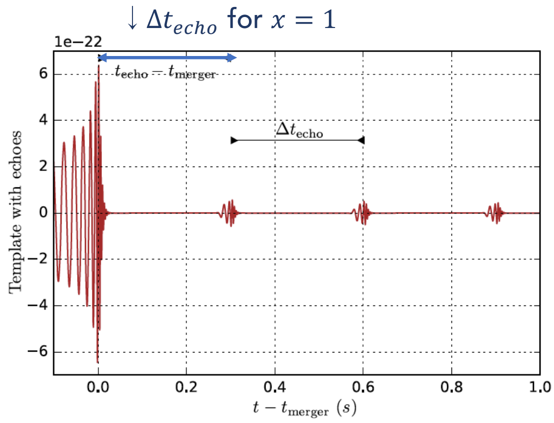

Searching events

(Abedi et al. (2017), Westerweck et al. (2018))

- Analyze the data set around each binary black hole event.
- Search the maximum signal-to-noise ratio (SNR) in the interval of

Peak of the first echo ↓ ↓Peak of the binary black hole merger

$$0.99 \leq x = \frac{t_{echo} - t_{merger}}{\Delta t_{echo}} \leq 1.01$$

Method of analysis 2

Background estimation (Westerweck et al. (2018))

- Perform the same analysis as the above for the rest of 4096 second-data.
- Count the number of data set whose SNR is above that of the event data set.
- p-value : number of data set that have higher SNR / number of total data set

16[s]				event					

4096 [s] (more than 200 data set)

Results (Preliminary)

Template

- Black hole spin and mass is fixed. $R_f(a, M, f) \to R_f(f)$
- Vary Δt_{echo} around the theoretical values. (Abedi et al. (2017))
- Length : 16 seconds

Data

- Of 4096 seconds LIGO open data for 3 events (GW150914, GW151226, LVT151012) (https://www.gw-openscience.org/events/)
- Sampling frequency: 4096Hz

SNR

- Matched filtering method

data↓ ↓template

$$\rho \equiv (x, s_t) = 4\,\mathrm{Re}\left(\int_0^\infty \frac{\tilde{x}(f)\tilde{s}_t^*(f)}{S_n(f)} df\right),$$

noise power spectrum ↑

Results (Preliminary)

p-values

	reflection rate	GW150914	GW151226	LVT151012	Total (Fisher's method)
Westerweck et al. (2018)	parameter	0.199	0.414	0.056	0.1
Our result	Depends on frequency	0.727	0.826	0.285	0.74

In general, critical p-value is 0.05 or 0.01.

Higher p-value ➡ consistent with noise.

Excluding LVT151012 makes p-value much higher. ➡Detected echo signals are consistent with the pure noise null hypothesis.(Westerweck et al. (2018))

Summary

- We have analyzed echo signals from LIGO open data.
- We use new templates whose reflection rate is obtained by solving black hole perturbation.
- We find no evidence for echoes from our template. (LVT151012 gives the lowest p-value.)

Future works

- Reflection rate and Δt_{echo} depend on black hole spin and mass (a, M).
- We should vary (a, M) .
- Analyze O2 events.

Takahiro Yamamoto
Kyoto University

“Analysis of Ringdown Gravitational Wave by Neural Network”

(10+5 min.)

[JGRG28 (2018) 110503]

Analysis of ringdown gravitational wave by neural network

Takahiro Yamamoto, Takahiro Tanaka
(Kyoto Univ.)

Gravitational Wave Physics and Astronomy Genesis

JGRG28
2018. 11. 05

Binary BH merger

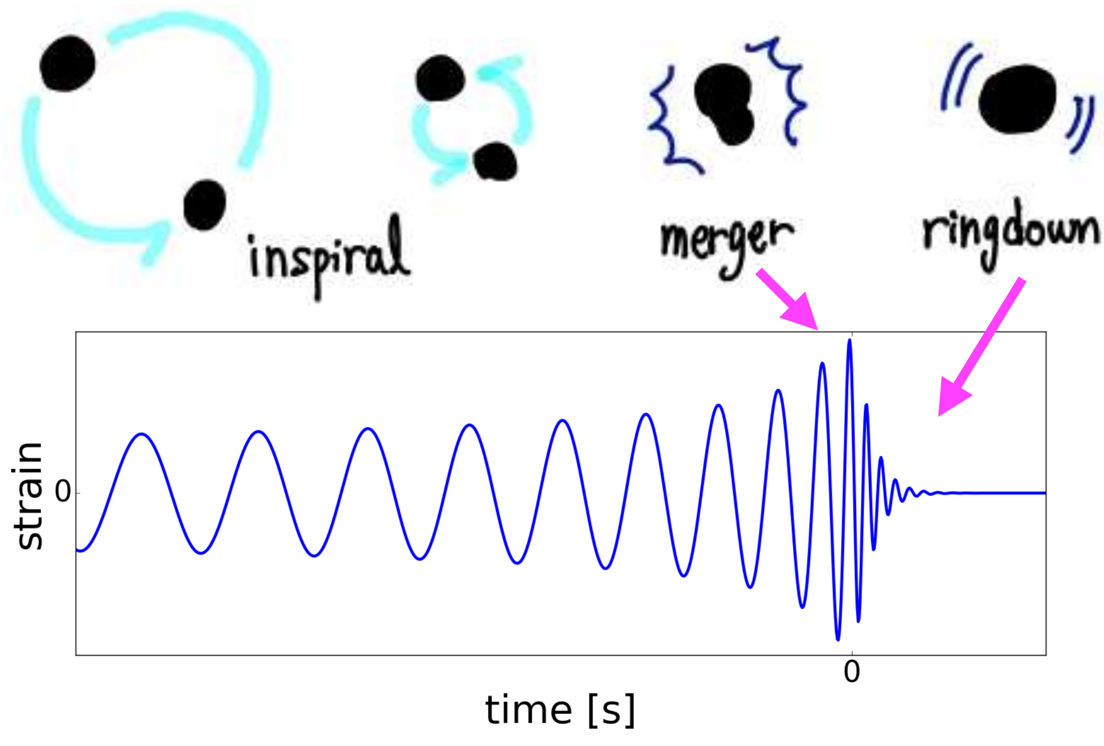

Black hole ringdown

- Ringdown is emitted when black hole is perturbed.
- Occupied with BH quasi-normal modes (QNMs)

$$h(t) = A\exp[-2\pi f_i(t-t_0)]\cos[2\pi f_r(t-t_0)-\phi_0]$$

$f_r,\ f_i:$ QNM frequency

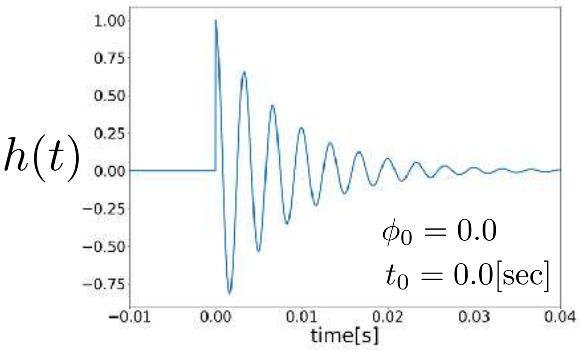

In general relativity, QNM frequency is determined by BH mass and spin.

※In general, ringdown is the linear combination of various modes. Usually, we focus on (l,m)=(2,2) mode which has the longest damping time.

Matched Filter(MF)

Calculate the correlation (SNR) between signal and templates.

The parameter maximizing SNR is the estimated value.

$$\mathrm{SNR} = 2\int_0^\infty \frac{\tilde{h}^*(f)\tilde{s}(f)+\tilde{h}(f)\tilde{s}^*(f)}{S_n(f)}df$$

Ringdown have 5 parameters $\{A, f_R, f_I, t_0, \phi_0\}$

The amplitude A can be replaced by the value of SNR.

The phase ϕ_0 can be optimized analytically.

Fixing the start time t_0 , search the QNM frequency $\{f_R, f_I\}$

e.g. GW150914

IMR: using inspiral-merger-ringdown waveform

If t_0 is around coalescence time,
estimation is biased by non-linearity.
If t_0 is late time, detector noise dominate.

$$h(t) = A\exp[-2\pi f_i(t-t_0)]\cos[2\pi f_r(t-t_0)-\phi_0]$$

$f_r,\ f_i:$ QNM frequency

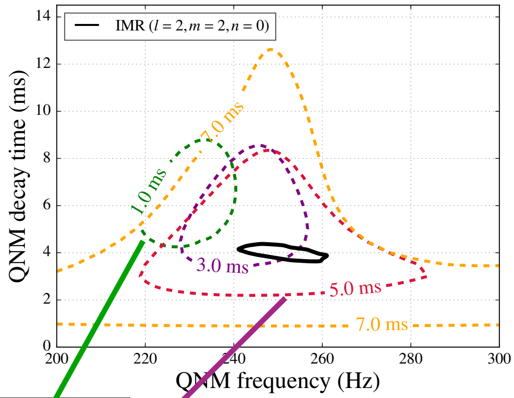

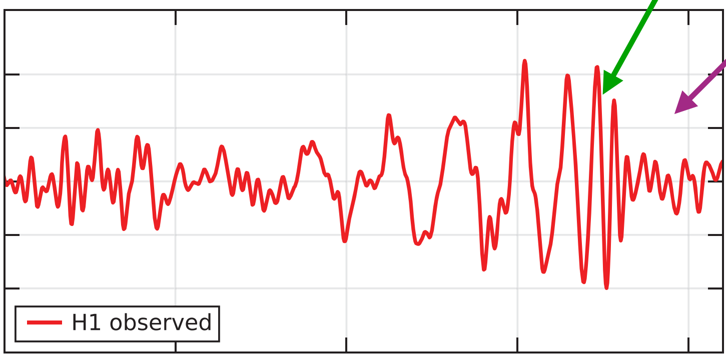

LIGO Scientific Collaboration and Virgo Collaboration (2016)

Mock Data Challenge

- Investigate the optimal method for analysis of ringdown
- Mockdata is based on the GR template and modified only ringdown part. We estimate QNM frequency of this modified waveform.
- We prepare 2 types of modification (A, B).
- For each templates (A, B), generate 15 signals. 5 are SNR=60, another 5 are SNR=30 and the last 5 are SNR=20. These 30 signals is used as mockdata.

ref) poster: Testing gravity theories using gravitational waves (T. Tanaka)

Mock Data Challenge

- Comparing 5 methods,

  - Hilbert-Huang transformation（Oohara, Sakai, Takahashi)
  - Auto-regressive model(Shinkai, Yamamoto)
  - plain MF (Tanaka, Uchikata)
  - improved MF (Tanaka)
  - neural network

- Here, I will talk about neural network method, compare with improved MF.

ref) poster: Testing gravity theories using gravitational waves (T. Tanaka)

Improved MF

Calculate the correlation (SNR) between signal and templates.

The parameter maximizing SNR is the estimated value.

$$\mathrm{SNR} = 2\int_0^\infty \frac{\tilde{h}^*(f)\tilde{s}(f) + \tilde{h}(f)\tilde{s}^*(f)}{S_n(f)} df$$

Modification：

・Use the template with modification A including the inspiral part

・Filter the template using the window function before calculate SNR

$$W(t) = \frac{1}{1 + e^{-50(t-t_c)\omega_I^{\mathrm{GR}}}}$$

Neural Network（NN)

- Find the (highly-nonlinear) relation between inputs and labels.

$$\text{output} = f(\text{input}; W)$$

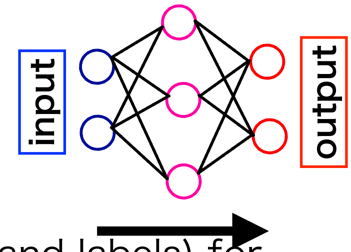

- Prepare the dataset (the pairs of inputs and labels) for training.

- Evaluate the error between labels and outputs for adjusting the parameter W

$$J(\text{label}, \text{output}) = |\text{label} - \text{output}|^2$$

Convolutional NN

Convolutional Layer

$$z'_{i,l'} = \sum_{l=1}^{L} \sum_{p=1}^{H} z_{i+p,l} h^{l}_{p,l'} + b_{i,l'}$$

Using “filter” to extract the local patterns
(L: size of input from previous layer、H: size of filter)

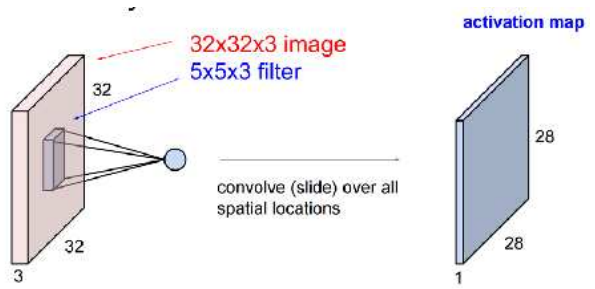

site)
https://qiita.com/icoxfog417/items/5fd55fad152231d706c2

layer	dimension
Input	(256, 2)
Conv	(256, 64)
Pooling	(128, 64)
ReLU	(128, 64)
Conv	(128, 128)
Pooling	(64, 128)
ReLU	(64, 128)
Conv	(64, 256)
Pooling	(32, 256)
ReLU	(32, 256)
Conv	(32, 512)
ReLU	(32, 512)
Flatten	32×512
Dense	256
ReLU	256
Dense	2
Output	2

Convolutional NN

Pooling Layer

$$z'_i = \max_{k=1,\dots,p} z_{si+k}$$

・Improve the validity against the small shift
・Suppress the computational cost

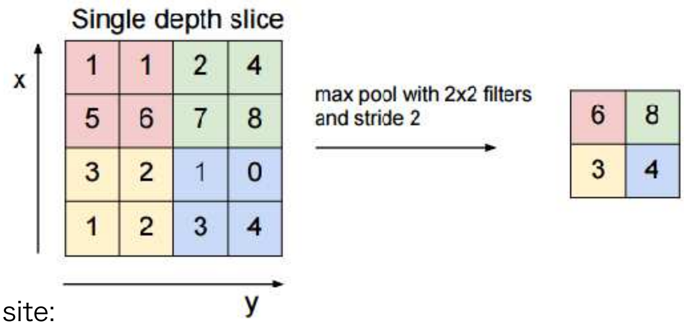

site:
https://qiita.com/icoxfog417/items/5fd55fad152231d706c2

layer	dimension
Input	(256, 2)
Conv	(256, 64)
Pooling	(128, 64)
ReLU	(128, 64)
Conv	(128, 128)
Pooling	(64, 128)
ReLU	(64, 128)
Conv	(64, 256)
Pooling	(32, 256)
ReLU	(32, 256)
Conv	(32, 512)
ReLU	(32, 512)
Flatten	32×512
Dense	256
ReLU	256
Dense	2
Output	2

Convolutional NN

Dense layer

Affine transform $$a_i^{(l)} = \sum_{j=1}^{n^{(l-1)}} w_{ij}^{(l)} z_j^{(l-1)} + w_{i0}^{(l)}$$

Nonlinear transformation

$$z_i^{(l)} = h(a_i^{(l)}) = \max(0, a_i^{(l)}) \quad \text{(ReLU)}$$

layer	dimension
Input	(256, 2)
Conv	(256, 64)
Pooling	(128, 64)
ReLU	(128, 64)
Conv	(128, 128)
Pooling	(64, 128)
ReLU	(64, 128)
Conv	(64, 256)
Pooling	(32, 256)
ReLU	(32, 256)
Conv	(32, 512)
ReLU	(32, 512)
Flatten	32×512
Dense	256
ReLU	256
Dense	2
Output	2

Dataset

- Training data consists of 441 templates A. They have various QNM frequencies covering enough area.
- Adding noise to the templates, the total number of signal is 8820.
- The noise amplitudes are adjusted so that their SNR are same as the testdata.
- Pick up 256 data points starting from the merger time.
- Use the plus and cross modes.

Detail

neural network and machine

- optimization algorithm: Adam
- library: Keras with TensorFlow backend
- GPU GeForce 1080 Ti (@Nagaoka University of Technology)

(x, y):
x is the size of input
y is the number of channels

layer	dimension
Input	(256, 2)
Conv	(256, 64)
Pooling	(128, 64)
ReLU	(128, 64)
Conv	(128, 128)
Pooling	(64, 128)
ReLU	(64, 128)
Conv	(64, 256)
Pooling	(32, 256)
ReLU	(32, 256)
Conv	(32, 512)
ReLU	(32, 512)
Flatten	32×512
Dense	256
ReLU	256
Dense	2
Output	2

Results for data A

real part

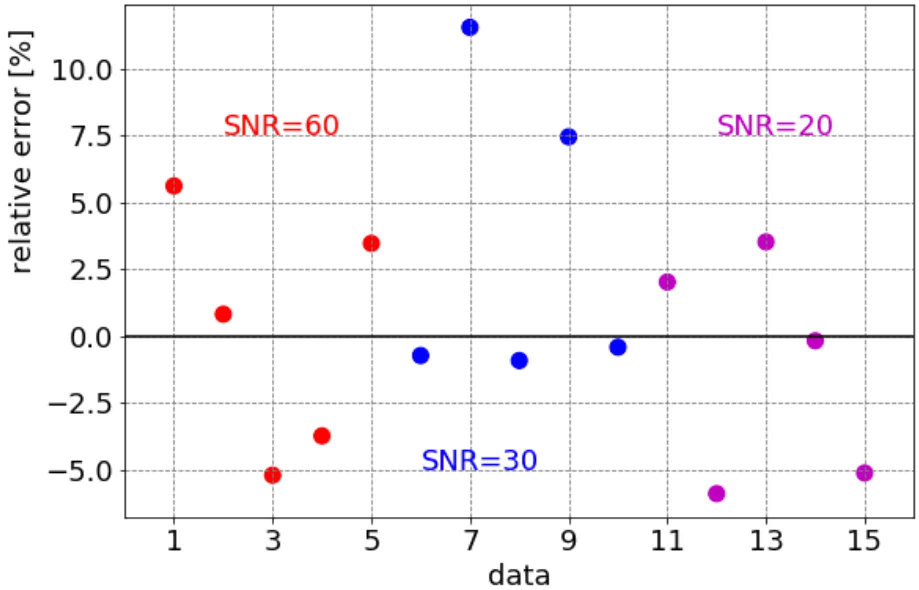

For real part, CNN can estimate less than 10% error.

Results for data A

Imaginary part

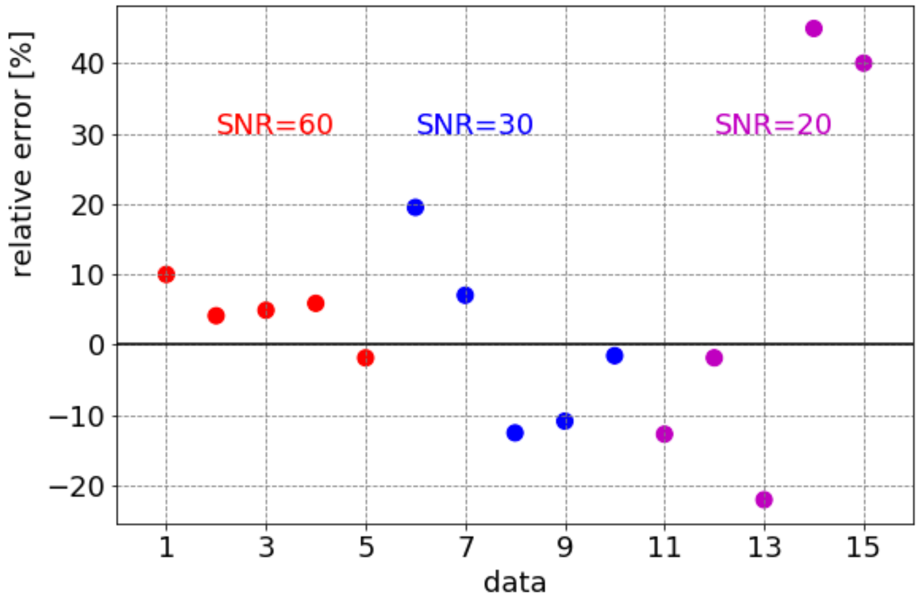

The smaller SNR is, the larger the error of the imaginary part.

Results for data B

real part

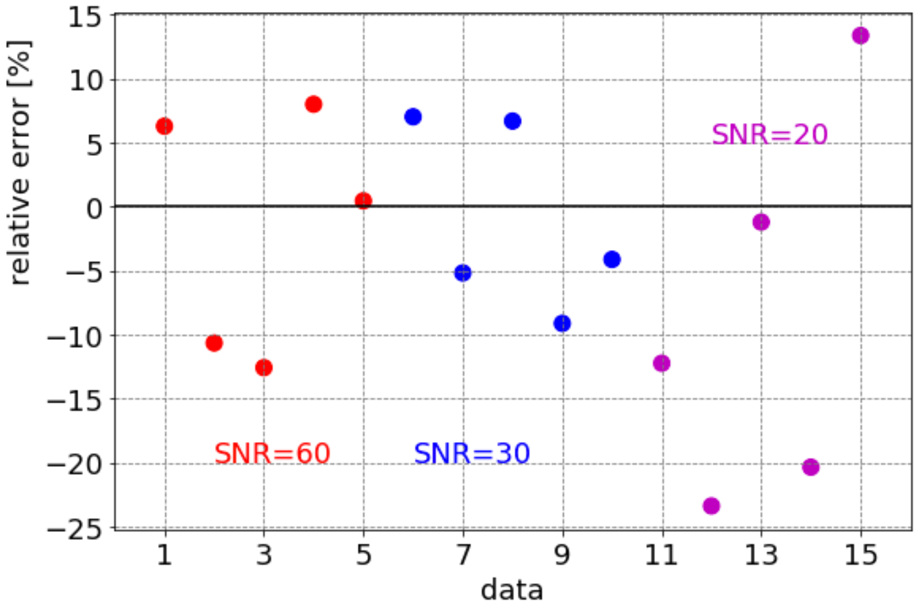

Error is about 20%, larger than for data A.

Results for data B

imaginary part

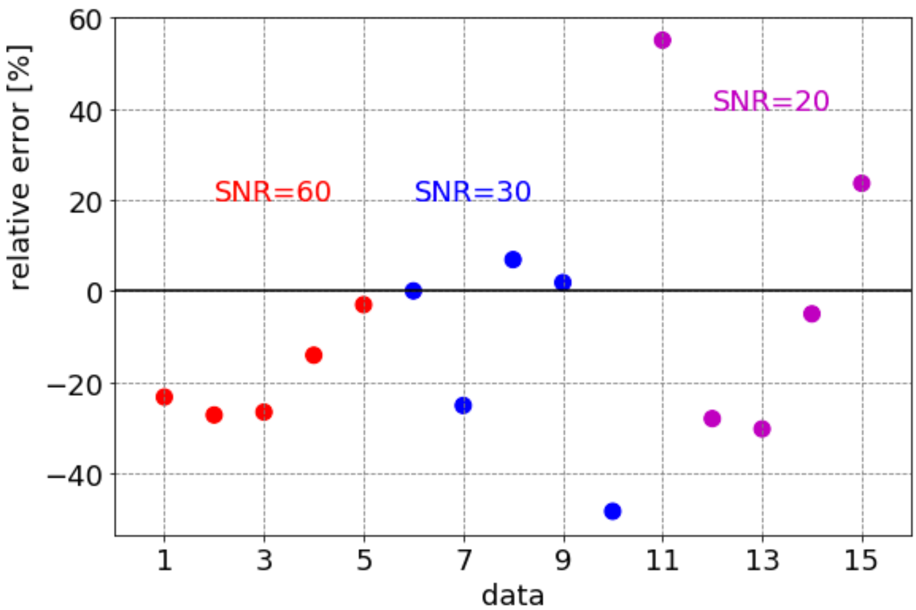

The errors become larger. For SNR~20, the error is ~60%.

Results

We evaluate the log error to suppress the variation of the error.

$$\overline{\delta \log Q} := \frac{1}{N}\sum_{n=1}^{N}\left(\log\frac{Q_n^{\mathrm{estimate}}}{Q_n^{\mathrm{true}}}\right) \qquad \sigma(Q) := \left[\frac{1}{N}\sum_{n=1}^{N}\left(\log\frac{Q_n^{\mathrm{estimate}}}{Q_n^{\mathrm{true}}}\right)^2\right]^{1/2}$$

		$\overline{\delta \log \omega_R}(\%)$	$\sigma(\omega_R)(\%)$	$\overline{\delta \log \omega_I}(\%)$	$\sigma(\omega_I)(\%)$
A	NN	0.69	4.75	3.36	16.67
	iMF	1.28	3.58	2.20	31.76
B	NN	-4.50	12.08	-13.48	29.34
	iMF	-0.79	11.65	15.51	31.35

Conclusion

- For both of templates, CNN have the comparable ability to the improved matched filtering.
- For now, NN can output the point value. We need to investigate the method how NN estimate the prediction error.
- We will implement the hierarchical training* so that NN can be applied to the signal having any SNR.

* George &Huerta (2017)

Hiroki Takeda
University of Tokyo

“Probing nontensorial polarization of inspiral gravitational waves with the third-generation detectors”

(10+5 min.)

[JGRG28 (2018) 110504]

2018. 11/5 JGRG28,
Rikkyo University

Probing nontensorial polarization of inspiral gravitational waves with the third-generation detectors

<u>Hiroki Takeda</u>(University of Tokyo)
Atsushi Nishizawa, Yuta Michimura, Koji Nagano, Kentaro Komori, Masaki Ando, and Kazuhiro Hayama

Abstract

・Observation of gravitational waves(GW) from compact binary coalescences(CBC) enabled some experimental studies to probe into the nature of space-time structure.

・Test of polarizations of GW is a powerful tool for pursuing the nature of gravity.

・We study separablity of polarization modes for inspiral GW from CBC and degeneracies among parameters with third-generation(3G) GW detectors.

・A single 3G detector could be used to test polarization of GW due to the effect of the Earth's rotation.

1. Polarization of Gravitational Wave

Polarization mode of GW

Generic metric theory allows 6 polarizations.

$$h_{ab}(t,\hat{\Omega}) = h_A(t) e^A_{ab}(\hat{\Omega}),$$

$$A = + \,, \times \,, x, \, y, \, b, \, l$$

Tensor

Plus $e^{+}_{ab} = \hat{e}_x \otimes \hat{e}_x - \hat{e}_y \otimes \hat{e}_y,$

Cross $e^{\times}_{ab} = \hat{e}_x \otimes \hat{e}_y + \hat{e}_y \otimes \hat{e}_x,$

Vector

Vector x $e^{x}_{ab} = \hat{e}_x \otimes \hat{e}_z + \hat{e}_z \otimes \hat{e}_x,$

Vector y $e^{y}_{ab} = \hat{e}_y \otimes \hat{e}_z + \hat{e}_z \otimes \hat{e}_y,$

Scalar

breathing $e^{b}_{ab} = \hat{e}_x \otimes \hat{e}_x + \hat{e}_y \otimes \hat{e}_y,$

longitudinal $e^{l}_{ab} = \sqrt{2}\hat{e}_z \otimes \hat{e}_z,$

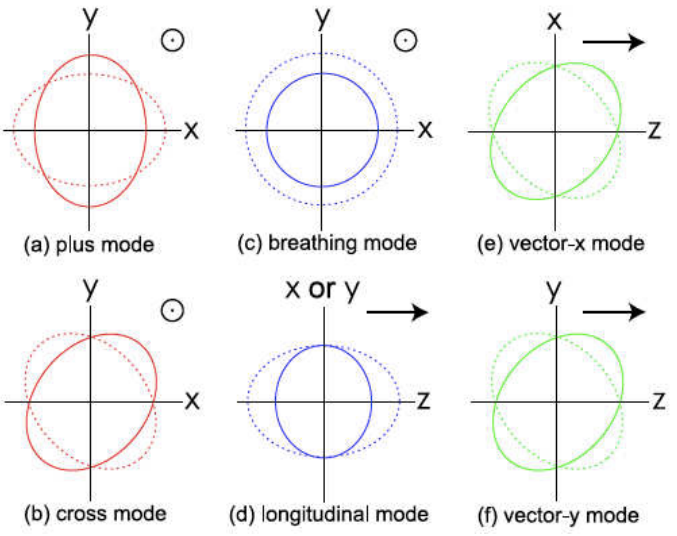

A. Nishizawa et al., Physical Review D 79, 082002 (2009).

Test of Gravity Theory with GW polarization

modes allowed in a theoretical model

Theory	Plus	Cross	Vector x	vector y	breathing	longitudinal
General Relativity	✓	✓				
Kaluza-Klein theory	✓	✓	✓	✓	✓	
Brans-Dicke theory	✓	✓			✓	✓
f(R) theory	✓	✓			✓	✓
Bimetric theory	✓	✓	✓	✓	✓	✓

Search for polarization modes can be used to test theories of gravity.

Separate and Reconstruct polarization modes model independently from detector signal

GW interferometric signal

Detector Signal

$$\boxed{h_I(t,\hat{\Omega}) = F_I^A(\hat{\Omega})h_A(t)}$$

Antenna pattern functions

GW amplitude for polarization mode A

$$F_I^A(\hat{\Omega}) := d_I^{ab} e^A_{ab}(\hat{\Omega}).$$

detector response to GW

Detector Tensor

$$d_I := \frac{1}{2}(\hat{u}_I \otimes \hat{u}_I - \hat{v}_I \otimes \hat{v}_I),$$

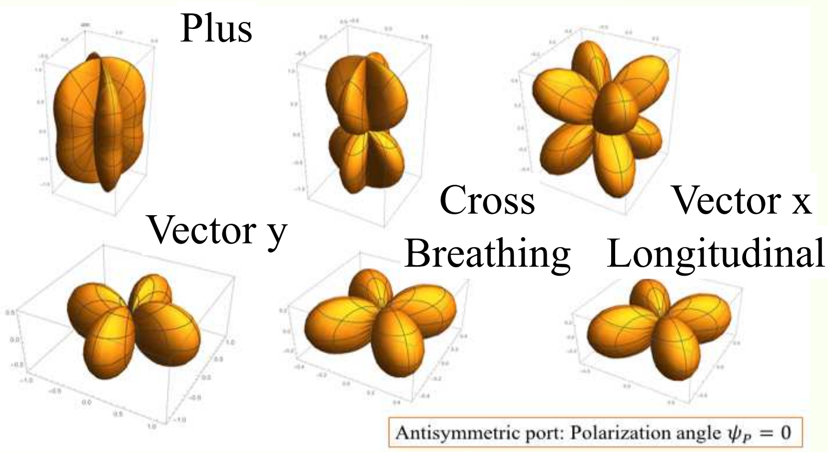

Antisymmetric port: Polarization angle $\psi_P = 0$

Reconstruction of GW polarization

In principle, (Num. of polarization modes) = (Num. of detectors)

e.g. The number of detector =3,
modes = (+ , × , *b*)

$$h_1 = F_1^+ h_+ + F_1^\times h_\times + F_1^b h_b$$
$$h_2 = F_2^+ h_+ + F_2^\times h_\times + F_2^b h_b$$
$$h_3 = F_3^+ h_+ + F_3^\times h_\times + F_3^b h_b$$

$$\begin{pmatrix} h_1 \\ h_2 \\ h_3 \end{pmatrix} = F \begin{pmatrix} h_+ \\ h_\times \\ h_b \end{pmatrix} \qquad F := \begin{pmatrix} F_1^+ & F_1^\times & F_1^b \\ F_2^+ & F_2^\times & F_2^b \\ F_3^+ & F_3^\times & F_3^b \end{pmatrix}$$

Reconstruction
(Inverse Problem)

$$\begin{pmatrix} h_+ \\ h_\times \\ h_b \end{pmatrix} = F^{-1} \begin{pmatrix} h_1 \\ h_2 \\ h_3 \end{pmatrix}$$

GW Detector network expansion → More polarization modes can be probed.

Polarization test with GW from CBC

	Theory	Data analysis	Observation
Burst	✓	△	✗
Chirp	△	✗	△
Stochastic	✓	✓	✓
Continuous	✓	✓	✗

GW waveforms from CBC have source model parameters,
which determine the frequency evolution in time and are correlated each other.

How do waveforms of CBC affect separation of GW polarization mode?
[separability, correlations and degeneracies among parameters]

Our previous work

PhysRevD.98.022008 (arXiv:1806.02182)

In each polarization model, parameter estimation errors and correlations between parameters for BBHs or BNSs with network of three or four detectors.

e.g. Tensor(+,×) scalar(dipole) model

model parameters in GR

$$h_I = \{\mathcal{G}_{T,I} + A_{S_1}\mathcal{G}_{S_1,I}\}h_{\rm GR}$$

polarization amplitude parameter

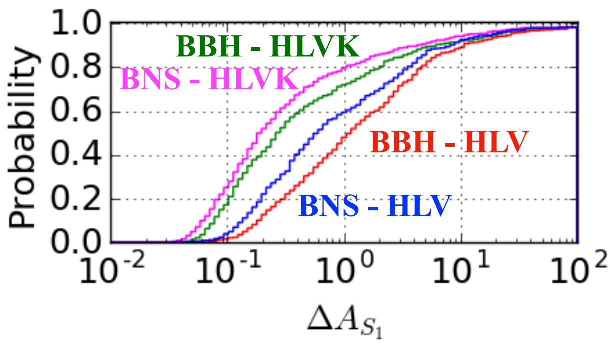

・Two conditions for separation of polarization modes;

(i) The same number of detectors as or more than number of polarization modes.
(ii) Significant SNR and the long duration of the signal.

2. Polarization test with third-generation gravitational wave detector

Third-generation gravitational-wave detector (3G GW detector)

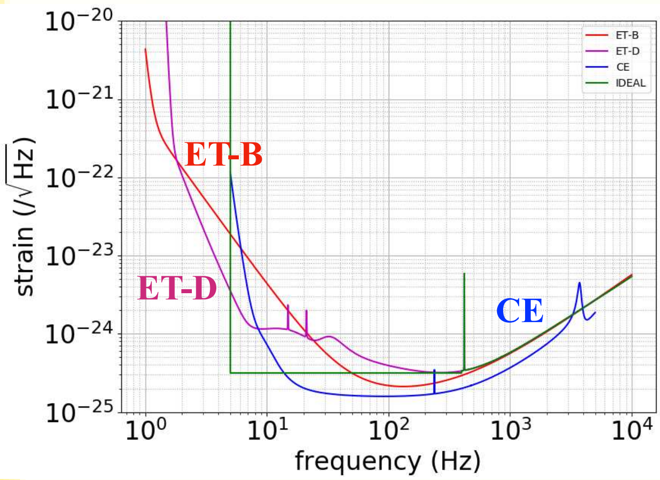

Einstein Telescope (ET) (ET-B, ET-D)

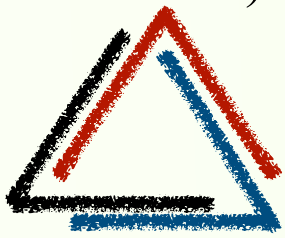

- **three V-shaped Michelson interferometer**

$f_{\mathrm{low}} = 1$ Hz

- **ETD is better at sub-10 Hz band than ETB.**

Cosmic Explorer (CE)

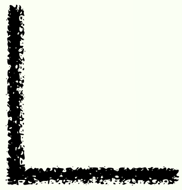

- **single L-shaped Michelson interferometer**
- **better above 8 Hz**

$f_{\mathrm{low}} = 5$ Hz

3G detectors would have extended sensitivity at lower frequencies than 2G detectors.

Difference between 2G and 3G detector

Earth's rotational effect need to be considered.

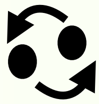

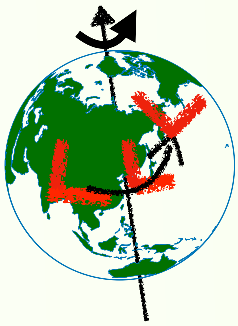

Waveforms of GW(stationary phase approximation)

$$h(f) = \mathcal{A} f^{-7/6} e^{i\Psi(f)} \left\{ \frac{5}{4} \mathscr{A}(t(f)) \right\} e^{-i(\phi_p(t(f)) + \phi_D(t(f)))},$$

relationship between time to merger and GW frequency

$$t(f) = t_c - \frac{5}{256} (G\mathcal{M}/c^3)^{-5/3} (\pi f)^{-8/3},$$

→ **NSNS(1.4-1.4),** $f_{\mathrm{low}} = 10$ Hz **- 0.28 hours**

$f_{\mathrm{low}} = 1$ Hz **- 5.44 days**

The duration of the signal in a detector band

An individual detector can be effectively treated as network including a set of detectors along its trajectory.

Zhao and Wen,
Phys. Rev. D **97**, 064031, 2018

Parameter estimation including nontensorial GW polarizations

setup

- **Parameter estimation by Fisher matrix** $\Gamma_{ij} := 4\mathrm{Re}\int_{f_{\min}}^{f_{\max}} df \sum_I \left(\frac{1}{S_{n,I}(f)} \frac{\partial h_I^*(f)}{\partial\lambda^i}\frac{\partial h_I(f)}{\partial\lambda^j}\right),$

- **Model TS1**

polarization amplitude parameter

Tensor(+,×) scalar(dipole) $h_I = \{\mathcal{G}_{T,I} + A_{S_1}\mathcal{G}_{S_1,I}\}h_{\mathrm{GR}}.$

- **Inspiral waveforms up to Newtonian order in amplitude & 3.5 PN in phase**

- **11 model parameters in GR** $(\log\mathcal{M}, \log\eta, t_c, \phi_c, \log d_L, \chi_s, \chi_a, \boxed{\theta_s, \phi_s, \cos\iota, \psi_p})$ **uniformly random**

+ additional polarization parameter A_{S_1} **, (fiducial values) = 1**

$\Delta A > 1$ ⇔ **Inseparable,** $\Delta A < 1$ ⇔ **Separable**

- **Sources (500) BNSs (equal mass** $1.4M_\odot$ at $z = 0.1$ **)**

- **Single 3G detector such as ET-B, ET-D, CE(desgin sensitivity) and ideal detector**

Result

Table 1: Medians of parameter estimation errors and their correlation coefficients.

	parameter	BNS(ET-B)	BNS(ET-D)	BNS(CE)	BNS(Ideal)
	SNR	57.8	50.7	104	170
ModelTS1	$\Delta\ln d_L$	0.979	0.355	6.67	0.197
	$\Delta\Omega_s[\mathrm{deg}^2]$	490	55.6	72105	7.56
	ΔA_{S1}	1.30	0.459	12.9	0.322
	$C(A_{S1}, \log d_L)$	0.982	0.985	0.911	0.994
	$C(A_{S1}, \cos\iota)$	-0.329	-0.217	-0.095	-0.370

ETB, CE: inseparable,
<u>ETD, Ideal: separable</u>
<u>(degeneracy broken)</u>

non-integer contribution to number of detectors by the Earth's rotation

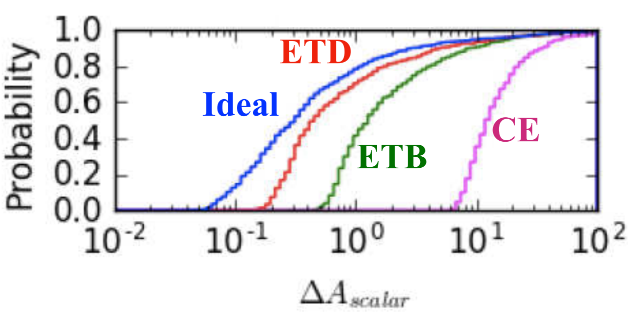

Result

Table 2: Medians of parameter estimation errors and their correlation coefficients.

	parameter	BNS(ET-D) fmin=1Hz	BNS(ET-D) fmin=5Hz	BNS(ET-D) fmin=10Hz
	SNR	50.7	49.8	41.6
ModelTS1	$\Delta \ln d_L$	0.355	0.910	2.31
	$\Delta\Omega_s[\mathrm{deg}^2]$	55.6	184	4308
	ΔA_{S1}	0.459	1.55	4.56
	$C(A_{S1}, \log d_L)$	0.985	0.992	0.965
	$C(A_{S1}, \cos\iota)$	-0.217	-0.277	-0.173

Changing the lower-cutoff frequency

sub-5 Hz region is crucial

ET-like detector :
antenna pattern changing → better resolution

CE-like detector :
better around 100 Hz → high SNR, detection rate

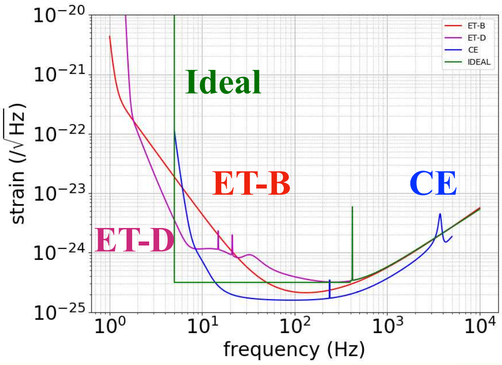

Conclusion and Outlook

- **We study separablity of polarization modes for inspiral GW from CBC and degeneracies among binary parameters with 3G detectors.**

- **A single detector could be used to test polarization of GW due to the effect of the Earth's rotation .** **e.g. ET-D:** $\Delta A = 0.46$

- **Sub-5 Hz region is crucial. ET-like → better resolution, CE-like → high SNR**

- **Developing the pipeline to reconstruct the polarization modes from CBC.**

Thank you for your attention!

Haruka Suzuki
Waseda university

“The Effect of Kozai-Lidov Mechanism on the Period Shift of the Binary Neutron Stars by Gravitational Waves”
(10+5 min.)

[JGRG28 (2018) 110505]

The Effect of Kozai-Lidov Mechanism on the Period Shift of the Binary Neutron Stars by Gravitational Waves

Waseda University D1 **Haruka Suzuki**

Collaborators: Priti Gupta (Waseda)
Hirotada Okawa (YITP,Waseda)
Kei-ichi Maeda (Waseda)

5 November 2018 JGRG28

Introduction

Hulse-Taylor binary

- binary Pulsar discovered in 1974
- orbit is shrinking by emission of GW
  ⇒ first evidence of existence of GW

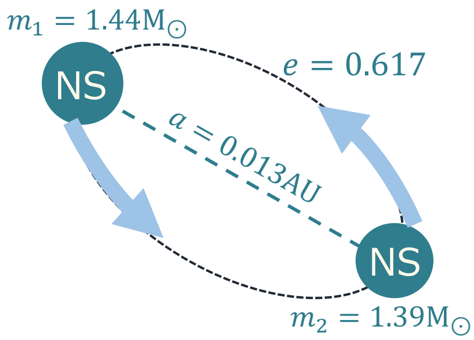

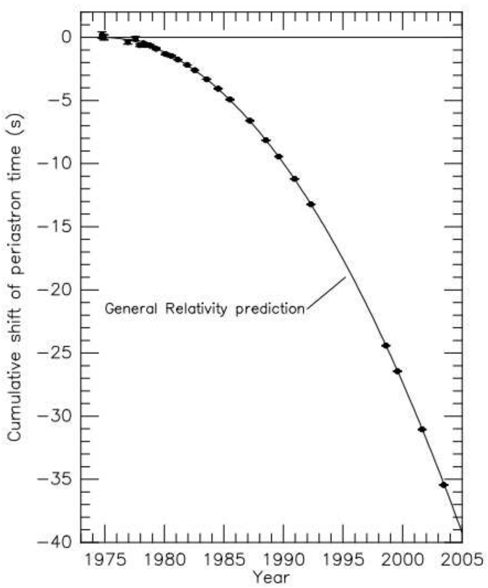

Weisberg & Taylor 2005

Russel Alan Hulse Joseph Hooton Taylor

The Nobel Prize in Physics 1993. NobelPrize.org. Nobel Media AB 2018. Fri. 2 Nov 2018.

Introduction

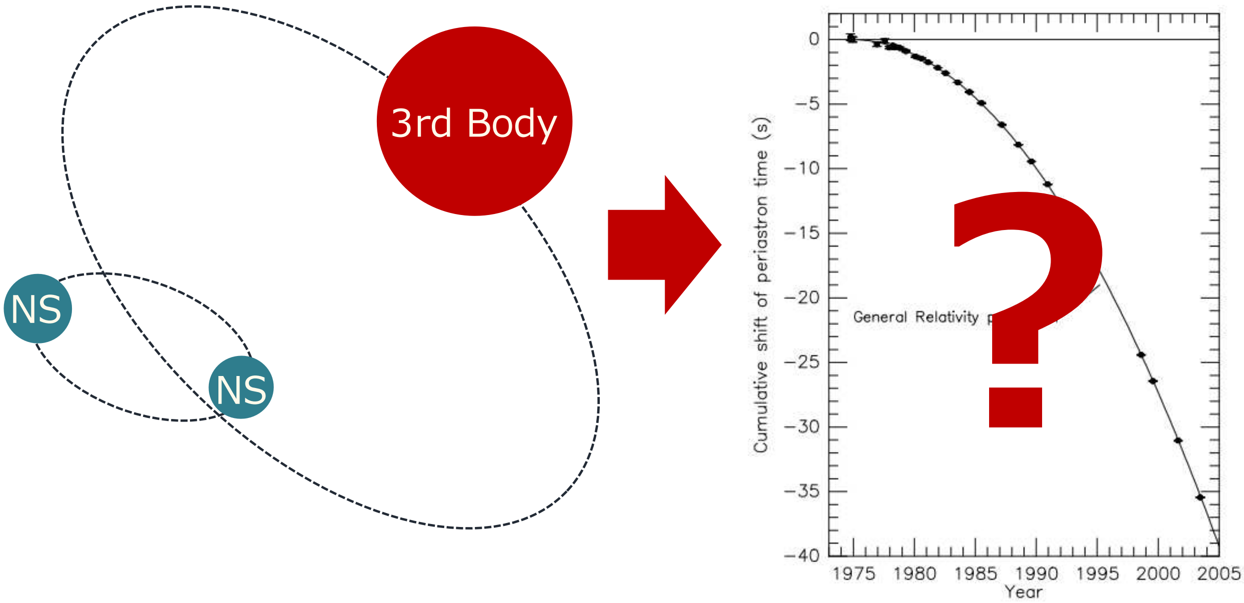

Kozai-Lidov Mechanism

hierarchical triple: binary + tertiary companion

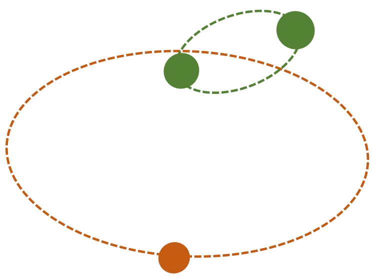

$$\Theta = \sqrt{1 - e_{\rm in}^2}\cos I = const.$$

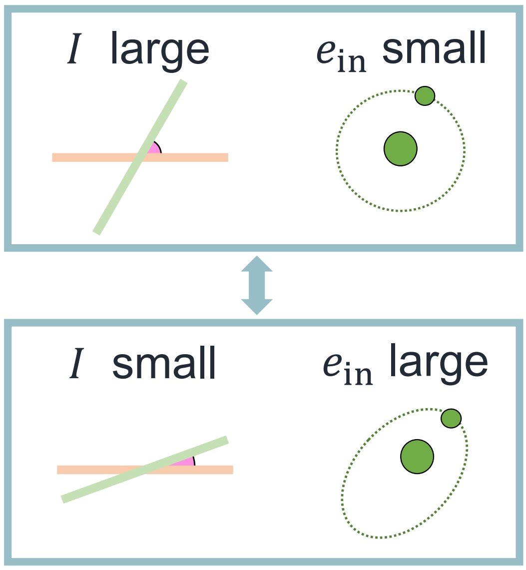

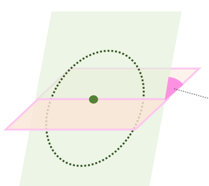

I : relative inclination

e : eccentricity

Kozai-Lidov Mechanism

hierarchical triple: binary + tertiary companion

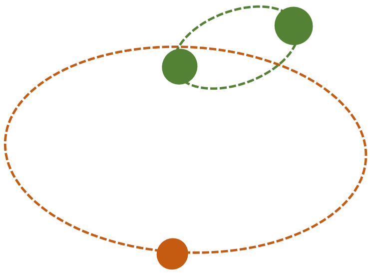

$$\Theta = \sqrt{1 - e_{\rm in}^2} \cos I = const.$$

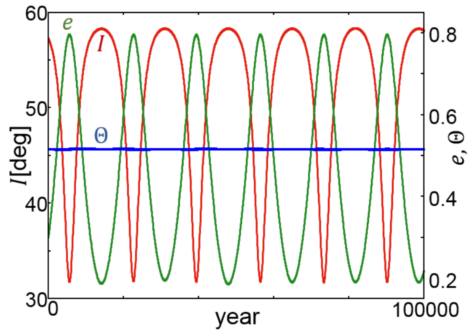

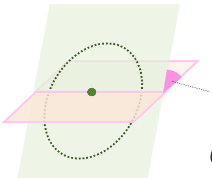

I : relative inclination

e : eccentricity

$$t_{KL} \simeq \frac{16}{15} \frac{a_{\rm out}^3}{a_{\rm in}^{3/2}} \sqrt{\frac{m_1}{G m_3^2}} (1 - e_{\rm out}^2)^{\frac{3}{2}}$$

Antognini 2015

Method

set model → calculate orbital evolution → calculate $\dot{P}$ and Δ_p

Method

set model → calculate orbital evolution → calculate $\dot{P}$ and Δ_p

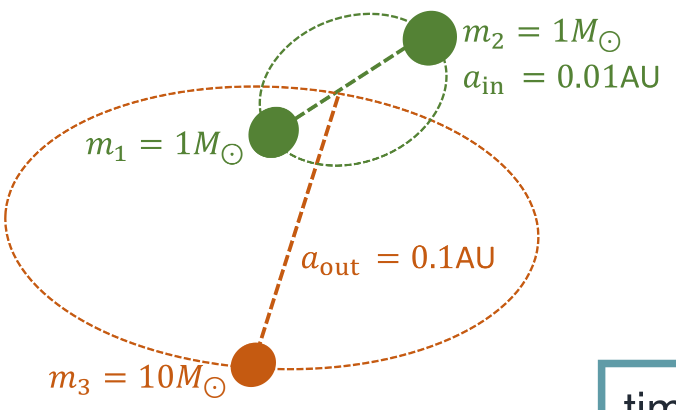

$e_{\rm in,0} = e_{\rm out,0} = 0$

$I_0 = 60^\circ$

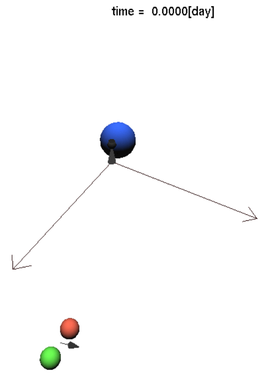

timescale $P_{\rm in} = 0.258$ day

$P_{\rm out} = 3.334$ day

$t_{\rm merger} \sim 10^9$ yr

Method

set model → calculate orbital evolution → calculate $\dot{P}$ and Δ_p

1st order post-Newtonian equation of motion

Einstein-Infeld-Hoffmann equation

$$
\begin{aligned}
\frac{d\boldsymbol{v}_k}{dt} = &-G\sum_{n\neq k} m_n \frac{\boldsymbol{x}_k-\boldsymbol{x}_n}{|\boldsymbol{x}_k-\boldsymbol{x}_n|^3} \\
&\times\left[1-4G\sum_{n'\neq k}\frac{m_{n'}}{|\boldsymbol{x}_k-\boldsymbol{x}_{n'}|}-\sum_{n'\neq n}\frac{m_{n'}}{|\boldsymbol{x}_n-\boldsymbol{x}_{n'}|}\left\{1-\frac{(\boldsymbol{x}_k-\boldsymbol{x}_n)\cdot(\boldsymbol{x}_n-\boldsymbol{x}_{n'})}{2|\boldsymbol{x}_n-\boldsymbol{x}_{n'}|^2}\right\}+v_k^2\right. \\
&\left.+2v_n^2-4\boldsymbol{v}_k\cdot\boldsymbol{v}_n-\frac{3}{2}\left\{\frac{(\boldsymbol{x}_k-\boldsymbol{x}_n)\cdot\boldsymbol{v}_n}{|\boldsymbol{x}_k-\boldsymbol{x}_n|}\right\}^2\right] \\
&-G\sum_{n\neq k} m_n\frac{\boldsymbol{v}_k-\boldsymbol{v}_n}{|\boldsymbol{x}_k-\boldsymbol{x}_n|^3}(\boldsymbol{x}_k-\boldsymbol{x}_n)\cdot(3\boldsymbol{v}_n-4\boldsymbol{v}_k) \\
&-\frac{7}{2}G^2\sum_{n\neq k}\frac{m_n}{|\boldsymbol{x}_k-\boldsymbol{x}_n|}\sum_{n'\neq n}\frac{m_{n'}(\boldsymbol{x}_n-\boldsymbol{x}_{n'})}{|\boldsymbol{x}_n-\boldsymbol{x}_{n'}|}
\end{aligned}
$$

integrate with 6th order Implicit Runge-Kutta method

※no GW back reaction

Method

set model → calculate orbital evolution → calculate $\dot{P}$ and Δ_p

convert $\boldsymbol{r}, \boldsymbol{v}$ into orbital elements $(a, e, i, \ldots)$

↓

take average for inner orbit $(\bar{a}, \bar{e})$

↓

calculate period shift of binary $\dot{P}$

$$\dot{P} = -\frac{192\pi}{5}\bar{a}_{\rm in}^{-\frac{5}{2}}\{G(m_1+m_2)\}^{\frac{1}{2}}\frac{G^2 m_1 m_2}{c^5}\frac{1}{(1-\bar{e}_{\rm in}^2)^{\frac{7}{2}}}\left(1+\frac{73}{24}\bar{e}_{\rm in}^2+\frac{37}{96}\bar{e}_{\rm in}^4\right)$$

Peters & Mathews 1963

↓

get cumulative shift of periastron time Δ_p

$$\Delta_p = \frac{\dot{P}}{2P}t^2$$

Result

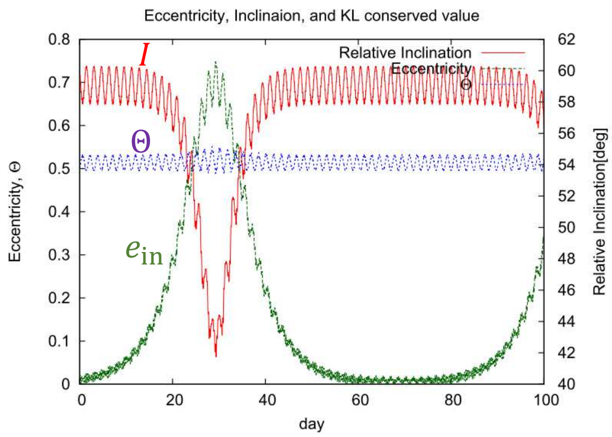

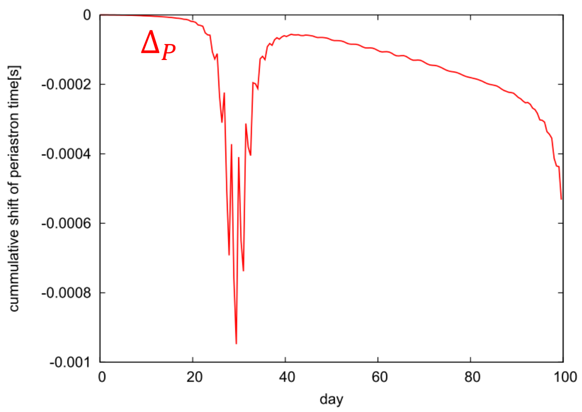

Result

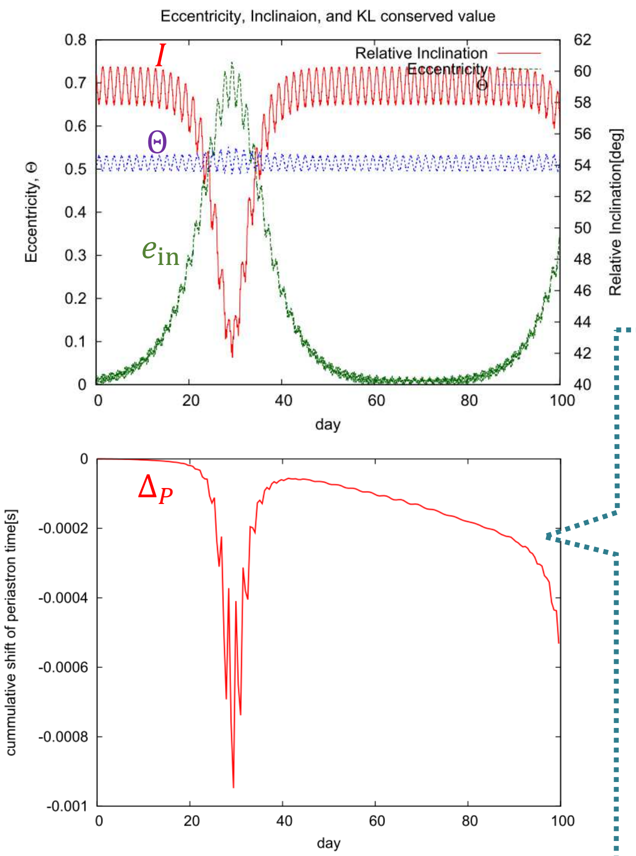

cf.) same model but no Kozai case
$(I_0 = 0)$

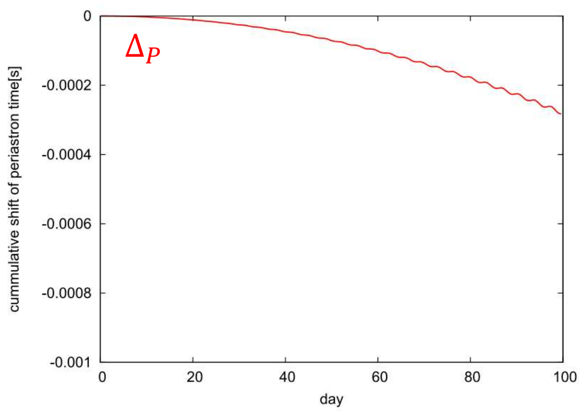

Result

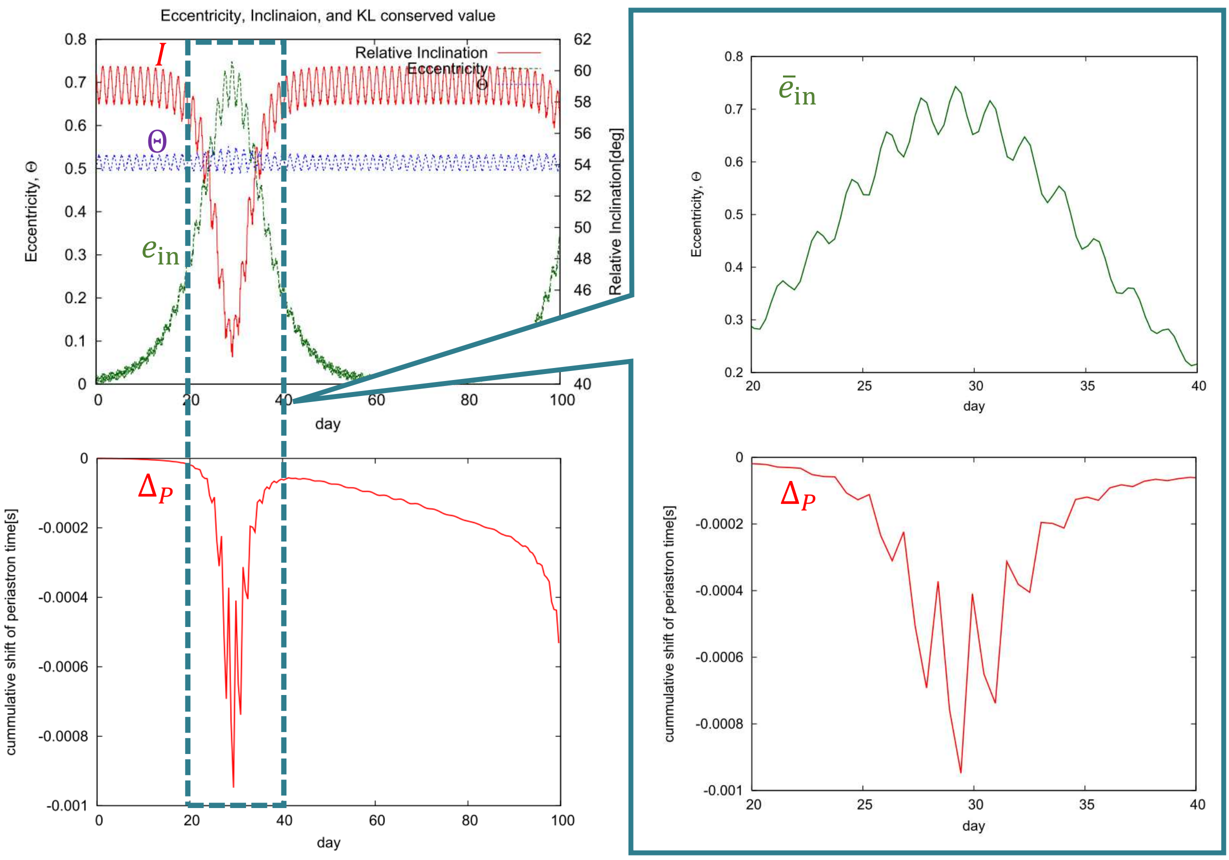

Summary and Future Work

- Kozai-Lidov effect can be seen in the time evolution of the cumulative shift of periastron time
- The oscillation timescales of the cumulative shift of periastron time correspond to the Kozai-Lidov timescale and the period of the outer orbit

- Now we are doing parameter search (detectable range) and analysis of the wave form
- calculating orbital evolution with back reaction is future work

Asuka Ito
Kobe University

“A strategy for detecting the bispectrum of stochastic gravitational waves”

(10+5 min.)

[JGRG28 (2018) 110506]

A strategy for detecting the bispectrum of stochastic GWs

Asuka Ito (Kobe Univ. Japan)

with Tsuneto Makoto, Toshifumi Noumi, Jiro Soda

in preparation

JGRG2018

Talk plan

1. Introduction and motivation
   - Stochastic GWs and its bispectra

2. A detection method for the bispectrum of stochastic GWs with gravitational wave detectors

3. Application to pulsar timing arrays

Stochastic GWs

The stochastic GWs are going through us randomly;
from all directions, with all frequencies.

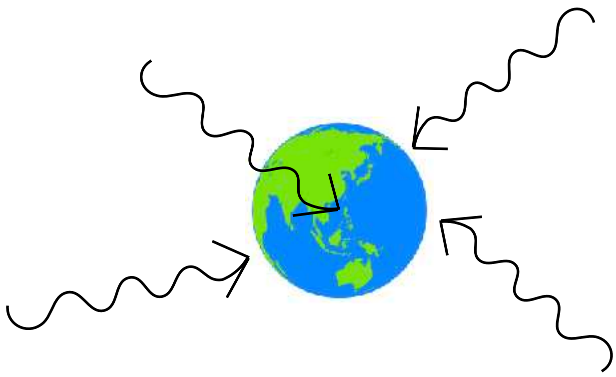

The main origin is the primordial GW.

The primordial GW is a remnant from the early universe.

→ It carries the information about the early universe!

Stochastic GWs

Since the stochastic GW is "stochastic", we must treat it statistically.

→ The observables are statistics: power spectra, bispectra, etc.

tell us the energy scale
of the inflation

tell us the detail of the
inflationary models;
such as interactions between
the graviton and other particles

Not only Observing the power spectrum, but also the bispectrum
is very important to distinguish the overflowing inflationary models!

The bispectrum

Expanding the GW in Fourier space:

$$\boxed{h_{ij}(t,\vec{x}) = \sum_A \int_{-\infty}^{\infty} \mathrm{d}f \int \mathrm{d}\hat{\Omega}\, e^{\mathrm{i}2\pi f(t-\hat{\Omega}\cdot\vec{x})}\, h_A(f,\hat{\Omega}) e^A_{ij}(\hat{\Omega})}$$

For the Fourier coefficient of the GW, the bispectrum is defined by

$$\boxed{< h_A(f,\hat{\Omega}) h_{A'}(f',\hat{\Omega}') h_{A''}(f'',\hat{\Omega}'') >= B_{AA'A''}(f,f',f'')\underline{\delta(f\hat{\Omega}+f'\hat{\Omega}'+f''\hat{\Omega}'')}}$$

Forming the momentum triangle

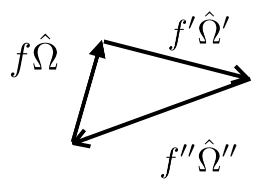

The shape of the Bispectrum

The shape of the bispectrum depends on the inflationary model,
Equilateral, squeezed, folded, etc.

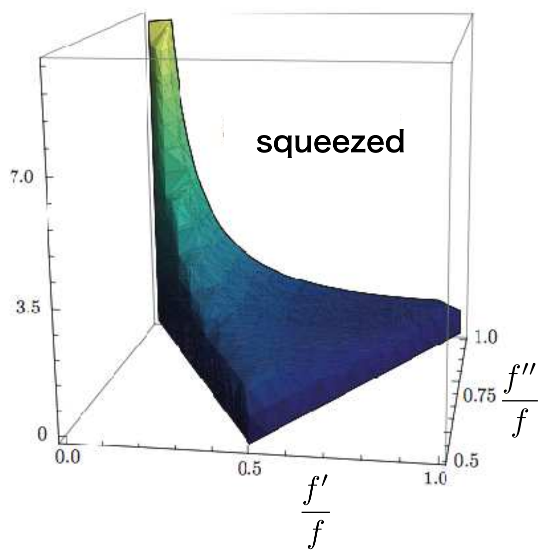

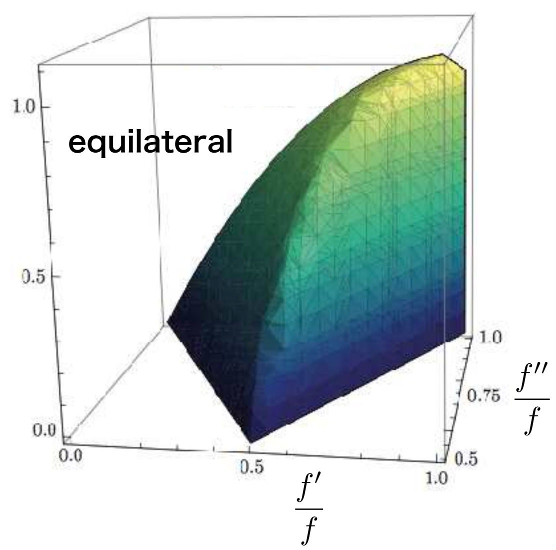

Observing the shape of the bispectrum is
a key to distinguish the inflationary models!

Talk plan

1. Introduction and motivation
   - Stochastic GWs and its bispectra

2. A detection method for the bispectrum of stochastic GWs with gravitational wave detectors

3. Application to pulsar timing arrays

GW signal in detectors

In general, a GW signal can be described as

$$\boxed{s(t) = h_{ij}(t, \boldsymbol{x}) D^{ij}}$$

h_{ij} is GWs : $ds^2 = -dt^2 + (\eta_{ij} + h_{ij}) dx^i dx^j$

D_{ij} is called the detector tensor, which contain the information about the detector

$$\boxed{< s(t)s(t) >=< \underline{h_{ij}(t, \boldsymbol{x}) h_{kl}(t, \boldsymbol{x}')} > D^{ij} D^{kl}}$$

$\downarrow$ Fourier transformation

$\boxed{\text{power spectrum}}$

Three point correlation

The three point correlation :

$$< s(t)s(t)s(t) >= \int\int\int df df' df'' \int\int\int d\hat{\Omega} d\hat{\Omega}' d\hat{\Omega}''$$
$$\times \sum_{A,A',A''} < h_A(f,\hat{\Omega}) h_{A'}(f',\hat{\Omega}') h_{A''}(f'',\hat{\Omega}'') > F^A(\hat{\Omega}) F^{A'}(\hat{\Omega}') F^{A''}(\hat{\Omega}'')$$

$$\left(F^A(\hat{\Omega}) \equiv e^A_{ij} D_{ij} \right)$$

Substituting the definition of bispectra

$$< h_A(f,\hat{\Omega}) h_{A'}(f',\hat{\Omega}') h_{A''}(f'',\hat{\Omega}'') >= B_{AA'A''}(f,f',f'')\delta(f\hat{\Omega} + f'\hat{\Omega}' + f''\hat{\Omega}'')$$

$$< s(t)s(t)s(t) >= \int\int\int df df' df'' \int\int\int d\hat{\Omega} d\hat{\Omega}' d\hat{\Omega}''$$
$$\times \sum_{A,A',A''} B_{AA'A''}(f,f',f'')\delta(f\hat{\Omega} + f'\hat{\Omega}' + f''\hat{\Omega}'') F^A(\hat{\Omega}) F^{A'}(\hat{\Omega}') F^{A''}(\hat{\Omega}'')$$

The shape of the bispectrum is degenerate (integrated)

However the shape is very important to probe the inflationary models.

How to resolve the degeneracy?

Three point correlation

Let us try to correlate the three signals as below:

$$S_{123} = \iiint_{-T/2}^{T/2} \mathrm{d}t_1 \mathrm{d}t_2 \mathrm{d}t_3 \; s_1(t_1) s_2(t_2) s_3(t_3) Q(t_1, t_2, t_3)$$

where T is the observation time and $Q(t_1, t_2, t_3)$ is a filter function

Now we take $\boxed{Q(t_1, t_2, t_3) = Q(at_1 + bt_2 + ct_3)}$

Moving on to the Fourier space,

$$S_{123} = \iiint_{-T/2}^{T/2} \mathrm{d}t_1 \mathrm{d}t_2 \mathrm{d}t_3 \iiiint_{-\infty}^{\infty} \mathrm{d}f_1 \mathrm{d}f_2 \mathrm{d}f_3 \mathrm{d}f \; \tilde{s}_1(f_1) \tilde{s}_2(f_2) \tilde{s}_3(f_3) \tilde{Q}\;(f)$$
$$\times e^{-2\pi i f_1 t_1} e^{-2\pi i f_2 t_2} e^{-2\pi i f_3 t_3} e^{2\pi i f (at_1 + bt_2 + ct_3)} .$$

Three point correlation

$$S_{123} = \iiint_{-T/2}^{T/2} \mathrm{d}t_1 \mathrm{d}t_2 \mathrm{d}t_3 \iiiint_{-\infty}^{\infty} \mathrm{d}f_1 \mathrm{d}f_2 \mathrm{d}f_3 \mathrm{d}f \; \tilde{s}_1(f_1)\tilde{s}_2(f_2)\tilde{s}_3(f_3)\tilde{Q}\;(f) \times e^{-2\pi i f_1 t_1} e^{-2\pi i f_2 t_2} e^{-2\pi i f_3 t_3} e^{2\pi i f(at_1+bt_2+ct_3)} .$$

Let us focus on frequencies which satisfy $\frac{1}{T} \ll f$,

Then we can approximately take $T \to \infty$.

Doing the time integrations, we obtain

$$S_{123} = \iiiint_{-\infty}^{\infty} \mathrm{d}f_1 \mathrm{d}f_2 \mathrm{d}f_3 \mathrm{d}f \; \tilde{s}_1(f_1)\tilde{s}_2(f_2)\tilde{s}_3(f_3)\tilde{Q}(f)\delta(f_1 - af)\delta(f_2 - bf)\delta(f_3 - cf)$$

Finally we arrive at

$$S_{123} = 2\int_0^{\infty} \mathrm{d}f \; \tilde{s}_1(af)\tilde{s}_2(bf)\tilde{s}_3(cf)\tilde{Q}(f)$$

Three point correlation

$$S_{123} = 2\int_0^{\infty} \mathrm{d}f \; \tilde{s}_1(af)\tilde{s}_2(bf)\tilde{s}_3(cf)\tilde{Q}(f)$$

Substituting the relation $\tilde{s}(f,\hat{\Omega}) = -\int d\hat{\Omega} \sum_A h_A(f,\hat{\Omega})F^A(\hat{\Omega})$

$$< S_{123} >= -2\int d\hat{\Omega} d\hat{\Omega}' d\hat{\Omega}'' \int df \sum_{A,A',A''} \underline{< h_A(af,\hat{\Omega}) h_{A'}(bf,\hat{\Omega}') h_{A''}(cf,\hat{\Omega}'') >} F^A(\hat{\Omega})F^{A'}(\hat{\Omega}')F^{A''}(\hat{\Omega}'')$$

$$= \underline{B_{AA'A''}(af,bf,cf)\delta(af\hat{\Omega} + bf\hat{\Omega}' + cf\hat{\Omega}'')}$$

(taking ensemble average)

A particular configuration of
the momentum triangle is extracted!

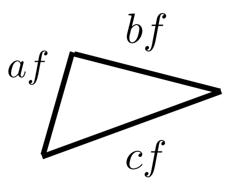

Three point correlation

- $< s_1(t_1)s_2(t_2)s_3(t_3) >$ $\longrightarrow$ **the shape is degenerate (integrated)**

- $$S_{123} = \int\int\int_{-T/2}^{T/2} dt_1 dt_2 dt_3 s_1(t_1)s_2(t_2)s_3(t_3)Q(at_1 + bt_2 + ct_3)$$

We can extract a particular configuration of the momentum triangle

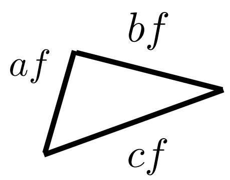

Talk plan

1. Introduction and motivation

   - Stochastic GWs and its bispectra

2. A detection method for the bispectrum of stochastic GWs with gravitational wave detectors

3. Application to pulsar timing arrays

Angular integration with three pulsars

There are about 100 millisecond pulsars which are being observed.
We can choose any three pulsars ideally.

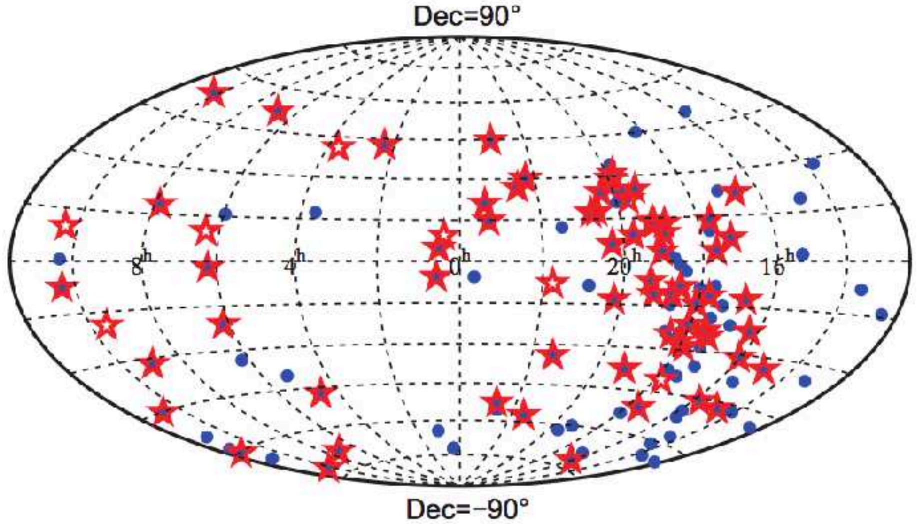

Ref: “Gravitational wave astronomy: the current status,” arxiv: 1602.02872

Application to pulsar

$$< S_{123} >= -2 \sum_{A,A',A''} \int df\, B_{AA'A''}(af,bf,cf) \int d\hat{\Omega} d\hat{\Omega}' d\hat{\Omega}'' \delta(af\hat{\Omega}+bf\hat{\Omega}'+cf\hat{\Omega}') F^{A}(\hat{p}_1,\hat{\Omega}) F^{A'}(\hat{p}_2,\hat{\Omega}') F^{A''}(\hat{p}_3,\hat{\Omega}'')$$

- depends on the inflationary model
- not depends on the inflationary model
- calculable to each $(a, b, c, \hat{p}_1, \hat{p}_2, \hat{p}_3, A, A', A'')$

The sensitivity depends on the shape of momentum triangle (a, b, c)
and the relative position of the pulsars $(\hat{p}_1, \hat{p}_2, \hat{p}_3)$

→ For instance, what is the configuration of three pulsars to maximize the sensitivity of $< S_{123} >$

Angular integration

co-aligned

$(a, b, c, \hat{p}_1, \hat{p}_1, \hat{p}_1, +, +, +)$

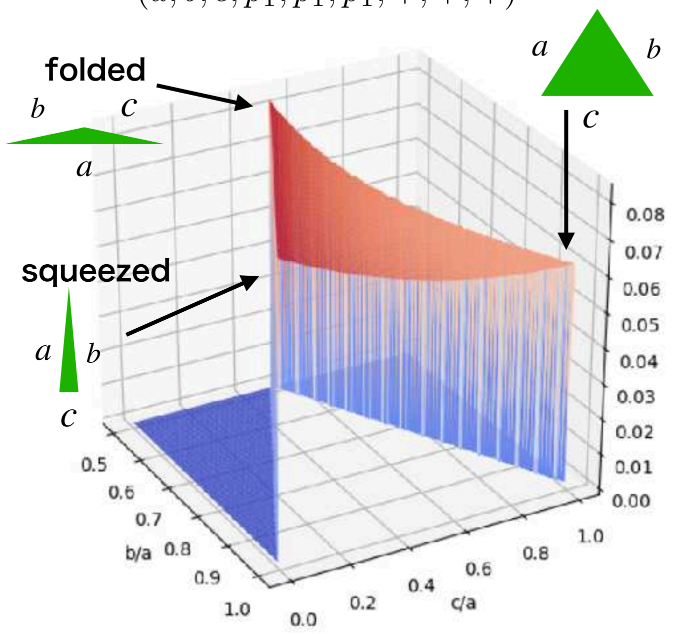

anti-aligned

$(a, b, c, \hat{p}_1, -\hat{p}_1, -\hat{p}_1, +, +, +)$

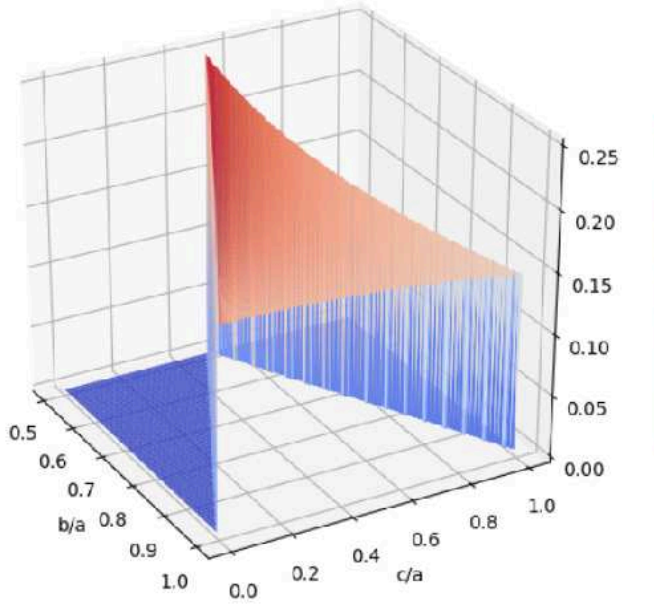

The pure sensitivity for $(+, +, +)$ mode can be increased by 3 times in the anti-aligned configuration compared with the co-aligned case!

Summary

- The bispectrum of the stochastic GWs is a clue of the early universe

- We suggested a method to detect the bispectrum, where a filter function $Q(at_1 + bt_2 + ct_3)$ enables us to extract a particular configuration of the bispectrum

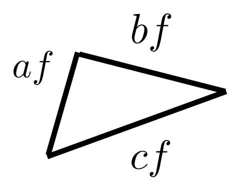

- The method was applied to pulsar timing arrays
  - We carried out the angular integration which does not depend on inflationary models
  - We found the configuration of pulsars which maximize the pure sensitivity ex) $(+, +, +)$ → anti-aligned

- Extension to the interferometer is also interesting and in preparation

Residual

The residual is written by $$\boxed{s(t) = h_{ij}(t, \boldsymbol{x}) D^{ij}}$$

where $$\boxed{D_{ij} = \frac{1}{2} \frac{\hat{p}^i \hat{p}^j}{1 + \hat{\Omega} \cdot \hat{p}}}$$

$\hat{p}$: the direction of a pulsar from the earth

$\hat{\Omega}$: the direction of a gravitational wave

Expanding the GW in Fourier space, the residual becomes

$$\boxed{s(t) = \int_{-\infty}^{\infty} \mathrm{d}f \int \mathrm{d}\hat{\Omega} \sum_A h_A(f, \hat{\Omega}) \; e^A_{ij} \frac{1}{2} \frac{\hat{p}^i \hat{p}^j}{1 + \hat{\Omega} \cdot \hat{p}}}$$

A relation

$$\begin{cases} h_{ij}(t,\vec{x}) = \sum_A \int \frac{d^3k}{(2\pi)^{3/2}} \tilde{h}^{(A)}(t,\vec{k}) e^{-i\vec{k}\vec{x}} e^{(A)}_{ij}(\hat{k}) \\ h_{ij}(t,\vec{x}) = \sum_A \int_{-\infty}^{\infty} \mathrm{d}f \int \mathrm{d}\hat{\Omega}\, e^{\mathrm{i}2\pi f(t-\hat{\Omega}\cdot\vec{x})}\, h_A(f,\hat{\Omega}) e^{A}_{ij}(\hat{\Omega}) \end{cases}$$

$$\boxed{< \tilde{h}^{(A)}(0,\vec{k})\tilde{h}^{(A')}(0,\vec{k}')\tilde{h}^{(A'')}(0,\vec{k}'') >= \frac{2^{9/2}\pi^{3/2}}{k^2k'^2k''^2} < h_A(f,\hat{\Omega})h'_A(f',\hat{\Omega}')h''_A(f'',\hat{\Omega}'') >}$$

Signal to noise ratio

$$\boxed{SNR = \frac{4T\int df \sum_{A,A',A''} B_{A,A',A''}(af,bf,cf)\tilde{Q}(f)(4\pi)^2\Gamma^{AA'A''}(a,b,c,\hat{p}_1,\hat{p}_2,\hat{p}_3)}{\left(\int df \tilde{Q}(f)^2 S_n^{(1)}(af)S_n^{(2)}(bf)S_n^{(3)}(cf)\right)^{1/2}}}$$

Then the optimal filter function is

$$\boxed{\tilde{Q}(f) = \frac{\sum_{A,A',A''} B_{A,A',A''}(af,bf,cf)\Gamma^{AA'A''}(a,b,c,\hat{p}_1,\hat{p}_2,\hat{p}_3)}{S_n^{(1)}(af)S_n^{(2)}(bf)S_n^{(3)}(cf)}}$$

R and L basises

$$\boxed{e_{ij}^{R} = \frac{e_{ij}^{+} + ie_{ij}^{\times}}{\sqrt{2}} , \quad e_{ij}^{L} = \frac{e_{ij}^{+} - ie_{ij}^{\times}}{\sqrt{2}} .}$$

$$h_{ij} \equiv h_R e_{ij}^{R} + h_L e_{ij}^{L} = h_+ e_{ij}^{+} + h_\times e_{ij}^{\times} ,$$

$$\boxed{h_R = \frac{h_+ - ih_\times}{\sqrt{2}}, \quad h_L = \frac{h_+ + ih_\times}{\sqrt{2}} .}$$

Invited lecture 14:00–14:45

[Chair: Misao Sasaki]

Mark Hindmarsh

University of Sussex

“Gravitational waves from phase transitions in the early Universe”

(40+10 min.)

[JGRG28 (2018) 110507]

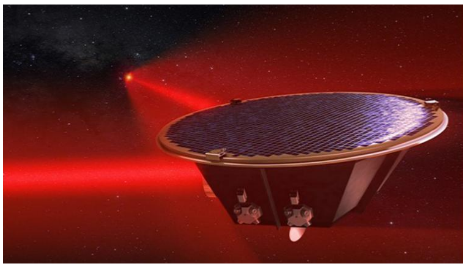

Gravitational waves from phase transitions in the early Universe

Mark Hindmarsh
Department of Physics & Astronomy
University of Sussex
and
Helsinki Institute of Physics & Dept of Physics, University of Helsinki

JGRG 28
Rikkyo U, Tokyo
5. marraskuuta 2018

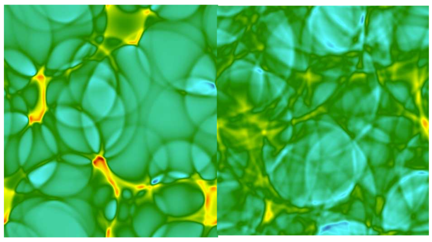

GW150914 strain and frequency spectrum

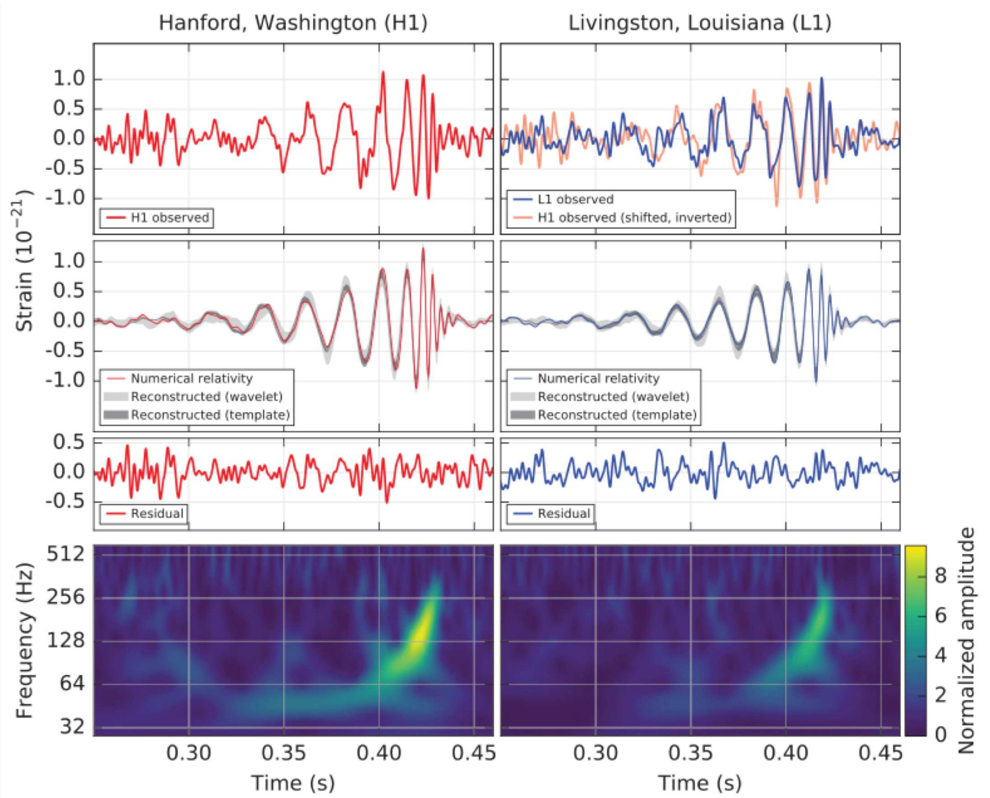

Detecting gravitational waves

- Compare distances between test masses in two directions with laser interferometer
- Strain ≈ Metric perturbation

$$\frac{\Delta l}{l} = \frac{1}{2}(h_{xx} - h_{yy})$$

- Sensitivity: $h \approx 10^{-21}$ @ 10^2 Hz
-

Name	Location	Arm length
GEO	Germany	600m
(a)LIGO	USA (2)	4km
(a)VIRGO	Italy	3km
KAGRA	Japan	3km
LIGO-India	India	4km

- Future: Einstein Telescope

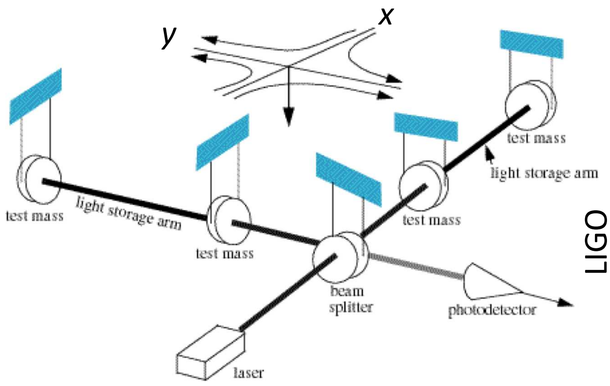

LIGO

LIGO

Gravitational wave astronomy

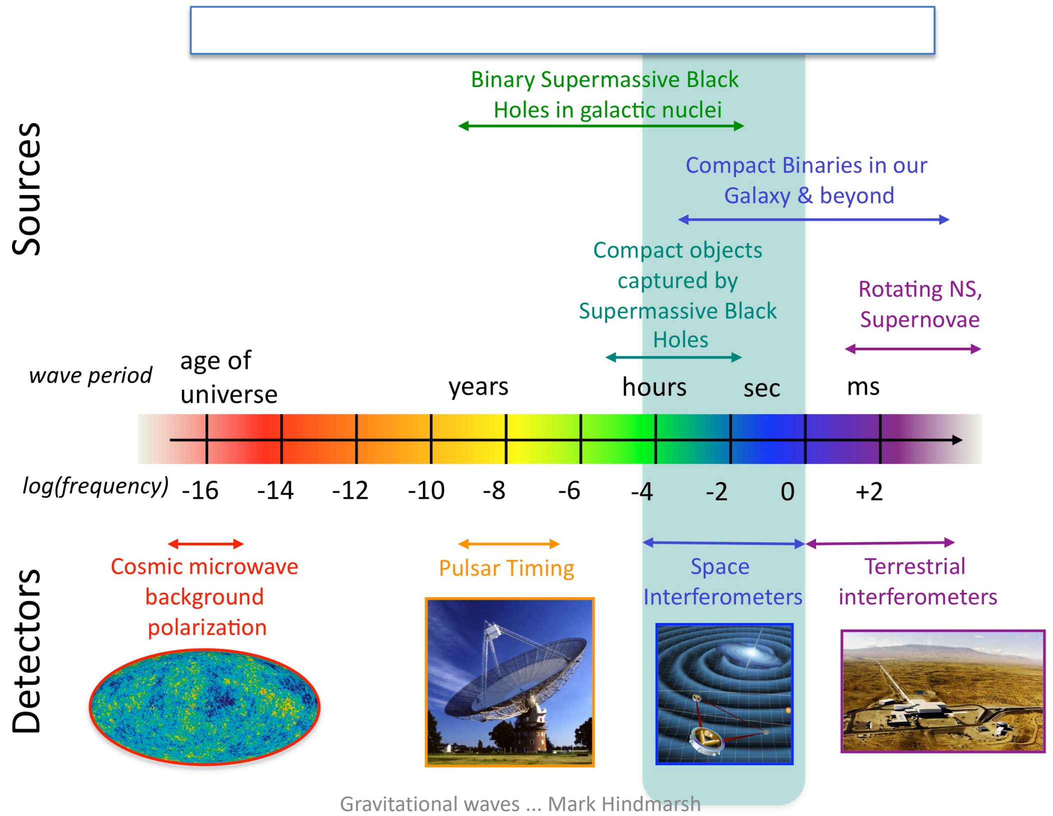

NASA

Gravitational wave cosmology

- Gravitational waves are hard to observe
- Once made, not absorbed by intervening matter
- Complete history of the universe visible in GWs

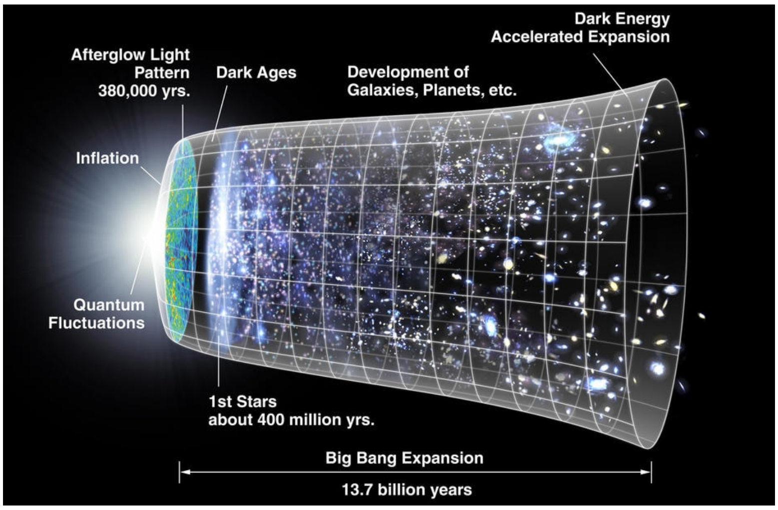

Space-based gravitational wave detectors

- Approved:
  - LISA (ESA L3 2034)
- LISA sensitivity
  - Peak: 10^{-3} - 10^{-2} Hz
  - $l \approx 10^{9}$ m
  - $\Delta l \approx 10^{-12}$ m
  - $h \approx 10^{-21}$
- Proposed:
  - DECIGO (Japan, ?)
  - Taiji (China, ?)
  - Big Bang Observer (USA, ?)

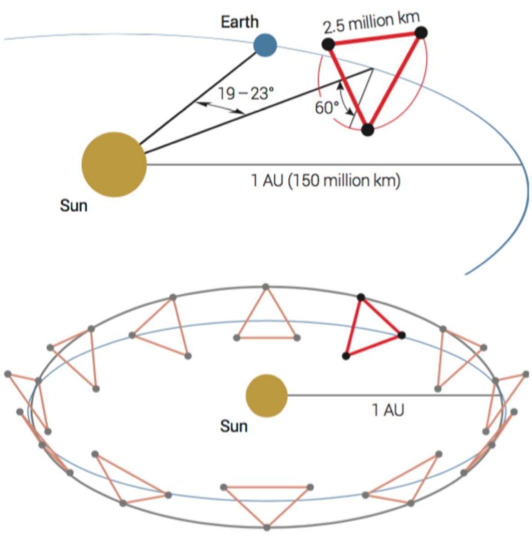

LISA

See talk by J. Gair, Wed 9:00 am

Generating gravitational waves

- Gravitational wave: a propagating shear in space

$$g_{ij} = \delta_{ij} + h_{ij}$$

- Classical source of gravitational waves: shear stress

$$\Box h_{ij} = -(16\pi G)S_{ij}$$

- Quantum production during inflation
  - c.f. Hawking radiation by black holes

  Gibbons, Hawking (1977), Starobinsky (1979)
- Equilibrium thermal production negligible

  Laine, Ghiglieri (2016)
- Departure from equilibrium required
  - e.g. phase transition

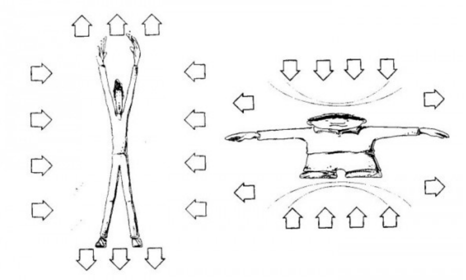

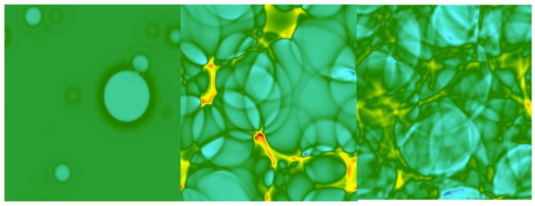

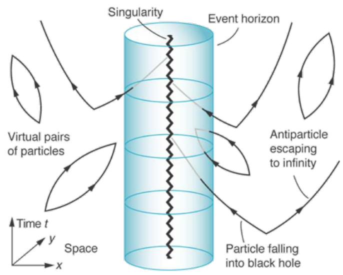

Gravitational waves from the early universe

- Events at time *t* generate waves with minimum frequency $f \approx 1/t$ (Hubble rate)
- Redshifted to a frequency now: $f_0 = (a(t)/a(t_0))f$
- Minimum frequencies (redshifted Hubble rates):

Event	Time/s	Temp/GeV	f_0/Hz
QCD phase transition	10^{-3}	0.1	10^{-8}
Higgs phase transition	10^{-11}	100	10^{-5}
?	10^{-25}	10^{9}	100 LIGO
End of inflation	$\geq 10^{-36}$	$\leq 10^{16}$	$\leq 10^{8}$

- Inflation and topological defects: waves on all scales

Measures of gravitational waves

- Unit vectors along interferometer arms: *l*$_i$ *m*$_i$
- Fourier transform of strain

$$\tilde{h}(f) = \frac{1}{2}\int_{-\infty}^{\infty} dt\, e^{-i2\pi f t} h_{ij}(l_i l_j - m_i m_j)$$

- One-sided power spectrum $S_h(f)$ ($f > 0$)

$$\langle \tilde{h}(f)\tilde{h}^*(f')\rangle = \frac{1}{2} S_h(f)\delta(f - f')$$

  – Characteristic strain (dimensionless) $h_c(f) = \sqrt{f S_h(f)}$
  – Root power spectral density ($\sqrt{\mathrm{Hz}^{-1}}$) $h(f) = \sqrt{S_h(f)}$
  – Energy density per logarithmic frequency interval:

$$\frac{d\rho_{\rm gw}}{d\ln f} = \frac{\pi}{G} f^3 S_h(f)$$

Measures of gravitational waves

- Unit vectors along interferometer arms: *l*$_i$ *m*$_i$
- Fourier transform of strain

$$\tilde{h}(f) = \frac{1}{2}\int_{-\infty}^{\infty} dt\, e^{-i2\pi f t} h_{ij}(l_i l_j - m_i m_j)$$

- One-sided power spectrum $S_h(f)$ ($f > 0$)

$$\langle \tilde{h}(f)\tilde{h}^*(f')\rangle = \frac{1}{2} S_h(f)\delta(f - f')$$

  – Characteristic strain (dimensionless) $h_c(f) = \sqrt{f S_h(f)}$
  – Root power spectral density ($\sqrt{\mathrm{Hz}^{-1}}$) $h(f) = \sqrt{S_h(f)}$
  – Fractional energy density per log frequency interval:

$$\frac{d\Omega_{\rm gw}}{d\ln f} = \frac{1}{\rho_{\rm tot}}\frac{d\rho_{\rm gw}}{d\ln f} = \frac{8\pi^2}{3H^2} f^3 S_h(f)$$

Cosmological gravitational waves

- Fractional energy density in GWs

$$\frac{d\Omega_{\rm gw}}{d\ln f} = \frac{8\pi^2}{3H^2} f^3 S_h(f)$$

- Hence

$$h_c(f) = \sqrt{\frac{3}{8\pi^2}\Omega_{\rm gw}}\left(\frac{H}{f}\right) \qquad H \simeq 2\times 10^{-18}\,{\rm s}^{-1}$$

- Higher frequency = smaller strain (given $\Omega_{\rm gw}$)

$$h_c \simeq 0.4\sqrt{\Omega_{\rm gw}}\times 10^{-20}\,(f/100\,{\rm Hz})^{-1}$$

- Big Bang Nucleosynthesis: $\Omega_{\rm gw}(t_{\rm BBN}) \lesssim 10^{-6}$
- LIGO: $\Omega_{\rm gw}(20 - 86\,{\rm Hz}) < 1.7\times 10^{-7}$ (95 % CL)

Gravitational wave spectrum

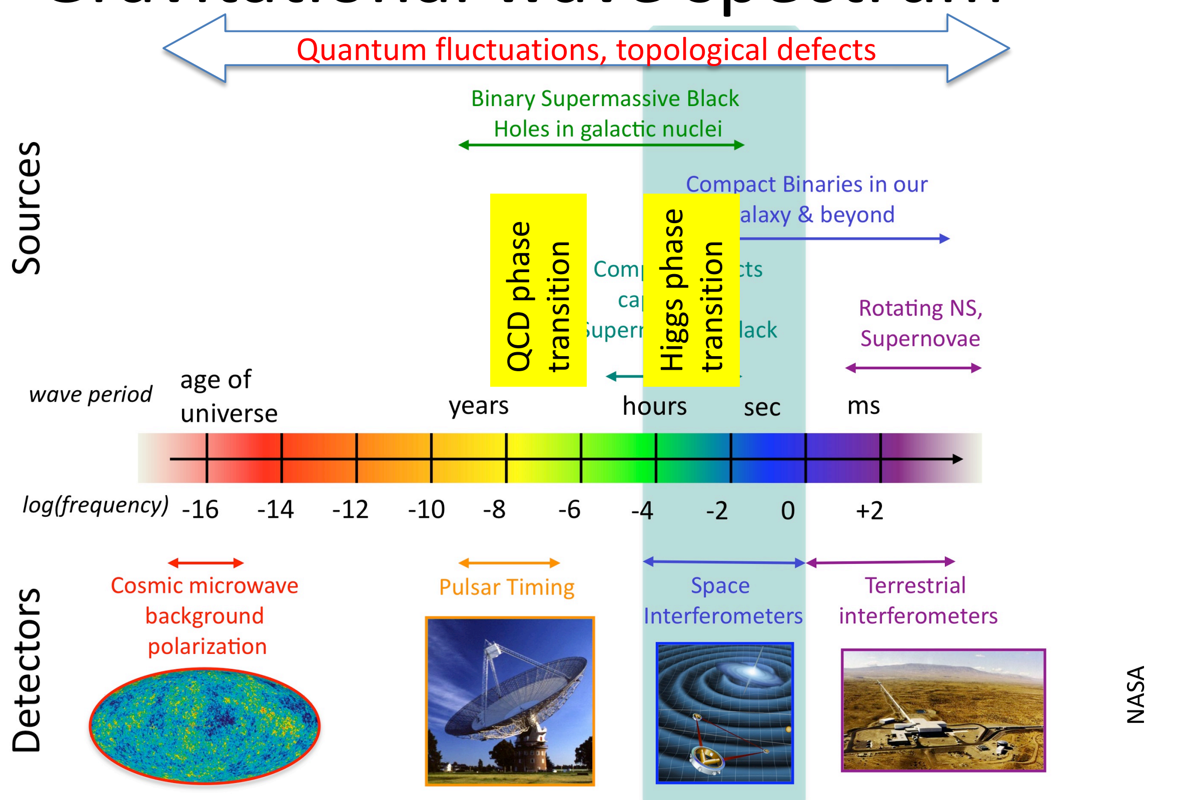

Phase transitions in the early Universe

- At very high temperatures and pressures, the state of matter in the Universe changes
  - Tc ~ 100 MeV quark-gluon plasma
  - Tc ~ 100 GeV all Standard model particles massless
  - Tc >> 100 GeV ???
- Departures from equilibrium and homogeneity (shear stress)
  - First order phase transition: relativistic condensation or `fizz'
    Steinhardt (1982)
  - Formation of topological defects
    Kibble (1976)

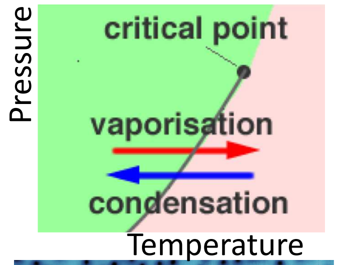

Supercritical fluid

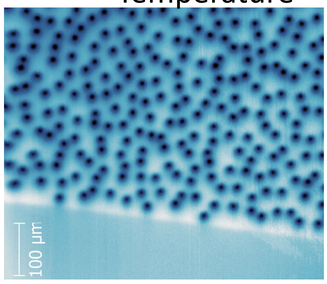

Abrikosov vortices

QCD phase transition

- QCD: rich phase diagram
- Universe: $n_B/n_\gamma \approx 6.1 \times 10^{-10}$
- Behaviour at low chemical potential well-established by lattice QCD Borsanyi et al (2016)
- Transition from QGP to hadronic phase is a cross-over

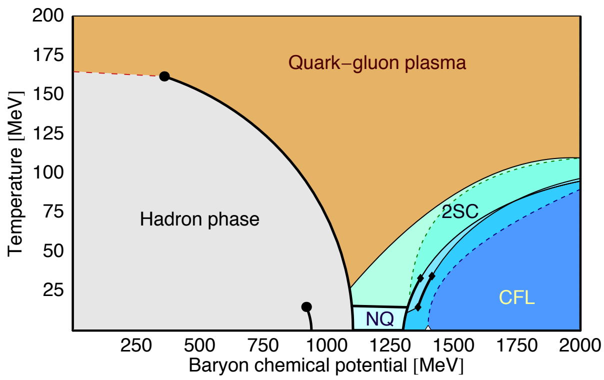

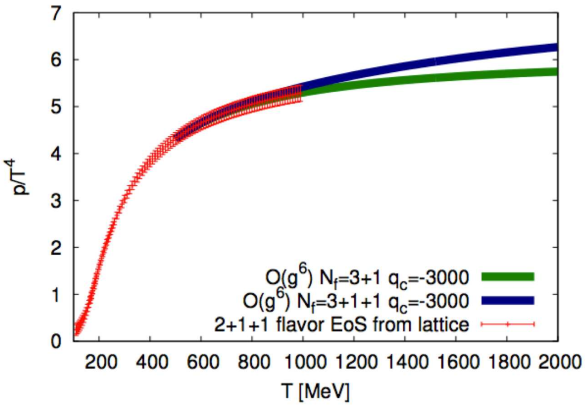

Borsanyi et al 2016

Higgs transition and beyond

- Low temperature:
  - Higgs phase
  - Higgs field is "on"
  - particles have mass
- High temperature:
  - symmetric phase
  - Higgs field is "off"
  - particles have no mass
- Phase transition at $T_c = 10^{15}$ K, t = 10 ps
- Standard Model transition
  - like a supercritical fluid Kajantie et al (1996)
  - no topological defects
- Beyond the Standard Model
  - may be first order
  - e.g. 2 Higgs doublets
  - Extra singlet
  - …

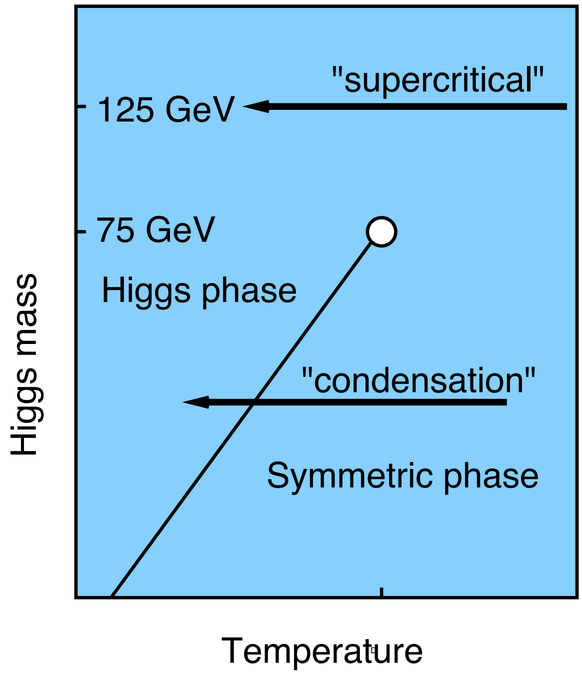

First order phase transitions

- 1st order transition proceeds by nucleation of bubbles of Higgs phase
- Expanding bubbles generate pressure waves in hot fluid
- Shear stresses - detectable gravitational waves?

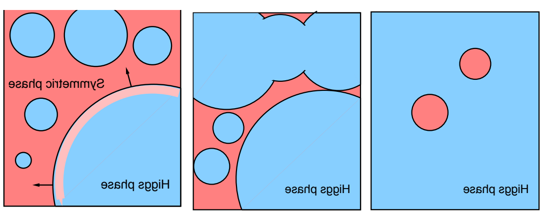

Steinhardt (1982); Gyulassy et al (1984); Witten (1984); Enqvist et al (1992)

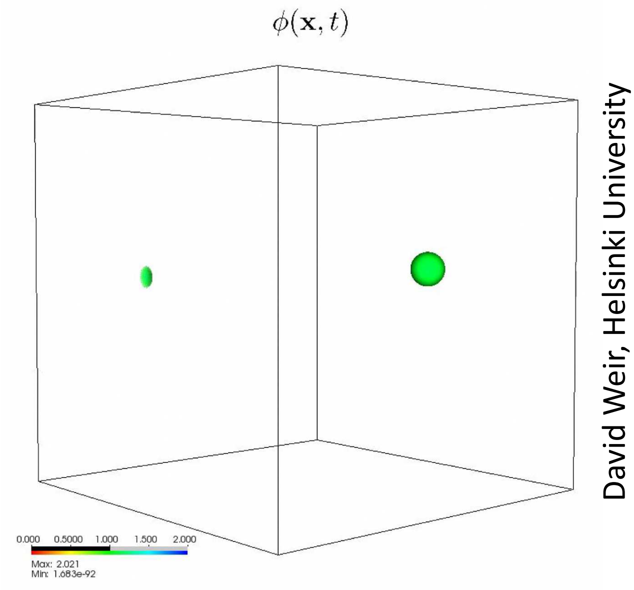

Scalar field

Hindmarsh, Huber, Rummukainen, Weir (2013)
Scalar only: Child, Giblin (2012)

GWs from first order phase transitions

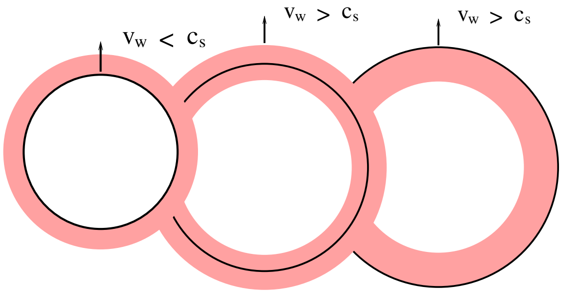

- Parametrise transition:
  - α = ("Latent heat")/(Thermal energy)
  - β = transition rate parameter
  - v_w = Bubble wall speed
  - H_n = Hubble rate at nucleation
- Derived parameters:
  - R_* = mean bubble separation (~v_w/β)
  - K = fluid kinetic energy fraction (depends on α, v_w)
    Steinhardt '84
    Espinosa et al 2010
- Aim: GW power spectrum

$$\frac{d\Omega_{\rm gw}}{d\ln f} = \frac{1}{\rho_{\rm tot}}\frac{d\rho_{\rm gw}}{d\ln f} = \frac{8\pi^2}{3H^2} f^3 S_h(f)$$

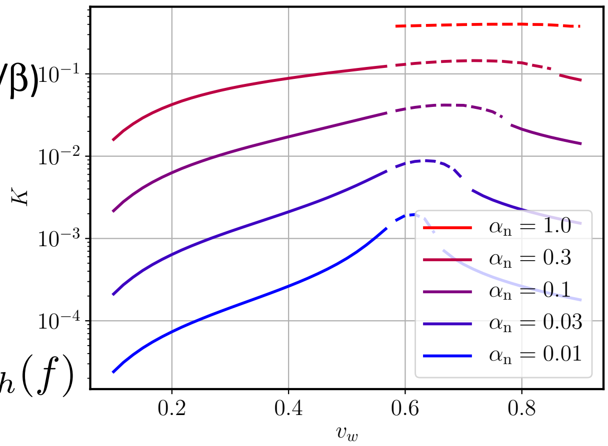

Simulations of phase transitions

- Preparatory: 1M hrs CSC, Finland
- 2015/6: 17M CPU-hours
  Tier-0 (Hazel Hen, Stuttgart)
- 4200^3 lattice on 24k cores
- Output: GW power spectrum

$$\frac{d\Omega_{\rm gw}}{d\ln f} = \frac{1}{\rho_{\rm tot}}\frac{d\rho_{\rm gw}}{d\ln f} = \frac{8\pi^2}{3H^2} f^3 S_h(f)$$

SUOMEN AKATEMIA
FINLANDS AKADEMI
ACADEMY OF FINLAND

Hindmarsh, Huber, Rummukainen, Weir 2017

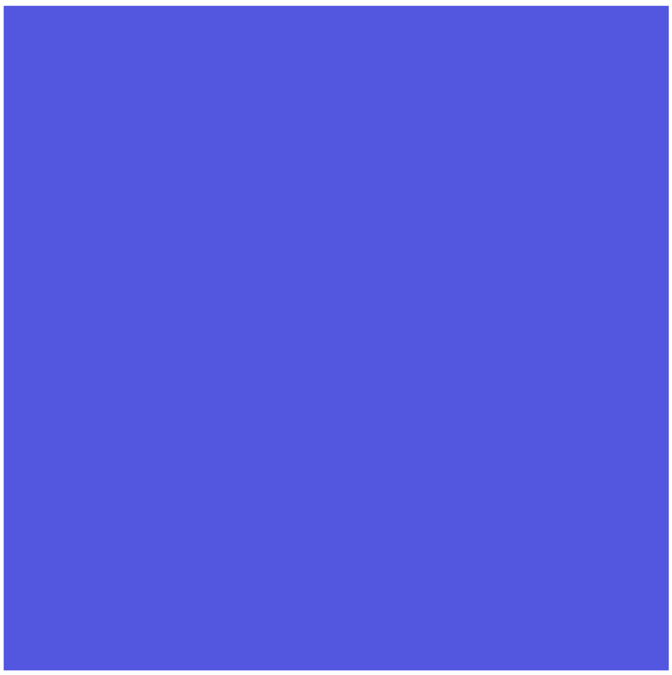

Fluid kinetic energy in slice (1200^3)

Weir 2017

GW energy density

$$\rho_{\mathrm{GW}} = \frac{1}{32\pi G}\langle \dot{h}_{ij}^2 \rangle.$$

- Fluid sources GWs continuously: $T_{ij} = (\bar{\epsilon}+\bar{p})V_iV_j|^{TT}$
- GW energy density grows with time $\rho_{\mathrm{GW}} \propto t\, G L_{\mathrm{f}}[(\bar{\epsilon}+\bar{p})\bar{U}_{\mathrm{f}}^2]^2$
- Final GW energy density depends on
  - Lifetime of source τ
  - Flow length scale $L_f \sim R_*$
  - Kinetic energy fraction squared K^2

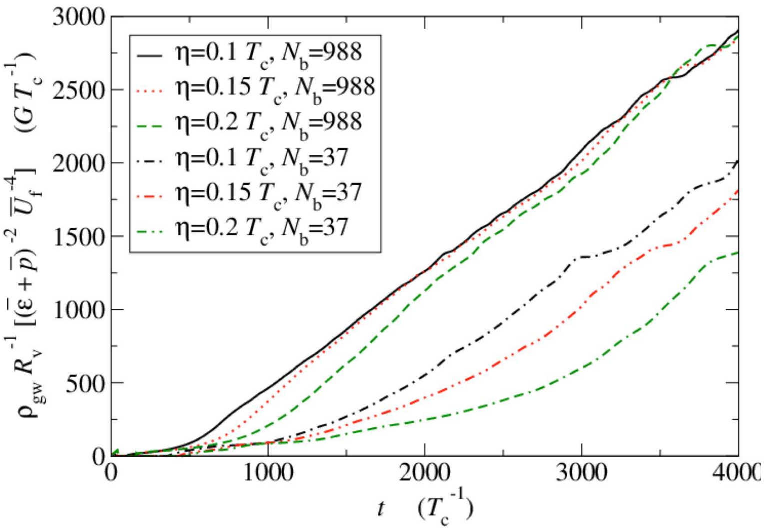

Hindmarsh, Huber, Rummukainen, Weir (2015)

GW power spectra: deflagration

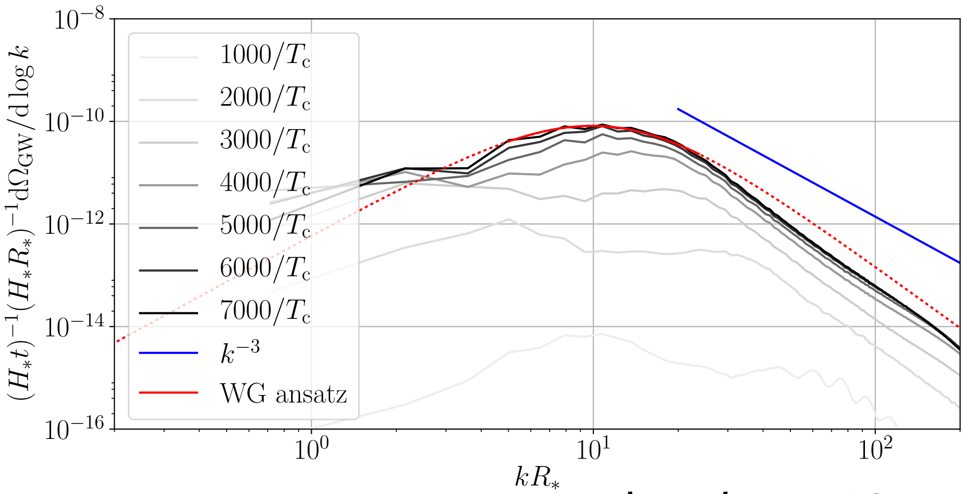

- Transition strength: α = 0.0046
- Wall speed: v_w = 0.44
- Mean bubble separation: R_* = 1900/T_c

- Peak at $kR_* \sim 10$
- Approx k^{-4} spectrum at high k

Hindmarsh, Huber, Rummukainen, Weir (2017)

GW power spectra: near c_s

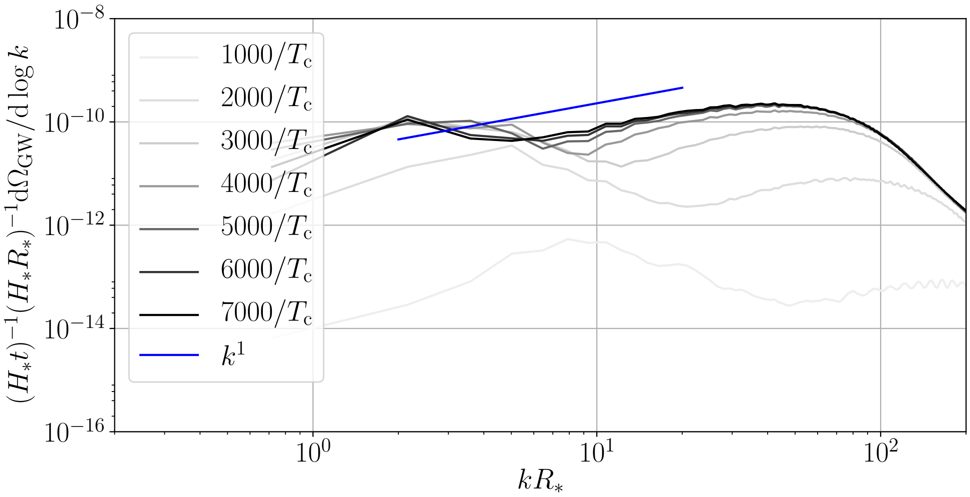

- Transition strength:
  $\alpha = 0.0046$
- Wall speed:
  $v_w = 0.56$
- Mean bubble separation:
  $R_* = 1900/T_c$

- Peak at $kR_* \sim 40$
- Approx k spectrum at lower k
- Peak length scale from sound shell thickness

Hindmarsh, Huber, Rummukainen, Weir (2017)

GW power spectra: detonation

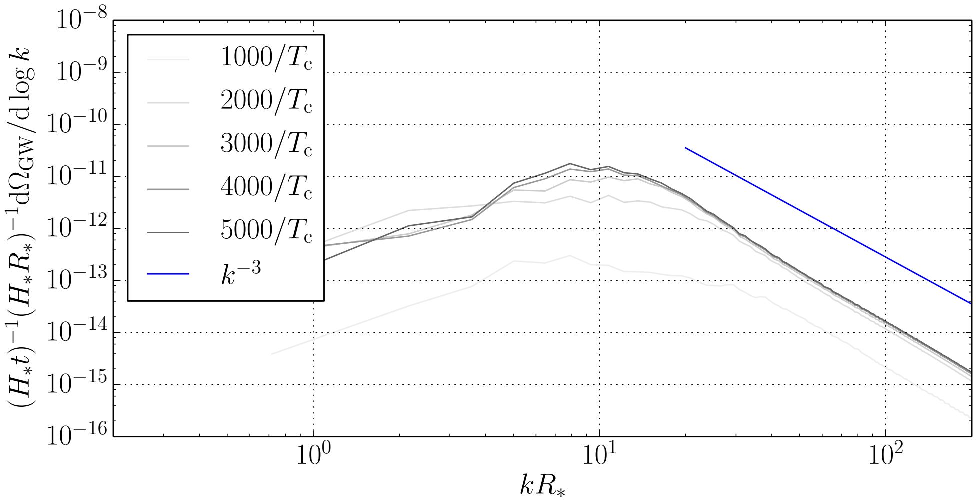

- Transition strength:
  $\alpha = 0.0046$
- Wall speed:
  $v_w = 0.92$
- Mean bubble separation:
  $R_* = 1900/T_c$

- Peak at $kR_* \sim 10$
- Approx k^{-3} spectrum at high k

Hindmarsh, Huber, Rummukainen, Weir (2017)

Sound shell model

- Velocity field model: linear superposition of 1-bubble $v(r)$ convolved with size distribution
- Many bubbles: Gaussian field
- Peak power proportional to:
  - Lifetime of source τ
  - Flow length scale $L_f \sim R_*$
  - Kinetic energy fraction squared K^2

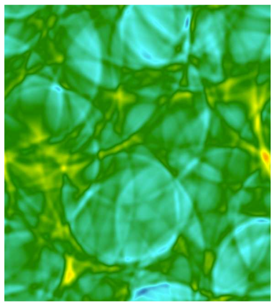

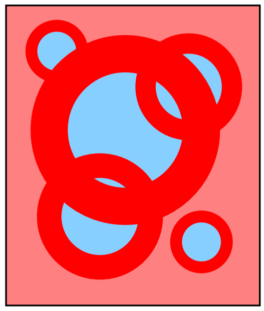

$$\Omega_{\mathrm{gw},0}^{\mathrm{peak}} \simeq 3 \times 10^{-6} (H_* R_*) K^2$$

$$f_{\mathrm{peak}} \simeq 26 \left(\frac{1}{H_* R_*}\right) \left(\frac{T_{\mathrm{n}}}{10^2\,\mathrm{GeV}}\right) \mu\mathrm{Hz},$$

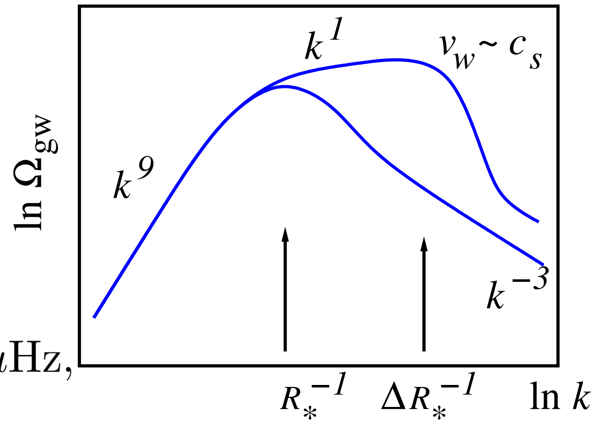

Hindmarsh (2017)

Shocks and turbulence

- Shocks develop after time $\tau_{\mathrm{s}} \sim R_*/\bar{U}_{\mathrm{f}}$
- Shocks source vorticity and turbulence
- Turbulence lifetime ~ autocorrelation time (eddy turn-over time) $\tau_{\mathrm{tu}} \sim R_*/\bar{U}_{\mathrm{f}}$
- Estimate GW power
  $\Omega_{\mathrm{GW}}^{\mathrm{tu}} \sim (H_* R_*/\bar{U}_{\mathrm{f}})^2 K^2 \sim (H_* R_*)^2 K$
- Non-linear behavior important if $\tau_{\mathrm{s}} \ll H_*^{-1}$
- Equivalent to $K \gg (H_{\mathrm{n}} R_*)^2$
- Disagreement about turbulence spectrum:
  - $f^{-2/3}$ Caprini, Durrer, Servant 2009
  - $f^{-9/2}$ Kamionkowsky, Kosowsky, Turner 1994; Gogoberidze, Kahniashvili, Kosowsky 2007
- No predictions for spectrum from shocks

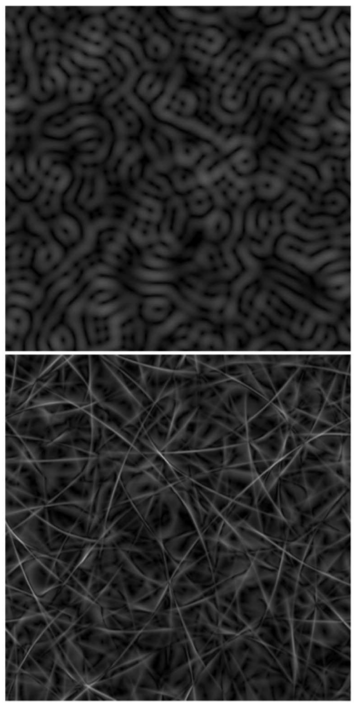

Pen, Turok 2015

Gravitational waves from a vacuum phase transition

- Extreme supercooling: shear stress dominated by scalar field
- Bubble walls accelerate: $v_w \to 1$

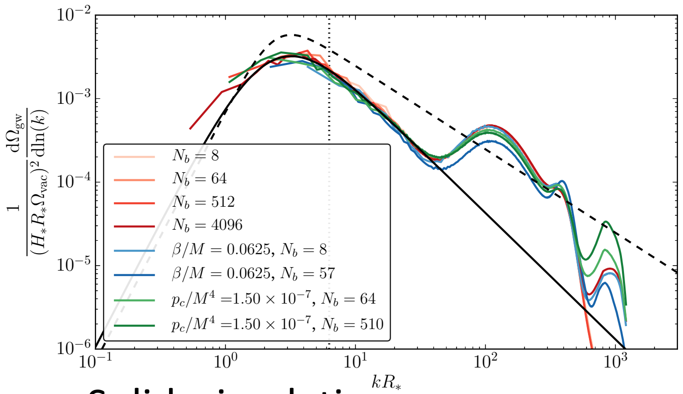

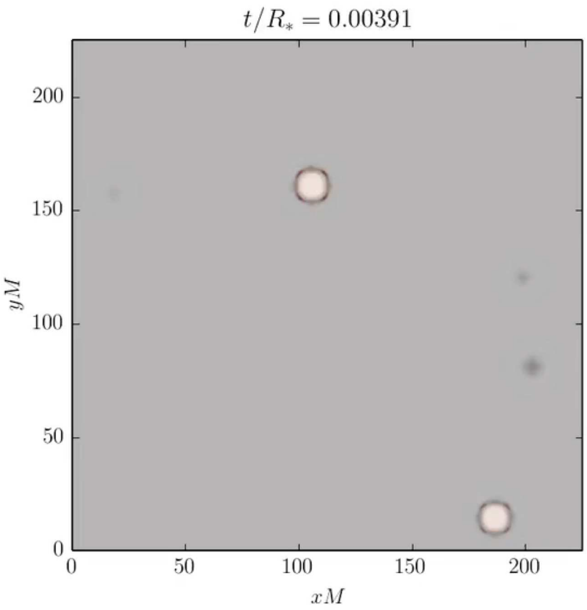

- Solid: simulations
- Dashed: Envelope Approximation

Kosowsky, Turner, Watkins 1992
Huber, Konstandin 2008

Cutting, Hindmarsh, Weir 2018

LISA prospects for EW phase transition

c.f. Caprini et al (2015) [LISA Cosmology Working Group]

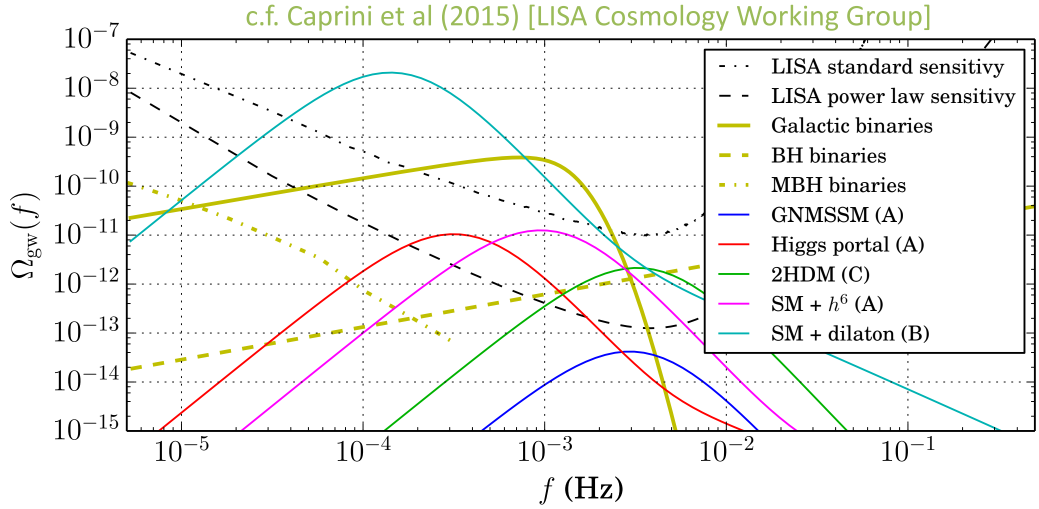

Model	T_n/GeV	α	β/H_n	v_w
GNMSSM A	112	0.037	277	0.95
Higgs portal A	70.6	0.09	47.35	0.95
2HDM C	51.6	0.111	663	0.95
SM + h^6 A	63	0.13	160	0.95
SM + dilaton B	100	1	15	0.95

Phase transitions: future challenges

- Full characterization of GW spectrum from phase transitions
  - Shocks and turbulence [$K > (H_n R_*)^2$]
  - Magnetic field dynamo?
- Phase transition parameters from underlying particle physics models
  - Perturbative 4D
  - DR & non-perturbative 3D
    Moore, Rummukainen (2000)
    Laine, Nardini, Rummukainen (2012) Really 1st order?
- Connection to collider (LHC …) data

  e.g. λ_{hhh}
- Distinguishing phase transitions from astrophysical GW foregrounds

LISA Cosmology Working Group

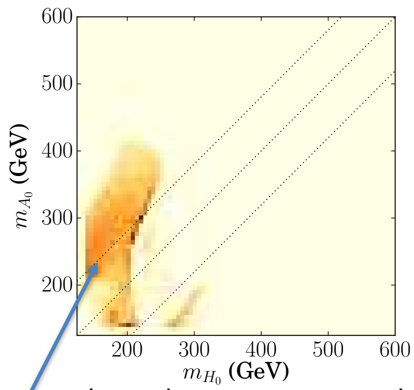

Andersen et al 2017

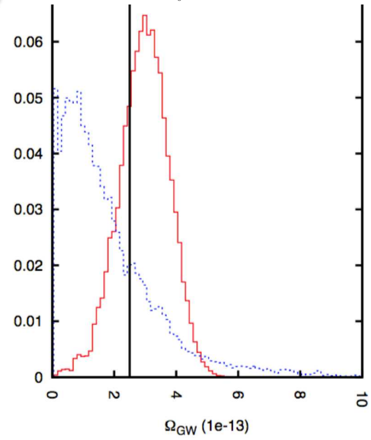

Adams, Cornish (2013)

Summary

- GWs probe of physics of early universe at very high energy
- LISA will probe physics of Higgs phase transition from 2034
- Aim: measure/constrain phase transition parameters
  - α = (Latent heat)/(Thermal energy)
  - β = transition rate parameter
  - v_w = Bubble wall speed
  - H_n = Hubble rate at nucleation
- LISA will complement LHC in search for new physics at TeV scale
- Lots of work to do
  - only 16 years to go!

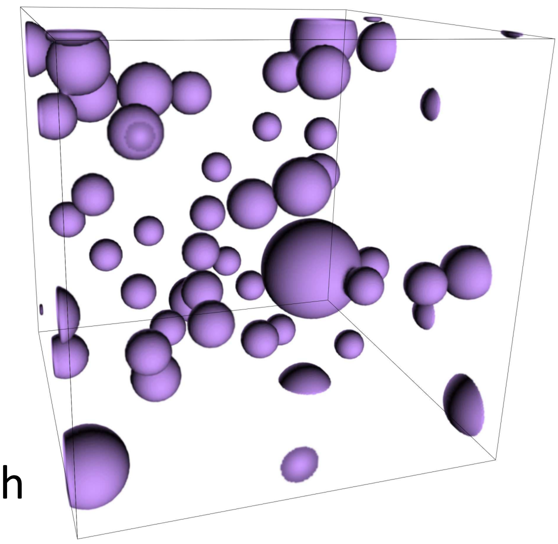

Session S1P1 14:45–15:15

[Chair: Misao Sasaki]

Osamu Seto

Hokkaido University

"Gravitational waves from seesaw phase tranistion"

(10+5 min.)

[JGRG28 (2018) 110508]

Gravitational wave from seesaw phase transition

Osamu Seto
(Hokkaido Univ.)

With: Nobuchika Okada (U. of Alabama)

Refs : Phys. Rev. D **98**, 063532 (2018)

§ Introduction

The most penetrable

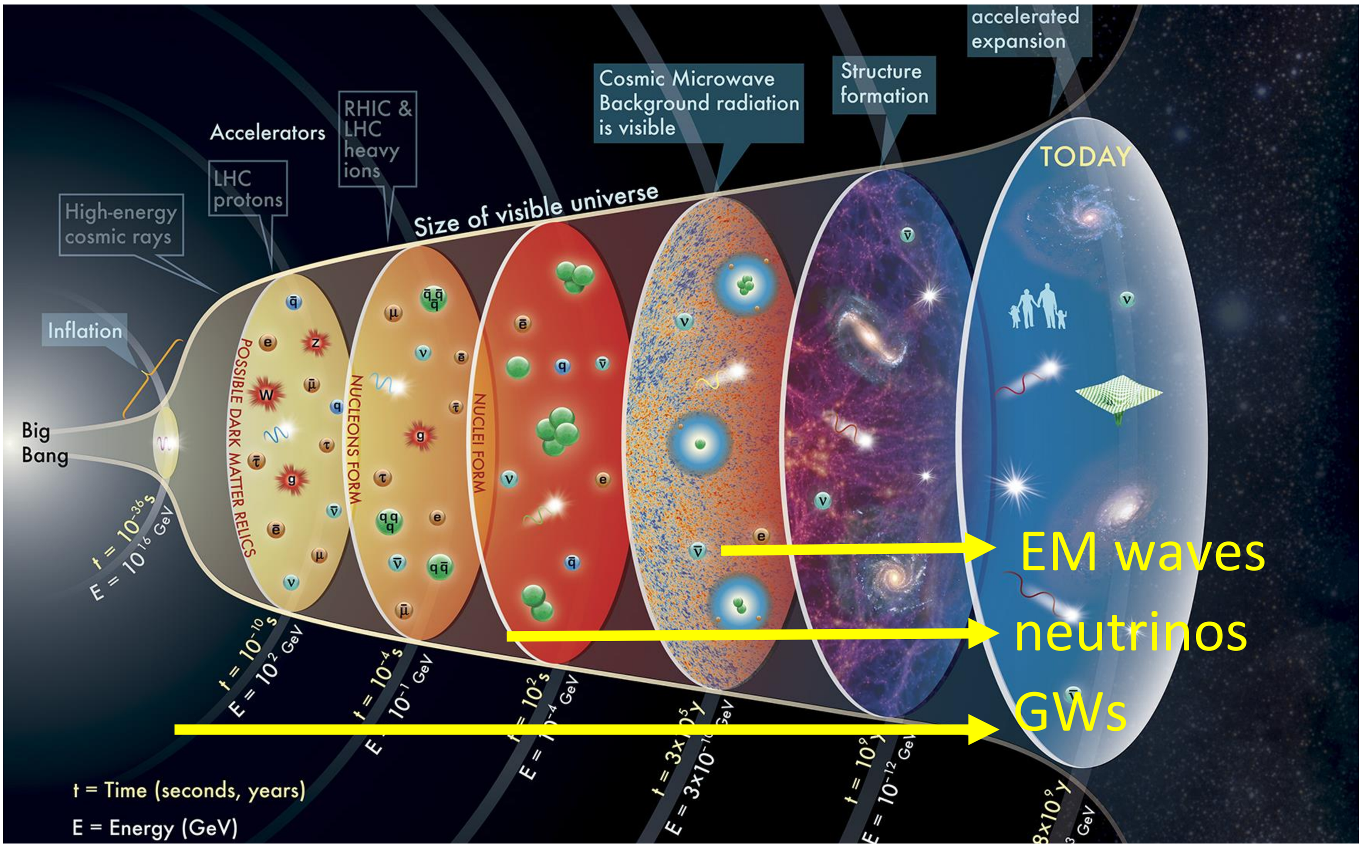

Phase transitions in the early Universe

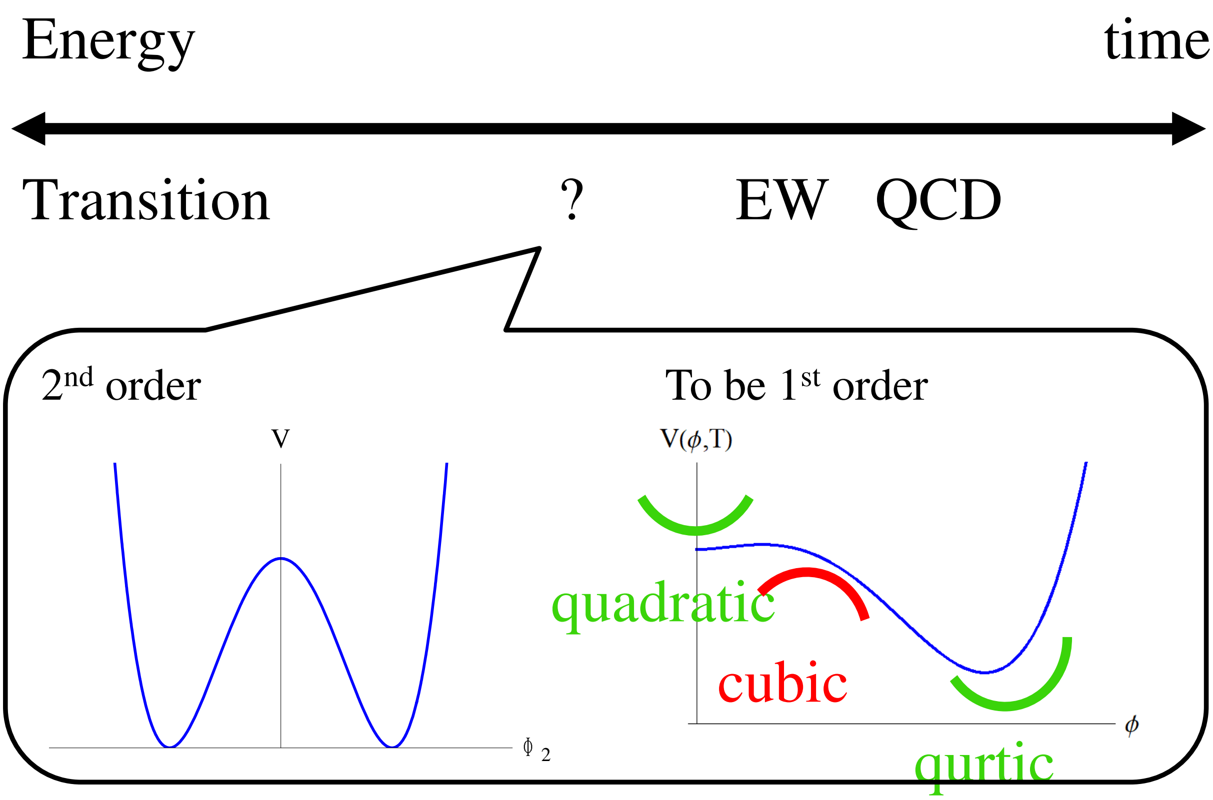

Nonvanishing neutrino mass

- Neutrino oscillation

  $\longrightarrow$ tiny (< 0.1 eV) but massive neutrino
- No mass in the renormalizable SM

- **Seesaw mechanism** for Majorana neutrino

  [Yanagida, Gell-Mann et al (1979)]

$$\begin{pmatrix} 0 & yv \\ yv & M_N \end{pmatrix} \rightarrow \begin{pmatrix} -(yv)^2/M_N & 0 \\ 0 & M_N \end{pmatrix}$$

M_N in Cosmology: Baryogenesis

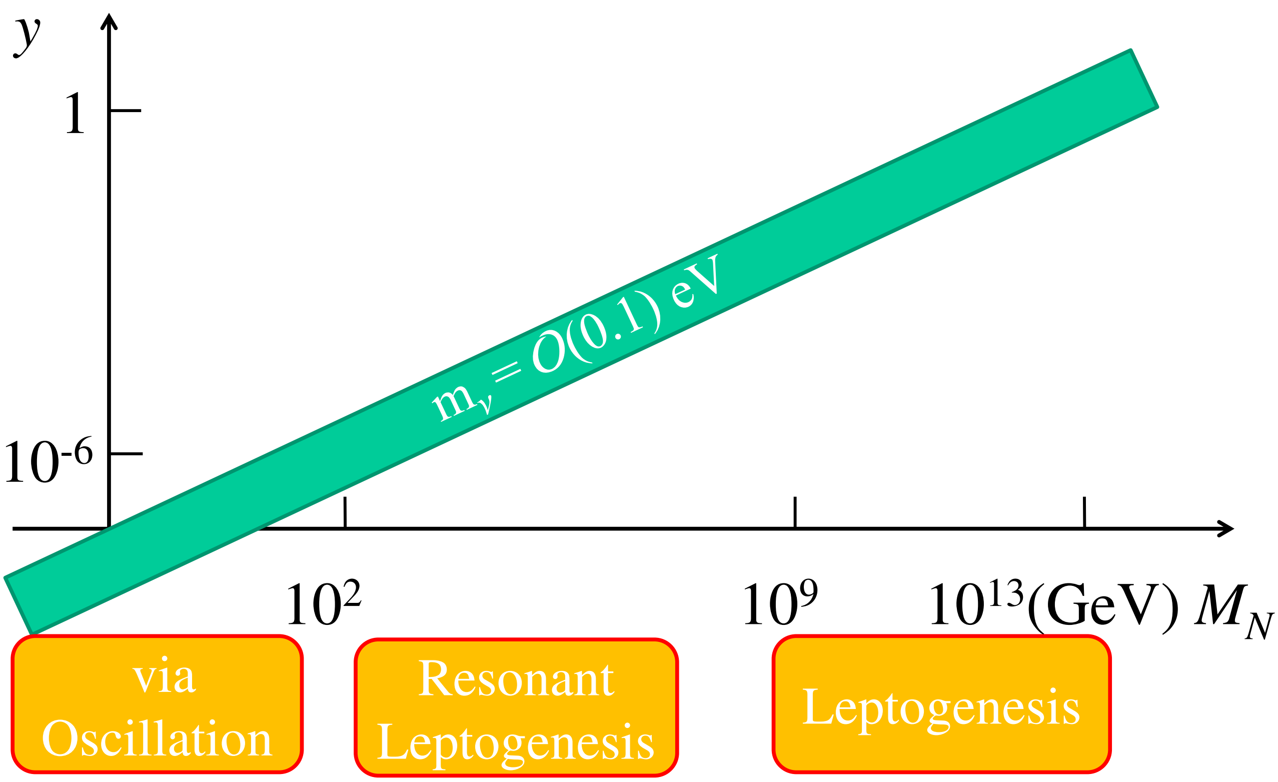

§ GW

GW from 1st order phase transitions

- Potential barrier and 1st order phase transition

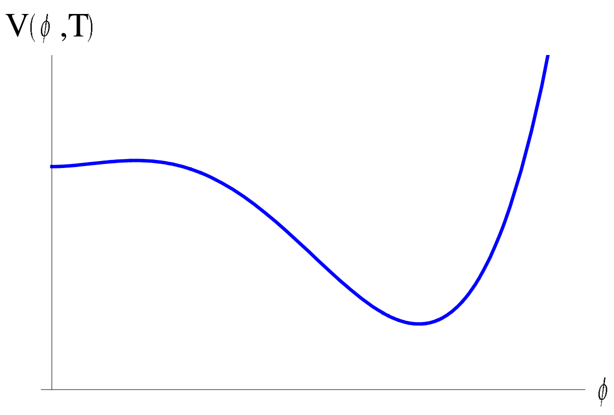

- Bubble formation

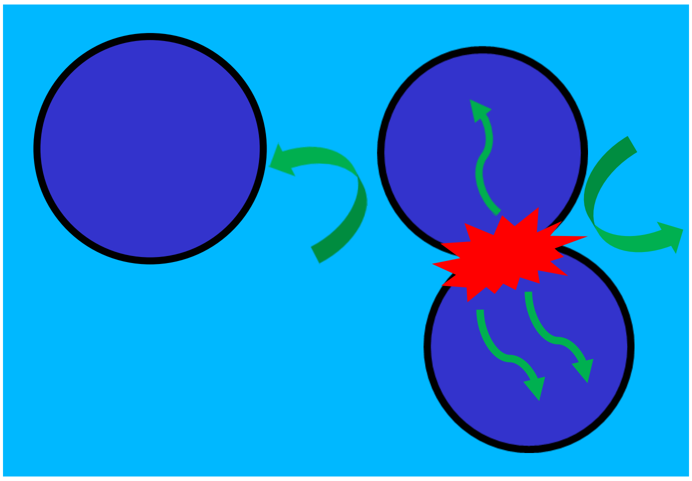

- Bubble collision
- Sound waves in the fluid
- Turbulence in the fluid

GWs spectrum

- At radiation dominated Universe
- The energy density of radiation $\rho_{\rm rad} = \frac{\pi^2 g_*}{30} T^4$
- The latent heat density

$$\epsilon = \left(V - T\frac{\partial V}{\partial T} \right)\bigg|_{\{\phi_{\rm high}, T_\star\}} - \left(V - T\frac{\partial V}{\partial T} \right)\bigg|_{\{\phi_{\rm low}, T_\star\}} \qquad \boxed{\alpha \equiv \frac{\epsilon}{\rho_{\rm rad}}}$$

- Transition time
  - Bubble nucleation rate $\Gamma(T) = \Gamma_0 e^{-S(T)} \simeq \Gamma_0 e^{-S_E^3(T)/T}$

$$\boxed{\frac{\beta}{H_\star} \simeq T\frac{dS}{dT}\bigg|_{T_\star} = T\frac{d(S_E^3/T)}{dT}\bigg|_{T_\star}}$$

GWs spectrum

- Bubble collision [Kosowsky and Turner (1993), Huber and Konstandin (2008)]

$$f_{\rm peak} \simeq 17 \left(\frac{f_\star}{\beta}\right)\left(\frac{\beta}{H_\star}\right)\left(\frac{T_\star}{10^8\,{\rm GeV}}\right)\left(\frac{g_*}{100}\right)^{1/6} {\rm Hz},$$

$$h^2\Omega_{GW}(f_{\rm peak}) \simeq 1.7\times 10^{-5}\kappa^2\Delta\left(\frac{\beta}{H_\star}\right)^{-2}\left(\frac{\alpha}{1+\alpha}\right)^2\left(\frac{g_*}{100}\right)^{-1/3},$$

- Sound waves [Hindmarsh et al (2014, 2015), Caprini et al (2016)]

$$f_{\rm peak} \simeq 19\frac{1}{v_b}\left(\frac{\beta}{H_\star}\right)\left(\frac{T_\star}{10^8\,{\rm GeV}}\right)\left(\frac{g_*}{100}\right)^{1/6} {\rm Hz},$$

$$h^2\Omega_{GW}(f_{\rm peak}) \simeq 2.7\times 10^{-6}\kappa_v^2 v_b\left(\frac{\beta}{H_\star}\right)^{-1}\left(\frac{\alpha}{1+\alpha}\right)^2\left(\frac{g_*}{100}\right)^{-1/3}.$$

- Turbulence [Kamionkowski et al (1994), Caprini et al (2009)]

$$f_{\rm peak} \simeq 27\frac{1}{v_b}\left(\frac{\beta}{H_\star}\right)\left(\frac{T_\star}{10^8\,{\rm GeV}}\right)\left(\frac{g_*}{100}\right)^{1/6} {\rm Hz},$$

$$h^2\Omega_{GW}(f_{\rm peak}) \simeq 3.4\times 10^{-4} v_b\left(\frac{\beta}{H_\star}\right)^{-1}\left(\frac{\kappa_{\rm turb}\alpha}{1+\alpha}\right)^{3/2}\left(\frac{g_*}{100}\right)^{-1/3}.$$

§ GW from $\mathrm{U(1)}_{\mathrm{B\text{-}L}}$ breaking

$\mathrm{U(1)}_{\mathrm{B\text{-}L}}$ gauge symmetry

- A simplest anomaly-free U(1) gauge theory
  - Three generations of RH neutrino
  - The origin of RH neutrino masses

$$m_{N_R^i} = \frac{Y_{N^i}}{\sqrt{2}} v_2$$

    - Higgs field with B-L charge "+2" Φ_2
    - $\mathcal{L} = y\, L\, \Phi N + \frac{1}{2} Y_N\, N\, \Phi_2\, N$

-1 +2 -1

  - One extra neutral gauge boson

$$M_{Z'}^2 = 4 g_{B-L}^2 v_2^2$$

Model: next to minimal

Content

	$SU(3)_c$	$SU(2)_L$	$U(1)_Y$	$U(1)_{B-L}$
q_L^i	**3**	**2**	1/6	1/3
u_R^i	**3**	**1**	2/3	1/3
d_R^i	**3**	**1**	−1/3	1/3
ℓ_L^i	**1**	**2**	−1/2	−1
e_R^i	**1**	**1**	−1	−1
H	**1**	**2**	−1/2	0
N_R^i	**1**	**1**	0	−1
Φ_1	**1**	**1**	0	+1
Φ_2	**1**	**1**	0	+2

Yukawa interaction

$$\mathcal{L}_{Yukawa} \supset -\sum_{i=1}^{3}\sum_{j=1}^{3} Y_D^{ij}\overline{\ell_L^i} H N_R^j - \frac{1}{2}\sum_{k=1}^{3} Y_{N^k}\Phi_2 \overline{N_R^{k\ C}} N_R^k + \text{H.c.}$$

Higgs potential

$$V(\Phi_1,\Phi_2) = \frac{1}{2}\lambda_1(\Phi_1\Phi_1^\dagger)^2 + \frac{1}{2}\lambda_2(\Phi_2\Phi_2^\dagger)^2 + \lambda_3\Phi_1\Phi_1^\dagger(\Phi_2\Phi_2^\dagger)$$
$$+ M_{\Phi_1}^2\Phi_1\Phi_1^\dagger - M_{\Phi_2}^2\Phi_2\Phi_2^\dagger - A(\Phi_1\Phi_1\Phi_2^\dagger + \Phi_1^\dagger\Phi_1^\dagger\Phi_2).$$

Higgs potential

$$V(\Phi_1,\Phi_2) = \frac{1}{2}\lambda_1(\Phi_1\Phi_1^\dagger)^2 + \frac{1}{2}\lambda_2(\Phi_2\Phi_2^\dagger)^2 + \lambda_3\Phi_1\Phi_1^\dagger(\Phi_2\Phi_2^\dagger)$$
$$+ M_{\Phi_1}^2\Phi_1\Phi_1^\dagger - M_{\Phi_2}^2\Phi_2\Phi_2^\dagger - A(\Phi_1\Phi_1\Phi_2^\dagger + \Phi_1^\dagger\Phi_1^\dagger\Phi_2).$$

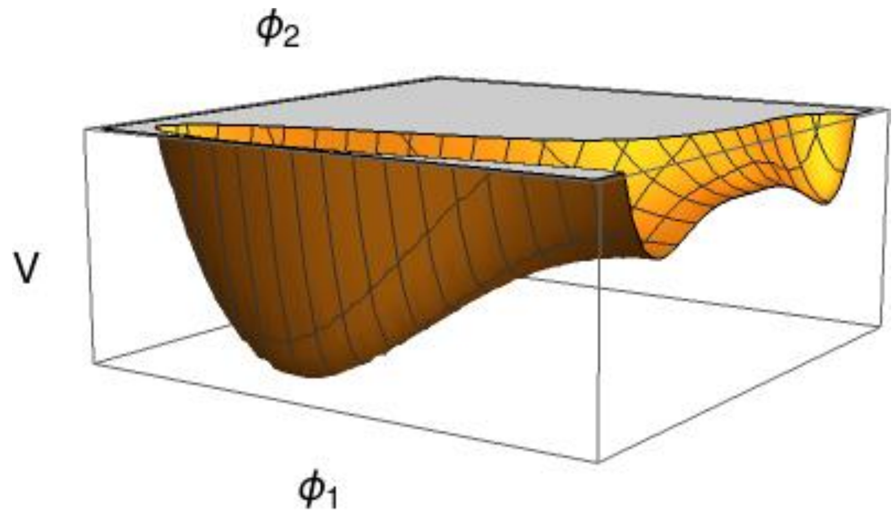

GW spectrum

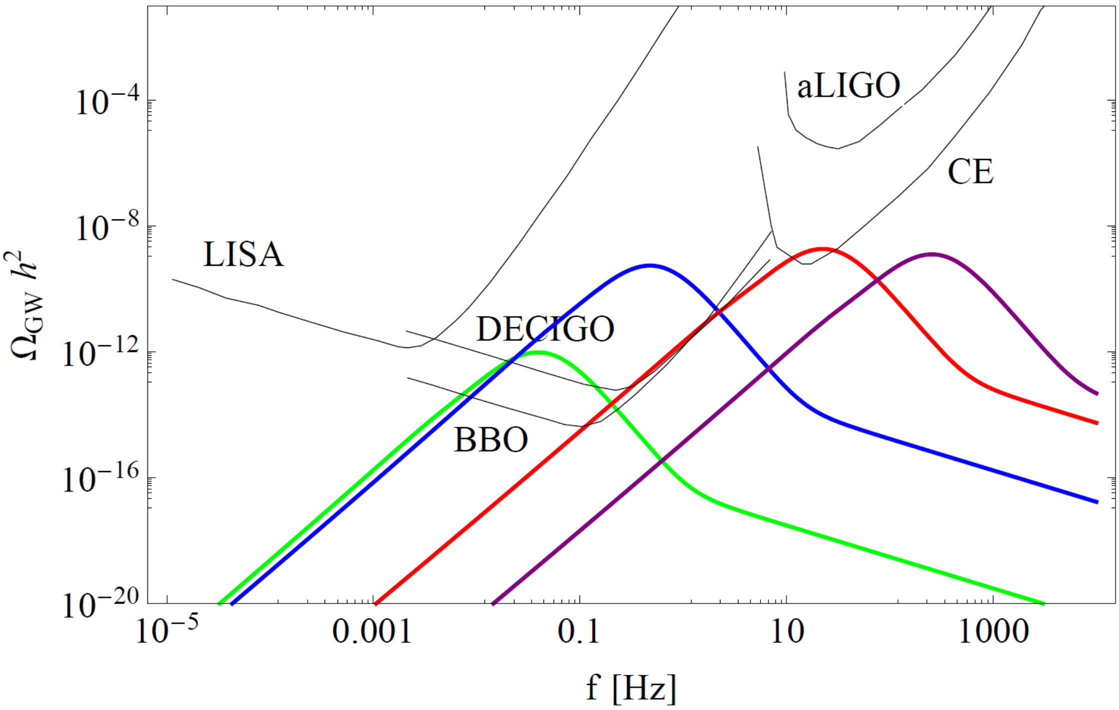

$v\ (=v_1=v_2) = 4,\ 10^2,\ 10^4,\ 10^5$ TeV

§ Summary

- The scale of gauged B-L symmetry could be probed by GWs
  - RH neutrino masses:
    - maybe much higher than the EW scale
  - ~~B-L~~ may be strong 1st order
  - Sources of cosmological GWs from an intermediate scale phase transition
    - Thermal history of the Universe
    - Implication to Baryogenesis
    - Inaccessible high scale particle physics for colliders
- Caveat
  - Gauge dependence problem [e.g., Chiang and Senaha (2017)]

Naonori Sugiyama

Kavli IPMU

“Limits on primordial statistical anisotropy from large-scale structure”

(10+5 min.)

[JGRG28 (2018) 110509]

Limits on Primordial Statistical Anisotropy from Large-Scale Structure

Naonori Sugiyama

Collaborators: Maresuke Shiraishi and Teppei Okumura

KAVLI IPMU INSTITUTE FOR THE PHYSICS AND MATHEMATICS OF THE UNIVERSE

JGRG28 @ Rikkyo University (Nov. 5-9, 2018)

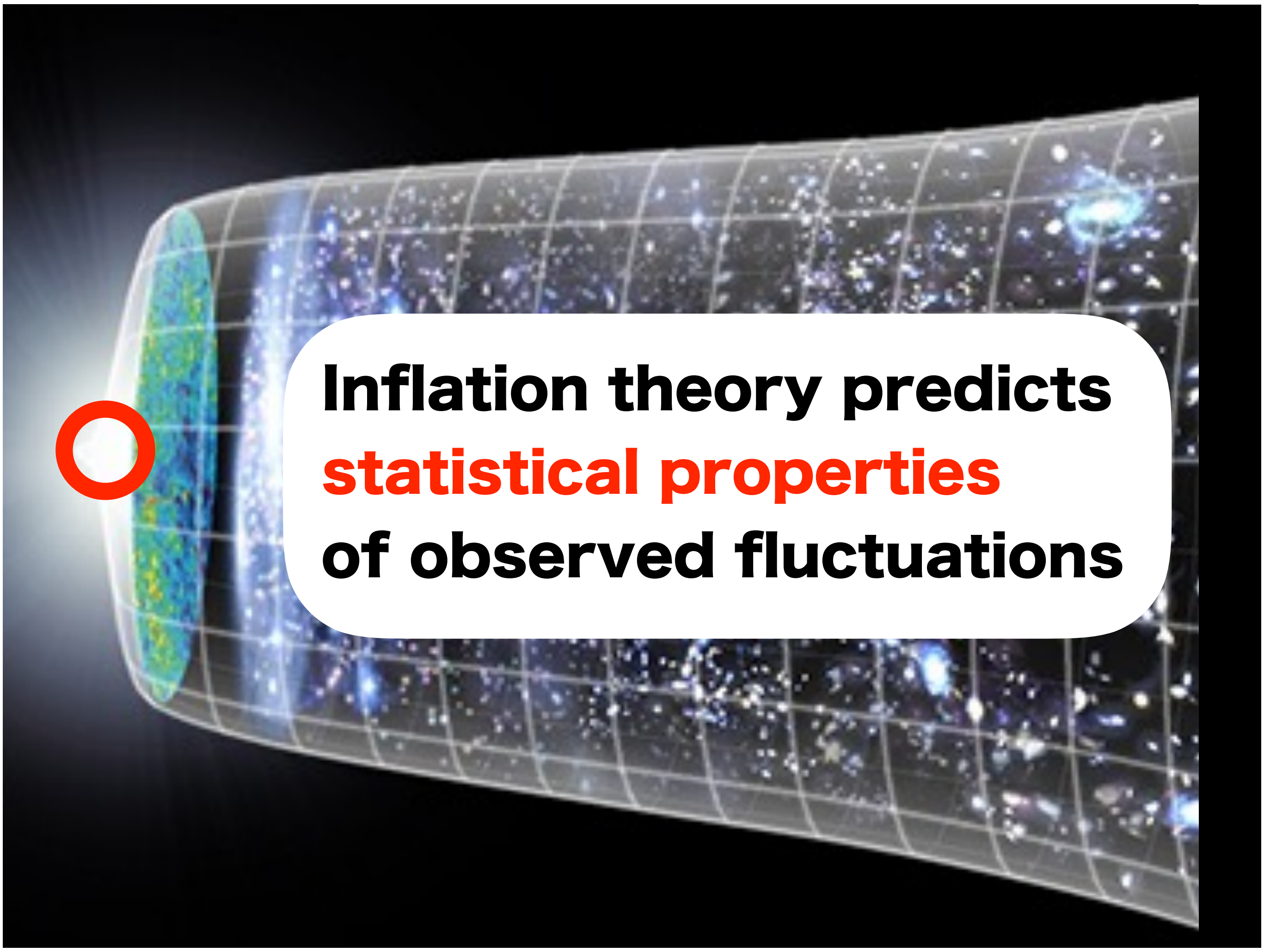

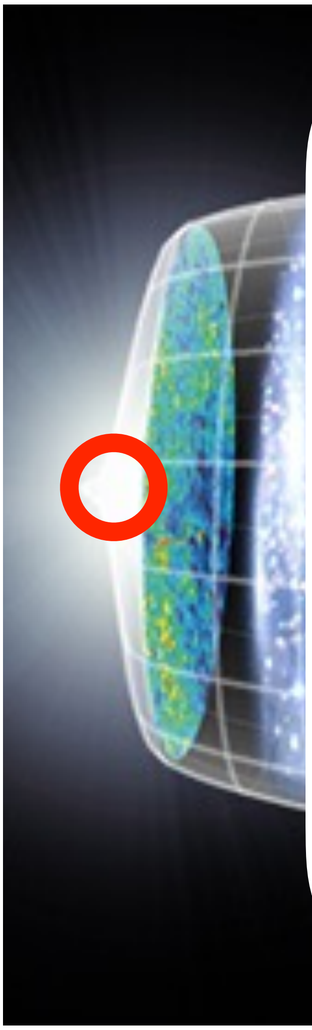

The standard theory (single-scalar slow-roll)

predicts:

- **Small non-Gaussianity**
- **Nearly scale-free**
- **Adiabaticity**
- **Parity-symmetry**
- **Translational symmetry**
- **Rotational symmetry**

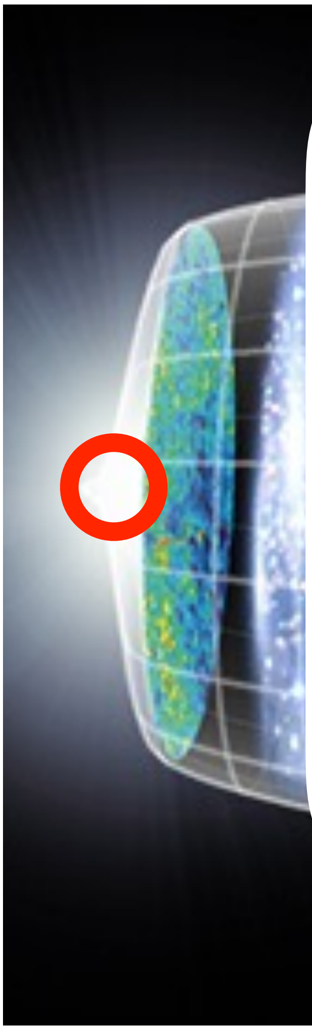

Rotational invariance:

$$P_\zeta(\vec{k}) = P_\zeta(|\vec{k}|)$$

Some kind of vector-field inflation theory can breaks the rotational invariance.

Quadrupolar anisotropy

Ackerman+2009

$$P_\zeta(\vec{k}) = P_{\rm iso}(|\vec{k}|)\left[1 + g_*\left(\left(\hat{k}\cdot\hat{p}\right)^2 - \frac{1}{3}\right)\right]$$

The simplest model
breaking statistical isotropy with preserving party-symmetry and translational invariance.

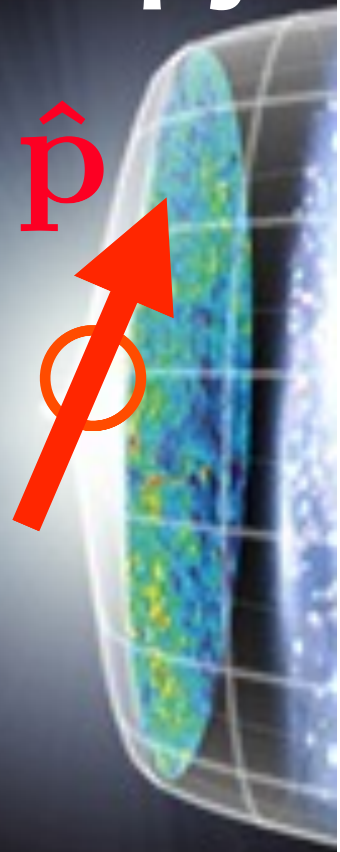

CMB experiments

Kim and Komatsu 2014:

$$\mathbf{g}_* = 0.002 \pm 0.016\ (68\%\mathrm{CL})$$

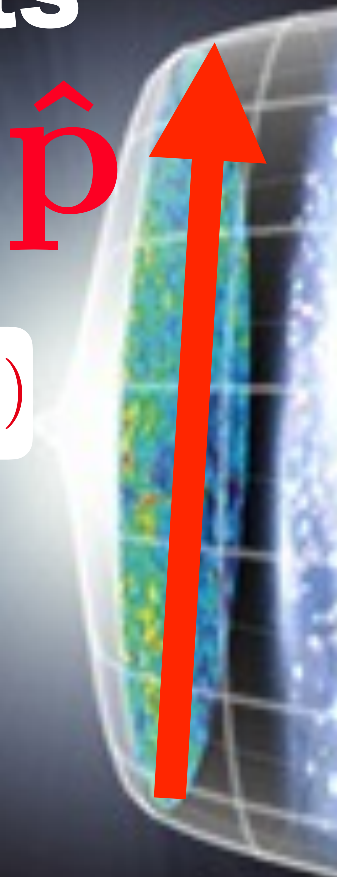

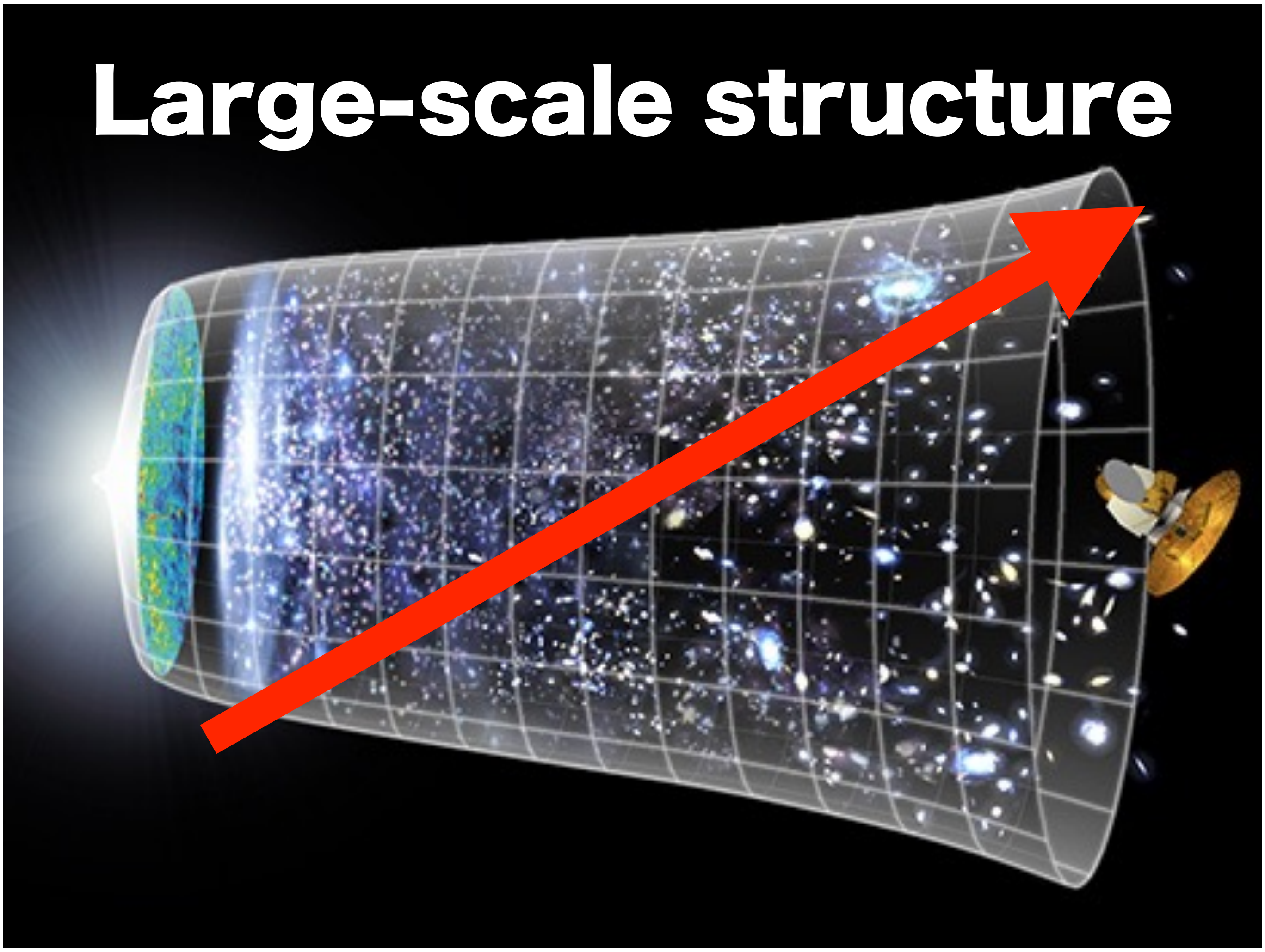

Why large-scale structure?

CMB (2D) vs. LSS (3D)

$$\boxed{\text{error} \propto 1/\sqrt{\text{Volume}}}$$

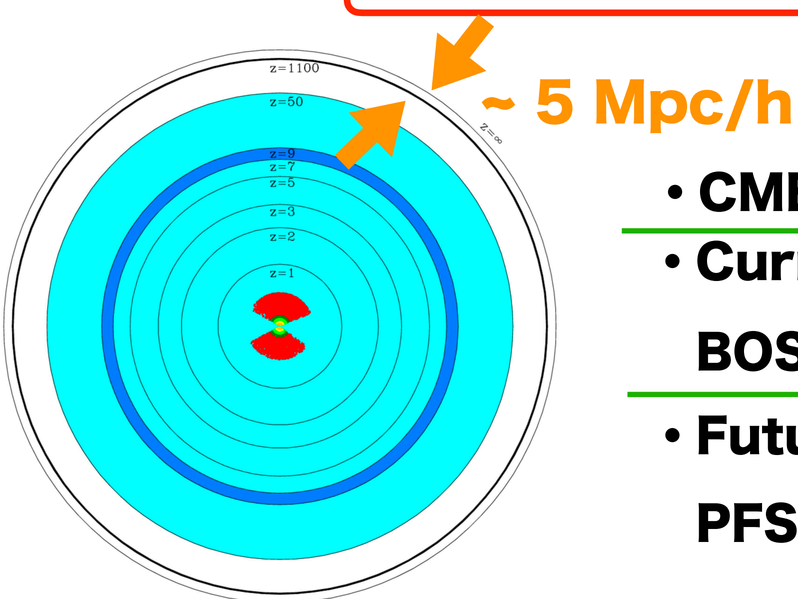

Tegmark and Zaldarriaga 2009

- CMB ~ 7 (Gpc/h)^3
- Current galaxy data

  BOSS ~ 4 (Gpch)^3
- Future galaxy data

  PFS ~ 10 (Gpc/h)^3

  DESI ~ 45(Gpc/h)^3

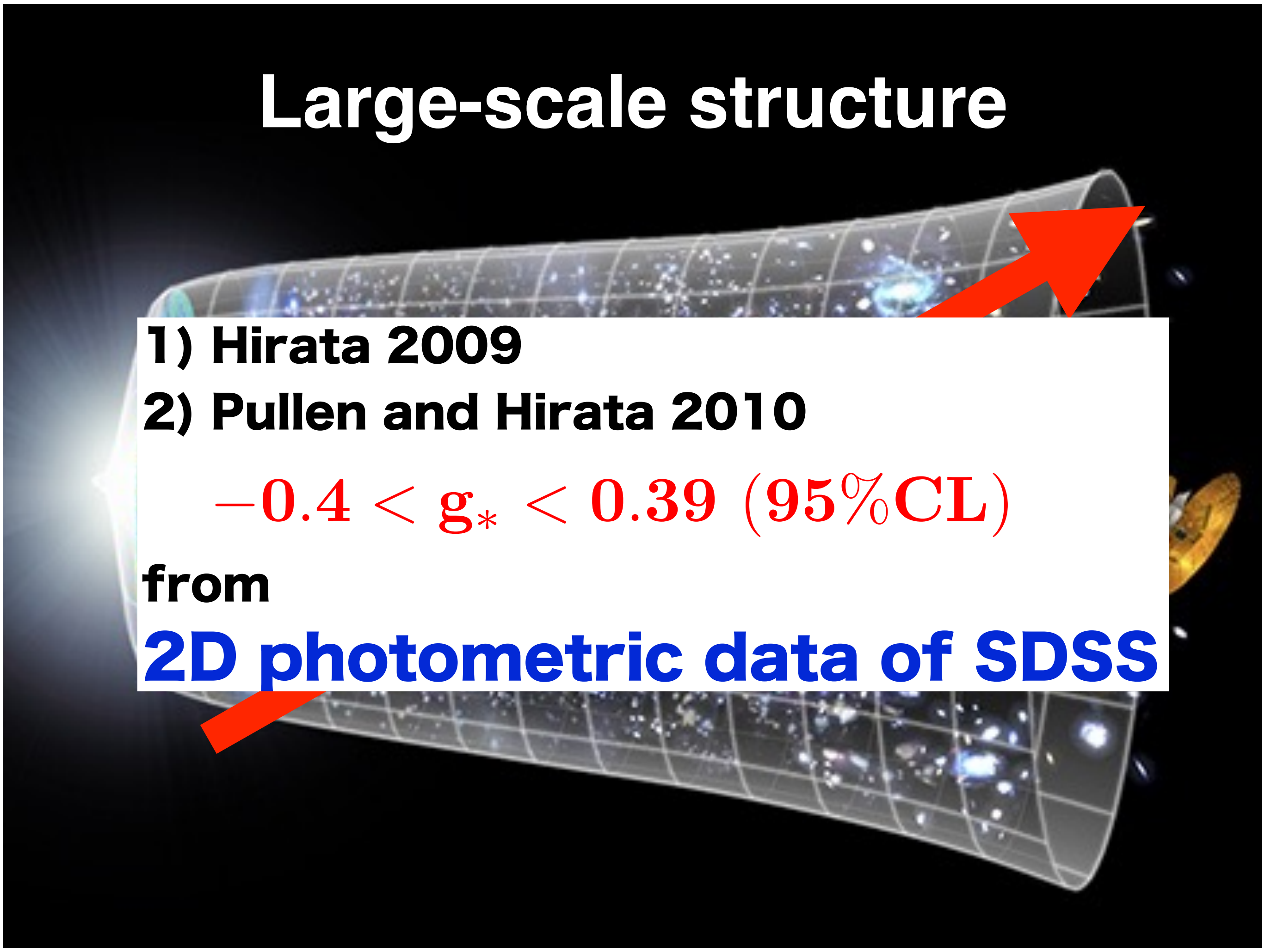
Large-scale structure
1) Hirata 2009
2) Pullen and Hirata 2010
$-0.4 < g_* < 0.39$ (95%CL)
from
2D photometric data of SDSS

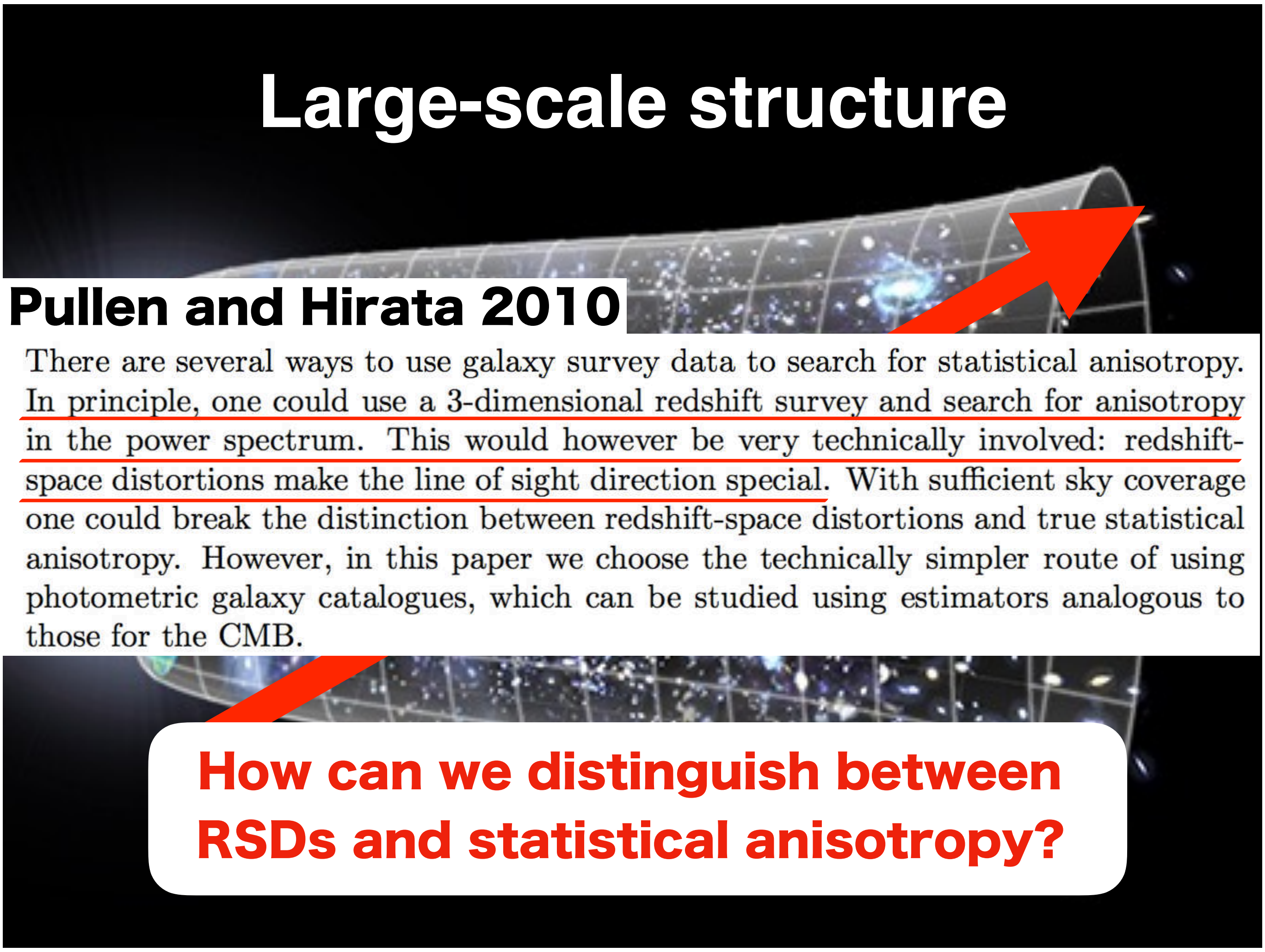
Large-scale structure
Pullen and Hirata 2010
There are several ways to use galaxy survey data to search for statistical anisotropy. In principle, one could use a 3-dimensional redshift survey and search for anisotropy in the power spectrum. This would however be very technically involved: redshift-space distortions make the line of sight direction special. With sufficient sky coverage one could break the distinction between redshift-space distortions and true statistical anisotropy. However, in this paper we choose the technically simpler route of using photometric galaxy catalogues, which can be studied using estimators analogous to those for the CMB.
How can we distinguish between RSDs and statistical anisotropy?

This talk:

1) presents an efficient way to distinguish the preferred angular dependence in the galaxy power spectrum from RSDs

2) for the first time, constrains the statistical anisotropy from spectroscopic 3D galaxy data (SDSS DR12 BOSS)

Galaxy power spectrum

$$P_{\rm g}(\vec{k},\ \underline{\hat{n}})$$

Line-of-sight direction

Legendre decomposition

Under statistical isotropy assumption:

$$P_{\mathrm{g}}(\vec{k},\,\hat{n}) = \sum_{\ell} P_{\ell}(k)\,\mathcal{L}_{\ell}\,(\hat{k}\cdot\hat{n})$$

Angular momentum, ell:
ell > 0 means the esistence of RSDs.

Galaxy power spectrum

$$P_{\mathrm{g}}(\vec{k},\,\hat{n},\,\hat{p})$$

Preferred direction

Decomposition into
Bipolar spherical harmonics

$$P_{\rm g}(\vec{k},\,\hat{n},\,\hat{p}) = \sum_{LM}\sum_{\ell\ell'} P^{LM}_{\ell\ell'}(k,\hat{p})\,\left(Y_\ell(\hat{k})\otimes Y_{\ell'}(\hat{n})\right)_{LM}$$

$$\sum_{m,m'}\begin{pmatrix} \ell & \ell' & L \\ m & m' & -M \end{pmatrix} Y_{\ell m}(\hat{k})\,Y_{\ell' m'}(\hat{n})$$

Angular momentum-coupling yields the total angular momentum, L

Decomposition into
Bipolar spherical harmonics

$$P_{\rm g}(\vec{k},\,\hat{n},\,\hat{p}) = \sum_{LM}\sum_{\ell\ell'} P^{LM}_{\ell\ell'}(k,\hat{p})\,\left(Y_\ell(\hat{k})\otimes Y_{\ell'}(\hat{n})\right)_{LM}$$

Total angular momentum, L:

L = 0 reduces to the Legendre expansion

L > 0 means the existence of anisotropy.

Quadrupolar anisotropy

$$P_\zeta(\vec{k}) = P_{\rm iso}(|\vec{k}|)\left[1 + g_*\left(\left(\hat{k}\cdot\hat{p}\right)^2 - \frac{1}{3}\right)\right]$$

$$\begin{aligned} P^{L=0,M}_{\ell\ell'}(k) &= \delta_{\ell\ell'} P_\ell(k) \\ P^{L=2,M}_{\ell\ell'}(k) &\propto g_*\, Y_{2M}(\hat{p}) \begin{pmatrix} \ell & \ell' & L \\ 0 & 0 & 0 \end{pmatrix}^2 P_{\ell'}(k) \end{aligned}$$

Survey geometry effect

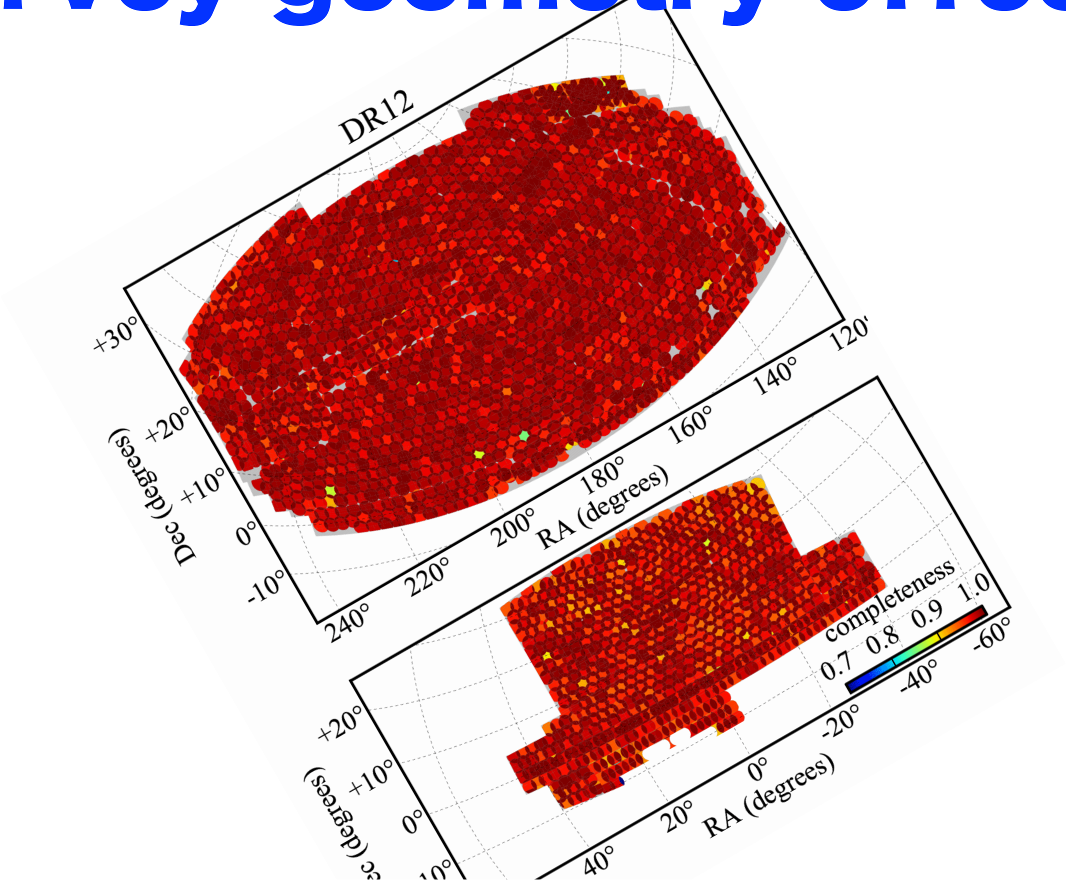

Survey geometry effect

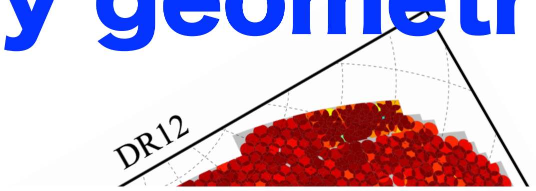

$$P_{\rm obs}(k) = \underbrace{W_{\rm aniso}}_{\text{Window effect}} \otimes \underbrace{P_{\rm iso}}_{\text{Signal}}$$

$$+ \; W_{\rm iso} \otimes \underbrace{P_{\rm aniso}}_{\text{What we want!}}$$

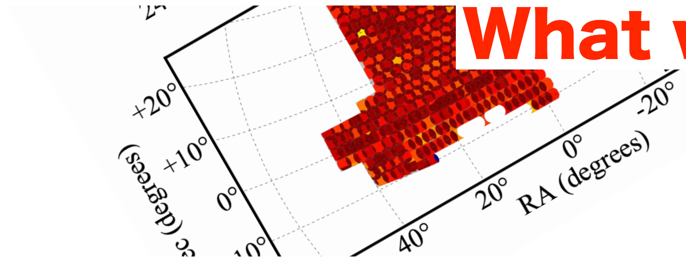

Power spectrum measurements

L = 2

M = -2,-1,0,1,2

SDSS DR12 BOSS

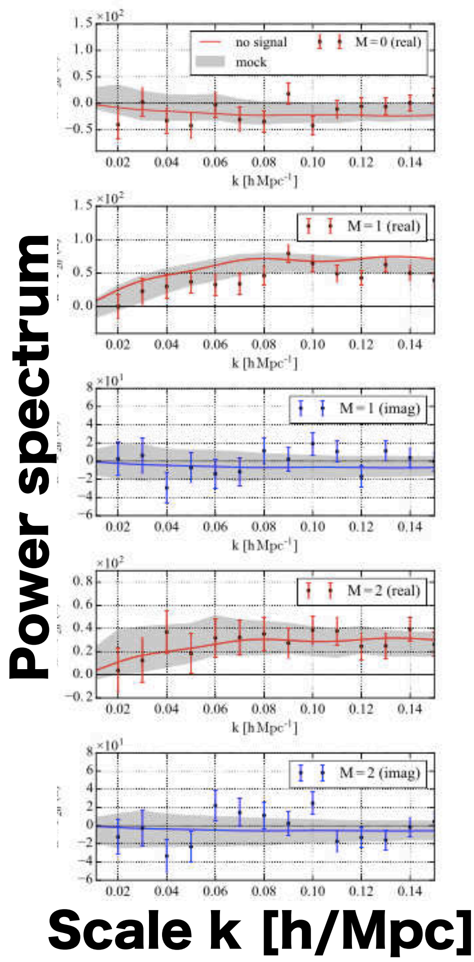

(L=2, M=2)

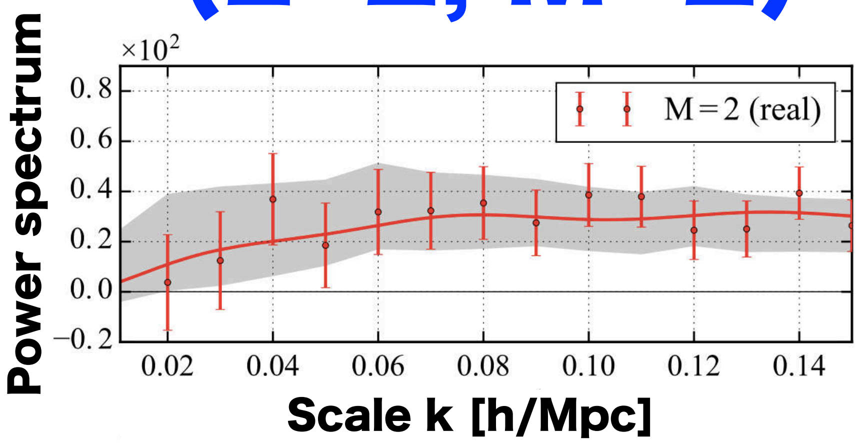

Shaded regions:

mocks without statistical anisotropic signal

Solid lines:

theory without statistical anisotropic signal

Data points:

observed data

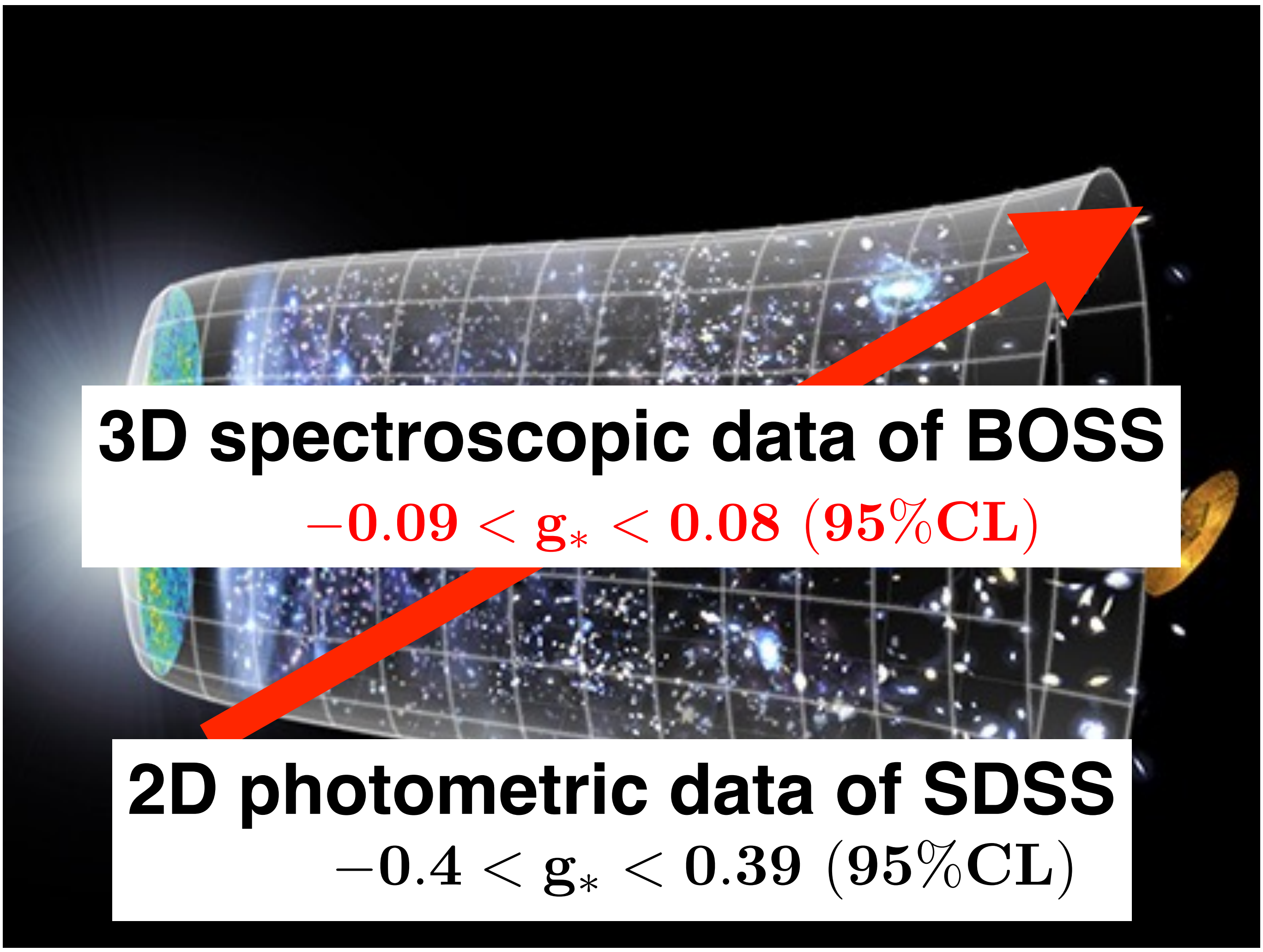

Future galaxy survey

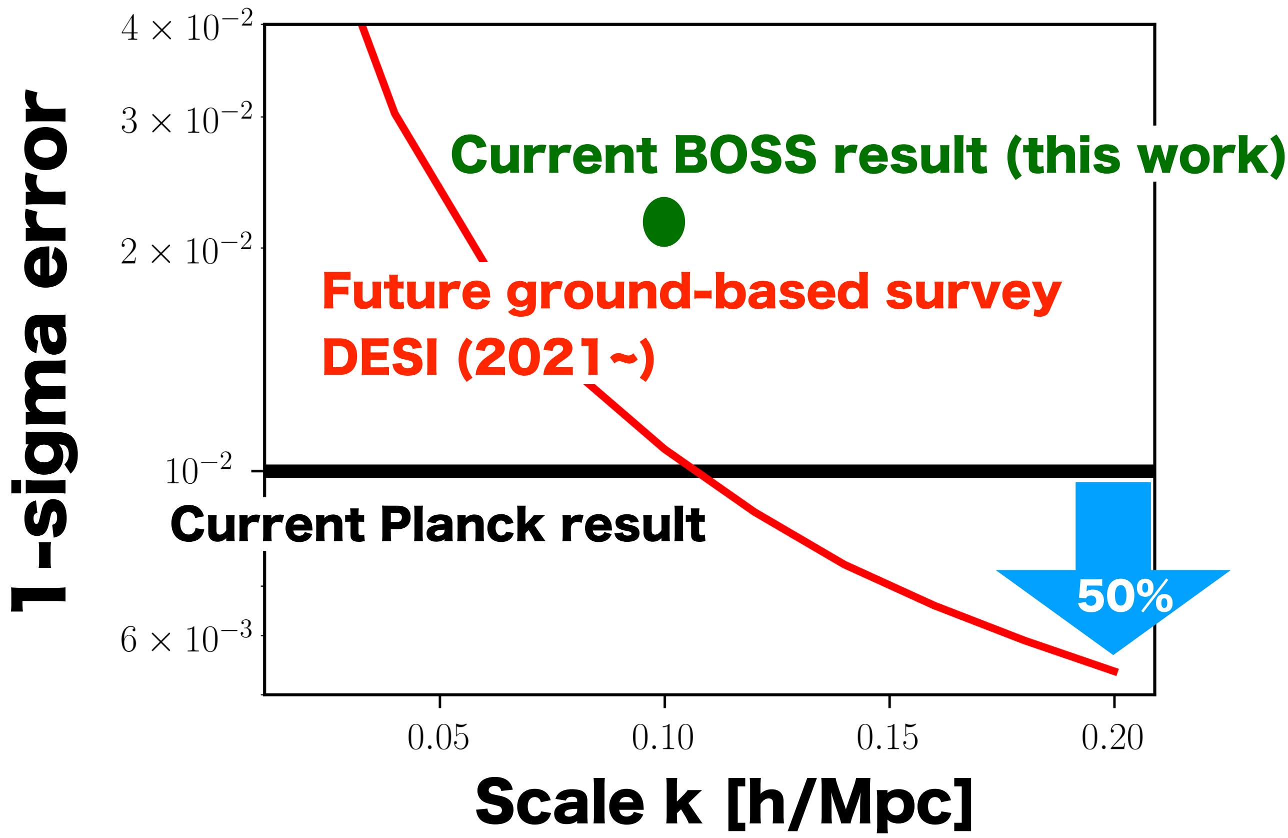

Summary

1) We proposed the **bipolar spherical harmonic** decomposition formalism to distinguish between the RSD effect and the primordial anisotropic signal.

2) We, **for the first time**, provided the constraint on the statistical anisotropic signal from 3D galaxy data (SDSS DR12).

3) While the current our constraint is weaker than the CMB result, **future galaxy surveys will provide the strongest constraint.**

arXiv:1612.02645 (Phys.Rev.D95, 063508)
arXiv:1704.02868 (MNRAS, 473, 2737-2752)

Session S1P2 16:45–18:30

[Chair: Kazuhiro Yamamoto]

Hayato Fukunaga

Nagoya University

“Flapping resonance instabilities and prospects on gravitational wave forest”

(10+5 min.)

[JGRG28 (2018) 110510]

JGRG @ Rikkyo University

2018 11/5

Flapping resonance instabilities and prospects on gravitational wave forest

Hayato Fukunaga (Nagoya University)

collaboration w/

Yuko Urakawa (Nagoya U. , Bielefeld U.)
Naoya Kitajima (Nagoya U.)

Motivation

black solid line : $\frac{1}{2}\mathrm{m}^2\phi^2$

There are many kinds of instabilities depending on models.

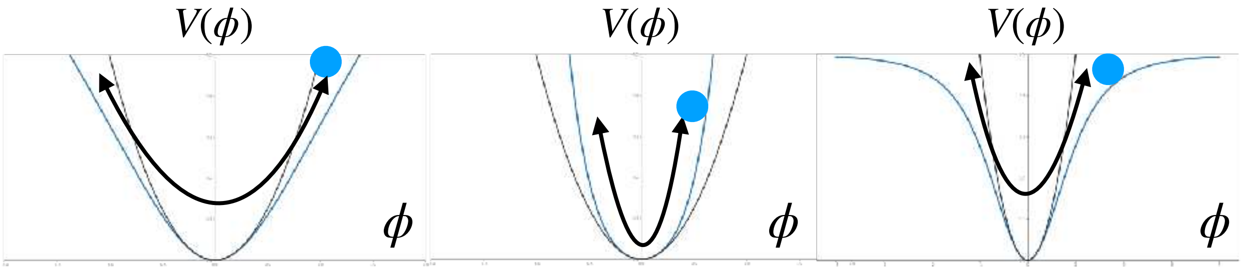

Narrow resonance   Broad resonance   Flapping resonance

Kitajima+ (18)

What is a new parameter which distinguish resonance instability ?

Resultant spectrums are different ?

Flapping Resonance

Kitajima et al. (18)

- tachyonic instability
- growth rate depends on k/am

$$\delta\ddot{\tilde{\phi}}_k + 3\frac{H}{m}\delta\dot{\tilde{\phi}}_k + \underbrace{\left[\left(\frac{k}{am}\right)^2 + \tilde{V}_{,\tilde{\phi}\tilde{\phi}}\right]}_{\equiv\, \omega_k^2}\delta\tilde{\phi}_k = 0$$

- tachy. inst.

if $\omega_k^2 < 0$ for modes

$$\frac{k}{am} < \sqrt{|\tilde{V}_{,\tilde{\phi}\tilde{\phi}}|}$$

-> grows exponentially

Oscillation between

$\tilde{V}_{,\tilde{\phi}\tilde{\phi}} < 0 \longleftrightarrow \tilde{V}_{,\tilde{\phi}\tilde{\phi}} > 0$

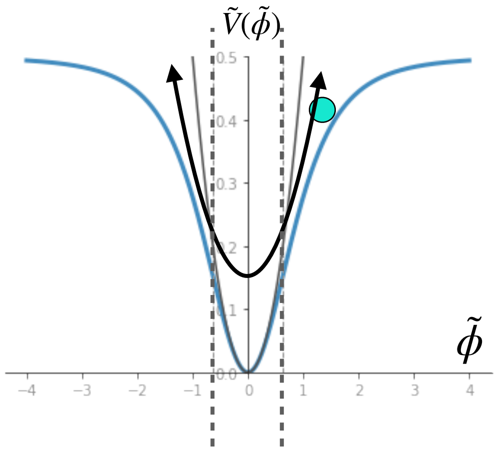

$\tilde{V}_{,\tilde{\phi}\tilde{\phi}} < 0$ $\tilde{V}_{,\tilde{\phi}\tilde{\phi}} > 0$ $\tilde{V}_{,\tilde{\phi}\tilde{\phi}} < 0$

$\omega_k^2 < 0$ $\omega_k^2 > 0$ $\omega_k^2 < 0$

Parametric resonance

Kofman et al. (97) ,etc...

Periodic external force (eg. swing)

→ **Enhancing the amplitude exponentially**

$$\delta\ddot{\tilde{\phi}}_k + (A_k - 2q\cos(2\tilde{t}))\delta\tilde{\phi}_k = 0$$

Mathieu equation

$q \ll 1$: Narrow resonance

$q \gg 1$: Broad resonance

Sustainable parametric res. for $H_{osc}/m \ll 1$

Narrow res. Broad res.

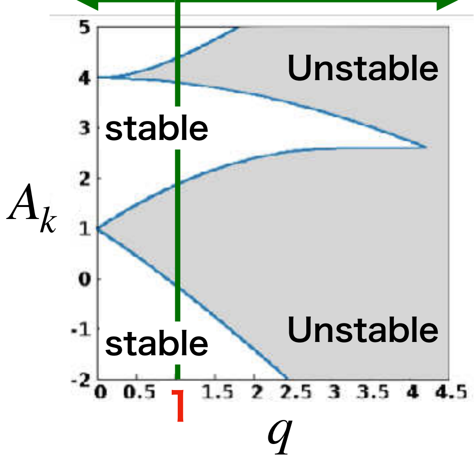

Parametric resonance

Periodic external force (eg. swing)

→ Enhancing the amplitude exponentially

We cannot apply parameter “q” to flapping resonance, which take place in anharmonic potential

$$\delta\phi_k + (A_k - 2q\cos(2t))\delta\phi_k = 0$$

Mathieu equation

$q \ll 1$: Narrow resonance
$q \gg 1$: Broad resonance

Sustainable parametric res. for $H_{osc}/m \ll 1$

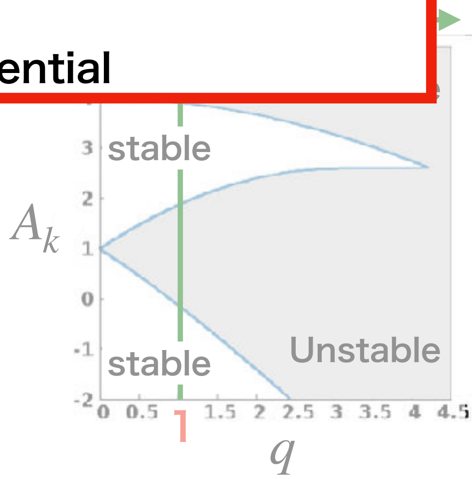

Classification

$$\ddot{\delta\tilde{\phi}}_k + 3\frac{H}{m}\dot{\delta\tilde{\phi}}_k + \left[\left(\frac{k}{am}\right)^2 + \tilde{V}_{,\tilde{\phi}\tilde{\phi}}\right]\delta\tilde{\phi}_k = 0$$

$$\frac{d^2f}{dz^2} + \omega^2 f = 0$$

- Mathieu eq. amp. of osc. term

$$\omega^2 = A - 2q\cos(2z)$$

applicable only this form

$$\begin{cases} q \ll 1 : \text{Narrow res.} \\ q \gg 1 : \text{Broad res.} \end{cases}$$

-general osc. eq.

include osc. term

$$\omega^2 = \left(\frac{k}{am}\right)^2 + \tilde{V}_{,\tilde{\phi}\tilde{\phi}}$$

amp.

$$\tilde{q} = \sqrt{\frac{<\tilde{V}_{,\tilde{\phi}\tilde{\phi}}^2> - <\tilde{V}_{,\tilde{\phi}\tilde{\phi}}>^2}{2}}$$

Classification

Fukunaga et al. (in progress)

$$\tilde{q} = \sqrt{\frac{< \tilde{V},^2_{\tilde{\phi}\tilde{\phi}} > - < \tilde{V},_{\tilde{\phi}\tilde{\phi}} >^2}{2}}$$

applicable to anharmonic potential

Intermediate res.	Narrow res.	Broad res.
$\tilde{q} \sim \mathcal{O}(1)$	$\tilde{q} \ll 1$	$\tilde{q} \gg 1$

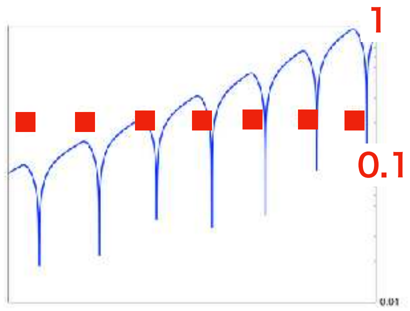

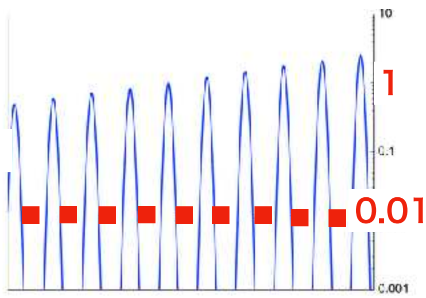

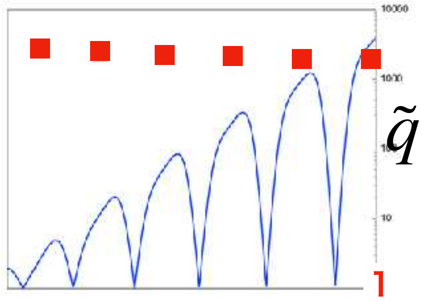

■ $\tilde{q}$ —— $|\delta\tilde{\phi}_k|$

* Intermediate res. ; if potential has $\tilde{V},_{\tilde{\phi}\tilde{\phi}} < 0$ region, flapping res. occurs

Spectrum

Fukunaga et al. (in progress)

$\tilde{q} \sim \mathcal{O}(1)$: Intermediate res.	$\tilde{q} \ll 1$: Narrow res.	$\tilde{q} \gg 1$: Broad res.
$\frac{k_{\rm peak}}{a_{\rm osc} m} \simeq \sqrt{\vert\tilde{V},^{(\rm plat)}_{\tilde{\phi}\tilde{\phi}}\vert}$ *Kitajima+ (18)*	$\frac{k_{\rm peak}}{a_{\rm osc} m} \simeq \sqrt{\frac{\tilde{q}}{2}}$	No peak

eg)

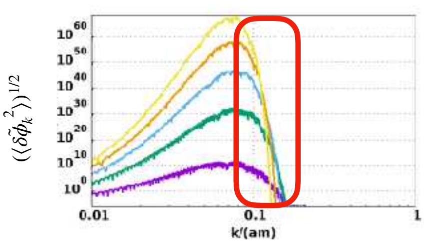

high-k->damp

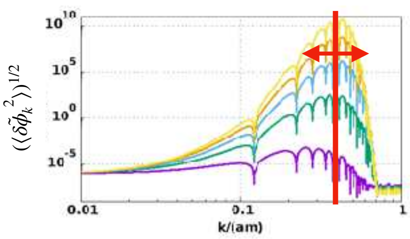

symmetry

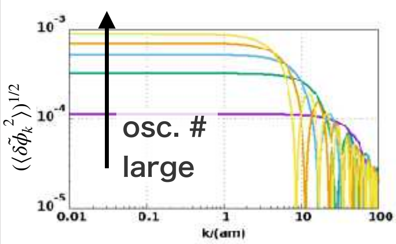

* if $H_{\rm osc}/m \ll 1$, narrow and flapping res. can continue longer

Growth rate

$\tilde{V}(\tilde{\phi}) = \frac{1}{2}\tilde{\phi}^2(1+\tilde{\phi}^2)^c$

Fukunaga et al. (in progress)

growth rate μ : $\delta\tilde{\phi}_k \propto e^{2\pi\mu N}$

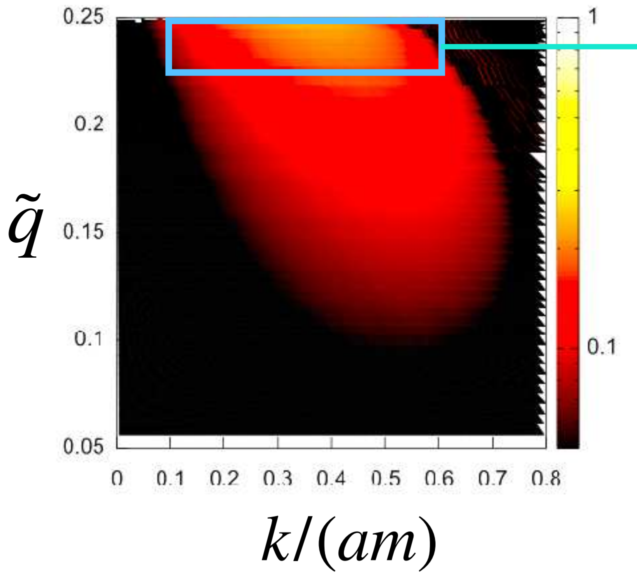

flapping res.

growth rate ~0.3

others : narrow res.

growth rate < 0.1

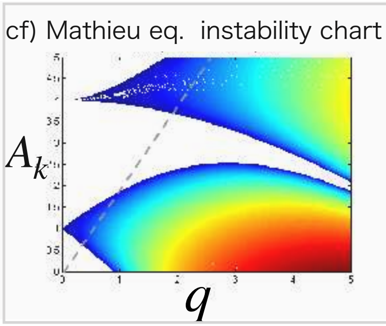

<u>Flapping res. leads to a rather efficient growth</u>

Cosine potential

$\tilde{V},_{\tilde{\phi}\tilde{\phi}} < 0$ region exist

-> flapping res. ?

$\tilde{V}(\tilde{\phi}) = 1 - \cos(\tilde{\phi})$

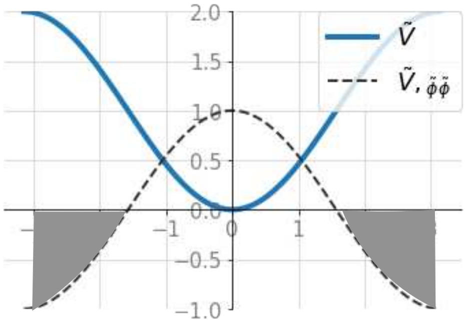

$H_{osc}/m \propto -1/\log(\dot{\tilde{\phi}}_i)$

Duration of flapping res. is short
even using tuned initial condition

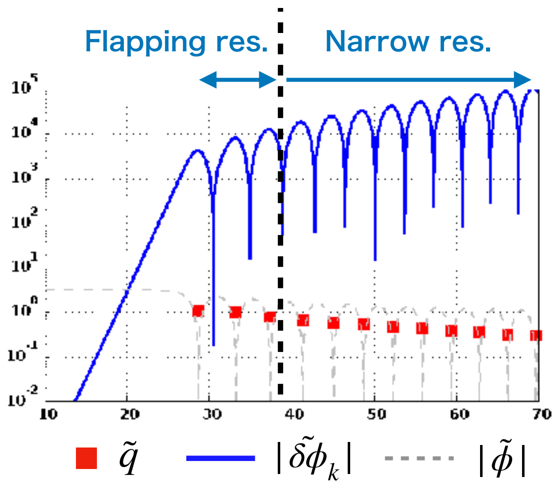

Cosine potential

Spectrum $\tilde{\phi}_i = \pi$

$\dot{\tilde{\phi}}_i = 10^{-5}$ $\dot{\tilde{\phi}}_i = 10^{-10}$

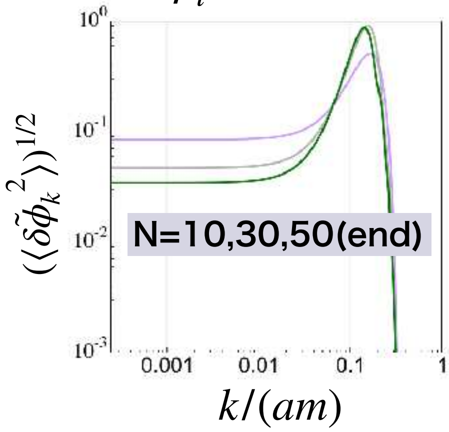

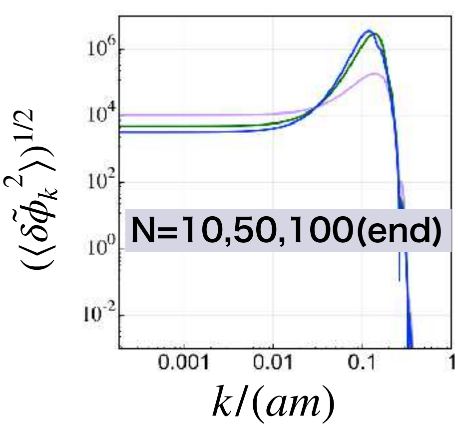

Initial velocity small -> Duration of narrow res. slightly long.

GW prospect

Future work

$$\Box h_{ij} = \frac{2}{M_p^2} T_{ij}$$

source term

$$T_{ij} \sim \partial_i \delta\phi \partial_j \delta\phi$$

$\downarrow$ sufficient growth

new way for axion search

Some information about linear analysis (spectrum shape, peak) can be propagated.

* We are planning to calculate GW spectrum using lattice simulation in future work

Summary and future works

- Proposal of new parameter

$$\tilde{q} \ll 1 \ : \ \text{Narrow res.}$$
$$\tilde{q} \gg 1 \ : \ \text{Broad res.}$$
$$\tilde{q} \sim \mathcal{O}(1) \ : \ \text{Intermediate res.}$$

  - Applicable to anharmonic background
  - Flapping resonance, which is an efficient mechanism of GW emission takes place for $\tilde{q} = \mathcal{O}(1)$

- In axion context, using conventional cosine potential, duration of flapping res. is short even using tuned initial condition.

Future works

Different resonance types lead to different non-linear dynamics and GW spectrums?

back-up slides

back-up

Normalization

Klein-Gordon eq.

ϕ : scalar field
f : decay const.
H : Hubble parameter
a : scale factor
p : 1/2 (radiation dominate)

Background

$$\partial_t^2\phi + 3H\partial_t\phi + V,_\phi = 0$$

Fourier mode of linear perturbation

$$\partial_t^2(\delta\phi_k) + 3H\partial_t(\delta\phi_k) + \left[\left(\frac{k}{a}\right)^2 + V,_{\phi\phi}\right]\delta\phi_k = 0$$

Using dimension-less variables

$$\tilde{t} \equiv mt \qquad \tilde{\phi} \equiv \frac{\phi}{f} \qquad V(\phi) = m^2 f^2 \tilde{V}(\tilde{\phi}) \qquad a \propto (mt)^p,\ H = \frac{p}{t}$$

$$\partial_{\tilde{t}}^2\tilde{\phi} + 3\frac{p}{\tilde{t}}\partial_{\tilde{t}}\tilde{\phi} + \tilde{V},_{\tilde{\phi}} = 0$$

$$\partial_{\tilde{t}}^2(\tilde{\delta\phi}_k) + 3\frac{p}{\tilde{t}}\partial_{\tilde{t}}(\tilde{\delta\phi}_k) + \left[\left(\frac{k}{am}\right)^2 + \tilde{V},_{\tilde{\phi}\tilde{\phi}}\right]\tilde{\delta\phi}_k = 0$$

back-up

String Axiverse

Arvanitaki et al. (10)

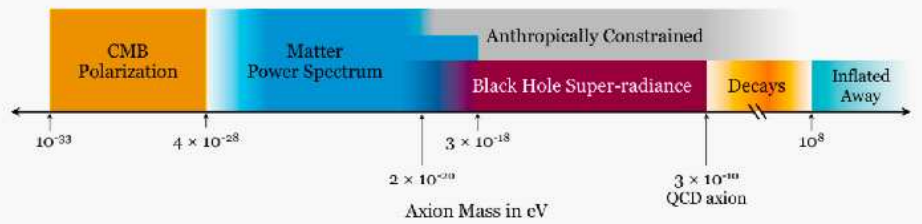

Figure 1: **Map of the Axiverse:** The signatures of axions as a function of their mass, assuming $f_a \approx M_{GUT}$ and $H_{inf} \sim 10^8$ eV. We also show the regions for which the axion initial angles are anthropically constrained not to over-close the Universe, and axions diluted away by inflation. For the same value of f_a we give the QCD axion mass. The beginning of the anthropic mass region (2×10^{-20} eV) as well as that of the region probed by density perturbations (4×10^{-28} eV) are blurred as they depend on the details of the axion cosmological evolution (see Section 2.3). 3×10^{-18} eV is the ultimate reach of density perturbation measurements with 21 cm line observations. The lower reach from black hole super-radiance is also blurred as it depends on the details of the axion instability evolution (see Section 2.5). The region marked as "Decays", outlines very roughly the mass range within which we expect bounds or signatures from axions decaying to photons, if they couple to $\vec{E} \cdot \vec{B}$. We will discuss axion decays in detail in a companion paper.

Neglect back-reaction on geometry

⟶ Axion's dynamics is independent of (m, f)

We can search axions with wide mass range !

back-up

GW forest

$$\nu_0 \propto \left(\frac{m}{H_{\rm rm}}\right)^{1/2} \left(\frac{m}{10^{-12}{\rm eV}}\right)^{1/2}$$

Kitajima et al. (18)

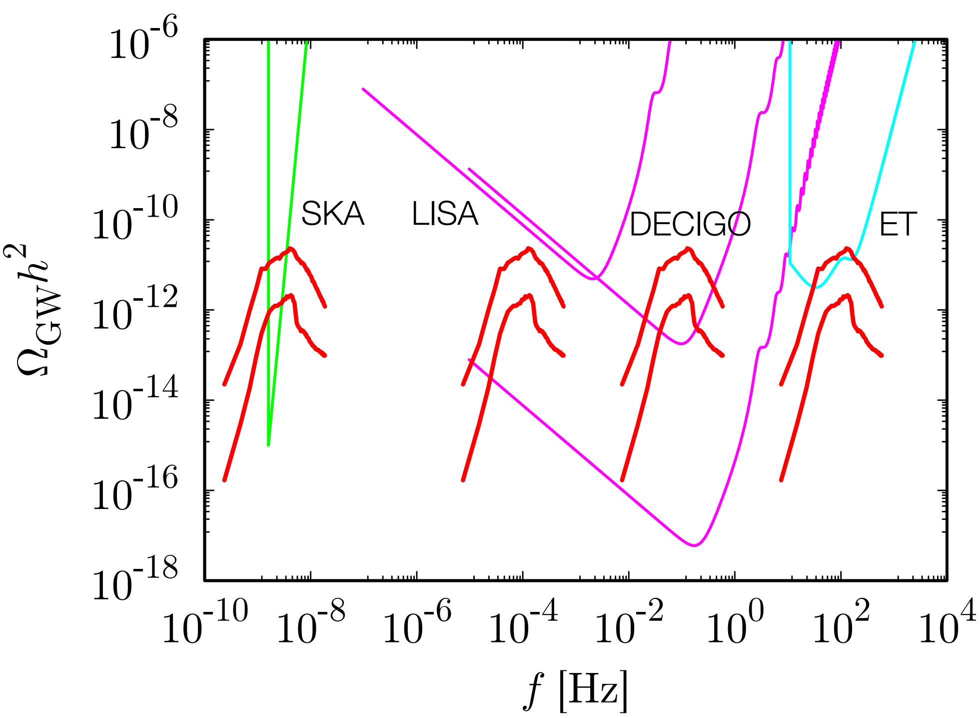

back-up

Phases of instability

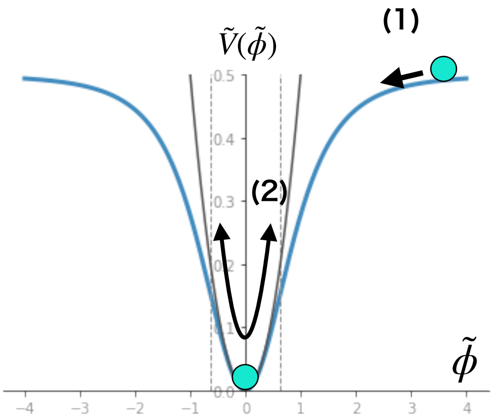

(3)* Oscillation in $\tilde{V},_{\tilde{\phi}\tilde{\phi}} > 0$

$|1-\tilde{V},_{\tilde{\phi}\tilde{\phi}}| > 1$

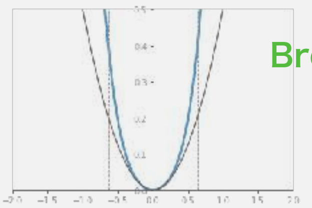

Broad res.

$\tilde{t}_{\rm osc}$

(1) Slowly rolling down in $\tilde{V},_{\tilde{\phi}\tilde{\phi}} < 0$

Tachyonic inst.

(2) Oscillation between

$$\tilde{V},_{\tilde{\phi}\tilde{\phi}} < 0 \longleftrightarrow \tilde{V},_{\tilde{\phi}\tilde{\phi}} > 0$$

Flapping res.

(3) Oscillation in $\tilde{V},_{\tilde{\phi}\tilde{\phi}} > 0$

$|1-\tilde{V},_{\tilde{\phi}\tilde{\phi}}| < 1$

Narrow res.

Flapping res. -> Narrow res.

-> Broad res.

back-up

GW spectrum

$$h_{ij} \propto \int \frac{d^3\mathbf{p}}{(2\pi)^{3/2}} p_l p_m \delta\phi(\mathbf{p})\delta\phi(\mathbf{k}-\mathbf{p})$$

peak and shape of GW spectrum ~ spectrum of $\delta\phi_k$

eg) spectrum peak

$$\frac{\omega}{m} = \frac{k^{\rm em}_{\rm peak}}{m a_{\rm em}} = \frac{k^{\rm res}_{\rm peak}}{m a_{\rm res}} \times \frac{k^{\rm em}_{\rm peak}/a_{\rm em}}{k^{\rm res}_{\rm peak}/a_{\rm res}}$$

momentum flow

described in terms of “$\tilde{q}$”

back-up

Oscillon formation

Kitajima et al. (18)

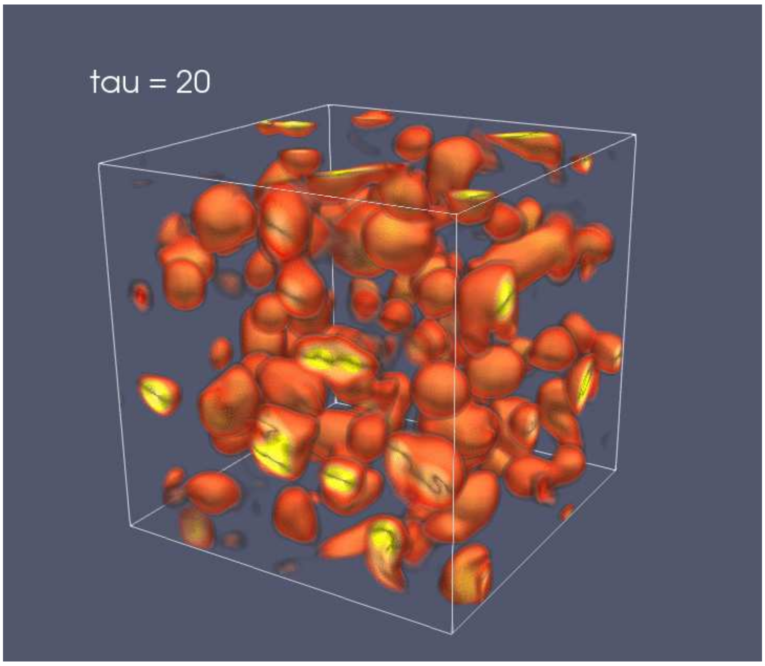

back-up

Growth rate and Spectrum

Flapping res. / Narrow res.

Flapping res. $\tilde V(\tilde\phi) = \frac{1}{2}\left(1 - \frac{1}{(1+\tilde\phi^2/c)^c}\right)$

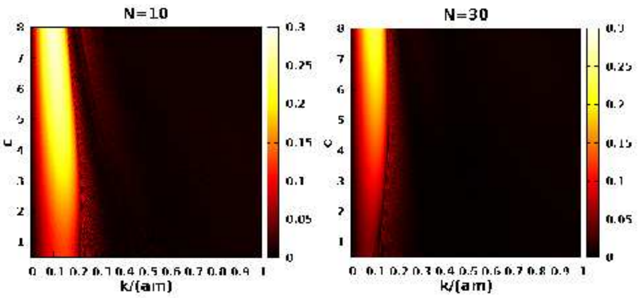

large c -> Hosc/m small

-> sustainable

growth rate ~ 0.3

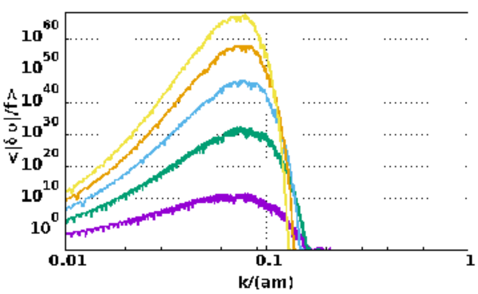

Narrow res. $\tilde V(\tilde\phi) = \frac{1}{2}\tilde\phi^2(1+\tilde\phi^2)^c$

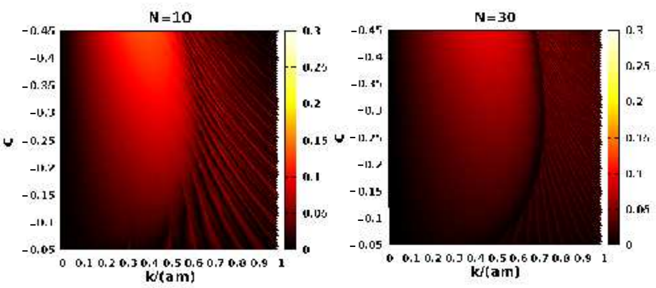

small c -> Hosc/m small

-> sustainable

growth rate ~ 0.1

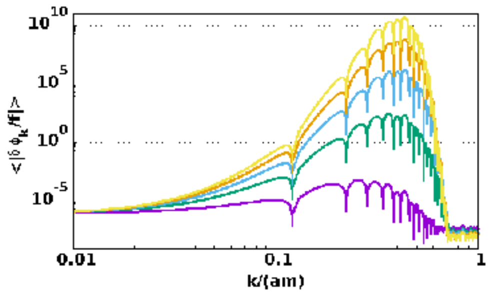

back-up

Growth rate and Spectrum

Broad res.

Broad res. $\tilde{V}(\tilde{\phi}) = \frac{1}{2}\tilde{\phi}^2(1+\tilde{\phi}^2)^c$

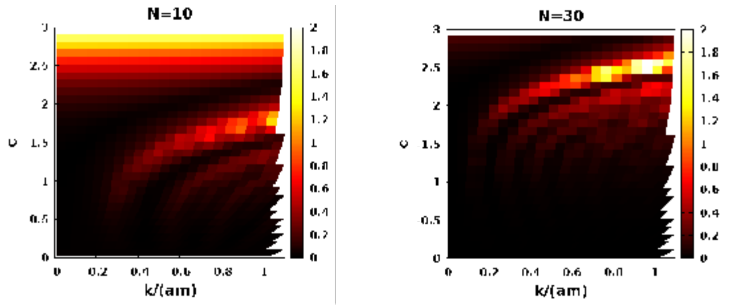

growth rate is larger than flapping res.

but not sustainable

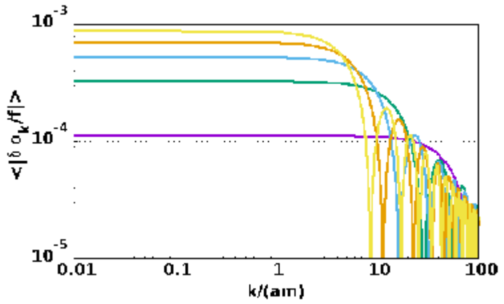

* no self-interaction in $|\tilde{\phi}| \ll 1$ -> broad res. cannot continue

back-up

Cosine potential

tuning initial velocity $\dot{\tilde{\phi}}|_{\tilde{t}_i}$,

$$H_{osc}/m \propto -1/\log(\dot{\tilde{\phi}}_i)$$

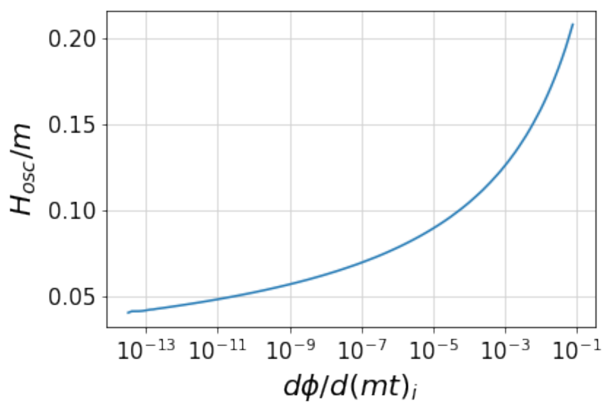

back-up

Cosine potential

During flapping res.   During narrow res.

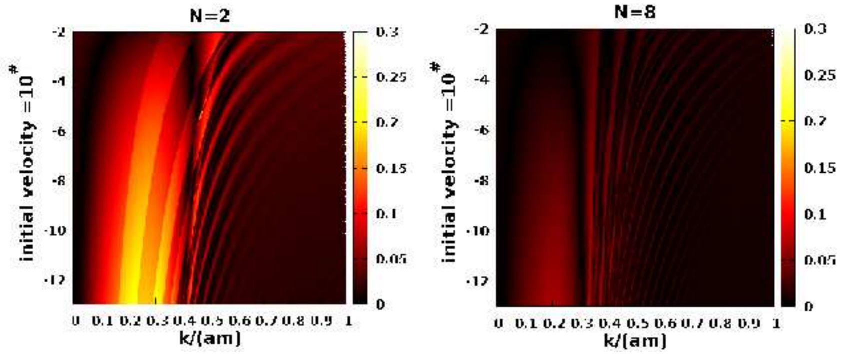

$\dot{\tilde{\phi}}_i = 10^{-5}$ $\dot{\tilde{\phi}}_i = 10^{-10}$

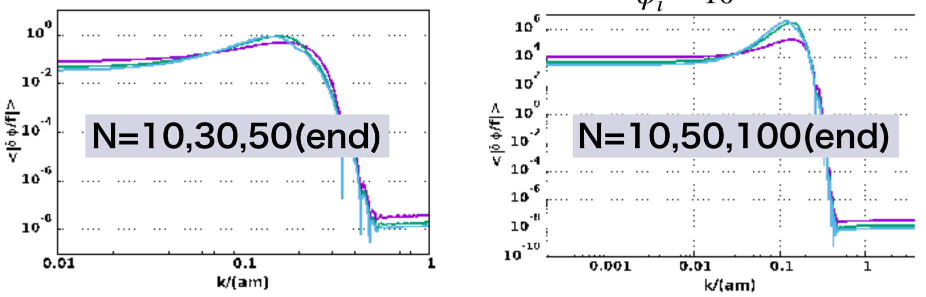

initial velocity small -> duration of narrow res. slightly longer

back-up

Growth rate

Narrow res. , Broad res.

$$\tilde{V}(\tilde{\phi}) = \frac{1}{2}\tilde{\phi}^2(1+\tilde{\phi}^2)^c$$

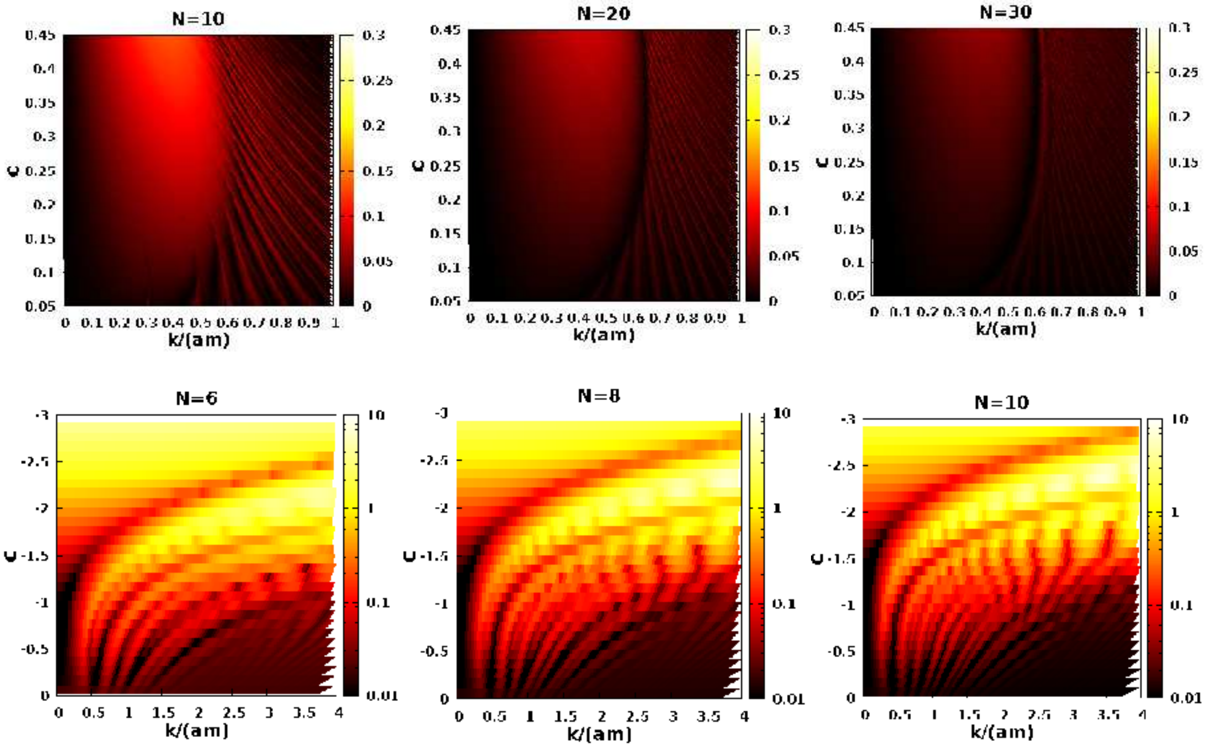

back-up

Growth rate

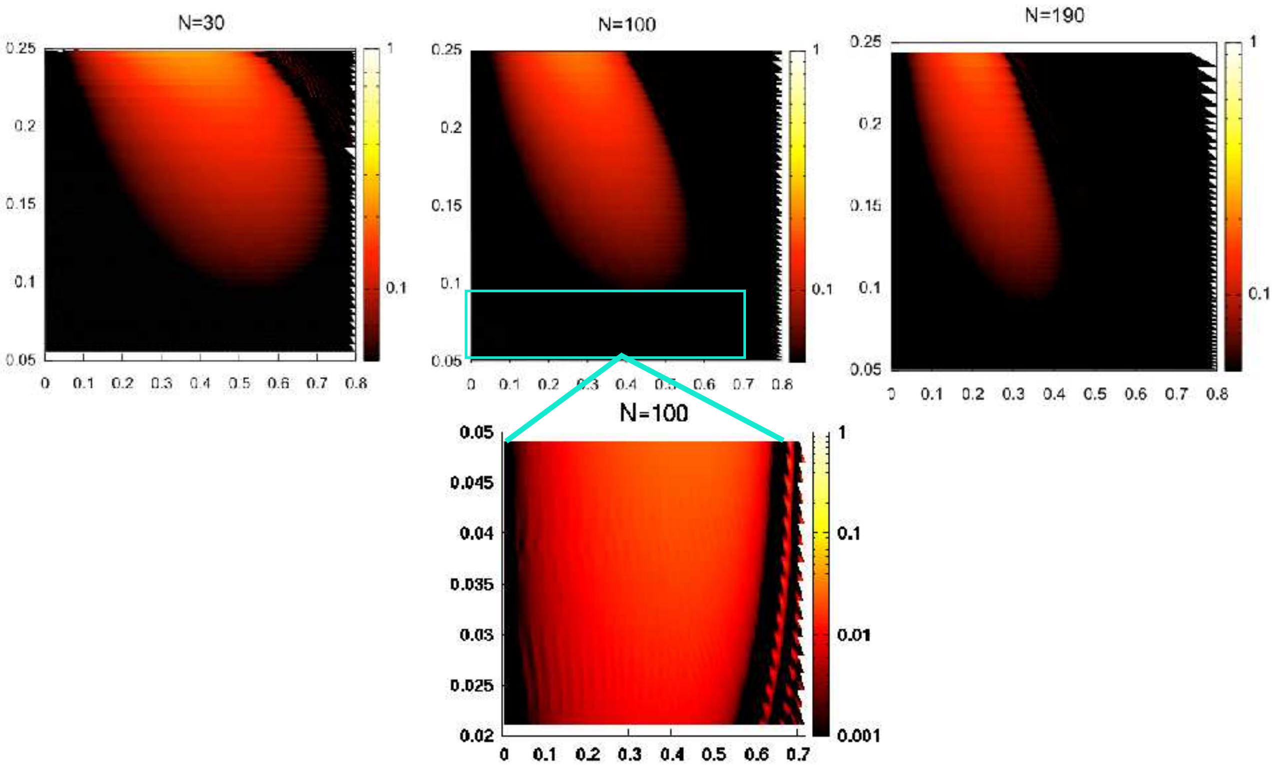

back-up

Parametric resonance

black dashed line : $\frac{1}{2}\mathrm{m}^2\phi^2$

$$\tilde{V}(\tilde{\phi}) = \frac{1}{2}\tilde{\phi}^2 + \frac{1}{4!}\lambda\phi^4 + \mathcal{O}(\tilde{\phi}^6)$$

$$q \sim \frac{\tilde{V},_{\tilde{\phi}\tilde{\phi}} - 1}{4}$$

$q \gg 1$: Broad resonance

$q \ll 1$: Narrow resonance

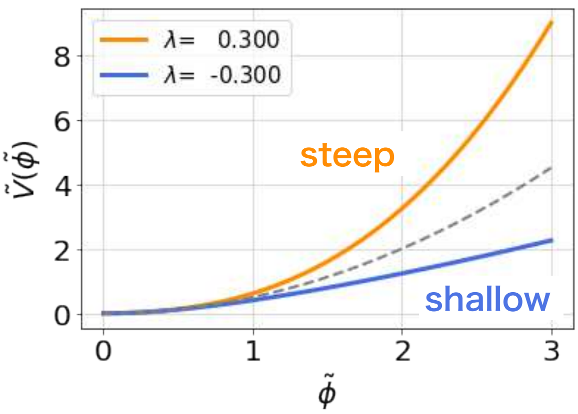

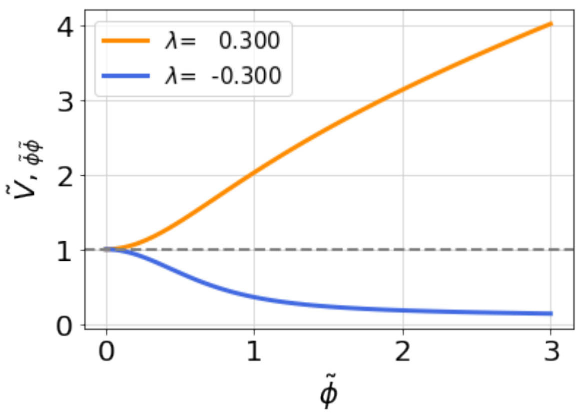

back-up

Spectrum

Fukunaga et al. (in progress)

$\tilde{q} \sim \mathcal{O}(1)$: Intermediate res.	$\tilde{q} \ll 1$: Narrow res.	$\tilde{q} \gg 1$: Broad res.
$\frac{k_{\rm peak}}{a_{\rm osc} m} \simeq \sqrt{\lvert \tilde{V}, ^{\rm (plat)}_{\tilde{\phi}\tilde{\phi}} \rvert}$ *Kitajima+ (18)*	$\frac{k_{\rm peak}}{a_{\rm osc} m} \simeq \sqrt{\frac{\tilde{q}}{2}}$	**No peak**

eg)

	$\tilde{V}(\tilde{\phi}) = \frac{1}{2}\tilde{\phi}^2(1+\tilde{\phi}^2)^c$ (-0.47<c<0)	$\tilde{V}(\tilde{\phi}) = \frac{1}{2}\tilde{\phi}^2(1+\tilde{\phi}^2)^c$ (0<c)

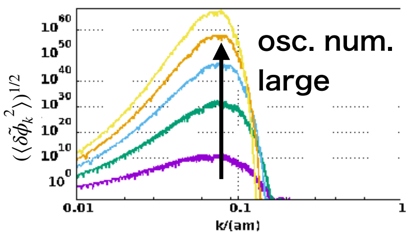

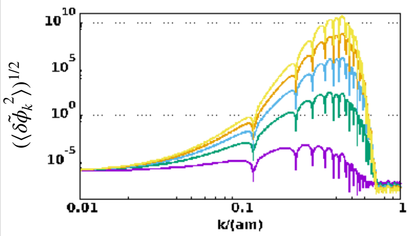

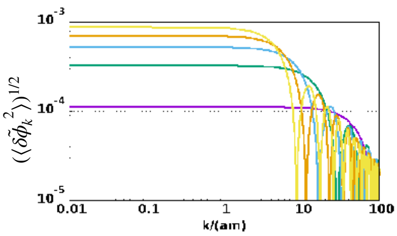

* if $H_{\rm osc}/m \ll 1$, narrow and flapping res. can continue longer

back-up

Intermediate resonance

$\tilde{V}, _{\tilde{\phi}\tilde{\phi}} < 0$	$\cancel{\tilde{V}, _{\tilde{\phi}\tilde{\phi}} < 0}$
flapping resonance	mild flapping resonance

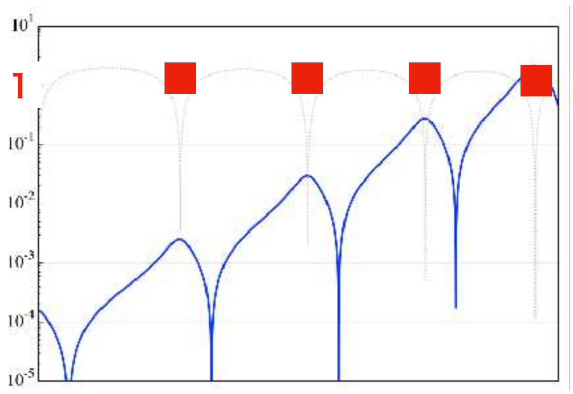

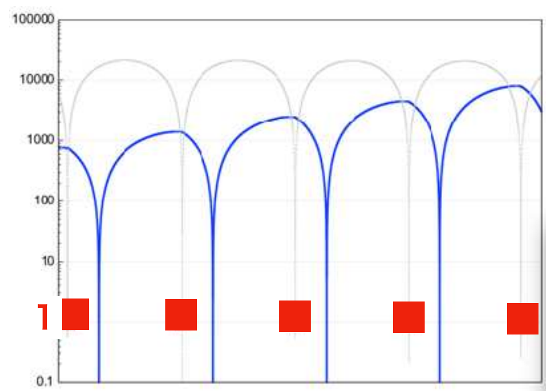

■ $\tilde{q}$ —— $\lvert \delta\tilde{\phi}_k \rvert$ - - - - $\lvert \tilde{\phi} \rvert$

both of two case $\tilde{q} \sim \mathcal{O}(1)$ but,

growth rate of flapping res. is much larger than mild flapping res.

Model pure natural inflation

$$\tilde{V}(\tilde{\phi}) = \frac{1}{2}\left(1 - \frac{1}{(1+\tilde{\phi}^2/c)^c}\right)$$

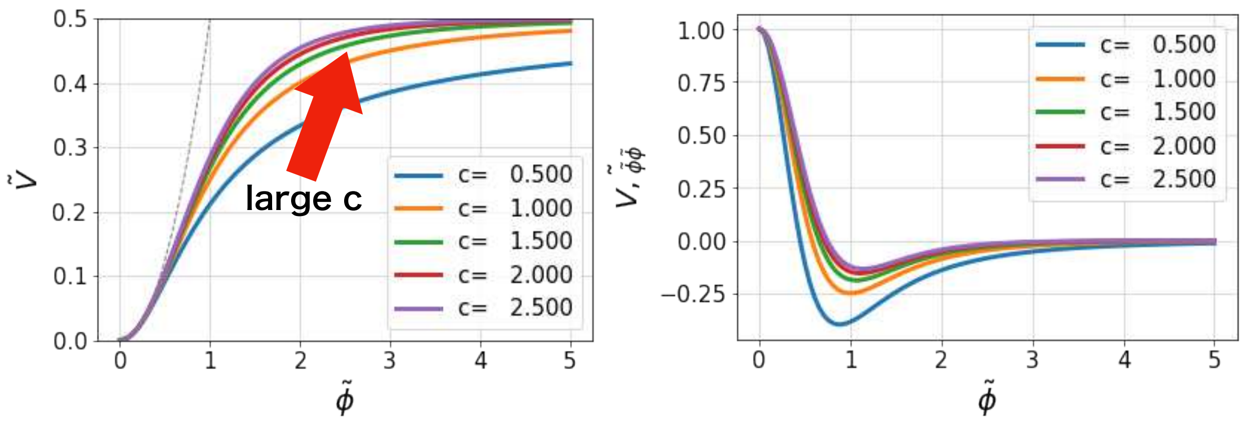

larger c -> more plateau -> Hosc/m small

Model power-law type potential

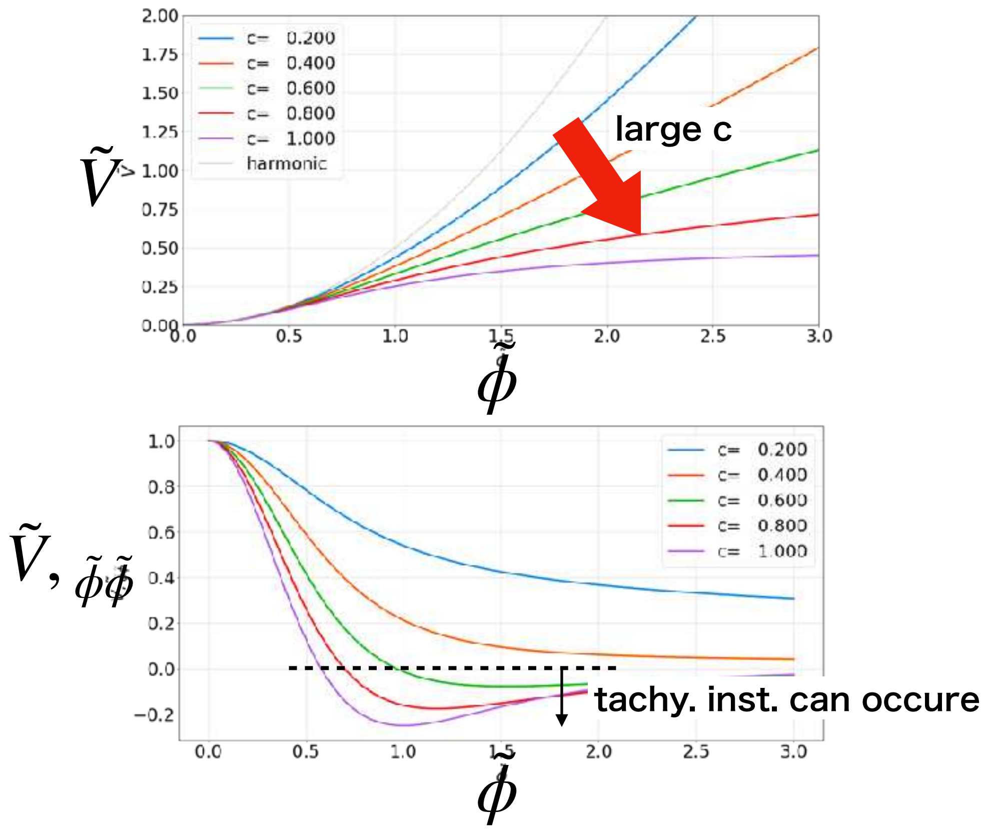

back-up

Narrow resonance

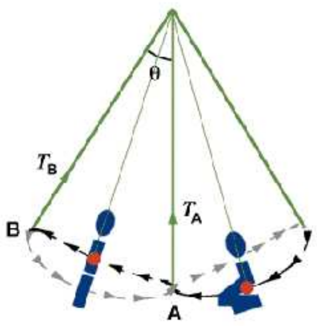

Repeat: Up & Down in a half of osc. period

→ Periodic ext. force

→ Enhancing the amplitude

Narrow resonance instability

Sustainable narrow resonance for H_{osc}/m<<1

Soda & Urakawa (17)

1) Redshift of modes in resonance band is inefficient.

2) Growth rate does not decrease over many oscillations.

$\delta\phi \propto e^{\gamma m t}$ ex. First band $\gamma \simeq \frac{q}{2} \propto \tilde{\phi}^2$

Flapping resonance instability

Kitajima, Soda & Y.U. (18)

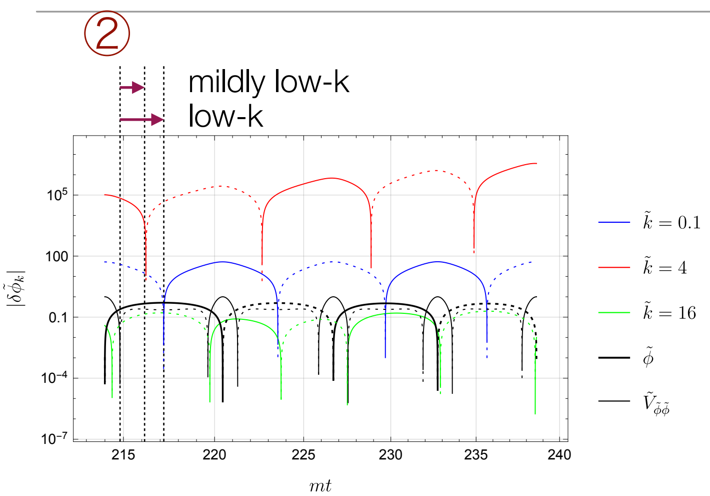

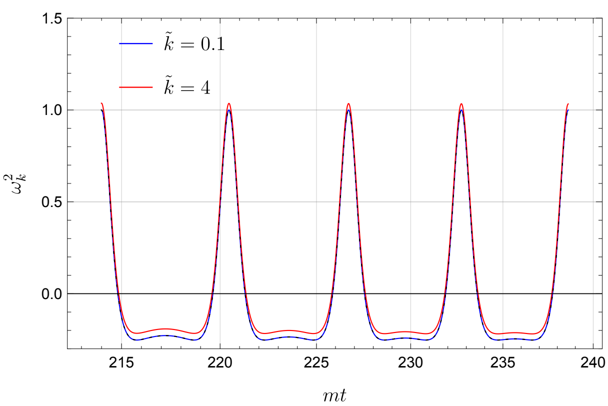

- For tachyonic instability $\frac{k}{am} \leq \sqrt{|\tilde{V}_{\tilde{\phi}\tilde{\phi}}|}$

- To shorten ② , larger *k*

$\Bigg\} \longrightarrow \frac{k_{\rm peak}}{a_{\rm res} m} \simeq \sqrt{|\tilde{V}^{(\rm plat)}_{\tilde{\phi}\tilde{\phi}}|}$

peak !!

Difference value of q

flapping res.
-> adiabatic condition is violated

narrow res.
-> adi. condition is not violated

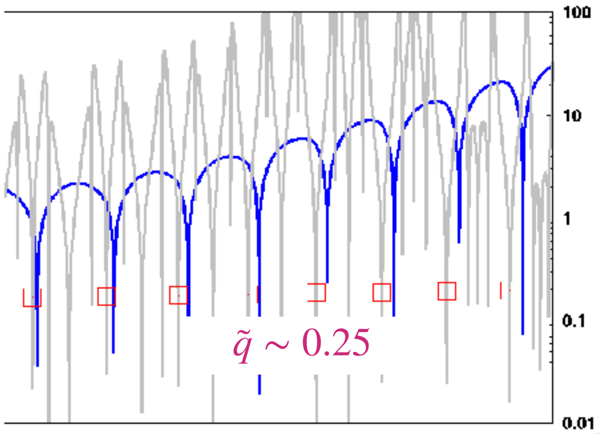

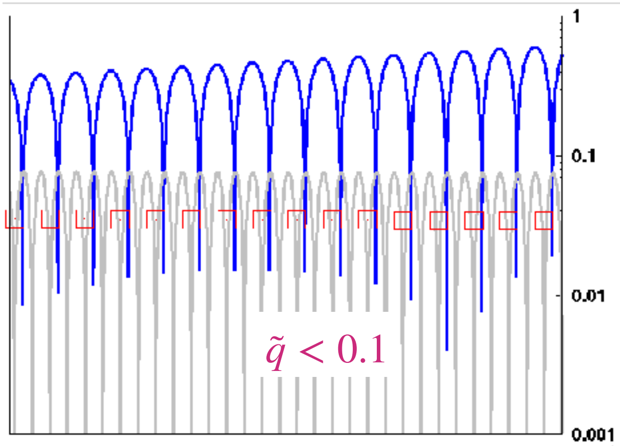

□ $\tilde{q}$ — $|\delta\tilde{\phi}_k|$ — adi. condition

Hiromasa Nakatsuka
ICRR,UTokyo

"Primordial black holes in an axion-like curvaton model"

(10+5 min.)

[JGRG28 (2018) 110514]

JGRG

Primordial black holes in an axion-like curvaton model

ICRR theory group M2

Hiromasa Nakatsuka (中塚洋佑)

Today's talk

- Formation of primordial black holes in an axionlike curvaton model
  Kenta Ando, Masahiro Kawasaki, and Hiromasa Nakatsuka
  Phys. Rev. D **98**, 083508

2018/11/05 Rikkyo University

Motivations of PBH study

- Binary BHs in the LIGO-Virgo
  - Relatively heavy mass?
  - $M_{PBH} = 30M_\odot \Leftrightarrow T = 50\mathrm{MeV}$
  - Binary formation in early universe
    [M. Sasaki, et. al., Phys. Rev. Lett. 117, 061101 (2016)]

LIGO event rate $\Leftrightarrow \frac{\Omega_{PBH}}{\Omega_{DM}} = 10^{-3}$

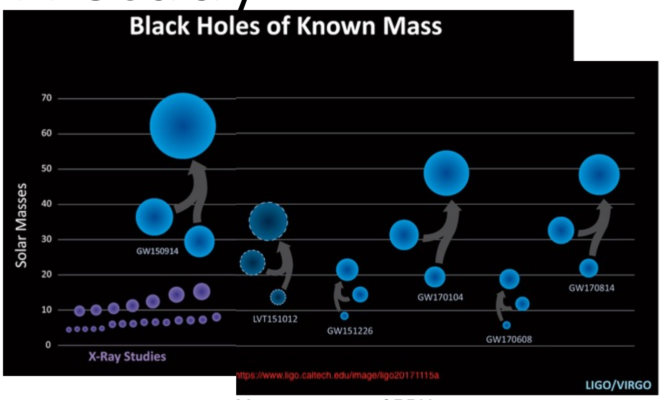

- PBH as Dark Matter
  - $\frac{\Omega_{PBH}}{\Omega_{DM}} = 1$
  - $M_{PBH} = 10^{-12}M_\odot$
    $\Leftrightarrow T = 10^5\mathrm{GeV}$

- PBHs on limited mass range
  ⇔ Curvature perturbation
  with peak-like spectrum

Mass spectrum of PBH

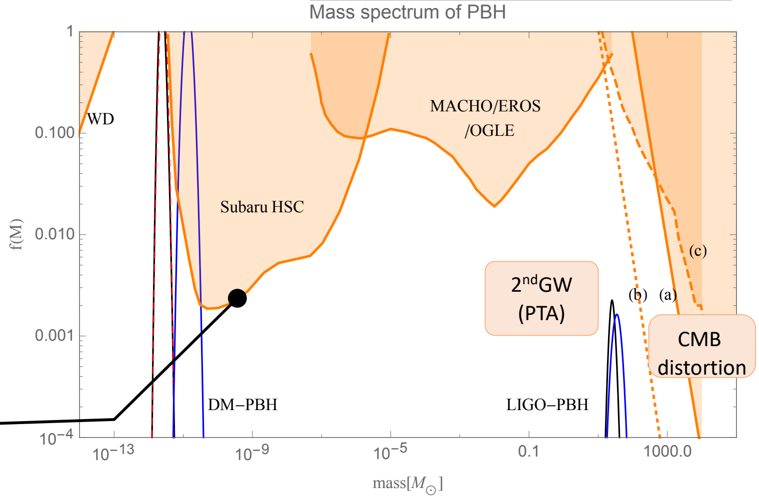

H. Niikura, M. Takada, N. Yasuda, R. H. Lupton, T. Sumi, S. More, A. More, M. Oguri, and M. Chiba, (2017), arXiv:1701.02151 [astro-ph.CO].

Primordial black holes in an axion-like curvaton model

- Motivations
- Perturbations $\mathcal{P}_\zeta(k)$ in our model

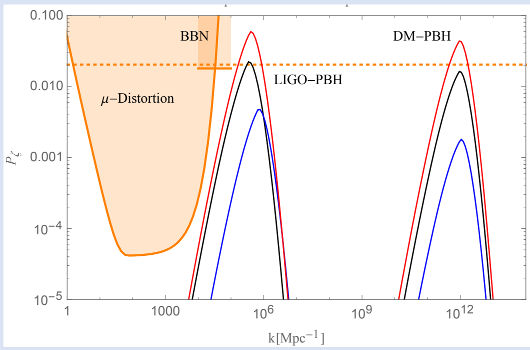

- PBH formation & 2nd GW
- Statistical property of the perturbations
- Conclusion

The mechanism of our model

- Axion-like curvaton model + inflaton coupling

● inflaton I ⇒ Inflation & CMB $(1\mathrm{Mpc} \sim\ 10^3\mathrm{Mpc})$

● complex scalar Φ with Higgs-like potential and

$$V_\Phi = g\, I^2|\Phi|^2 + \frac{\lambda}{4}\left(|\Phi|^2 - \frac{v^2}{2}\right)^2 - v^3\epsilon(\Phi+\Phi^*)$$

⇒ Small scale perturbation

Inflaton coupling

Higgs-like potential

Bias term

- To solve Cosmic string problem
- To avoid stochastic region

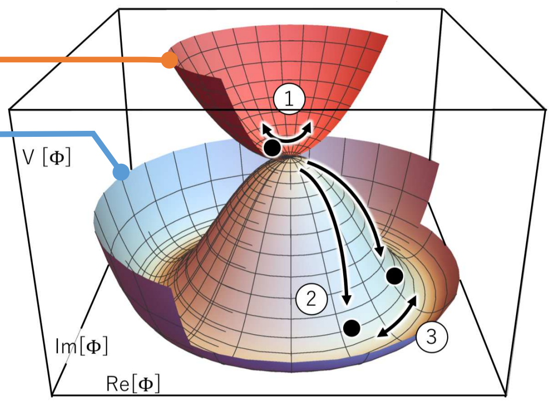

Perturbations of $\Phi = \frac{\varphi}{\sqrt{2}} e^{i\tilde{\sigma}/\varphi}$

- Hubble perturbations
  - Generated at horizon crossing
  - $\left(\frac{H}{2\pi}\right)^2 = \mathcal{P}_\varphi = \mathcal{P}_{\tilde{\sigma}} = 2|\Phi|^2\mathcal{P}_\theta$
  - $\mathcal{P}_\theta(\mathrm{k}) = \left(\frac{H(t_k)}{2\pi}\right)^2 \frac{1}{2|\Phi(t_k)|^2}$

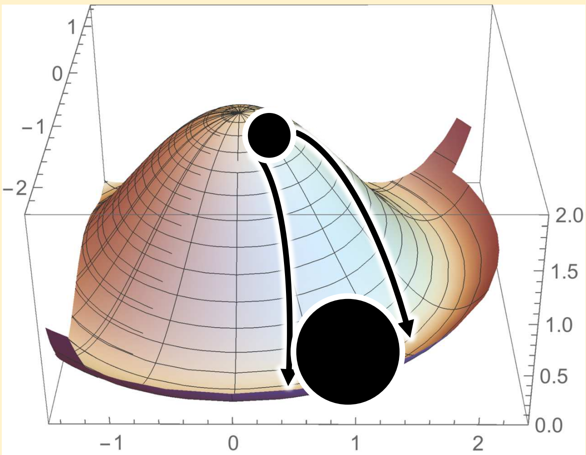

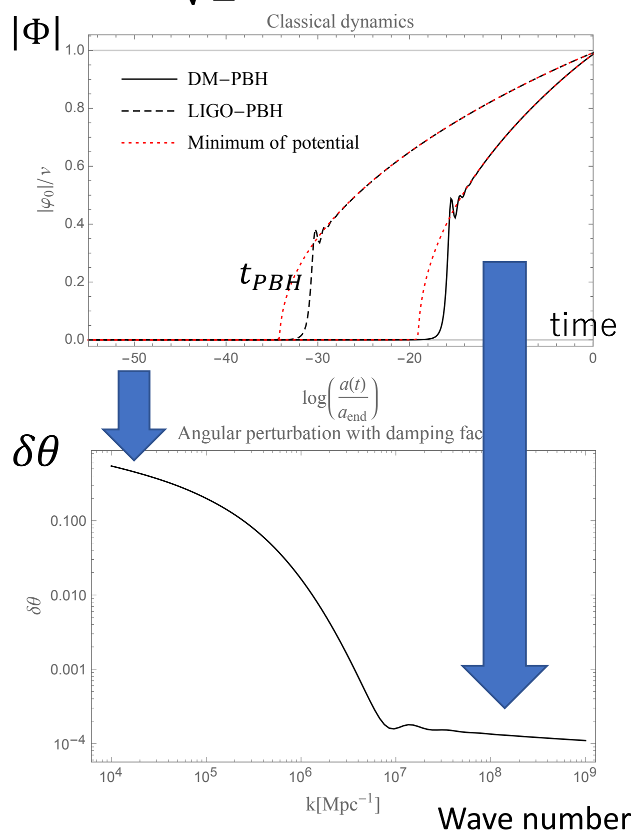

Perturbations of $\Phi = \frac{\varphi}{\sqrt{2}} e^{i\tilde{\sigma}/\varphi}$

- Hubble friction

$$\left(\partial_t^2 + \boxed{3H\partial_t} + a^{-2}k^2 + m_{eff}^2\right)\delta\Phi_k = 0$$

  - At ①, $m_{eff}^2 > \mathrm{H}^2$,
  - Φ oscillates and Hubble friction decreases $\delta\Phi$

$$\delta\Phi(\mathrm{k}) \propto \boxed{\frac{3}{2}\ln\left(\frac{k}{k_{PBH}}\right)}$$

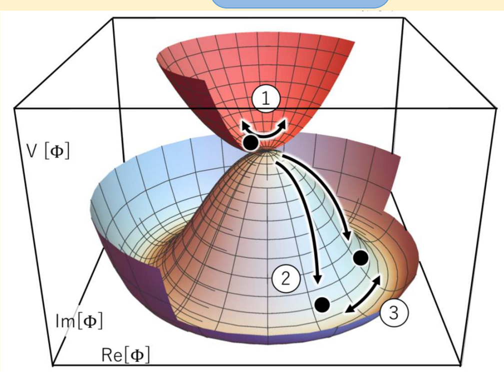

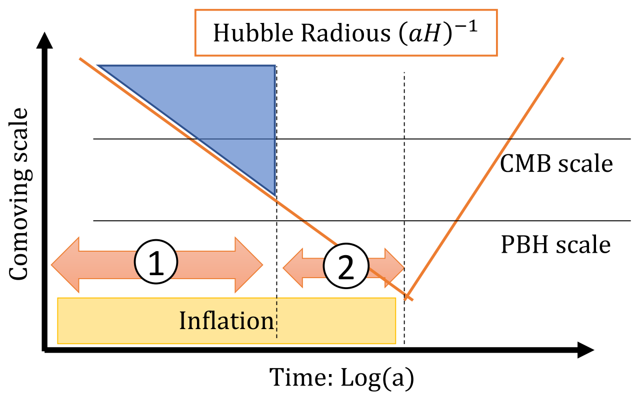

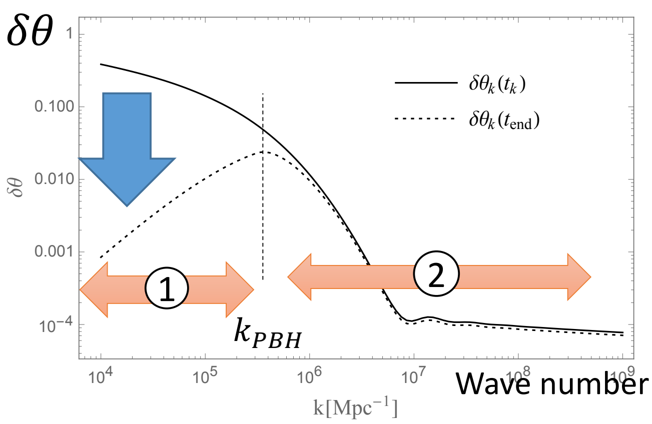

Evaluation of PBH formation rate

$\mathcal{P}_\zeta(k)$: curvature power spectrum

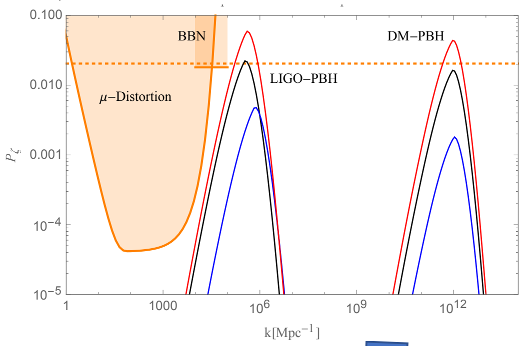

$f(M)$

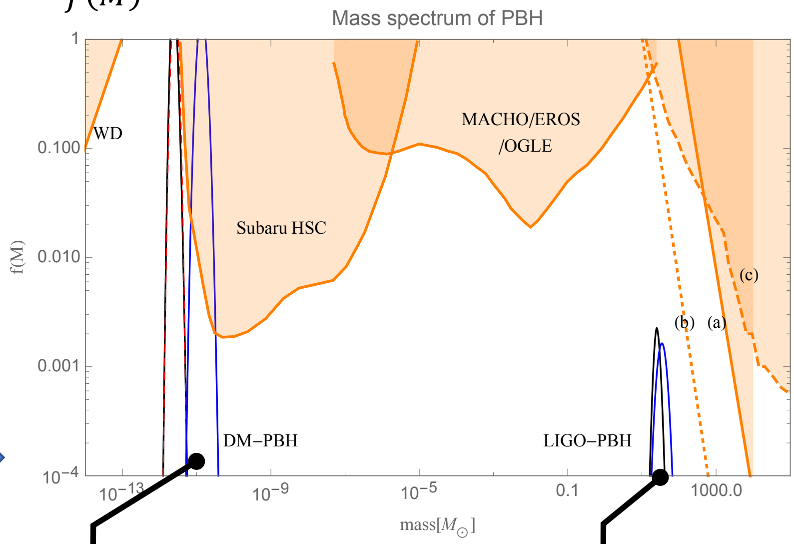

〈Colors〉
Blue: top-hat type
Black: delta function type
Red: Gaussian type

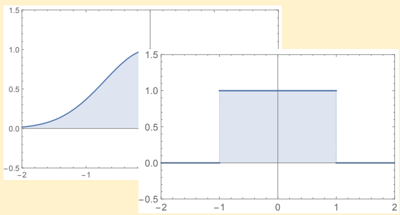

K. Ando, K. Inomata, and M. Kawasaki, (2018), arXiv:1802.06393

- DM PBH

$$\frac{\Omega_{PBH}}{\Omega_{DM}} = \int \mathrm{d}(\ln M)\, f(M) = 1$$

- LIGO PBH

$$\frac{\Omega_{PBH}}{\Omega_{DM}} = 10^{-3}$$

Secondary gravitational waves

- GWs are sourced by the scalar perturbation in 2nd order,

$$h_{ij}'' + 2aHh_{ij}' - \nabla^2 h_{ij} = -4T_{ij}^{lm}\, S_{lm} \quad , \quad S_{lm} = O(\zeta^2)$$

R. Saito and J. 'i. Yokoyama , Phys. Rev. Lett. 102, 161101 (2009)

E. Bugaev and P. Klimai, , Phys. Rev. Lett. 102, 161101 (2009)

$\mathcal{P}_\zeta$: curvature power spectrum

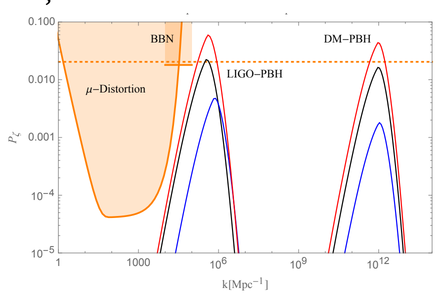

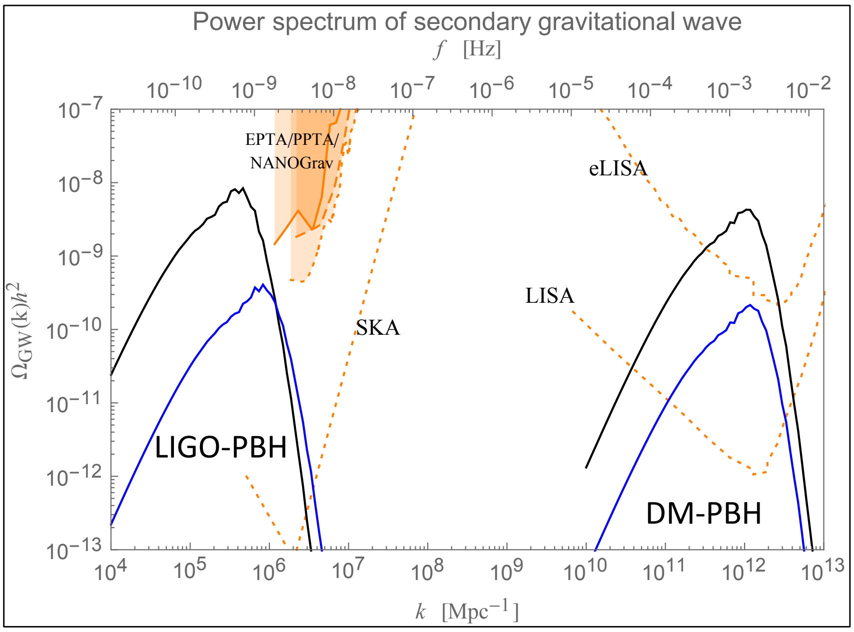

The effect of non-Gaussianity

- In our curvaton model: $f_{NL}(k_{PBH}) \sim 2.7, \quad (r = 0.5)$
- For PBH formation
  - With non-Gaussianity, PBH formation rate $\beta(M)$ increases.

  $\Leftrightarrow$ We can achieve $\beta(M) = 10^{-3}/1$ by smaller $\mathcal{P}_\zeta(k)$.

  〈Dotted: assuming Gaussian／Solid: including non-Gaussianity〉

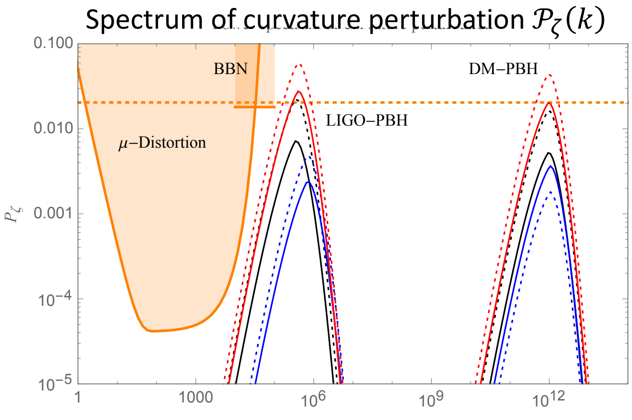

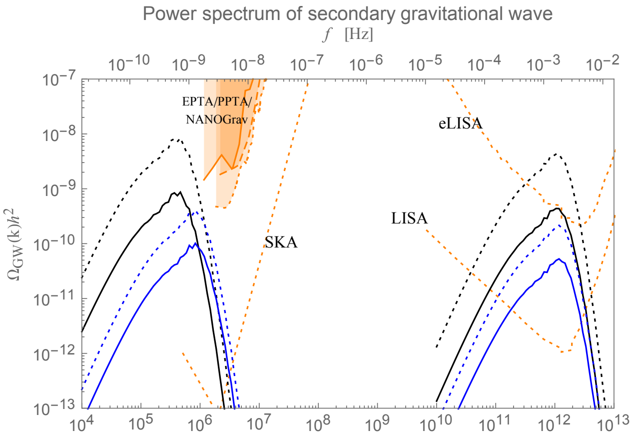

- non-Gaussianity helps to avoid current constraints
- Future GW constraints check both scenarios with/without NG

Results& Conclusion

- We have constructed the model to form enough PBHs for BBHs in LIGO/VIRGO or DM.
- But, the results depend on the uncertainties of PBH formation.

- The detailed analysis?
- I focus on non-Gaussianity. (Ongoing)

The mechanism of our model

- Classical dynamics: Φ

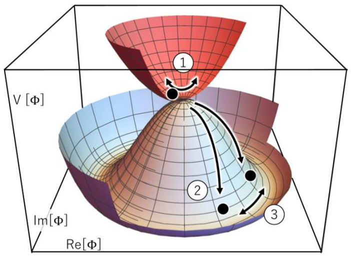

- PBH formation

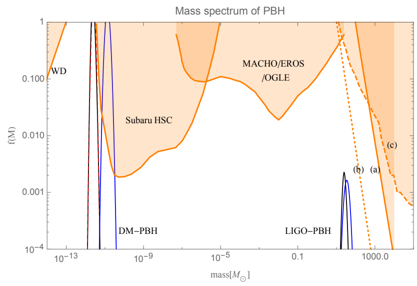

- Perturbations $\mathcal{P}_\zeta(k)$

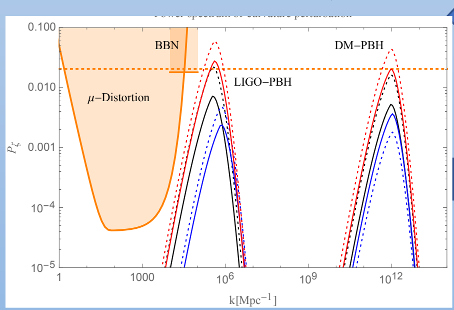

- 2^{nd} GW

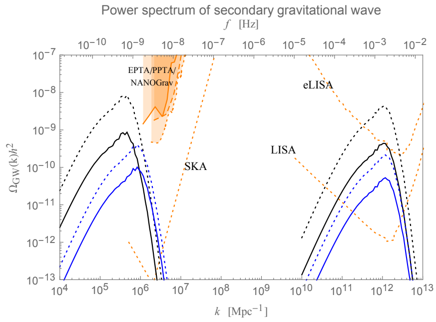

The effect of non-Gaussianity

Kensuke Akita
Tokyo Institute of Technology

"Affleck-Dine baryogenesis in the SUSY DFSZ axion model without R-parity"

(10+5 min.)

[JGRG28 (2018) 110515]

Affleck-Dine baryogenesis in the SUSY DFSZ axion model without R-parity

Kensuke Akita (Tokyo Institute of Technology)

Based on
arXiv:1809.04361
with Hajime Otsuka (Waseda University)

@Rikkyo University ''JGRG28'', Nov. 5, 2018

Introduction

Problems of the Standard Model:

- the origin of the tiny neutrino masses

Previously proposed solutions:

- Seesaw mechanism introducing the heavy right-handed neutrinos

- Small R-parity (lepton number) violating terms in supersymmetric (SUSY) theories

  NOT introducing the right-handed neutrinos

  R-parity: $R_p = (-1)^{2S+3B+L}$

  R-parity violating term: $\mathcal{L} \supset \underbrace{\mu_i \nu_i \tilde{H}_u}_{\text{Neutrino mass terms}} + \text{c.c}$

  S : spin
  B : baryon number
  L : lepton number

We focus on this

Requirement: explanation of the smallness of R-parity violation.

Introduction

The SUSY DFSZ axion model achieves the small R-parity violation.

R-parity violating term: $\mathcal{L} \supset y_i \frac{S_1^3}{M_P^2} \nu_i \tilde{H}_u + \text{c.c}$

Planck mass

	S_1	ν_i	$\tilde{H}_u$
$U(1)_{PQ}$	1	-2	-1

(S_1 : PQ field)

Symmetry breaking of $U(1)_{\text{PQ}}$:

$$\mathcal{L} \supset \underbrace{y_i \frac{\langle S_1 \rangle^3}{M_P^2}}_{\text{The effective coupling}} \nu_i \tilde{H}_u + \text{c.c}$$

The magnitude of R-parity violation: controlled and suppressed for $\langle S_1 \rangle \ll M_P$

In addition the SUSY DFSZ axion model

- solves strong CP problem
- includes the axion which is a candidate of dark matter

The SUSY DFSZ axion model can solve several problems.

How about the baryon asymmetry?

$$\boxed{\frac{n_B}{s} \simeq 10^{-10}}$$

Our universe is baryon asymmetric to explain BBN and CMB observation

Previously proposed solutions:

- Thermal leptogenesis

induced by the decay of heavy right-handed neutrinos.

- Affleck-Dine(AD) mechanism

induced by the scalar field in supersymmetric theory.

Can the SUSY DFSZ axion model explain the baryon asymmetry via the AD mechanism without the right-handed neutrinos?

Affleck-Dine baryogenesis

Affleck, Dine, Nucl. Phys. B249, 361 (1985)
Dine, Randall, Thomas , Nucl. Phys. B291, 458 (1996)

Affleck-Dine(AD) baryogenesis

- In SUSY theory, scalar fields(squark, slepton) have baryon/lepton charge.
- Scalar potential of MSSM include flat directions ϕ (AD field) at renormalizable level and supersymmetric limit.
- B/L number density: $n_{B/L} \propto i(\dot{\phi}^* \phi - \phi^* \dot{\phi}) = 2|\phi|^2 \dot{\theta} \quad (\phi = |\phi| e^{i\theta})$

Dynamics of AD field via B/L violating operator $\Rightarrow$ Generate B/L number

- B/L violating operator:

Conventional case: $W = \dfrac{\phi^n}{M^{n-3}} \; (n \geq 4)$

This case: $\boxed{W = \dfrac{S_1^m \phi^n}{M_P^{n+m-3}} \; (n, m \in N)}$

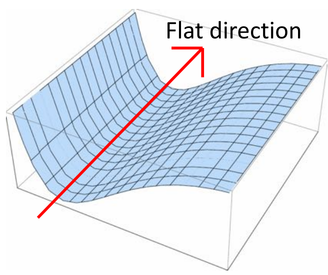

Set-up

	S_1	L	H_u
$U(1)_{PQ}$	1	-2	-1

- L violating operator:

$$\boxed{W_{AD} = y\frac{S_1^3 L H_u}{M_P^2} = y\frac{S_1^3\phi^2}{M_P^2}}$$

$$L = \frac{1}{\sqrt{2}}\begin{pmatrix}\phi\\0\end{pmatrix},\quad H_u = \frac{1}{\sqrt{2}}\begin{pmatrix}0\\\phi\end{pmatrix}$$

- The scalar potential for ϕ, S_1 :

Assumption: $c_\phi, c_1 > 0$

$$V = (m_\phi^2 \underline{- c_\phi} H^2)|\phi|^2 + (m_{S_1}^2 \underline{- c_1} H^2)|S_1|^2 + \frac{y^2|S_1|^6|\phi|^2}{M_P^4} +$$
$$\underline{+ (a_H H + a_m m_{3/2})\frac{y S_1^3\phi^2}{M_P^2} + \text{h.c.}} + \ldots$$

Phase dependent terms: L,CP-violating terms

$(m_\phi \simeq m_{S_1} \simeq m_{3/2})$

Let us investigate the potential and dynamics of AD/PQ scalar fields

Dynamics of ϕ, S_1 during inflation: $H = H_{\rm inf} > m_{3/2}$

$$V = (\cancel{m_\phi^2} - c_\phi H^2)|\phi|^2 + (\cancel{m_{S_1}^2} - c_1 H^2)|S_1|^2 + \frac{y^2|S_1|^6|\phi|^2}{M_P^4} +$$

negative mass!

$$+ (a_H H + \cancel{a_m m_{3/2}})\frac{y S_1^3\phi^2}{M_P^2} + \text{h.c.} + \ldots$$

A minimum for $a_H \gg c_\phi, c_1$:

$(m_\phi \simeq m_{S_1} \simeq m_{3/2})$

$$\boxed{\begin{aligned}&\langle|\phi|\rangle \simeq \langle|S_1|\rangle \simeq (HM_P^2)^{1/3}\\ &\langle 2\theta + 3\theta_{S_1} + \arg a_H\rangle = 0\end{aligned}}$$

$(\phi = |\phi|e^{i\theta},\ S_1 = |S_1|e^{i\theta_{S_1}})$

ϕ, S_1 will settle at the above minimum: $\boxed{n_L = |\phi|^2\dot\theta = 0}$

Dynamics of ϕ, S_1 after inflation: $H = \dfrac{2}{3t} > m_{3/2}$

$$V = (\cancel{m_\phi^2} - c_\phi H^2)|\phi|^2 + (\cancel{m_{S_1}^2} - c_1 H^2)|S_1|^2 + \frac{y^2|S_1|^6|\phi|^2}{M_P^4} +$$
$$+ \cancel{(a_H H + a_m m_{3/2})\frac{y S_1^3 \phi^2}{M_P^2}} + \mathrm{h.c.} + \ldots$$
$$\to 0 \quad (H \propto \langle I \rangle = 0)$$

The inflaton start to oscillate.

inflaton

$$(m_\phi \simeq m_{S_1} \simeq m_{3/2})$$

The minimum → a saddle point!

We can follow the trajectory of ϕ, S_1 numerically.

$\dot{\theta} = 0$ because new phase-dependent potential is not produced.

$$\boxed{n_L = |\phi|^2\dot{\theta} = 0} \quad (\phi = |\phi| e^{i\theta})$$

Dynamics of ϕ, S_1 at $H = \dfrac{2}{3t} < m_{3/2}$

$$V = (m_\phi^2 - \cancel{c_\phi H^2})|\phi|^2 + (m_{S_1}^2 - \cancel{c_1 H^2})|S_1|^2 + \frac{y^2|S_1|^6|\phi|^2}{M_P^4} +$$

positive mass

$$+ \underbrace{(\cancel{a_H H} + a_m m_{3/2})\frac{y S_1^3 \phi^2}{M_P^2}}_{\text{New phase-dependent term}} + \mathrm{h.c.} + \ldots$$

$$(m_\phi \simeq m_{S_1} \simeq m_{3/2})$$

New phase-dependent term

:the minimum of θ changes ➡ $\dot{\theta} \neq 0$

ϕ start to rotate around $\langle \phi \rangle = 0$.

➡ $$\boxed{n_L = |\phi|^2 \dot{\theta} \neq 0} \quad (\phi = |\phi| e^{i\theta})$$

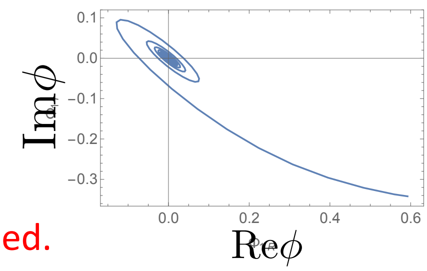

The lepton asymmetry is produced.

Baryon asymmetry

Using E.O.M of ϕ

$$\frac{\partial n_L}{\partial t} + 3Hn_L = -\mathrm{Im}\left[\frac{\partial V}{\partial \phi}\phi\right]$$

$t_{\rm osc} \simeq \frac{1}{m_\phi}$

These values are calculated numerically at $H \simeq m_\phi$

$$\boxed{n_L(t_{\rm osc}) \simeq \frac{1}{m_\phi}\frac{S_1^3(t_{\rm osc})\phi^2(t_{\rm osc})}{M_P^2}|ya_m|m_{3/2}\delta_{\rm eff}}$$

$$\delta_{\rm eff} = \sin(\arg(ya_m) + 3\arg(S_1) + 2\theta)$$

Baryon asymmetry: $\frac{n_B}{s} \simeq \frac{8}{23}\frac{n_L}{s}$ Kuzmin, Rubakov, Shaposhnikov, Phys. Lett. B155, 36 (1985)

$$\boxed{\frac{n_B}{s} \simeq \begin{cases} 0.7\times 10^{-10}\left(\frac{T_{\rm reh}}{10^7\mathrm{GeV}}\right)\left(\frac{1}{|y|}\right)^{\frac{1}{3}}\left(\frac{m_{3/2}}{m_\phi}\right)\left(\frac{m_\phi}{1\mathrm{TeV}}\right)^{-\frac{1}{3}} & \text{for } c_\phi = \frac{1}{5},\ c_1 = \frac{1}{4} \\ 0.68\times 10^{-10}\left(\frac{T_{\rm reh}}{10^5\mathrm{GeV}}\right)\left(\frac{1}{|y|}\right)^{\frac{1}{3}}\left(\frac{m_{3/2}}{m_\phi}\right)\left(\frac{m_\phi}{1\mathrm{TeV}}\right)^{-\frac{1}{3}} & \text{for } c_\phi = c_1 = 1 \end{cases}}$$

The enough amount of baryon asymmetry is produced!

Conclusion

The SUSY DFSZ axion model

- explain the baryon asymmetry via Affleck-Dine mechanism
- may explain neutrino masses and baryon asymmetry in supersymmetric theory without introducing new fields such as right-handed neutrinos.

Future work

- Investigating the detail of neutrino sector

Fabio Chibana
Tokyo Institute of Technology

“Redshift space distortions in the presence of non-minimally coupled dark matter”

(10+5 min.)

[JGRG28 (2018) 110516]

Redshift space distortions in the presence of non-minimally couple dark matter

Fabio Chibana

Tokyo Institute of Technology

JGRG 28 (Rikkyo University)
2018/11/05

In collaboration with: R. Kimura, T. Suyama, M.Yamaguchi, D. Yamauchi, S. Yokoyama

Outline

I. **Introduction:**
   a. **Redshift space distortions in standard cosmology**
   b. **Kaiser formula**

II. **Coupled dark matter**
   a. **Disformal coupling**
   b. **Modified Kaiser formula**

III. **Forecasts**
   a. **Constraints from future galaxy surveys**

IV. **Summary**

Introduction:
Redshift space distortions

Redshift space distortions

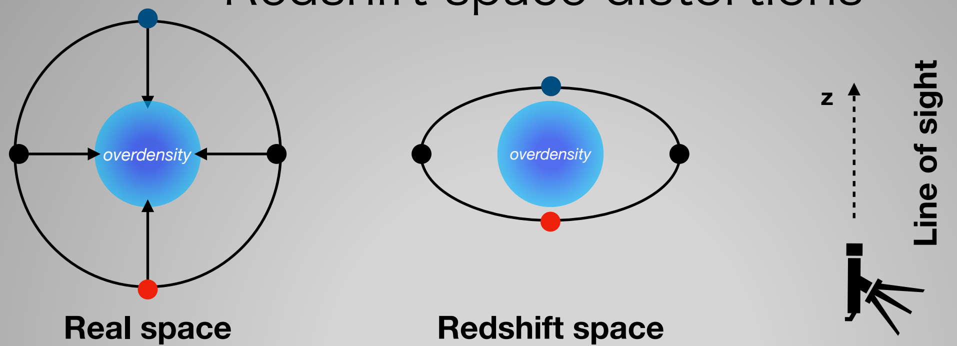

From real to redshift space:

Position

$$\mathbf{s} = \mathbf{x} + \frac{v_{\mathrm{g,z}}}{aH}\hat{z}$$

galaxy's peculiar velocity along the line of sight

Redshift space distortions

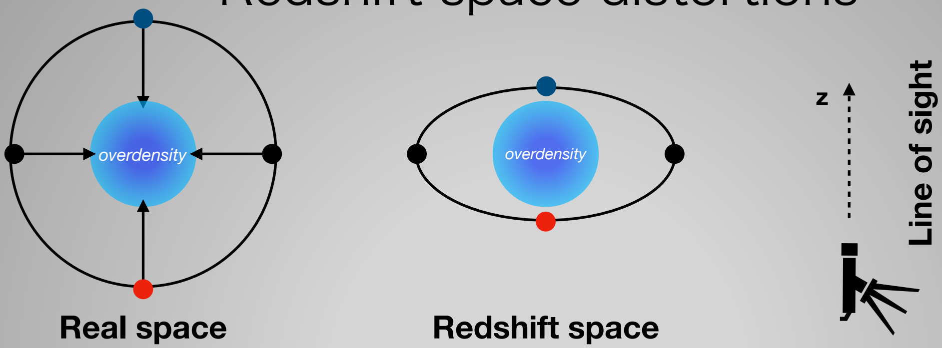

From real to redshift space:

Position $$\mathbf{s} = \mathbf{x} + \frac{v_{\rm g,z}}{aH}\hat{z}$$

galaxy's peculiar velocity along the line of sight

Density contrast $$\delta_{\rm g,s} = \delta_{\rm g} - \frac{\nabla_z v_{\rm g,z}}{aH}$$

$n_{\rm g} = \bar{n}_{\rm g}(1+\delta_g)$

$n_{\rm g}$: *number density*

$\bar{n}_{\rm g}$: *ave. number density*

Redshift space distortions

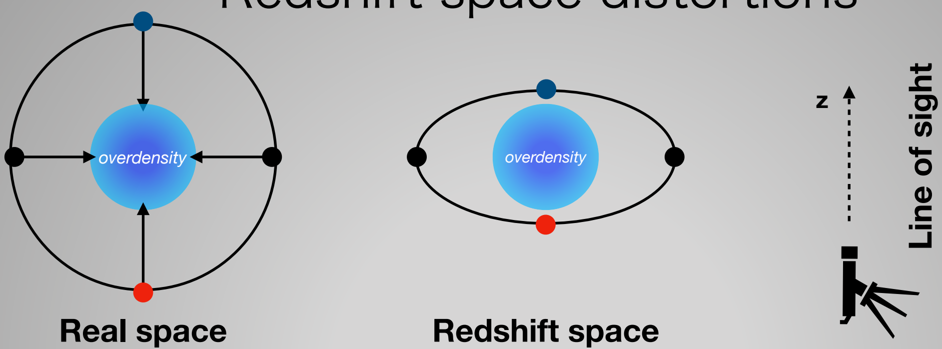

From real to redshift space:

Position $$\mathbf{s} = \mathbf{x} + \frac{v_{\rm g,z}}{aH}\hat{z}$$

$n_{\rm g} = \bar{n}_{\rm g}(1+\delta_g)$

$n_{\rm g}$: *number density*

$\bar{n}_{\rm g}$: *ave. number density*

Density contrast $$\delta_{\rm g,s} = \delta_{\rm g} - \frac{\nabla_z v_{\rm g,z}}{aH}$$

$\delta_{\rm g} = b_g \delta_{\rm m}$ (linear bias)

$v_{\rm g} \approx v_{\rm m}$

Standard cosmology: linear perturbation

Newtonian gauge:
$\mathrm{d}s^2 = -[1+2\Phi(t,\mathbf{x})]\mathrm{d}t^2 + a^2(t)[1-2\Psi(t,\mathbf{x})]\mathrm{d}\mathbf{x}^2$

Sub-horizon approximation: $\frac{k}{aH} \gg 1$

Poisson, continuity and Euler equations (in Fourier space):

$$\frac{k^2}{a^2}\Phi = -4\pi G\rho_{\rm m}\delta_{\rm m}$$
$$\dot{\delta}_{\rm m} + \frac{k^2}{a^2}v_{\rm m} = 0$$
$$\dot{v}_{\rm m} - \Phi = 0$$

EoM for the density contrast

$$\ddot{\delta}_{\rm m} + 3H\,\dot{\delta}_{\rm m} - 4\pi G\rho_{\rm m}\delta_{\rm m} = 0$$

Growth function $\quad \delta_{\rm m}(t,k) = D_{\rm m}(t)\delta_0(k)$

δ_0 : Initial density contrast

Linear growth rate $\quad f_{\rm m}(t) = \frac{\mathrm{d}\log D_{\rm m}}{\mathrm{d}\log a}$

Standard cosmology: linear perturbation

Newtonian gauge:
$\mathrm{d}s^2 = -[1+2\Phi(t,\mathbf{x})]\mathrm{d}t^2 + a^2(t)[1-2\Psi(t,\mathbf{x})]\mathrm{d}\mathbf{x}^2$

Sub-horizon approximation: $\frac{k}{aH} \gg 1$

Poisson, continuity and Euler equations (in Fourier space):

$$\frac{k^2}{a^2}\Phi = -4\pi G\rho_{\rm m}\delta_{\rm m}$$
$$\dot{\delta}_{\rm m} + \frac{k^2}{a^2}v_{\rm m} = 0$$
$$\dot{v}_{\rm m} - \Phi = 0$$

EoM for the density contrast

$$\ddot{\delta}_{\rm m} + 3H\,\dot{\delta}_{\rm m} - 4\pi G\rho_{\rm m}\delta_{\rm m} = 0$$

Growth function $\quad \delta_{\rm m}(t,k) = D_{\rm m}(t)\delta_0(k)$

δ_0 : Initial density contrast

Linear growth rate $\quad f_{\rm m}(t) = \frac{\mathrm{d}\log D_{\rm m}}{\mathrm{d}\log a}$

$$v_{\rm m} = -\frac{a^2 H}{k^2} f_{\rm m}\delta_{\rm m}$$

Equation for the velocity

Standard cosmology: power spectrum

- Power spectrum (PS): $P_\delta(k) \sim |\delta_k|^2$
- **Kaiser formula**

$\mu = \cos\theta = \hat{k}\cdot\hat{z}$

$$\boxed{P_{\rm g,s}(\mathbf{k};t) = \left[b_{\rm g} + \mu^2 f_m(t)\right]^2 P_{\rm m}(k;t) \quad \textit{(Kaiser, 1987)}}$$

Galaxy PS in redshift space — Matter PS in real space

Standard cosmology: power spectrum

- Power spectrum (PS): $P_\delta(k) \sim |\delta_k|^2$
- **Kaiser formula**

$\mu = \cos\theta = \hat{k}\cdot\hat{z}$

$$\boxed{P_{\rm g,s}(\mathbf{k};t) = \left[b_{\rm g} + \mu^2 f_m(t)\right]^2 P_{\rm m}(k;t) \quad \textit{(Kaiser, 1987)}}$$

Galaxy PS in redshift space — Matter PS in real space

Linear growth rate can be measured by RSD

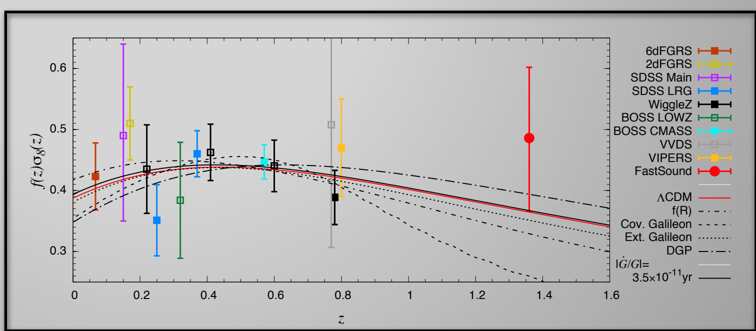

Okumura, et al. Publ. Astron. Soc. Jap. 68 (2016) no.3, 38

Non-minimally coupled dark matter

Non-minimally coupled dark matter: set up

Action:

$$S = \int \mathrm{d}^4x\sqrt{-g}\left[\underbrace{\frac{M_{\mathrm{Pl}}^2}{2}R[g]}_{\text{General relativity}} + \underbrace{\mathcal{L}_\phi[g,\phi]}_{\text{Scalar field (DE)}}\right] + \underbrace{S_{\mathrm{m}}}_{\text{Matter (baryons + CDM)}}$$

$$\boxed{S_{\mathrm{m}} = S_{\mathrm{b}} + S_{\mathrm{c}}}$$

Non-minimally coupled dark matter: set up

Action: $$S = \int \mathrm{d}^4x\sqrt{-g}\left[\underbrace{\frac{M_{\rm Pl}^2}{2}R[g]}_{\text{GR}} + \underbrace{\mathcal{L}_\phi[g,\phi]}_{\text{DE}}\right] + \underbrace{S_{\rm m}}_{\text{Matter}}$$

$$\boxed{S_{\rm m} = S_{\rm b} + S_{\rm c}}$$

Baryons: constraints from solar system experiments => **minimal coupling**

$$S_{\rm b} = \int \mathrm{d}^4x\sqrt{-g}\,\mathcal{L}_{\rm b}[g,\psi_{\rm b}]$$

Non-minimally coupled dark matter: set up

Action: $$S = \int \mathrm{d}^4x\sqrt{-g}\left[\underbrace{\frac{M_{\rm Pl}^2}{2}R[g]}_{\text{GR}} + \underbrace{\mathcal{L}_\phi[g,\phi]}_{\text{DE}}\right] + \underbrace{S_{\rm m}}_{\text{Matter}}$$

$$\boxed{S_{\rm m} = S_{\rm b} + S_{\rm c}}$$

Baryons: constraints from solar system experiments => **minimal coupling**

$$S_{\rm b} = \int \mathrm{d}^4x\sqrt{-g}\,\mathcal{L}_{\rm b}[g,\psi_{\rm b}]$$

CDM: insensitive to solar system experiments => **non-minimal coupling**

$$S_{\rm c} = \int \mathrm{d}^4x\,\sqrt{-\tilde{g}}\,\mathcal{L}_{\rm c}\left[\tilde{g},\psi_{\rm c}\right]$$

$$\boxed{\tilde{g}_{\mu\nu} = \underbrace{A(\phi,X)}_{\text{conformal factor}}g_{\mu\nu} + \underbrace{B(\phi,X)}_{\text{disformal factor}}\partial_\mu\phi\partial_\nu\phi}$$

(Bekenstein, 1993)

Coupled DM: linear perturbation

(sub-horizon + quasistatic approx.)

- Poisson and baryon equations: unchanged
- Continuity and Euler equations for CDM are modified

Coupled DM: linear perturbation

(sub-horizon + quasistatic approx.)

- Poisson and baryon equations: unchanged
- Continuity and Euler equations for CDM are modified

EoM for the density contrast of CDM

$$\ddot{\delta}_{\rm c} + 3H_{\rm eff}\,\dot{\delta}_{\rm c} - 4\pi G_{\rm eff}\rho_{\rm m}\delta_{\rm m} = 0$$

Velocity equation

$$v_{\rm m}(t,\mathbf{k}) = -\frac{a^2 H}{k^2} f_{\rm m}^{\rm eff}(t)\,\delta_{\rm m}(t,\mathbf{k})$$

Coupled DM: linear perturbation

(sub-horizon + quasistatic approx.)

- Poisson and baryon equations: unchanged
- Continuity and Euler equations for CDM are modified

EoM for the density contrast of CDM

$$\ddot{\delta}_{\rm c} + 3H_{\rm eff}\,\dot{\delta}_{\rm c} - 4\pi G_{\rm eff}\,\rho_{\rm m}\delta_{\rm m} = 0$$

Velocity equation

$$v_{\rm m}(t,\mathbf{k}) = -\frac{a^2 H}{k^2} f_{\rm m}^{\rm eff}(t)\,\delta_{\rm m}(t,\mathbf{k})$$

$$\boxed{f_{\rm m}^{\rm eff} = f_{\rm m} + \Delta f_{\rm m}^{\rm eff}}$$

Actual growth rate

$$f_{\rm m} = \frac{{\rm d}\log D_{\rm m}}{{\rm d}\log a}$$

DM-DE coupling effect depends on the conformal and disformal functions

Coupled DM: linear perturbation

(sub-horizon + quasistatic approx.)

- Poisson and baryon equations: unchanged
- Continuity and Euler equations for CDM are modified

EoM for the density contrast of CDM

$$\ddot{\delta}_{\rm c} + 3H_{\rm eff}\,\dot{\delta}_{\rm c} - 4\pi G_{\rm eff}\,\rho_{\rm m}\delta_{\rm m} = 0$$

Velocity equation

$$v_{\rm m}(t,\mathbf{k}) = -\frac{a^2 H}{k^2} f_{\rm m}^{\rm eff}(t)\,\delta_{\rm m}(t,\mathbf{k})$$

$$\boxed{f_{\rm m}^{\rm eff} = f_{\rm m} + \Delta f_{\rm m}^{\rm eff}}$$

Actual growth rate

$$f_{\rm m} = \frac{{\rm d}\log D_{\rm m}}{{\rm d}\log a}$$

DM-DE coupling effect depends on the conformal and disformal functions

DM-DE interactions change both the growth function & growth rate!

Coupled DM: power spectrum

Modified Kaiser formula

$$\boxed{P_{\mathrm{g,s}}(\mathbf{k};t) = \left[b_{\mathrm{g}} + \mu^2 f_{\mathrm{m}}^{\mathrm{eff}}(t)\right]^2 P_{\mathrm{m}}(k;t)}$$

Coupled DM: power spectrum

Modified Kaiser formula

$$\boxed{P_{\mathrm{g,s}}(\mathbf{k};t) = \left[b_{\mathrm{g}} + \mu^2 f_{\mathrm{m}}^{\mathrm{eff}}(t)\right]^2 P_{\mathrm{m}}(k;t)}$$

- Standard scenario (minimally coupled DM)

$$D_{\mathrm{m}} = D_{\mathrm{c}} = D_{\mathrm{b}} \qquad\qquad f_{\mathrm{m}}^{\mathrm{eff}} = f_{\mathrm{m}}$$

- Coupled DM

RSD measures the effective growth rate (actual growth rate + DM-DE interaction)

Coupled DM: power spectrum

Modified Kaiser formula

$$\boxed{P_{\rm g,s}(\mathbf{k};t) = \left[b_{\rm g} + \mu^2 f_{\rm m}^{\rm eff}(t)\right]^2 P_{\rm m}(k;t)}$$

- Standard scenario (minimally coupled DM)

$$D_{\rm m} = D_{\rm c} = D_{\rm b} \qquad\qquad f_{\rm m}^{\rm eff} = f_{\rm m}$$

- Coupled DM

RSD measures the effective growth rate (actual growth rate + DM-DE interaction)

Could we actually measure it?

Forecasts

Forecast: set up

- Canonical scalar field:

$$\mathcal{L}_\phi = -\frac{1}{2}\partial^\mu\phi\partial_\mu\phi - V(\phi)$$

$$V(\phi) = V_0\phi^{-n}, \quad n > 0$$

$$X \equiv -\frac{1}{2}g_{\mu\nu}\partial^\mu\phi\partial^\nu\phi$$

$$\hat{\phi} \equiv \frac{\phi}{M_{\rm Pl}}$$

- Coupling:

$$\tilde{g}_{\mu\nu} = A g_{\mu\nu} + B\partial_\mu\phi\partial_\nu\phi$$

Model I (conf.) $A(\phi) = e^{-2\alpha\hat{\phi}}, \quad B = 0$ (*Amendola, 2000*)

Model II (conf.) $A(\phi) = e^{-\alpha\hat{\phi}^2}, \quad B = 0$

Model III (disf.) $A = 1, \quad B(X) = \frac{\alpha}{X}$ → *No interaction at background level.*

Forecast: Fisher matrix analysis

Galaxy survey:

- Phase two of the Square Kilometer Array project (SKA2)
  - (proposed) Network of radio telescopes in South Africa and Australia.
  - Estimated to start in 2025.
  - Survey specifications based on (*Yahya, et al. 2015)*
- Euclid space satellite
  - Estimated launch: 2021
  - Survey specifications based on (*Amendola, et al. 2016)*

Fisher matrix analysis:

Estimation of the constraints a future experiment

$$F_{\alpha\beta} = \sum_{z_i}\int_{k_{\rm min}}^{k_{\rm min}} \frac{{\rm d}^3\mathbf{k}}{(2\pi)^3} V_{\rm eff}(\mathbf{k}, z_i) \frac{\partial \ln P_{\rm obs}(\mathbf{k}, z_i)}{\partial\theta^\alpha}\frac{\partial \ln P_{\rm obs}(\mathbf{k}, z_i)}{\partial\theta^\beta}$$

$$P_{\rm obs}(\vec{k}, z) = \mathcal{N}_{\rm AP}(z)\left(b + f_{\rm m}^{\rm eff}\mu^2\right)^2 P_{\rm m}(k, z)e^{-k^2\mu^2\sigma_{\rm NL}^2}.$$

Forecast: results (preliminary)

Model	α (Fid.)	Survey	$10^3 \times \sigma(\alpha)$	
I	0.04	Euclid	5.90	~15%
		SKA2	3.72	~ 9%
II	0.04	Euclid	26.37	~66%
		SKA2	19.99	~50%
III	-0.1	Euclid	15.00	~15%
		SKA2	5.36	~5%

Table 9. Marginalized mean values and 68% C.L. intervals for coupled DE (see Sect. 5.3.4).

CDE models	*Planck* TT+lowP	*Planck* TT+lowP +BSH	*Planck* TT+lowP +WL	*Planck* TT+lowP +BAO/RSD	*Planck* TT+lowP +WL+BAO/RSD	
β	<0.066 (95%)	$0.037^{+0.018}_{-0.015}$	$0.043^{+0.026}_{-0.022}$	$0.034^{+0.019}_{-0.016}$	$0.037^{+0.020}_{-0.016}$	~50%
α	$0.43^{+0.15}_{-0.33}$	$0.29^{+0.077}_{-0.26}$	$0.44^{+0.18}_{-0.29}$	$0.40^{+0.15}_{-0.29}$	$0.45^{+0.17}_{-0.33}$	
H_0 (km s^{-1} Mpc^{-1}) .	$65.4^{+3.2}_{-2.6}$	$67.47^{+0.88}_{-0.79}$	67.6 ± 2.8	66.7 ± 1.1	66.9 ± 1.1	
σ_8	$0.812^{+0.031}_{-0.026}$	0.829 ± 0.018	$0.819^{+0.031}_{-0.026}$	0.817 ± 0.017	0.810 ± 0.017	

Planck Collaboration: Planck 2015 results. XIV.

Forecast: results (preliminary)

Model	α (Fid.)	Survey	$10^3 \times \sigma(\alpha)$	
I	0.04	Euclid	5.90	~15%
		SKA2	3.72	~ 9%
II	0.04	Euclid	26.37	~66%
		SKA2	19.99	~50%
III	-0.1	Euclid	15.00	~15%
		SKA2	5.36	~5%

Best case scenario: constraints improve to ~9%

Table 9. Marginalized mean values and 68% C.L. intervals for coupled DE (see Sect. 5.3.4).

CDE models	*Planck* TT+lowP	*Planck* TT+lowP +BSH	*Planck* TT+lowP +WL	*Planck* TT+lowP +BAO/RSD	*Planck* TT+lowP +WL+BAO/RSD	
β	<0.066 (95%)	$0.037^{+0.018}_{-0.015}$	$0.043^{+0.026}_{-0.022}$	$0.034^{+0.019}_{-0.016}$	$0.037^{+0.020}_{-0.016}$	~50%
α	$0.43^{+0.15}_{-0.33}$	$0.29^{+0.077}_{-0.26}$	$0.44^{+0.18}_{-0.29}$	$0.40^{+0.15}_{-0.29}$	$0.45^{+0.17}_{-0.33}$	
H_0 (km s^{-1} Mpc^{-1}) .	$65.4^{+3.2}_{-2.6}$	$67.47^{+0.88}_{-0.79}$	67.6 ± 2.8	66.7 ± 1.1	66.9 ± 1.1	
σ_8	$0.812^{+0.031}_{-0.026}$	0.829 ± 0.018	$0.819^{+0.031}_{-0.026}$	0.817 ± 0.017	0.810 ± 0.017	

Planck Collaboration: Planck 2015 results. XIV.

Summary

- DM-DE interactions change both the growth function & growth rate;
- RSD measures the effective growth rate:
  - combination of the actual growth rate & DM-DE interaction effects;
- Future galaxy surveys: able to put constraints on the interaction (~9%);

Thank you!

Extra: Effective growth rate

For CDM

$$f_{\rm c}^{\rm eff} = f_{\rm c} - \frac{\Upsilon_2}{1-\Upsilon_1}\left(f_{\rm c} - \frac{Q_0}{\mathcal{A}H\dot{\phi}}\right) \equiv f_{\rm c} + \Delta f_{\rm c}\,.$$

For total matter

$$\begin{aligned} f_{\rm m}^{\rm eff} &= \frac{\omega_{\rm c} D_{\rm c} f_{\rm c}^{\rm eff} + \omega_{\rm b} D_{\rm b} f_{\rm b}}{\omega_{\rm c} D_{\rm c} + \omega_{\rm b} D_{\rm b}} \\ &= f_{\rm m} + \omega_{\rm c}\frac{D_{\rm c}}{D_{\rm m}}\Delta f_{\rm c} - \omega_{\rm b}\frac{Q_0\dot{\phi}}{H\rho_{\rm m}}\frac{D_{\rm c}-D_{\rm b}}{D_{\rm m}} \equiv f_{\rm m} + \Delta f_{\rm m}\,, \end{aligned}$$

Extra: EoM for density constrast

$$\boxed{(1-\Upsilon_1-\Upsilon_2)\,\ddot{\delta}_c + 2H(1-\mathcal{E}_1)\,\dot{\delta}_c - 4\pi G\Big[(1-\mathcal{E}_2)\,\rho_c\delta_c + (1-\Upsilon_1)\,\rho_b\delta_b\Big] = 0}$$

Model I

$$\mathcal{E}_1 = \frac{\alpha}{2}\frac{\dot{\phi}}{M_{\rm Pl}H}\,, \qquad \mathcal{E}_2 = -2\alpha^2\,.$$

$$\Upsilon_1 = \Upsilon_2 = 0,$$

Model II

$$\mathcal{E}_1 = \frac{\alpha}{2}\frac{\phi\,\dot{\phi}}{M_{\rm Pl}^2 H}, \qquad \mathcal{E}_2 = -2\alpha^2\frac{\phi^2}{M_{\rm Pl}^2}.$$

Model III

$$\mathcal{E}_1 = -\frac{2\alpha^2\rho_c\dot{\phi}\left(3\dot{\phi}+2V_\phi\right)}{H\left(\dot{\phi}^2-2\alpha\rho_c\right)\left[(1-2\alpha)\dot{\phi}^2-2\alpha\rho_c\right]}$$

$$\mathcal{E}_2 = \frac{2\alpha\dot{\phi}^2}{\dot{\phi}^2-2\alpha\rho_c}.$$

$$\Upsilon_1 = -\Upsilon_2 = \mathcal{E}_2.$$

Tuesday 6th November
Invited lecture 9:00–9:45
[Chair: Junichi Yokoyama]

David F. Mota
University of Oslo

“Nonlinear astrophysical phenomena and the viability of screening mechanisms in gravity beyond General Relativity”
(40+10 min.)

[JGRG28 (2018) 110601]

Nonlinear astrophysical phenomena and the viability of screening mechanisms in gravity beyond General Relativity

David F. Mota

UiO : Institute of Theoretical Astrophysics
University of Oslo

General Relativity is quite unique

Curvature

$$\frac{1}{16\pi G}\int d^4x\sqrt{-g}R(g) + \int d^4x\sqrt{-g}\mathcal{L}(g,\mathrm{matter})$$

Metric of space time

Lovelock's theorem (1971) :*"The only second-order, local gravitational field equations derivable from an action containing solely the 4D metric tensor (plus related tensors) are the Einstein field equations with a cosmological constant."*

Higher dimensions

Non-local

Higher-order

Modified Gravity

New degrees of freedom

Tessa Baker 2013

Common Feature to Modified Gravity

Screening Mechanisms!

Solar System Bounds

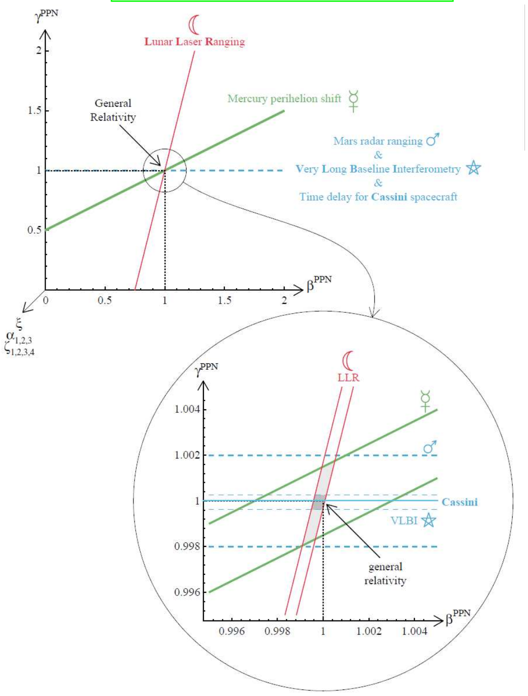

Cosmological Bounds

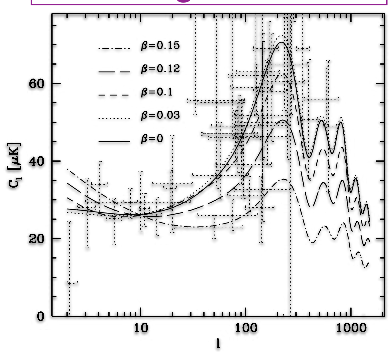

Astrophysical Bounds

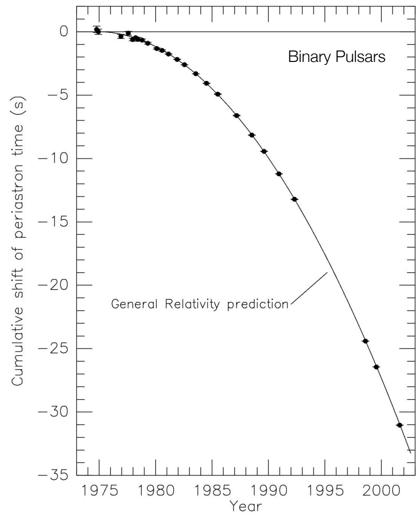

Screening Mechanisms in Scalar-Tensor Gravity

$$\mathcal{L} = -\frac{1}{2}Z^{\mu\nu}(\phi,\partial\phi,\ldots)\partial_\mu\phi\partial_\nu\phi - V(\phi) + g(\phi)T^{\mu}_{\mu}$$

1. Weak coupling

2. Large mass

$$V(r) = -\frac{g^2(\bar{\phi})}{Z(\bar{\phi})c_s^2(\bar{\phi})}\,\frac{e^{-\frac{m(\bar{\phi})}{\sqrt{Z(\bar{\phi})}c_s(\bar{\phi})}r}}{4\pi r}\mathcal{M}$$

3. Large inertia

Couplings, Mass, Inertia environmental dependent

Screening mechanism ≠ Theory of gravity

$$\mathcal{L} = -\frac{1}{2}Z^{\mu\nu}(\phi,\partial\phi,\ldots)\partial_\mu\phi\partial_\nu\phi - V(\phi) + g(\phi)T^{\mu}_{\mu}$$

$$V(r) = -\frac{g^2(\bar{\phi})}{Z(\bar{\phi})c_s^2(\bar{\phi})}\,\frac{e^{-\frac{m(\bar{\phi})}{\sqrt{Z(\bar{\phi})}c_s(\bar{\phi})}r}}{4\pi r}\mathcal{M}$$

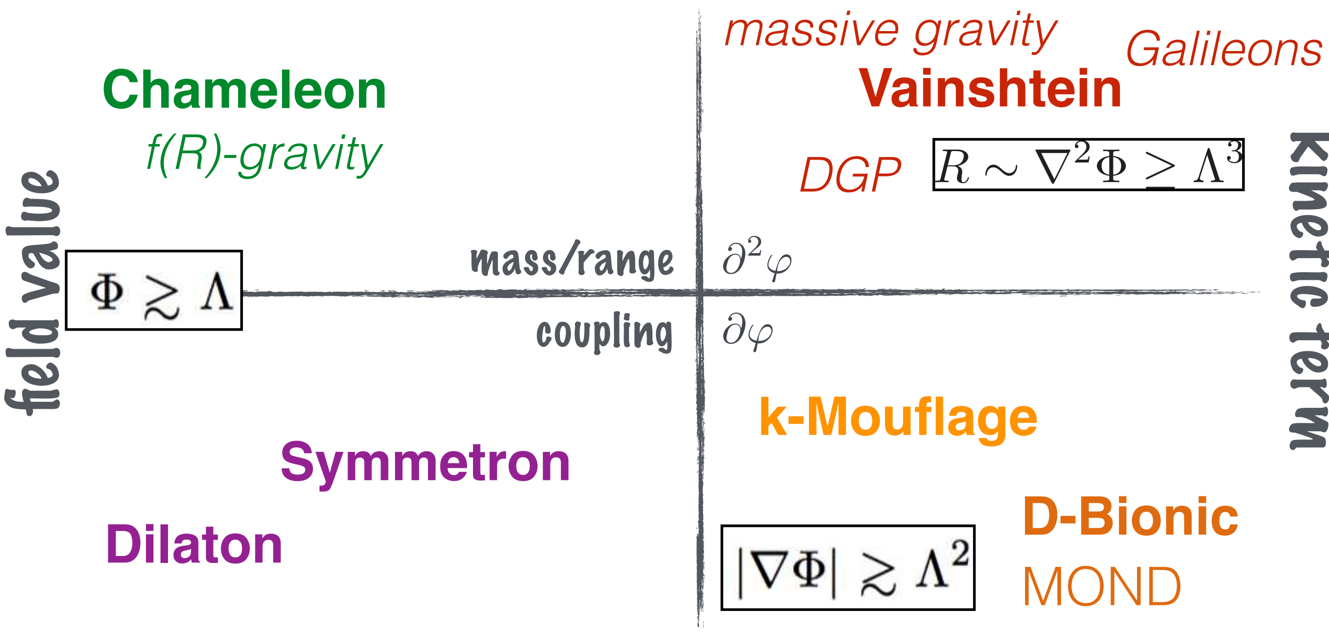

Symmetron Screening

Strength of fifth force depends on local density

$$S = \int \mathrm{d}^4x\sqrt{-g}\left(\frac{M_{\rm Pl}^2}{2}R - \frac{1}{2}(\partial\phi)^2 - V(\phi)\right) + S_{\rm matter}\left[A^2(\phi)g_{\mu\nu},\psi\right]$$

$$\Psi(r) = -\frac{GM}{r}\left(1+\alpha e^{-r/\lambda}\right)$$

$$A(\phi) = 1 + \frac{1}{2M^2}\phi^2$$

coupling

$$V_{\rm eff}(\phi) = \frac{1}{2}\left(\frac{\rho}{M^2} - \mu^2\right)\phi^2 + \frac{1}{4}\lambda\phi^4$$

(High density)

No coupling!

$A(\phi) = 1$

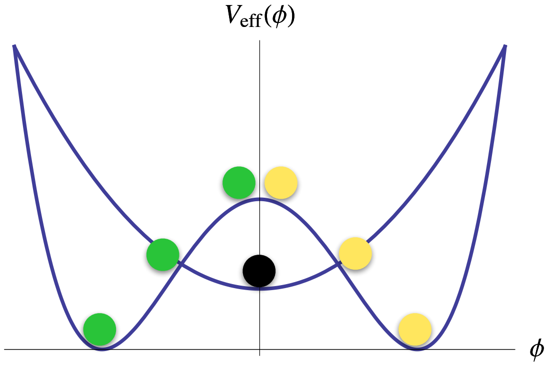

(Low density)

coupled!

$A(\phi) = 1 + \frac{1}{2M^2}\phi^2_{\rm vev}$

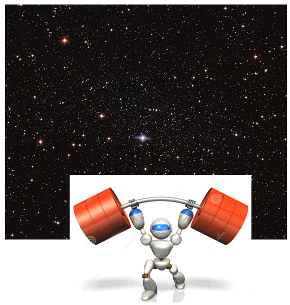

Chameleon Screening

Mass/Range of field depends on local density

$$S = \int \mathrm{d}^4x\sqrt{-g}\left(\frac{M_{\rm Pl}^2}{2}R - \frac{1}{2}(\partial\phi)^2 - V(\phi)\right) + S_{\rm matter}\left[A^2(\phi)g_{\mu\nu},\psi\right]$$

$$m_{\rm eff}^2(\bar\phi) = V^{\rm eff}_{,\phi\phi}(\bar\phi) = V_{,\phi\phi}(\bar\phi) + A_{,\phi\phi}(\bar\phi)\rho$$

$$A(\phi) \simeq 1 + \xi\frac{\phi}{M_{\rm Pl}} \qquad V(\phi) = \frac{M^{4+n}}{\phi^n}$$

Low density region

Small mass

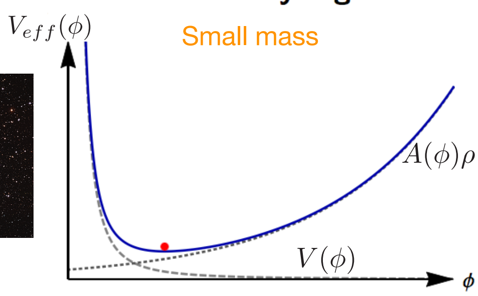

$V''(\phi) \ll 1 \rightarrow$ Unscreened

Chameleon f(R)-gravity

$$S = \frac{M_{\rm Pl}^2}{2}\int \mathrm{d}^4x\sqrt{-g}\Big(R + f(R)\Big) + S_{\rm matter}[g_{\mu\nu},\psi]$$

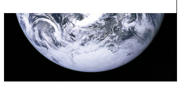

$$f(R) = -\frac{aM^2}{1+\left(\frac{R}{M^2}\right)^{-\alpha}}$$

Constrains on Modified Gravity

Post-Newtonian Parameter

$$\mathrm{d}s^2 = (-1 + 2\frac{GM}{r})\,\mathrm{d}t^2 + (1 + 2\gamma\frac{GM}{r})\,\mathrm{d}x^2$$

"How much space is curved by a unit rest mass"

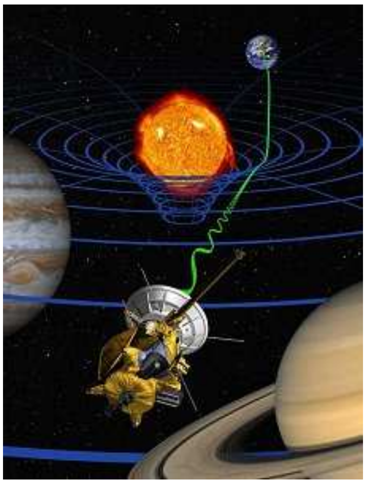

$$\gamma - 1 = (2.1 \pm 2.3) \times 10^{-5}$$

$$\gamma - 1 = 0, \qquad \mathrm{GR}$$

$$\gamma - 1 = -\frac{\phi^2}{M^2}\frac{2}{\frac{\phi^2}{M^2} + 2\Psi(1 + \frac{\phi^2}{M^2})}$$

Computing the profile of the field in the solar system

$$S = \int \mathrm{d}^4x\sqrt{-g}\left(\frac{M_{\rm Pl}^2}{2}R - \frac{1}{2}(\partial\phi)^2 - V(\phi)\right) + S_{\rm matter}\left[A^2(\phi)g_{\mu\nu}, \psi\right]$$

- Scalar field equation of motion

$$\ddot{\phi} + 3H\dot{\phi} - \frac{1}{a^2}\nabla^2\phi = -V_{\mathrm{eff},\phi}(\rho, \phi)$$

- A damped **wave equation**

Quasi-static approximation

Field profile doesn’t change in virialised/quasi-static systems

- Scalar field equation of motion

$$\frac{1}{a^2}\nabla^2\phi = -V_{\mathrm{eff},\phi}(\rho,\phi)$$

- **Quasi-static** approximation

$$S = \int \mathrm{d}^4x\sqrt{-g}\left(\frac{M_{\mathrm{Pl}}^2}{2}R - \frac{1}{2}(\partial\phi)^2 - V(\phi)\right) + S_{\mathrm{matter}}\left[A^2(\phi)g_{\mu\nu},\psi\right]$$

Quasi-static approximation

Field profile does change in virialised/quasi-static systems

- Scalar field equation of motion

$$\frac{1}{a^2}\nabla^2\phi = -V_{\mathrm{eff},\phi}(\rho,\phi)$$

- **Quasi-static** approximation

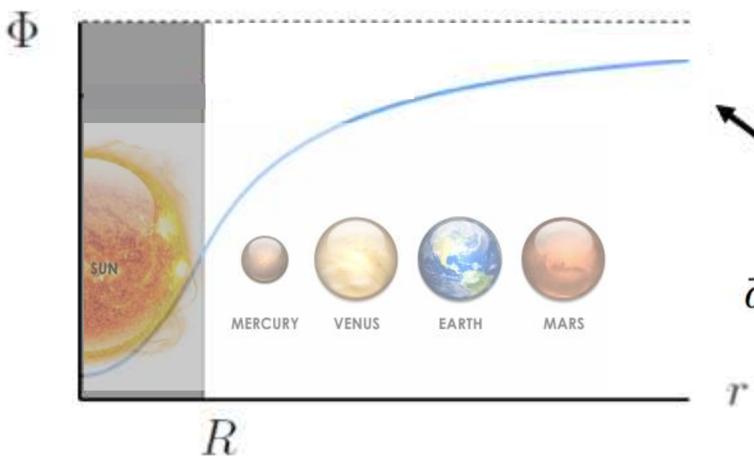

ϕ

$$\vec{a} = -\vec{\nabla}\Phi - \frac{\mathrm{d}\ln A(\phi)}{\mathrm{d}\phi}\vec{\nabla}\phi$$

Newtonian

$$S = \int \mathrm{d}^4x\sqrt{-g}\left(\frac{M_{\mathrm{Pl}}^2}{2}R - \frac{1}{2}(\partial\phi)^2 - V(\phi)\right) + S_{\mathrm{matter}}\left[A^2(\phi)g_{\mu\nu},\psi\right]$$

Quasi-static approximation

Field profile does change in virialised/quasi-static systems

- Scalar field equation of motion

$$\frac{1}{a^2}\nabla^2\phi = -V_{\mathrm{eff},\phi}(\rho,\phi)$$

- **Quasi-static** approximation

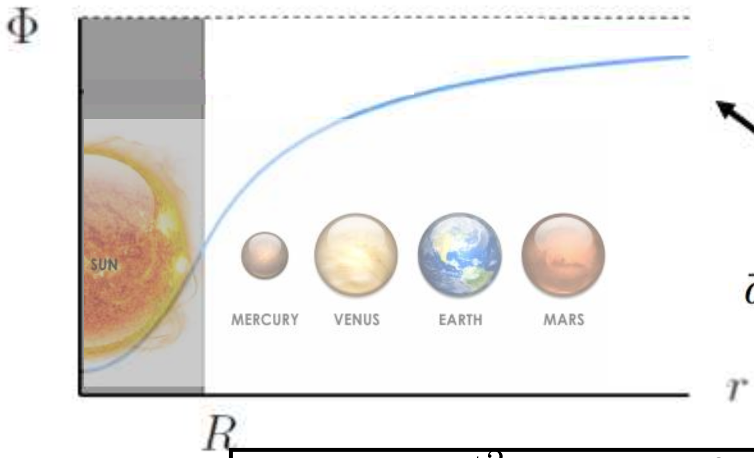

ϕ

$$\vec{a} = \underbrace{-\vec{\nabla}\Phi}_{\text{Newtonian}} - \frac{\mathrm{d}\ln A(\phi)}{\mathrm{d}\phi}\vec{\nabla}\phi$$

$$\boxed{\gamma - 1 = -\frac{\phi^2}{M^2}\frac{2}{\frac{\phi^2}{M^2} + 2\Psi\left(1+\frac{\phi^2}{M^2}\right)}}$$

The Thin Shell Effect

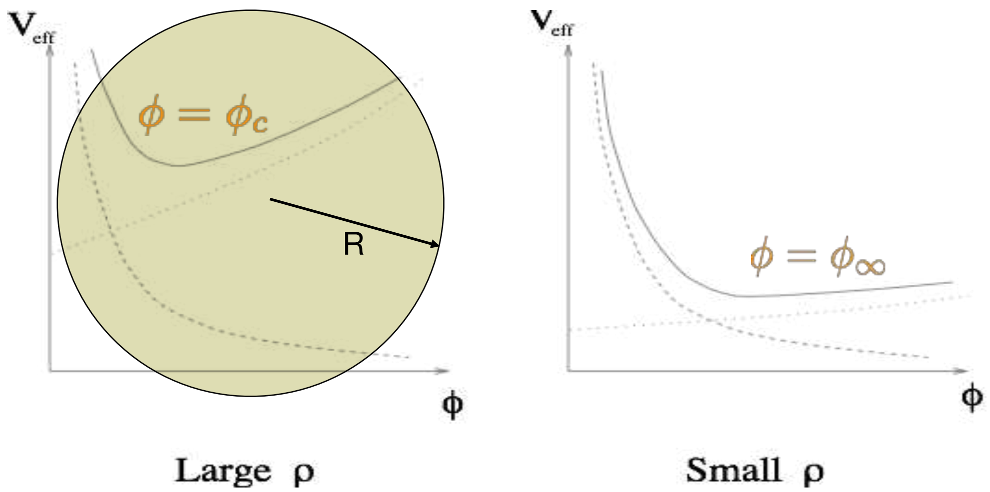

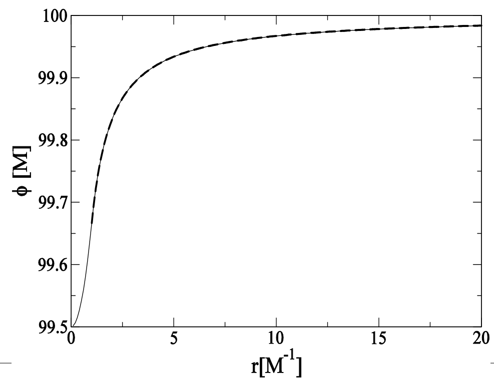

The Thin Shell Effect

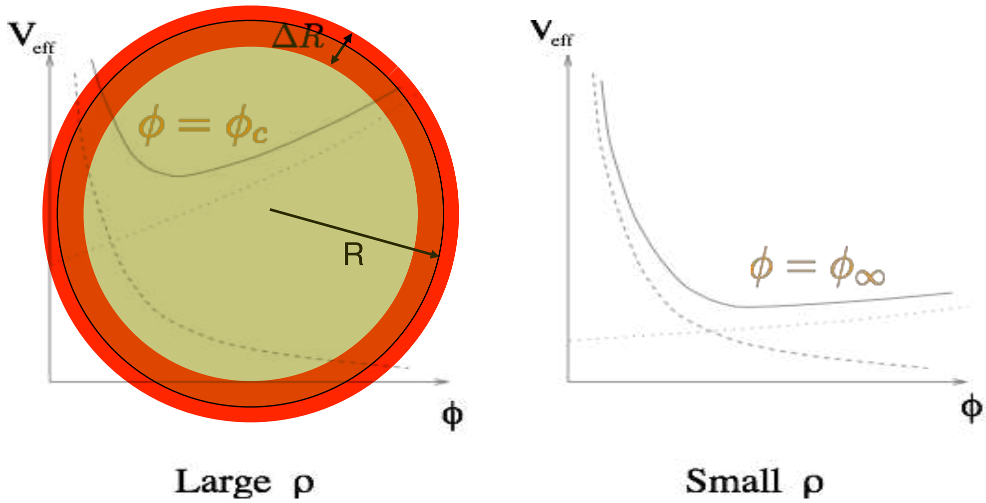

Field reaches effectiv

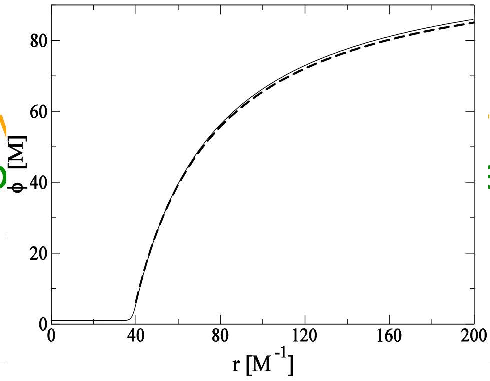

ywhere in the body

All field variations co ear body surface

This region is called

Thin shell effect

Screening mechanisms suppress value field and gradient

$$\vec{a} = -\vec{\nabla}\Phi - \frac{\mathrm{d}\ln A(\phi)}{\mathrm{d}\phi}\vec{\nabla}\phi = -\vec{\nabla}\Big(\Phi + \ln A(\phi)\Big)$$

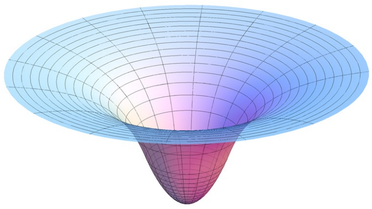

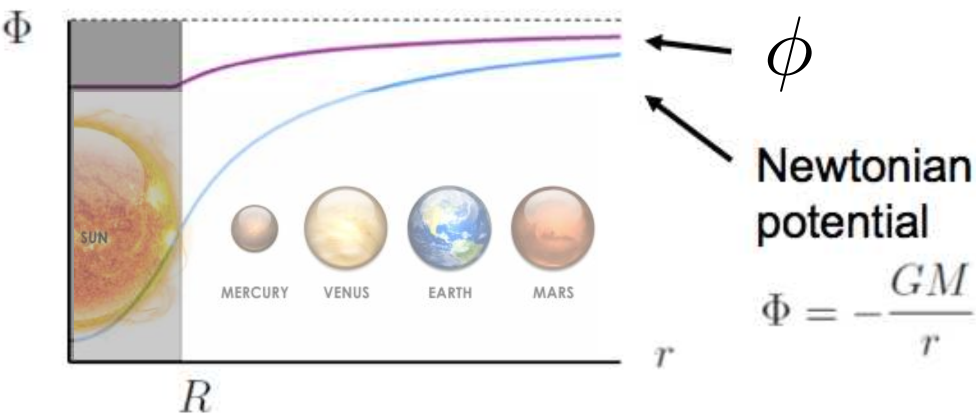

$$\Phi = -\frac{GM}{r}$$

$$\boxed{F_\phi \ll F_N}$$

$$\boxed{\gamma - 1 = -\frac{\phi^2}{M^2}\frac{2}{\frac{\phi^2}{M^2} + 2\Psi(1 + \frac{\phi^2}{M^2})} \ll 1}$$

Waves from Supernovae

Chameleon Potential

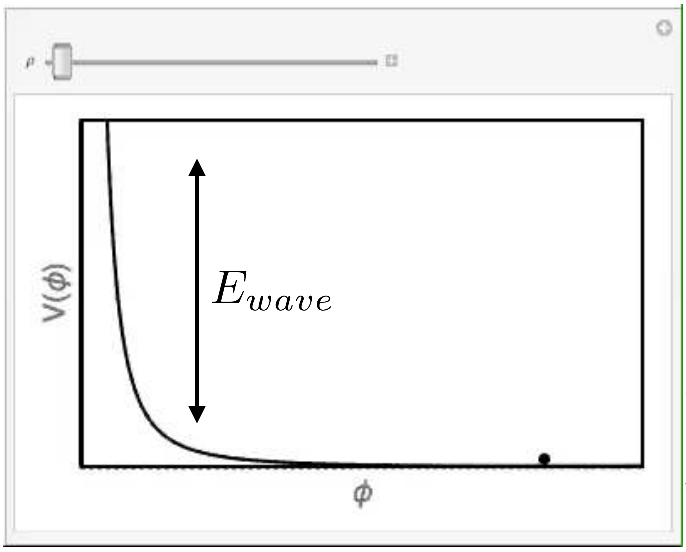

Profile of field

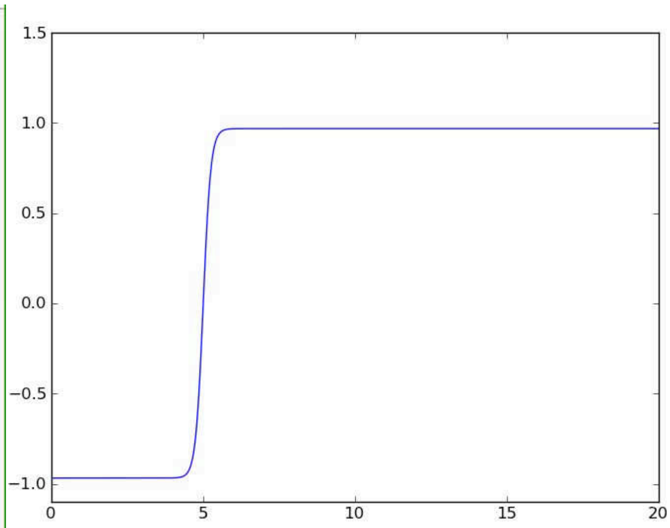

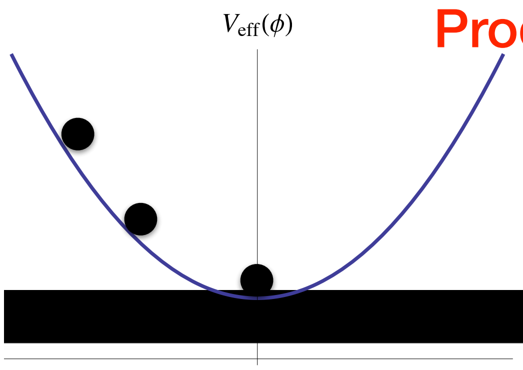

Production of waves
Symmetron

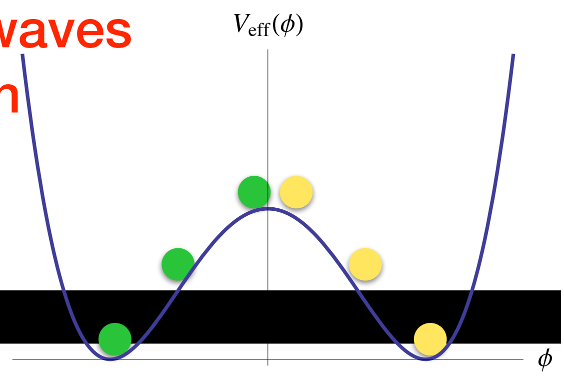

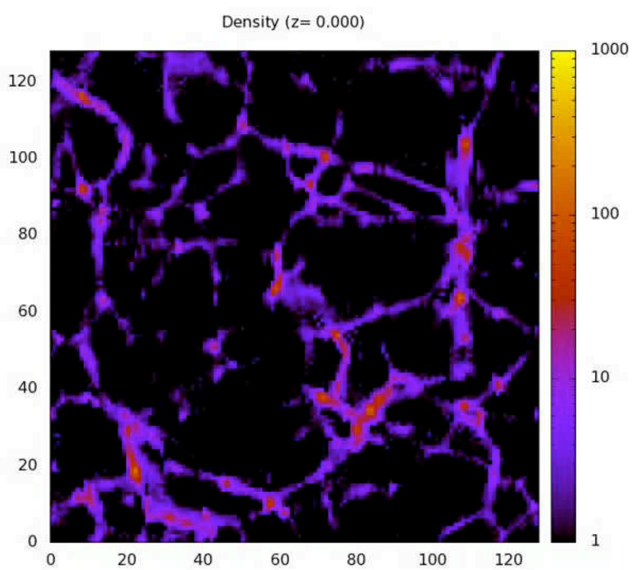

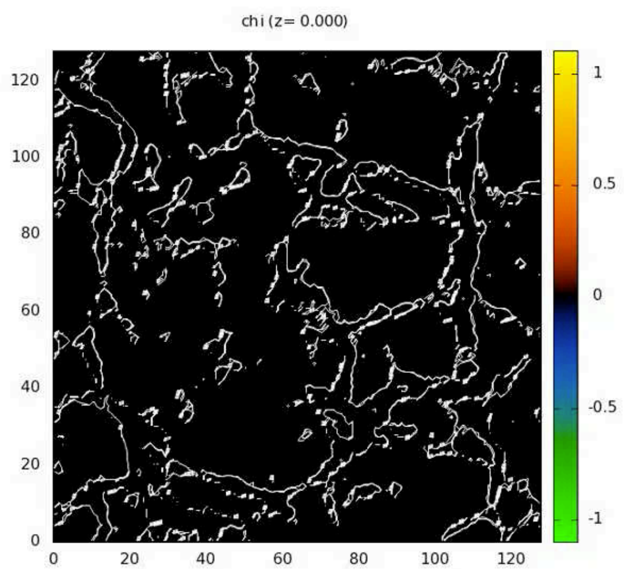

Llinares, DFM, PRL

Waves from collapse of domain walls

[redacted]

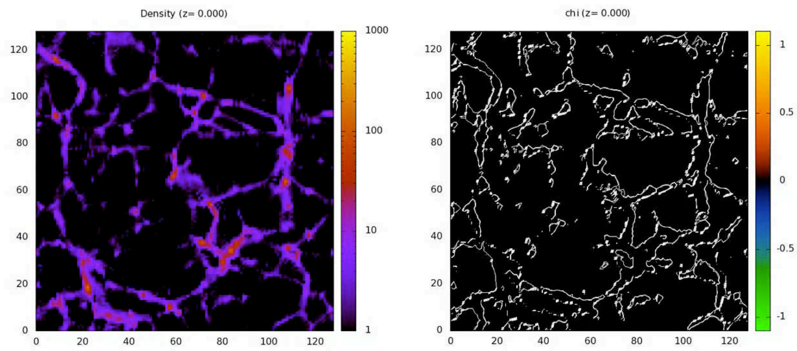

Profile of field [redacted]

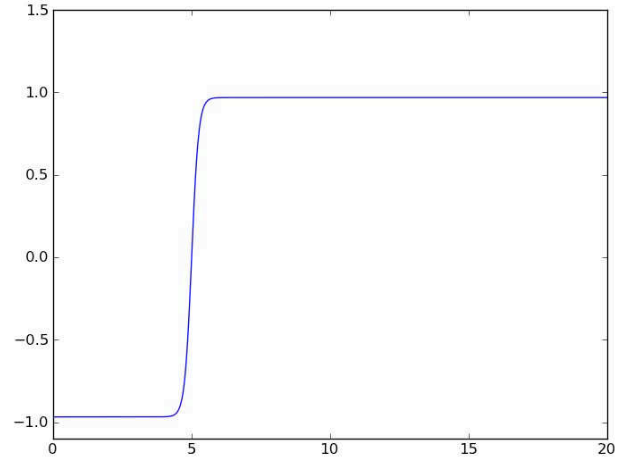

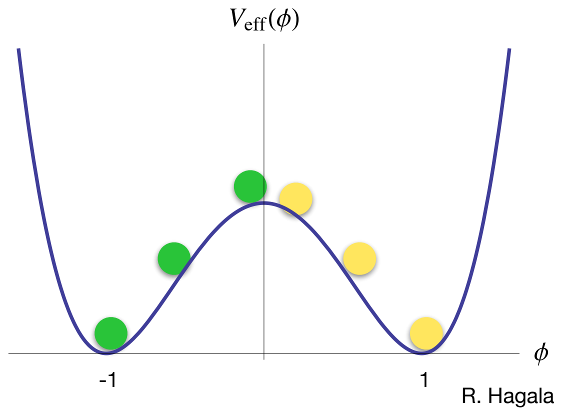

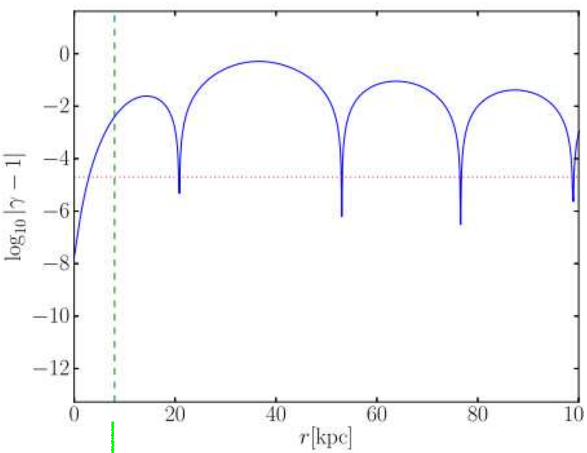

Distance from milky way centre

Solar System

Cassini bound

$$\gamma - 1 = -\frac{\phi^2}{M^2}\frac{2}{\frac{\phi^2}{M^2} + 2\Psi(1+\frac{\phi^2}{M^2})}$$

Hagala, Llinares, DFM, PRL

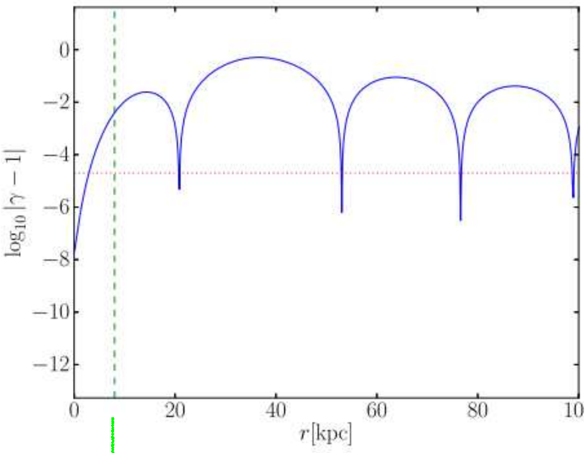

Cassini bound

$$\gamma - 1 = -\frac{\phi^2}{M^2}\frac{2}{\frac{\phi^2}{M^2} + 2\Psi(1 + \frac{\phi^2}{M^2})}$$

Distance from milky way centre

Solar System

Hagala, Llinares, DFM, PRL

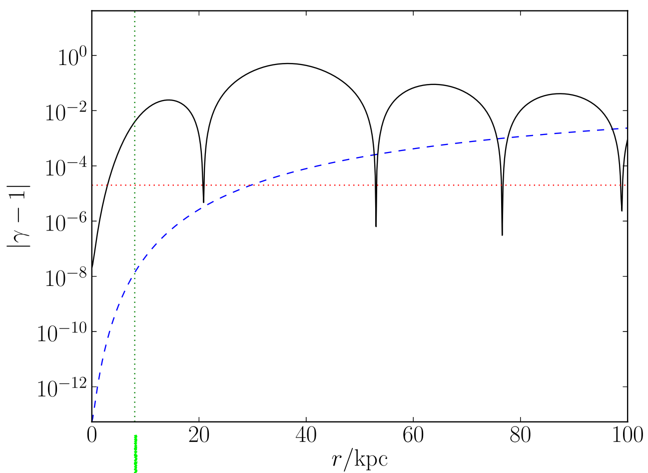

Cassini bound

$$\gamma - 1 = -\frac{\phi^2}{M^2}\frac{2}{\frac{\phi^2}{M^2} + 2\Psi(1 + \frac{\phi^2}{M^2})}$$

Distance from milky way centre

Solar System

Screening disrupted!

Scalar waves increase the PPN parameter and fifth force several orders in magnitude!

Oscillations are a smoking gun!

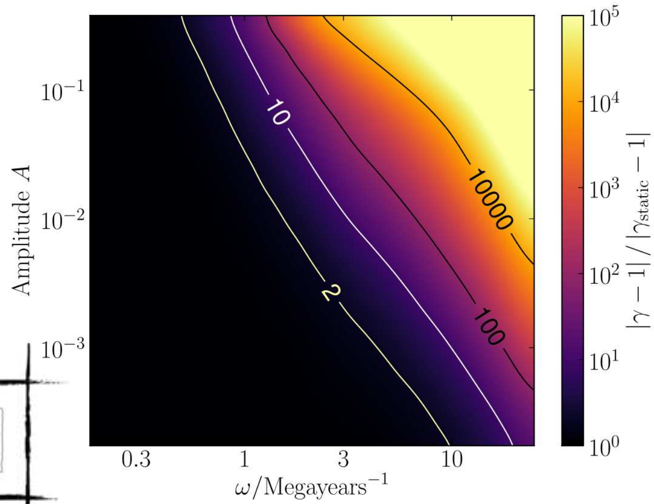

Hagala, Llinares, DFM, PRL

Summary

- A light extra degree of freedom in the gravity sector is viable only if a screening mechanism is efficient to suppress it at local scales

- The viability and efficiency of screening mechanism generally relies on the quasi-static approximation

- Astrophysical events can create waves and the quasi-static approximation is no longer valid

- Waves diminish the screening mechanism efficiency in several orders of magnitude reducing the viability of many modified gravity theories

Session S2A1 9:45–10:15

[Chair: Junichi Yokoyama]

Katsuki Aoki

Waseda University

"Ghost-free scalar-tensor theories in metric-affine formalism"

(10+5 min.)

[JGRG28 (2018) 110602]

Ghost-free scalar-tensor theories in metric-affine formalism

Katsuki Aoki, **Waseda University**
with K. Shimada
Based on Phys.Rev. D98 (2018) 044038 (arXiv: 1806.02589)
and in preparation

Introduction

GR is 1) a theory of massless spin-2 field
→ Gravity determine dynamics of a symmetric tensor $g_{\mu\nu}$.

2) a theory of curved geometry
→ Gravity determine all geometrical quantities.

Physics should require how to measure the distance and the derivative.
→ **two independent objects, metric** $g_{\mu\nu}$ **and connection** $\Gamma^{\mu}_{\alpha\beta}$.

Riemannian geometry: metric is only independent object

$$\Gamma^{\mu}_{\alpha\beta} = \left\{ {\mu \atop \alpha\beta} \right\} := \frac{1}{2} g^{\mu\nu}(\partial_\alpha g_{\beta\nu} + \partial_\beta g_{\alpha\nu} - \partial_\nu g_{\alpha\beta})$$

in which $\nabla_\mu g_{\alpha\beta} = 0\,, \quad \Gamma^{\mu}_{[\alpha\beta]} = 0$

Preserving inner product and torsionless **Just a special case!**

Metric and Metric-affine formalisms

- **Metric formalism**: Gravity is a theory of metric (= spin-2 field)
  → Gravity determine dynamics of a symmetric tensor $g_{\mu\nu}$.
- **Metric-affine (Palatini) formalism**: Gravity is a theory of geometry
  → Gravity determine not only the metric but also the connection.

Two formalisms generally give different theories.

Einstein gravity: Riemannian = beyond Riemannian

Beyond Einstein: Riemannian ≠ beyond Riemannian

For example, $\phi^2 R(g) \neq \phi^2 \overset{\Gamma}{R}(g,\Gamma)$ Bauer and Demir, 2008

$\phi\Box\phi \neq \phi\overset{\Gamma}{\Box}\phi$ see next talk!

Why are two different?

For convenience, we introduce the distortion tensor κ

$$\kappa^{\mu}{}_{\alpha\beta} := \Gamma^{\mu}_{\alpha\beta} - \left\{ {\mu \atop \alpha\beta} \right\} \qquad \left\{ {\mu \atop \alpha\beta} \right\} = \frac{1}{2} g^{\mu\nu}(\partial_\alpha g_{\beta\nu} + \partial_\beta g_{\alpha\nu} - \partial_\nu g_{\alpha\beta})$$

The metric-affine formalism = The metric formalism with κ.

$$\overset{\Gamma}{R}{}^{\mu}{}_{\alpha\beta\gamma}(\Gamma) = R^{\mu}{}_{\alpha\beta\gamma}(g) + 2\nabla_{[\alpha}\kappa^{\mu}_{\beta]\nu} + \kappa^{\mu}_{[\alpha|\sigma}\kappa^{\sigma}_{\beta]\nu}$$

$\text{linear in curvature} \sim M_{\rm pl}^2 R(g) + M_{\rm pl}^2 \kappa^2$: mass term of distortion

$\text{higher curvature} \supset (\nabla\kappa)^2$: kinetic term of distortion

When higher curvatures can be ignored, κ can be integrated out.

$$S_{\rm ST}[g,\kappa,\phi] = S_{\rm ST}[g,\kappa(g,\phi),\phi]$$ KA and K. Shimada, 2018

✓ Einstein gravity $\Rightarrow \kappa^{\mu}{}_{\alpha\beta} = 0$

✓ Beyond Einstein $\Rightarrow \kappa^{\mu}{}_{\alpha\beta} \neq 0$

cf. The metric formalism
$\Leftrightarrow \kappa^{\mu}{}_{\alpha\beta} = 0$

What can we get from metric-affine?

In low energy scales,

Integrating out κ

$$S_{\rm ST}[g,\kappa,\phi]=S_{\rm ST}[g,\kappa(g,\phi),\phi]$$

We can discuss metric-affine theories in the metric formalism.

However,

✓ Two formalisms give different predictions. (e.g. $\phi\Box\phi \neq \phi\overset{\Gamma}{\Box}\phi$)

✓ The metric-affine may reveal a hidden structure of ghost-free theories.

$$\mathcal{L}=\frac{M_{\rm pl}^2}{2}\overset{\Gamma}{R}(g,\Gamma)+\mathcal{L}_\phi(g,\phi,\overset{\Gamma}{\nabla}_\mu\phi,\overset{\Gamma}{\nabla}_\mu\overset{\Gamma}{\nabla}_\nu\phi) + \text{non-minimal couplings}$$

is ghost free if 1) the theory is projective invariant
2) we can take the unitary gauge $\phi=\phi(t)$

Projective invariance

Let's back to Einstein gravity.

$$\kappa^\mu{}_{\alpha\beta}:=\Gamma^\mu_{\alpha\beta}-\left\{{\mu \atop \alpha\beta}\right\}$$

$$\mathcal{L}_{\rm EH}(g,\Gamma)=\frac{M_{\rm pl}^2}{2}\overset{\Gamma}{R}=\frac{M_{\rm pl}^2}{2}\left(R(g)+\kappa^\alpha{}_{\alpha\beta}\kappa^{\beta\gamma}{}_\gamma-\kappa^{\alpha\beta}{}_\gamma\kappa^\gamma{}_{\alpha\beta}\right)+\text{total divergence}$$

The EH action has an additional symmetry, **"projective invariance"**,

$$\Gamma^\mu_{\alpha\beta}\to\Gamma^\mu_{\alpha\beta}+\delta^\mu_\beta U_\alpha(x) \quad \text{or} \quad \kappa^\mu{}_{\alpha\beta}\to\kappa^\mu{}_{\alpha\beta}+\delta^\mu_\beta U_\alpha(x)$$

The projective transformation preserves the geodesic equation

$$\frac{d^2x^\mu}{d\lambda^2}+\Gamma^\mu_{\alpha\beta}\frac{dx^\alpha}{d\lambda}\frac{dx^\beta}{d\lambda}=0$$

and the change of the angle for parallel transport (a conformal symmetry)

$$\delta_{\rm PT}\left(\frac{\mathbf{A}\cdot\mathbf{B}}{|\mathbf{A}||\mathbf{B}|}\right)\to\delta_{\rm PT}\left(\frac{\mathbf{A}\cdot\mathbf{B}}{|\mathbf{A}||\mathbf{B}|}\right)$$

Scalar field with projective invariance

Consider the Lagrangian

$$\mathcal{L} = \frac{M_{\rm pl}^2}{2}\overset{\Gamma}{R}(g,\Gamma) + \mathcal{L}_\phi(g,\phi,\overset{\Gamma}{\nabla}_\mu\phi,\overset{\Gamma}{\nabla}_\mu\overset{\Gamma}{\nabla}_\nu\phi)$$

Higher derivatives of ϕ have the connection

$$\overset{\Gamma}{\nabla}_\mu\phi = \partial_\mu\phi\,, \quad \overset{\Gamma}{\nabla}_\mu\overset{\Gamma}{\nabla}_\nu\phi = \partial_\mu\partial_\nu\phi - \Gamma^\alpha_{\nu\mu}\partial_\alpha\phi$$

Projective invariance $\Gamma^\mu_{\alpha\beta} \to \Gamma^\mu_{\alpha\beta} + \delta^\mu_\beta U_\alpha(x)$ is realized by invariance under

$$\overset{\Gamma}{\nabla}_\mu\overset{\Gamma}{\nabla}_\nu\phi \to \overset{\Gamma}{\nabla}_\mu\overset{\Gamma}{\nabla}_\nu\phi - U_\mu\partial_\nu\phi$$

In the gauge $\phi = \phi(t)$

$$\overset{\Gamma}{\nabla}_\mu\overset{\Gamma}{\nabla}_\nu\phi \to \overset{\Gamma}{\nabla}_\mu\overset{\Gamma}{\nabla}_\nu\phi - A_* U_\mu\, n_\nu$$

$$A_* = n^\mu\partial_\mu\phi\,, n^\mu \text{ is the normal vector}$$

Scalar field with projective invariance

In the gauge $\phi = \phi(t)$

$$\overset{\Gamma}{\nabla}_\mu\overset{\Gamma}{\nabla}_\nu\phi \to \overset{\Gamma}{\nabla}_\mu\overset{\Gamma}{\nabla}_\nu\phi - A_* U_\mu\, n_\nu$$

$$A_* = n^\mu\partial_\mu\phi\,, n^\mu \text{ is the normal vector}$$

Since U_μ is an arbitrary vector, we can choose $U_\mu \propto n_\mu$.

$$\overset{\Gamma}{\nabla}_\mu\overset{\Gamma}{\nabla}_\nu\phi \to \overset{\Gamma}{\nabla}_\mu\overset{\Gamma}{\nabla}_\nu\phi - U(x)\, n_\mu n_\nu$$

This symmetry implies the 00 component is just a gauge mode.

$$\overset{\Gamma}{\nabla}_\mu\overset{\Gamma}{\nabla}_\nu\phi = \pounds_n A_* n_\mu n_\nu + \cdots \qquad (A_* = -\dot{\phi}/N)$$

$$\Rightarrow \mathcal{L}_\phi(g,\phi,\overset{\Gamma}{\nabla}_\mu\phi,\overset{\Gamma}{\nabla}_\mu\overset{\Gamma}{\nabla}_\nu\phi) = \mathcal{L}(t,N,K_{ij},D_iN,\kappa)$$

The Ostrogradsky ghost (= lapse) does not appear in the unitary gauge.
(trivially degenerated)

Ghost-free scalar tensor theory

We found more general ghost-free Lagrangian

$$\mathcal{L} = f_1 \overset{\Gamma}{R} + f_2 \overset{\Gamma}{G}{}^{\mu\nu} \overset{\Gamma}{\nabla}_\mu \phi \overset{\Gamma}{\nabla}_\nu \phi + f_3 \overset{\Gamma}{G}{}^{\mu\alpha\nu\beta} \overset{\Gamma}{\nabla}_\mu \phi \overset{\Gamma}{\nabla}_\nu \phi \overset{\Gamma}{\nabla}_\alpha \overset{\Gamma}{\nabla}_\beta \phi + f_d \overset{\Gamma}{R}_{\mu\nu} \overset{\Gamma}{\nabla}{}^\mu \phi \overset{\Gamma}{\nabla}{}^\nu \phi + \mathcal{L}_\phi$$

where

$$f_1 = f_1(g, \phi, \overset{\Gamma}{\nabla}_\mu \phi, \overset{\Gamma}{\nabla}_\mu \overset{\Gamma}{\nabla}_\nu \phi) \quad \text{and so on}$$

are assumed to be projective invariant.

$$\overset{\Gamma}{G}{}^{\mu\nu\alpha\beta} := \frac{1}{4} \epsilon^{\mu\nu\rho\sigma} \epsilon^{\alpha\beta\gamma\delta} \overset{\Gamma}{R}_{\rho\sigma\gamma\delta} \qquad \text{dual Riemann tensor}$$

$$\overset{\Gamma}{G}{}^{\mu\nu} := \overset{\Gamma}{G}{}^{\mu\alpha\nu}{}_\alpha \qquad \text{Einstein tensor}$$

Up to the quadratic in the connection,
we can explicitly get the solution $\kappa = \kappa(g, \phi)$ and integrate κ out.

Quadratic projective invariant theory

Expanding the functions in terms of $\overset{\Gamma}{\nabla} \overset{\Gamma}{\nabla} \phi$ and ignoring higher orders

$$\begin{aligned}\mathcal{L}(g, \Gamma, \phi) = {} & f_1 \overset{\Gamma}{R} + f_2 \overset{\Gamma}{G}{}^{\mu\nu} \overset{\Gamma}{\nabla}_\mu \phi \overset{\Gamma}{\nabla}_\nu \phi + f_d \overset{\Gamma}{R}_{\mu\nu} \overset{\Gamma}{\nabla}{}^\mu \phi \overset{\Gamma}{\nabla}{}^\nu \phi + F_2 + F_3 \mathcal{L}_3^{\mathrm{gal}\Gamma} + F_4 \mathcal{L}_4^{\mathrm{gal}\Gamma} \\ & + C_1 \epsilon^{\mu\nu\rho\sigma} \epsilon^{\mu'\nu'\rho'}{}_\sigma \overset{\Gamma}{\nabla}_\mu \phi \overset{\Gamma}{\nabla}_{\mu'} \phi \overset{\Gamma}{\nabla}_\nu \overset{\Gamma}{\nabla}_{\nu'} \phi \overset{\Gamma}{\nabla}_{[\rho} \overset{\Gamma}{\nabla}_{\rho']} \phi + C_2 (\mathcal{L}_3^{\mathrm{gal}\Gamma})^2 \\ & + C_3 (g^{\mu\beta} g^{\nu\delta} g^{\alpha\gamma} - g^{\mu\nu} g^{\alpha\gamma} g^{\beta\delta}) \overset{\Gamma}{\nabla}_\mu \phi \overset{\Gamma}{\nabla}_\nu \phi \overset{\Gamma}{\nabla}_\alpha \overset{\Gamma}{\nabla}_\beta \phi \overset{\Gamma}{\nabla}_\gamma \overset{\Gamma}{\nabla}_\delta \phi\end{aligned}$$

= The most general projective invariant
scalar-tensor theories up to quadratic order

After integrating out the connection,
the theory is reduced to the quadratic U-DHOST theory.

$$\begin{aligned}\mathcal{L}(g, \phi) = {} & f R(g) + P + Q_1 g^{\mu\nu} \phi_{\mu\nu} + Q_2 \phi^\mu \phi_{\mu\nu} \phi^\nu + \left(\kappa_1 + \frac{f}{X}\right) L_1^{(2)} + \left(\kappa_2 - \frac{f}{X}\right) L_2^{(2)} + \left(\frac{2f}{X^2} - \frac{4f_X}{X} + 2\sigma\kappa_1 + 2\left[3\sigma - \frac{1}{X}\right]\kappa_2\right) L_3^{(2)} \\ & + \left(\alpha + \frac{2f_X}{X} - \frac{2f}{X^2} - \frac{2\kappa_1}{X}\right) L_4^{(2)} + \left(-\frac{\alpha}{X} + \frac{2f_X}{X^2} + \kappa_1 \left[\frac{1}{X^2} + 3\sigma^2 - \frac{2\sigma}{X}\right] + \kappa_2 \left[3\sigma - \frac{1}{X}\right]^2\right) L_5^{(2)}\end{aligned}$$

Hidden structure of ghost-free theories

Up to quadratic order in the connection

✓ The most general ST theory = The (quadratic) U-DHOST theory

De Felice, et al. 2018

$$\begin{aligned}\mathcal{L}(g,\Gamma,\phi) &= f_1\overset{\Gamma}{R} + f_2\overset{\Gamma}{G}{}^{\mu\nu}\overset{\Gamma}{\nabla}_\mu\phi\overset{\Gamma}{\nabla}_\nu\phi + f_d\overset{\Gamma}{R}_{\mu\nu}\overset{\Gamma}{\nabla}{}^\mu\phi\overset{\Gamma}{\nabla}{}^\nu\phi + F_2 + F_3\mathcal{L}_3^{\mathrm{gal}\Gamma} + F_4\mathcal{L}_4^{\mathrm{gal}\Gamma}\\ &+ C_1\epsilon^{\mu\nu\rho\sigma}\epsilon^{\mu'\nu'\rho'}{}_\sigma\overset{\Gamma}{\nabla}_\mu\phi\overset{\Gamma}{\nabla}_{\mu'}\phi\overset{\Gamma}{\nabla}_\nu\overset{\Gamma}{\nabla}_{\nu'}\phi\overset{\Gamma}{\nabla}_{[\rho}\overset{\Gamma}{\nabla}_{\rho']}\phi + C_2(\mathcal{L}_3^{\mathrm{gal}\Gamma})^2\\ &+ C_3(g^{\mu\beta}g^{\nu\delta}g^{\alpha\gamma} - g^{\mu\nu}g^{\alpha\gamma}g^{\beta\delta})\overset{\Gamma}{\nabla}_\mu\phi\overset{\Gamma}{\nabla}_\nu\phi\overset{\Gamma}{\nabla}_\alpha\overset{\Gamma}{\nabla}_\beta\phi\overset{\Gamma}{\nabla}_\gamma\overset{\Gamma}{\nabla}_\delta\phi\end{aligned}$$

The degeneracy conditions are satisfied only in the unitary gauge.

✓ Projective invariance + Galileon type combinations = (quadratic) DHOST

Langlois and Noui 2016

$$\mathcal{L}(g,\Gamma,\phi) = f_1\overset{\Gamma}{R} + f_2\overset{\Gamma}{G}{}^{\mu\nu}\overset{\Gamma}{\nabla}_\mu\phi\overset{\Gamma}{\nabla}_\nu\phi + F_2 + F_3\mathcal{L}_3^{\mathrm{gal}\Gamma} + F_4\mathcal{L}_4^{\mathrm{gal}\Gamma}$$

The degeneracy conditions are satisfied in any gauge.

✓ **Theories beyond quadratic order = new theories**

Relations between Palatini and metric

✓ (Conventional) non-minimal coupling

$$\mathcal{L} = \frac{M_{\mathrm{pl}}^2}{2}g^{\mu\nu}\overset{\Gamma}{R}_{\mu\nu} - \frac{1}{2}(\partial\phi)^2 - V(\phi) - \underline{\frac{\xi}{2}\phi^2\overset{\Gamma}{R}}$$

$$\Leftrightarrow \mathcal{L} = \frac{M_{\mathrm{pl}}^2}{2}R(g) - \frac{M_{\mathrm{pl}}^2 - \xi(1+6\xi)\phi^2}{2(M_{\mathrm{pl}}^2 - \xi\phi^2)}(\partial\phi)^2 - V(\phi) - \frac{\xi}{2}\phi^2\overset{\Gamma}{R}$$

Non-canonical kinetic term

✓ Kinetic non-minimal coupling

$$\mathcal{L} = \underline{f(X)\overset{\Gamma}{R}} + P(X)$$

$$X = (\partial\phi)^2$$

$$\Leftrightarrow \mathcal{L} = f(X)R(g) + P(X) + \frac{6f_X^2}{f}\phi^\alpha\phi^\beta\phi_{\alpha\gamma}\phi^\gamma_\beta$$

“counter term” to eliminate the ghost (NOT ad-hoc!)

⇒ should rediscuss well-known models which give new phenomenology.

Summary and Discussions

- Metric-affine formalism: metric and connection are independent.
- Beyond Einstein gravity: metric-affine formalism ≠ metric formalism

  Integrating out Γ (in low energy)

  $S_{\rm ST}[g,\Gamma,\phi] = S_{\rm ST}[g,\Gamma(g,\phi),\phi]$ Γ ≠ Levi-Civita connection

- Projective invariance → Ghost-free theories (in the unitary gauge)

  $$\mathcal{L} = \frac{M_{\rm pl}^2}{2}\overset{\Gamma}{R}(g,\Gamma) + \mathcal{L}_\phi(g,\phi,\overset{\Gamma}{\nabla}_\mu\phi,\overset{\Gamma}{\nabla}_\mu\overset{\Gamma}{\nabla}_\nu\phi) + \text{non-minimal couplings}$$

  In particular, beyond quadratic = new theories

  *Non-projective invariant theory is also possible

- Phenomenology? e.g. inflation

  see next talk for the simplest case! $(\phi\Box\phi \neq \phi\overset{\Gamma}{\Box}\phi)$

Keigo Shimada
Waseda University

“Inflation in Metric-affine Gravity”
(10+5 min.)

[JGRG28 (2018) 110603]

Inflation in Metric-affine Gravity

The 28th Workshop on General Relativity and Gravitation in Japan
@Rikkyo U.

KEIGO SHIMADA (WASEDA U.)

COLLABORATING WITH K. AOKI-SAN AND K. MAEDA-SAN (WASEDA)

BASED ON KS, K.AOKI, K.MAEDA[$arxiv$:1811.XXXX]

Prelude:

1. K.Aoki-san's Talk: [The Formulation]
   " Ghost-free scalar-tensor theories in metric-affine formalism"

➢The Idea:
Metric-affine Formalism + Projective Invariance = Ghost-free?

2. My Talk: [The Phenomenology]

➢The Idea:
Inflationary scenarios differ depending on Geometry
➢Not necessarily Projective Invariant Theories

Introduction: Non-Riemannian Geometry

Non-Riemannian Geometry(What do we keep and what we don't)

In (Pseudo-)Riemannian Geometry…

1. Riemann Metric $g_{\mu\nu}$:
   Defines length $\mathrm{d}s^2 = g_{\mu\nu}\mathrm{d}x^\mu \mathrm{d}x^\nu$
   Symmetric two-rank tensor

2. Connection $\left\{ {\lambda \atop \mu\nu} \right\}$: (Riemann-)Levi-Civita Connection
   Defines parallel transport
   Symmetric ($\left\{ {\lambda \atop \mu\nu} \right\} = \left\{ {\lambda \atop \nu\mu} \right\}$), Metric-Compatible ($\nabla_\lambda g_{\mu\nu} = 0$)

Introduction: Non-Riemannian Geometry

Non-Riemannian Geometry(What do we keep and what we dont)

In (Pseudo-)Rieman

⇓ Decided from the gravitational action

1. Riemann Metric $g_{\mu\nu}$:
   …nes length $\mathrm{d}s^2 = g_{\mu\nu}\mathrm{d}x^\mu \mathrm{d}x^\nu$

Fundamentally different geometrical variables

POINT

2. Connection $\left\{ {\lambda \atop \mu\nu} \right\}$: (Riemann-)Levi-Civita Connection
   Defines pa…

⇑ Decided by hand ⇑

Symmetric … Compatible ($\nabla_\lambda g_{\mu\nu} = 0$)

Extending the Geometry

Introduction: Metric-Affine Geometry

Metric-Affine Geometry

In Metric-affine Geometry…

1. Riemann Metric $g_{\mu\nu}$: ⇐ **Keep the metric as Riemann**
   Defines length $ds^2 = g_{\mu\nu} dx^\mu dx^\nu$
   Symmetric two-rank tensor

POINT

Let's let 'the action' decide the connection

2. Connection $\Gamma^\lambda{}_{\mu\nu}$: Arbitrary Connection
   Defines parallel transport
   ~~Symmetric ($\Gamma^\lambda{}_{\mu\nu} = \Gamma^\lambda{}_{\nu\mu}$), Metric-Compatible ($\nabla_\lambda g_{\mu\nu} = 0$)~~
   $T^\lambda{}_{\mu\nu} := \Gamma^\lambda{}_{\mu\nu} - \Gamma^\lambda{}_{\nu\mu}$ $\quad Q_\alpha{}^{\beta\gamma} := \nabla^\Gamma_\alpha g^{\beta\gamma}$

Metric-Affine Gravity

Introduction: Metric-Affine Geometry

Metric Affine

Arbitrary Affine-Connection

$\Gamma^\lambda{}_{\sigma\rho}$

Non-metricity Tensor

$Q_\alpha{}^{\beta\gamma} := \nabla^\Gamma_\alpha g^{\beta\gamma}$

Length/angle does not conserve

(Under Parallel Transport)

Torsion Tensor

$T^\lambda{}_{\mu\nu} := \Gamma^\lambda{}_{\mu\nu} - \Gamma^\lambda{}_{\nu\mu}$

Spacetime is Twisted

$[\nabla_\mu, \nabla_\nu] V^\lambda = R^\lambda{}_{\sigma\mu\nu} V^\sigma - T^\sigma{}_{\mu\nu} \nabla_\sigma V^\lambda$

Introduction: Metric-Affine Geometry

Metric Affine

Arbitrary Affine-Connection

$$\Gamma^{\lambda}{}_{\sigma\rho}$$

Non-metricity Tensor

$$Q_{\alpha}{}^{\beta\gamma} := \nabla_{\alpha}^{\Gamma} g^{\beta\gamma}$$

Torsion Tensor

$$T^{\lambda}{}_{\mu\nu} := \Gamma^{\lambda}{}_{\mu\nu} - \Gamma^{\lambda}{}_{\nu\mu}$$

$$\boxed{\Gamma^{\lambda}{}_{\mu\nu} = \left\{ {\lambda \atop \mu\nu} \right\} + \frac{1}{2}\left(T^{\lambda}{}_{\mu\nu} - 2T_{(\mu\nu)}{}^{\lambda} - Q^{\lambda}{}_{\mu\nu} + 2Q_{(\mu\nu)}{}^{\lambda} \right)}$$

Metric Affine Gravity allows one to 'Select' the Geometry

$$T^{\lambda}{}_{\mu\nu} := \Gamma^{\lambda}{}_{\mu\nu} - \Gamma^{\lambda}{}_{\nu\mu}$$

$$Q_{\alpha}{}^{\beta\gamma} := \nabla_{\alpha}^{\Gamma} g^{\beta\gamma}$$

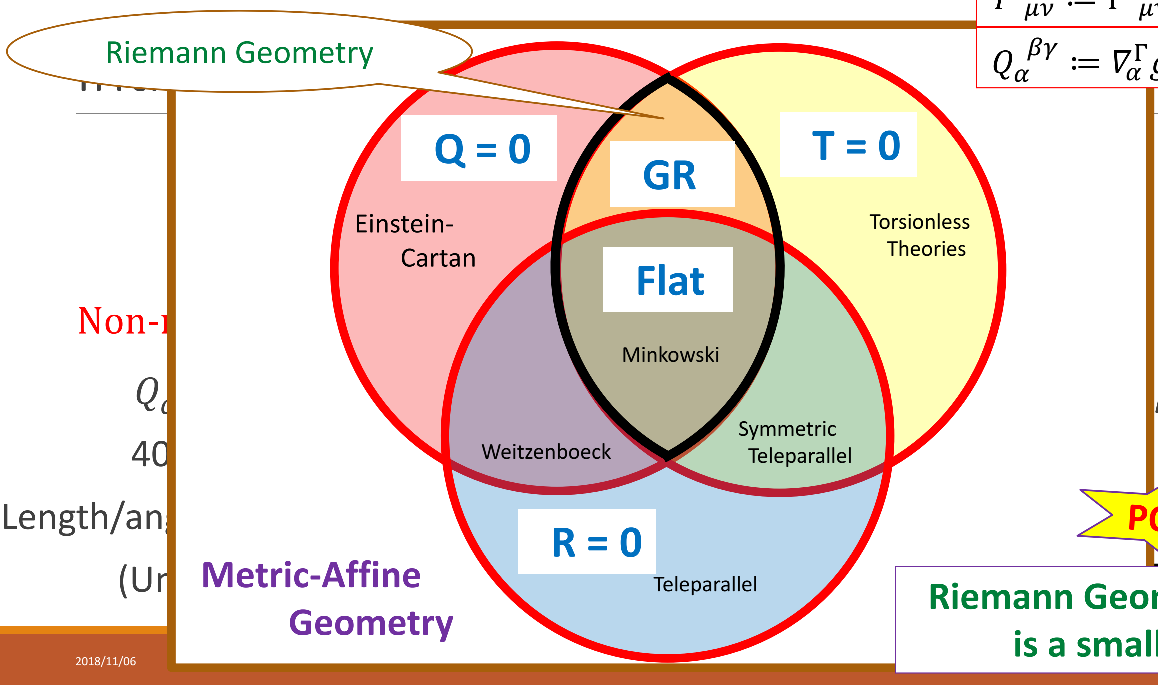

POINT

Riemann Geometry is a small subset

$$R^{\alpha}{}_{\beta\mu\nu}(\Gamma) \equiv \partial_{\mu}\Gamma^{\alpha}{}_{\nu\beta} - \partial_{\nu}\Gamma^{\alpha}{}_{\mu\beta} + \Gamma^{\alpha}{}_{\mu\lambda}\Gamma^{\lambda}{}_{\nu\beta} - \Gamma^{\alpha}{}_{\nu\lambda}\Gamma^{\lambda}{}_{\mu\beta}$$

Metric-Affine Formalism In GR

NON-RIEMANNIAN

Metric-affine Formalism (Einstein,1925):

Symmetric metric $g_{\mu\nu}$ and Connection $\Gamma^{\lambda}{}_{\sigma\rho}$ are independent

$$S = \frac{M_{Pl}^2}{2}\int d^4x\sqrt{-g}\, R(g,\Gamma) + S_M(g,\{\ \ \})$$

METRIC-AFFINE

$$\Downarrow$$

$$\Gamma^{\lambda}_{\sigma\rho} = \left\{ {\lambda \atop \sigma\rho} \right\} + U_{\sigma}\delta^{\lambda}_{\rho}$$

c.f. Aoki-san's Talk

U_{σ}: Projective Mode

$$R^{\alpha}{}_{\beta\mu\nu}(\Gamma) \equiv \partial_{\mu}\Gamma^{\alpha}{}_{\nu\beta} - \partial_{\nu}\Gamma^{\alpha}{}_{\mu\beta} + \Gamma^{\alpha}{}_{\mu\lambda}\Gamma^{\lambda}{}_{\nu\beta} - \Gamma^{\alpha}{}_{\nu\lambda}\Gamma^{\lambda}{}_{\mu\beta}$$

Metric-Affine Formalism In GR

NON-RIEMANNIAN

Metric-affine Formalism (Einstein,1925):

Symmetric metric $g_{\mu\nu}$ and Connection $\Gamma^{\lambda}{}_{\sigma\rho}$ are independent

$$S = \frac{M_{Pl}^2}{2}\int d^4x\sqrt{-g}\, R(g,\Gamma) + S_M(g,\{\ \ \})$$

METRIC-AFFINE

$$\Downarrow$$

$$\Gamma^{\lambda}_{\sigma\rho} = \left\{ {\lambda \atop \sigma\rho} \right\}$$

POINT

1. Gauge Fixing: $U_{\sigma} = 0$
2. Levi-Civita became a 'solution'
   - ✓ But not unique!

c.f. Aoki-san's Talk

$$R^{\alpha}{}_{\beta\mu\nu}(\Gamma) \equiv \partial_{\mu}\Gamma^{\alpha}{}_{\nu\beta} - \partial_{\nu}\Gamma^{\alpha}{}_{\mu\beta} + \Gamma^{\alpha}{}_{\mu\lambda}\Gamma^{\lambda}{}_{\nu\beta} - \Gamma^{\alpha}{}_{\nu\lambda}\Gamma^{\lambda}{}_{\mu\beta}$$

Metric-Affine Formalism In GR

As a 'second' approach…

NON-RIEMANNIAN

$$S = \frac{M_{Pl}^2}{2}\int d^4x\sqrt{-g}\,R(g,\Gamma) + S_M(g,\{\ \ \})$$

We could also '*select*' the geometry

A priori / Assume the geometry before variation

1. Riemann Geometry $\Gamma^{\lambda}{}_{\mu\nu} = \left\{ {\lambda \atop \mu\nu} \right\}$
2. Einstein-Cartan Geometry $T^{\lambda}{}_{\mu\nu} \neq 0 \quad Q_{\lambda}{}^{\mu\nu} = 0$
3. Weyl Geometry $T^{\lambda}{}_{\mu\nu} = 0 \quad Q_{\lambda}{}^{\mu\nu} = A_{\lambda}g^{\mu\nu}$

⋮

etc…

$$T^{\lambda}{}_{\mu\nu} := \Gamma^{\lambda}{}_{\mu\nu} - \Gamma^{\lambda}{}_{\nu\mu}$$
$$Q_{\alpha}{}^{\beta\gamma} := \nabla^{\Gamma}_{\alpha} g^{\beta\gamma}$$

$$R^{\alpha}{}_{\beta\mu\nu}(\Gamma) \equiv \partial_{\mu}\Gamma^{\alpha}{}_{\nu\beta} - \partial_{\nu}\Gamma^{\alpha}{}_{\mu\beta} + \Gamma^{\alpha}{}_{\mu\lambda}\Gamma^{\lambda}{}_{\nu\beta} - \Gamma^{\alpha}{}_{\nu\lambda}\Gamma^{\lambda}{}_{\mu\beta}$$

Metric-Affine Formalism In GR

Metric-affine Formalism (Einstein,1925):

Symmetric metric $g_{\mu\nu}$ and Connection $\Gamma^{\lambda}{}_{\sigma\rho}$ are independent

NON-RIEMANNIAN

$$S = \frac{M_{Pl}^2}{2}\int d^4x\sqrt{-g}\,R(g,\Gamma) + S_M(g,\{\ \ \})$$

$$\boxed{T^{\lambda}{}_{\mu\nu} = 0 \text{ or } Q_{\alpha}{}^{\beta\gamma} = 0}$$

'*Select*' the geometry

METRIC-AFFINE

$$\Gamma^{\lambda}{}_{\sigma\rho} = \left\{ {\lambda \atop \sigma\rho} \right\}$$

$$\boxed{T^{\lambda}{}_{\mu\nu} = 0 \text{ and } Q_{\alpha}{}^{\beta\gamma} = 0}$$

$Q_\alpha{}^{\beta\gamma} \coloneqq \nabla_\alpha^\Gamma g^{\beta\gamma} \quad T^\lambda{}_{\mu\nu} \coloneqq \Gamma^\lambda{}_{\mu\nu} - \Gamma^\lambda{}_{\nu\mu}$

Metric-Affine Formalism In GR: short summary

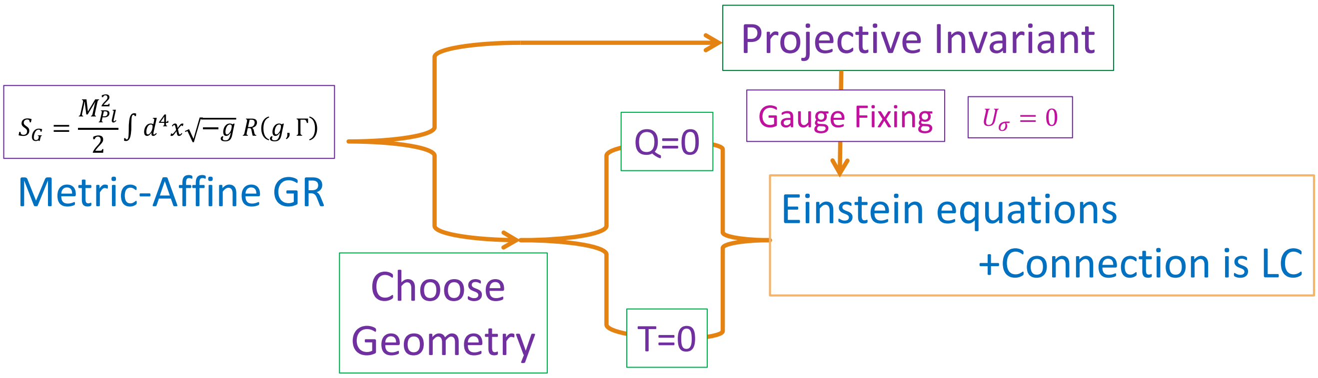

$Q_\alpha{}^{\beta\gamma} \coloneqq \nabla_\alpha^\Gamma g^{\beta\gamma} \quad T^\lambda{}_{\mu\nu} \coloneqq \Gamma^\lambda{}_{\mu\nu} - \Gamma^\lambda{}_{\nu\mu}$

Metric-Affine Formalism In GR: short summary

However
General metric-affine gravitational theories
do not admit L.C. connection as a solution
Metric-affine and Riemann geometry
computes different results in
"Extended Theories of Gravity"

Application to Inflation

$\Box^{\eta} := \eta^{\mu\nu}\partial_\mu\partial_\nu$

How to apply the framework to Cosmology?

Starting point: A 'Non-minimal' coupled Lagrangian

$$L_{\phi,flat} = \frac{1}{2}\phi\Box^{\eta}\phi - V(\phi)$$

$$\parallel$$

Up to surface term

$$-\frac{1}{2}\eta^{\mu\nu}\partial_\mu\phi\partial_\nu\phi - V(\phi)$$

Covariantize: 'Curve' space-time onto Metric-Affine space

Application to Inflation

- Flat Space

$$L_{\phi,flat} = \frac{1}{2}\phi\Box^{\eta}\phi - V(\phi)$$

- Curved Riemann Space

$\Box^{g}$: d'Alembertian Operator with the L.C. connection

$$L_{g\Gamma\phi} = \frac{M_{Pl}^2}{2}R(g,\Gamma) + \frac{1}{2}\phi\Box^{g}\phi - V(\phi)$$

Covariantization is trivial

$$\parallel$$

$$\frac{M_{Pl}^2}{2}R(g,\Gamma) - \frac{1}{2}g^{\mu\nu}\nabla_\nu^g\phi\nabla_\nu^g\phi - V(\phi)$$

Application to Inflation

- Flat Space

$$L_{\phi,flat} = \frac{1}{2}\phi\Box^{\eta}\phi - V(\phi)$$

- Curved Metric-Affine Space

$$\boxed{\Box^{\Gamma} := \alpha\nabla^{\mu}\nabla_{\mu} + (1-\alpha)\nabla_{\mu}\nabla^{\mu}}$$

POINT

Covariantization is non-trivial

$$L_{g\Gamma\phi} = \frac{M_{Pl}^2}{2}R(g,\Gamma) + \frac{1}{2}\phi\Box^{\Gamma}\phi - V(\phi)$$
$$\not\parallel$$
$$\frac{M_{Pl}^2}{2}R(g,\Gamma) - \frac{1}{2}g^{\mu\nu}\partial_\mu\phi\partial_\nu\phi - V(\phi)$$

Due to Non-metricity

$$\nabla_\mu\nabla^\mu = \nabla_\mu(g^{\mu\nu}\nabla_\nu) = Q_\mu{}^{\mu\nu} + \nabla^\mu\nabla_\mu \neq \nabla^\mu\nabla_\mu$$

Equal only for certain Γs

$$\boxed{\Box^{\Gamma} := \alpha\nabla^{\Gamma\mu}\nabla^{\Gamma}_{\mu} + (1-\alpha)\nabla^{\Gamma}_{\mu}\nabla^{\Gamma\mu}}$$

$$\frac{\delta L_{g\Gamma\phi}}{\delta\Gamma^{\lambda}_{\mu\nu}}\delta^{\lambda}_{\mu} = 0$$

Solving the Connection

$$L_{g\Gamma\phi} = \frac{M_{Pl}^2}{2}R(g,\Gamma) + \frac{1}{2}\phi\Box^{\Gamma}\phi + V(\phi)$$

Metric-Affine Scalar-Tensor

Impose PI

Q=0

Choose Geometry

T=0

⋮

etc

I. Projective Invariant:

$\Gamma^{\lambda}{}_{\mu\nu} =$

II. Metric-compatible

$\Gamma^{\lambda}{}_{\mu\nu} =$

III. Torsionless

$\Gamma^{\lambda}{}_{\mu\nu} =$

$$\Box^{\Gamma} := \alpha \nabla^{\Gamma\mu}\nabla^{\Gamma}_{\mu} + (1-\alpha)\nabla^{\Gamma}_{\mu}\nabla^{\Gamma\mu}$$

Solving the Connection

E.L. eq for Γ is Algebraic

$$L_{g\Gamma\phi} = \frac{M_{Pl}^2}{2} R(g,\Gamma) + \frac{1}{2}\phi\Box^{\Gamma}\phi + V(\phi)$$

Metric-Affine
Scalar-Tensor

Impose PI

Q=0

Choose Geometry

T=0

I. Projective Invariant: Fixes $\alpha = \frac{1}{2}$

$$\Gamma^{\lambda}{}_{\mu\nu} = \left\{ {\lambda \atop \mu\nu} \right\} + \frac{\phi}{4M_{Pl}^2}\left(\delta^{\lambda}_{\mu}\partial_{\nu}\phi - g_{\mu\nu}\partial^{\lambda}\phi\right) + U_{\mu}\delta^{\lambda}_{\nu}$$

II. Metric-compatible

$$\Gamma^{\lambda}{}_{\mu\nu} = \left\{ {\lambda \atop \mu\nu} \right\} + \frac{\phi}{4M_{Pl}^2}\left(\delta^{\lambda}_{\mu}\partial_{\nu}\phi - g_{\mu\nu}\partial^{\lambda}\phi\right)$$

III. Torsionless

$$\Gamma^{\lambda}{}_{\mu\nu} = \left\{ {\lambda \atop \mu\nu} \right\} + \frac{\phi}{6M_{Pl}^2}\left[3(\alpha-1)g_{\mu\nu}\partial^{\lambda}\phi + 2(\alpha+1)\delta^{\lambda}_{(\mu}\partial_{\nu)}\phi\right]$$

$$\Box^{\Gamma} := \alpha \nabla^{\Gamma\mu}\nabla^{\Gamma}_{\mu} + (1-\alpha)\nabla^{\Gamma}_{\mu}\nabla^{\Gamma\mu}$$

Solving the Connection

E.L. eq for Γ is Algebraic

POINT

The connection does not have any new d.o.f
(does not propagate)

$\because$ $L_{g\Gamma\phi}$ does not have a kinetic term of Γ

Can Integrate out Γ

I. Projective Invariant: Fixes $\alpha = \frac{1}{2}$

$$\Gamma^{\lambda}{}_{\mu\nu} = \left\{ {\lambda \atop \mu\nu} \right\} + \frac{\phi}{4M_{Pl}^2}\left(\delta^{\lambda}_{\mu}\partial_{\nu}\phi - g_{\mu\nu}\partial^{\lambda}\phi\right) + U_{\mu}\delta^{\lambda}_{\nu}$$

II. Metric-compatible

$$\Gamma^{\lambda}{}_{\mu\nu} = \left\{ {\lambda \atop \mu\nu} \right\} + \frac{\phi}{4M_{Pl}^2}\left(\delta^{\lambda}_{\mu}\partial_{\nu}\phi - g_{\mu\nu}\partial^{\lambda}\phi\right)$$

III. Torsionless

$$\Gamma^{\lambda}{}_{\mu\nu} = \left\{ {\lambda \atop \mu\nu} \right\} + \frac{\phi}{6M_{Pl}^2}\left[3(\alpha-1)g_{\mu\nu}\partial^{\lambda}\phi + 2(\alpha+1)\delta^{\lambda}_{(\mu}\partial_{\nu)}\phi\right]$$

To the ‘Riemannian’ frame

$$X = -\frac{1}{2}\partial^\mu \phi \partial_\mu \phi$$

$$\boxed{\Box^\Gamma := \alpha \nabla^{\Gamma\mu}\nabla^\Gamma_\mu + (1-\alpha)\nabla^\Gamma_\mu \nabla^{\Gamma\mu}}$$

Integrating out Γ

$$L_{g\Gamma\phi} = \frac{M_{Pl}^2}{2} R(g,\Gamma) + \frac{1}{2}\phi\Box^\Gamma\phi - \frac{1}{2}m^2\phi^2$$

Γ has no new d.o.f. $\Downarrow$ $\Gamma^\lambda_{\mu\nu} = \{\quad\} + \cdots$

$$L_{g\phi} = \frac{M_{Pl}^2}{2} R(g,\{\}) + \left(1 + B(\alpha)\frac{\phi^2}{M_{Pl}^2}\right) X - \frac{1}{2}m^2\phi^2$$

The only variables are the metric and the scalar
Selected Geometry is encoded in $B(\alpha)$

$$B(\alpha) = \begin{cases} -\frac{3}{8} & \text{PI and Q} = 0 \\ \frac{1}{6}(11\alpha^2 - 8\alpha - 1) & \text{T} = 0 \end{cases}$$

Consider $B(\alpha) > 0$ ex) Torsionless MAG

Observational Constraints $(n_s - r)$

0.25

r:
Tensor-to-Scalar
Ratio

0.00

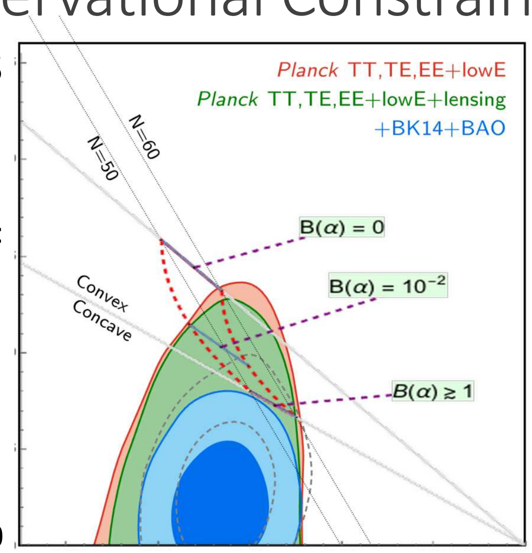

0.94 n_s:Spectral Index 1.0

$B(\alpha)$ as a new parameter

Planck 2018 Data

$$V(\phi) = \frac{1}{2}m^2\phi^2$$

$$\boxed{\Box^\Gamma := \alpha \nabla^{\Gamma\mu}\nabla^\Gamma_\mu + (1-\alpha)\nabla^\Gamma_\mu \nabla^{\Gamma\mu}}$$

Ex) For the Torsionless case...

$$\alpha \gtrsim 0.84 \quad \text{or} \quad \alpha \lesssim -0.12$$

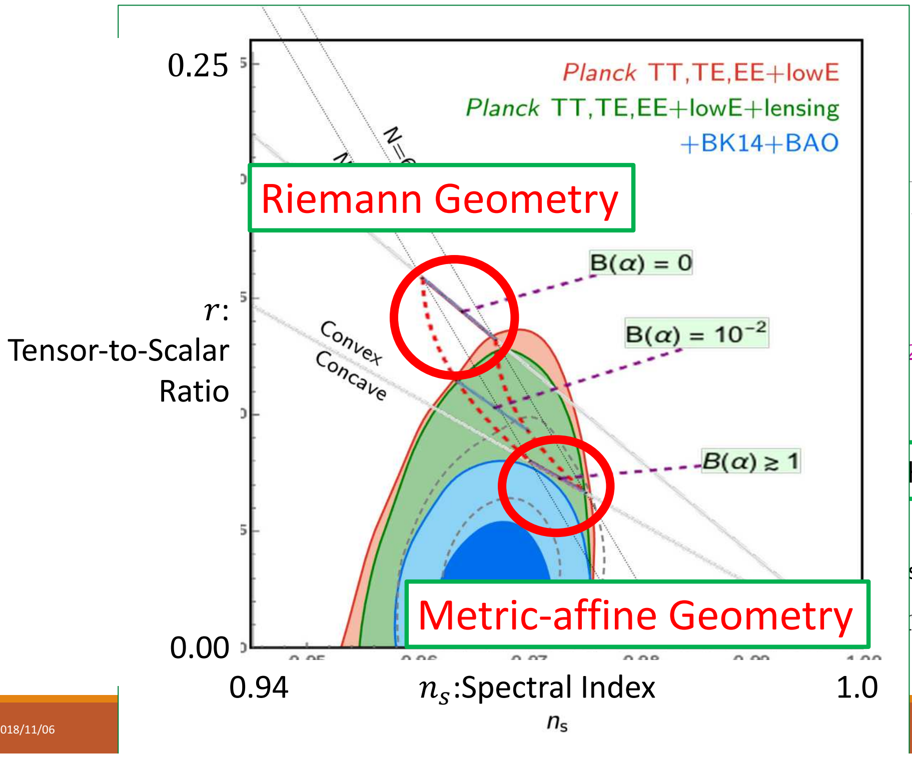

rameter

$^2\phi^2$

$+ (1-\alpha)\nabla^\Gamma_\mu \nabla^{\Gamma\mu}$

ss case…

$\alpha \lesssim -0.12$

Discussion

1. In Metric-affine Geometry covariantization is nontrivial
2. The (arbitrary) connection does not propagate
   1. The connection could be integrated out
   2. Existence of a ‘Riemann Frame’
3. Different ‘Geometry Postulates’ computes different results

   Riemann, Einstein-Cartan, Weyl, Torsionless… etc etc
4. Observational variables changes
   - Greatly differs from the Riemann counterpart
     - ✓ Some may seem observationally viable?

Summary

✓Metric-Affine Formalism is

an extension of gravity that could (should?) be considered.

✓It is possible to formulate viable metric-affine models

that differs from its purely metric counterpart.

✓When Γ is non-propagating,

one could obtain classically equivalent actions between

Riemann and Metric-affine geometry theories

Future Prospects:

1. Theoretical/Observational constraints from the spin half/integer difference
   - In MAG, SM particles with spin 1/2 and 0,1 act differently
     1. Different interaction with scalar(inflaton)
     2. Different Geodesics (Calculable from WKB approximation)
2. Including Higher derivatives/curvatures
   - Great difference between MAG and Riemannian
     - Connection propagates!!
   - Hamiltonian analysis is crucial (In progress)
     - How many new physical d.o.f.s? Observational constraints?

Session S2A2 10:45–12:15

[Chair: Yasusada Nambu]

Zhi-Bang Yao

School of Physics and Astronomy, Sun Yat-Sen University

“Spatially Covariant Gravity with Velocity of the Lapse Function”

(10+5 min.)

[JGRG28 (2018) 110604]

JGRG28@ Rikkyo university

Spatially covariant gravity with velocity of the lapse function

Speaker: Zhi-Bang Yao (姚志邦)
Supervisor: Xian Gao (高顯)
Department of Physics and Astronomy
Sun Yat-Sen University
Date: Nov. 6th, 2018

Reference: X. Gao and Z-B. Yao, [arXiv: 1806.02811]

Introduction

How to modified gravity ?

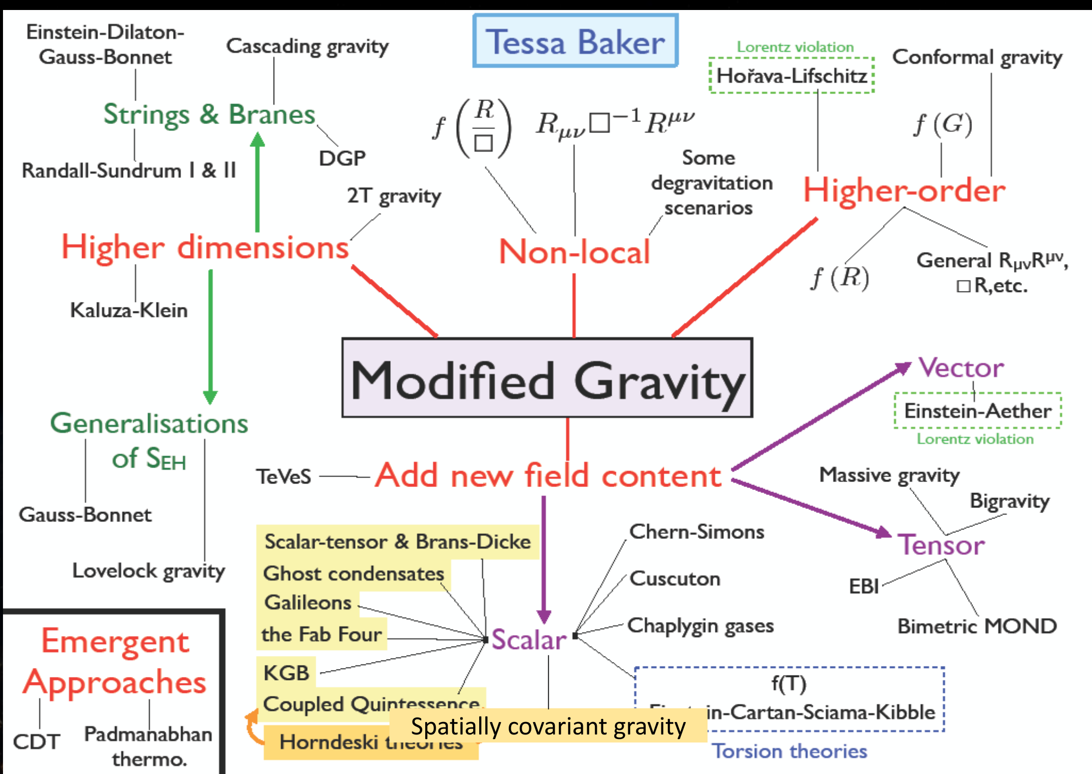

[Bull et. al, 2016]

Introduction

Why spatially covariant?

Modified Gravity

New degrees of freedom

Add scalar field

1974 Horndeski theory
2011 Generalized Galileons
2013 Mimetic Dark Matter
2014 GLPV theory
2015 Quadratic theory
2016 DHOST

Reduce symmetries

2004 Ghost condensate
2007 EFT of inflation
2009 Hořava gravity
2014 Spatially covariant gravity

$t=\phi$

Unitary gauge →

← Stuckelberg trick

$$\mathcal{L}\left(g_{\mu\nu}, {}^{(4)}R_{\mu\nu\rho\sigma}, \phi, \nabla_\mu\right) \xleftarrow{\phi(t,\vec{x})=t} \mathcal{L}\left(N, {}^{(3)}h_{ij}, {}^{(3)}R_{ij}, K_{ij}, \mathscr{L}_{\vec{n}}N, \nabla_i; t\right)$$

The action

How to determine the Lagrangian?

[Xian Gao, PRD, 2014]

$$\xrightarrow{\text{scalar-tensor}} \mathcal{L}\left(\phi, g_{\mu\nu}, {}^{(4)}R_{\mu\nu}; \nabla_\mu\right)$$

$$\xrightarrow{\text{ADM}} \mathcal{L}\left(\phi, N, h_{\mu\nu}, {}^{(3)}R_{\mu\nu}; \pounds_{\vec{n}}, D_\mu\right)$$

$$\xrightarrow{\text{unitary gauge}} \mathcal{L}\left(t, N, h_{ij}, {}^{(3)}R_{ij}; \pounds_{\vec{n}}, \nabla_i\right)$$

$$\xrightarrow{\text{special case}} \mathcal{L}\left(t, N, h_{ij}, {}^{(3)}R_{ij}, \pounds_{\vec{n}}h_{ij}; \nabla_i\right)$$

$$\xrightarrow{\text{extending}} \mathcal{L}\left(t, N, h_{ij}, {}^{(3)}R_{ij}, \pounds_{\vec{n}}N, \pounds_{\vec{n}}h_{ij}; \nabla_i\right)$$

Spatially Covariant Gravity with velocity of lapse function

To the XG theory, DoF is 3, but, naively thinking, to the extended one, the DoF generally should be 4.

Under what conditions it's reduced to 3 only ?

Hamiltonian analysis

Dealing with the action

Action in unitary gauge:

$$S^{(\mathrm{u.g.})} = \int dtd^3xN\sqrt{h}\mathcal{L}\left(t, N, h_{ij}, R_{ij}, F, K_{ij}, \nabla_i\right)$$

$$F = \pounds_{\vec{n}}N$$

$$K_{ij} = \frac{1}{2}\pounds_{\vec{n}}h_{ij}$$

The equivalent action with Lagrange multipliers:

$$S^{(\mathrm{eq})} = S_{AB} + \int dtd^3x\left[\frac{\delta S_{AB}}{\delta A}(F - A) + \frac{\delta S_{AB}}{\delta B_{ij}}(K_{ij} - B_{ij})\right]$$

Phase space:

$$\begin{pmatrix} N & N^i & h_{ij} & A & B_{ij} \\ \pi & \pi_i & \pi^{ij} & p & p^{ij} \end{pmatrix} \qquad \mathrm{dim} = 2\times(10+7) = 34$$

[Rio Saitou, PRD, 2016]

Hamiltonian analysis

Consistency conditions

Primary constraints:

$$\pi_i \approx 0 \qquad p \approx 0 \qquad p^{ij} \approx 0$$

$$\tilde{\pi} := \pi - \frac{1}{N}\frac{\delta S_{AB}}{\delta A} \approx 0 \qquad \tilde{\pi}^{ij} := \pi^{ij} - \frac{1}{2N}\frac{\delta S_{AB}}{\delta B_{ij}} \approx 0$$

Consistency conditions of primary constraints:

$$\int d^3y \begin{bmatrix} [\cdot,\cdot] & \pi_k & p & p^{kl} & \tilde{\pi} & \tilde{\pi}^{kl} \\ \pi_i & 0 & 0 & 0 & 0 & 0 \\ p & 0 & 0 & 0 & [p(\vec{x}),\tilde{\pi}(\vec{y})] & [p(\vec{x}),\tilde{\pi}^{kl}(\vec{y})] \\ p^{ij} & 0 & 0 & 0 & [p^{ij}(\vec{x}),\tilde{\pi}(\vec{y})] & [p^{ij}(\vec{x}),\tilde{\pi}^{kl}(\vec{y})] \\ \tilde{\pi} & 0 & [\tilde{\pi}(\vec{x}),p(\vec{y})] & [\tilde{\pi}(\vec{x}),p^{kl}(\vec{y})] & [\tilde{\pi}(\vec{x}),\tilde{\pi}(\vec{y})] & [\tilde{\pi}(\vec{x}),\tilde{\pi}^{kl}(\vec{y})] \\ \tilde{\pi}^{ij} & 0 & [\tilde{\pi}^{ij}(\vec{x}),p(\vec{y})] & [\tilde{\pi}^{ij}(\vec{x}),p^{kl}(\vec{y})] & [\tilde{\pi}^{ij}(\vec{x}),\tilde{\pi}(\vec{y})] & [\tilde{\pi}^{ij}(\vec{x}),\tilde{\pi}^{kl}(\vec{y})] \end{bmatrix} \begin{bmatrix} \lambda^k \\ \mu \\ \mu_{kl} \\ \lambda \\ \lambda_{kl} \end{bmatrix}(\vec{y}) \approx \begin{bmatrix} \mathcal{C}_i \\ 0 \\ 0^{ij} \\ C' \\ T^{ij} \end{bmatrix}(\vec{x}$$

$$\begin{aligned} \#_{\mathrm{dof}} &= \frac{1}{2}(\#_{\mathrm{var}}\times 2 - \#_{\mathrm{1st}}\times 2 - \#_{\mathrm{2nd}}) \\ &= \frac{1}{2}(17\times 2 - 6\times 2 - 14) \\ &= 4 \end{aligned}$$

Hamiltonian analysis

Consistency conditions

Primary constraints:

$$\pi_i \approx 0 \qquad p \approx 0 \qquad p^{ij} \approx 0$$

$$\tilde{\pi} := \pi - \frac{1}{N}\frac{\delta S_{AB}}{\delta A} \approx 0 \qquad \tilde{\pi}^{ij} := \pi^{ij} - \frac{1}{2N}\frac{\delta S_{AB}}{\delta B_{ij}} \approx 0$$

Consistency conditions of primary constraints:

$$\int d^3y \begin{bmatrix} [\cdot,\cdot] & \pi_k & \bar{p} & p^{kl} & \bar{\pi} & \tilde{\pi}^{kl} \\ \pi_i & 0 & 0 & 0 & 0 & 0 \\ \bar{p} & 0 & 0 & 0 & -\mathcal{D}(\vec{y},\vec{x}) & 0 \\ p^{ij} & 0 & 0 & 0 & 0 & [p^{ij}(\vec{x}),\tilde{\pi}^{kl}(\vec{y})] \\ \bar{\pi} & 0 & \mathcal{D}(\vec{x},\vec{y}) & 0 & \mathcal{F}(\vec{x},\vec{y}) & 0 \\ \tilde{\pi}^{ij} & 0 & 0 & [\tilde{\pi}^{ij}(\vec{x}),p^{kl}(\vec{y})] & 0 & [\tilde{\pi}^{ij}(\vec{x}),\tilde{\pi}^{kl}(\vec{y})] \end{bmatrix} \begin{bmatrix} \lambda^k \\ \mu \\ \mu_{kl} \\ \lambda \\ \lambda_{kl} \end{bmatrix}(\vec{y}) \approx \begin{bmatrix} \mathcal{C}_i \\ 0 \\ 0^{ij} \\ \mathcal{C} \\ T^{ij} \end{bmatrix}(\vec{x})$$

$$\begin{aligned} \#_{\text{dof}} &= \frac{1}{2}\left(\#_{\text{var}} \times 2 - \#_{\text{1st}} \times 2 - \#_{\text{2nd}}\right) \\ &= \frac{1}{2}(17 \times 2 - 6 \times 2 - 14) \\ &= 4 \end{aligned}$$

Hamiltonian analysis

Consistency conditions

$$\int d^3y \begin{bmatrix} [\cdot,\cdot] & \pi_k & \bar{p} & p^{kl} & \bar{\pi} & \tilde{\pi}^{kl} \\ \pi_i & 0 & 0 & 0 & 0 & 0 \\ \bar{p} & 0 & 0 & 0 & -\mathcal{D}(\vec{y},\vec{x}) & 0 \\ p^{ij} & 0 & 0 & 0 & 0 & [p^{ij}(\vec{x}),\tilde{\pi}^{kl}(\vec{y})] \\ \bar{\pi} & 0 & \mathcal{D}(\vec{x},\vec{y}) & 0 & \mathcal{F}(\vec{x},\vec{y}) & 0 \\ \tilde{\pi}^{ij} & 0 & 0 & [\tilde{\pi}^{ij}(\vec{x}),p^{kl}(\vec{y})] & 0 & [\tilde{\pi}^{ij}(\vec{x}),\tilde{\pi}^{kl}(\vec{y})] \end{bmatrix} \begin{bmatrix} \lambda^k \\ \mu \\ \mu_{kl} \\ \lambda \\ \lambda_{kl} \end{bmatrix}(\vec{y}) \approx \begin{bmatrix} \mathcal{C}_i \\ 0 \\ 0^{ij} \\ \mathcal{C} \\ T^{ij} \end{bmatrix}(\vec{x})$$

$$\begin{aligned} \#_{\text{dof}} &= \frac{1}{2}\left(\#_{\text{var}} \times 2 - \#_{\text{1st}} \times 2 - \#_{\text{2nd}}\right) \\ &= \frac{1}{2}(17 \times 2 - 6 \times 2 - 14) \\ &= 4 \end{aligned}$$

$$\int d^3y \begin{bmatrix} [\cdot,\cdot] & \pi_k & \bar{p} & p^{kl} & \bar{\pi} & \tilde{\pi}^{kl} \\ \pi_i & 0 & 0 & 0 & 0 & 0 \\ \bar{p} & 0 & 0 & 0 & 0 & 0 \\ p^{ij} & 0 & 0 & 0 & 0 & [p^{ij}(\vec{x}),\tilde{\pi}^{kl}(\vec{y})] \\ \bar{\pi} & 0 & 0 & 0 & \mathcal{F}(\vec{x},\vec{y}) & 0 \\ \tilde{\pi}^{ij} & 0 & 0 & [\tilde{\pi}^{ij}(\vec{x}),p^{kl}(\vec{y})] & 0 & [\tilde{\pi}^{ij}(\vec{x}),\tilde{\pi}^{kl}(\vec{y})] \end{bmatrix} \begin{bmatrix} \lambda^k \\ \mu \\ \mu_{kl} \\ \lambda \\ \lambda_{kl} \end{bmatrix}(\vec{y}) \approx \begin{bmatrix} \mathcal{C}_i \\ 0 \\ 0^{ij} \\ \mathcal{C} \\ T^{ij} \end{bmatrix}(\vec{x})$$

$$\begin{aligned} \#_{\text{dof}} &= \frac{1}{2}\left(\#_{\text{var}} \times 2 - \#_{\text{1st}} \times 2 - \#_{\text{2nd}}\right) \\ &= \frac{1}{2}(17 \times 2 - 7 \times 2 - 13) \\ &= 3.5 \end{aligned}$$

Hamiltonian analysis

Consistency conditions

$$\int d^3y \begin{bmatrix} [\cdot,\cdot] & \pi_k & \bar{p} & p^{kl} & \bar{\pi} & \tilde{\pi}^{kl} \\ \pi_i & 0 & 0 & 0 & 0 & 0 \\ \bar{p} & 0 & 0 & 0 & -\mathcal{D}(\vec{y},\vec{x}) & 0 \\ p^{ij} & 0 & 0 & 0 & 0 & [p^{ij}(\vec{x}),\tilde{\pi}^{kl}(\vec{y})] \\ \bar{\pi} & 0 & \mathcal{D}(\vec{x},\vec{y}) & 0 & \mathcal{F}(\vec{x},\vec{y}) & 0 \\ \tilde{\pi}^{ij} & 0 & 0 & [\tilde{\pi}^{ij}(\vec{x}),p^{kl}(\vec{y})] & 0 & [\tilde{\pi}^{ij}(\vec{x}),\tilde{\pi}^{kl}(\vec{y})] \end{bmatrix} \begin{bmatrix} \lambda^k \\ \mu \\ \mu_{kl} \\ \lambda \\ \lambda_{kl} \end{bmatrix} (\vec{y}) \approx \begin{bmatrix} \mathcal{C}_i \\ 0 \\ 0^{ij} \\ \mathcal{C} \\ T^{ij} \end{bmatrix} (\vec{x})$$

$$\begin{aligned} \#_{\rm dof} &= \frac{1}{2}\left(\#_{\rm var}\times 2 - \#_{\rm 1st}\times 2 - \#_{\rm 2nd}\right) \\ &= \frac{1}{2}\left(17\times 2 - 6\times 2 - 14\right) \\ &= 4 \end{aligned}$$

$$\int d^3y \begin{bmatrix} [\cdot,\cdot] & \pi_k & \bar{p} & p^{kl} & \bar{\pi} & \tilde{\pi}^{kl} \\ \pi_i & 0 & 0 & 0 & 0 & 0 \\ \bar{p} & 0 & 0 & 0 & 0 & 0 \\ p^{ij} & 0 & 0 & 0 & 0 & [p^{ij}(\vec{x}),\tilde{\pi}^{kl}(\vec{y})] \\ \bar{\pi} & 0 & 0 & 0 & 0 & 0 \\ \tilde{\pi}^{ij} & 0 & 0 & [\tilde{\pi}^{ij}(\vec{x}),p^{kl}(\vec{y})] & 0 & [\tilde{\pi}^{ij}(\vec{x}),\tilde{\pi}^{kl}(\vec{y})] \end{bmatrix} \begin{bmatrix} \lambda^k \\ \mu \\ \mu_{kl} \\ \lambda \\ \lambda_{kl} \end{bmatrix} (\vec{y}) \approx \begin{bmatrix} \mathcal{C}_i \\ 0 \\ 0^{ij} \\ \mathcal{C} \\ T^{ij} \end{bmatrix} (\vec{x})$$

$$\begin{aligned} \#_{\rm dof} &= \frac{1}{2}\left(\#_{\rm var}\times 2 - \#_{\rm 1st}\times 2 - \#_{\rm 2nd}\right) \\ &= \frac{1}{2}\left(17\times 2 - 7\times 2 - 14\right) \\ &= 3 \end{aligned}$$

Hamiltonian analysis

Results

Spatially covariant gravity with velocity of the lapse function:

$$S^{(\rm u.g.)} = \int dt d^3x N\sqrt{h}\mathcal{L}\left(t, N, h_{ij}, F, K_{ij}, R_{ij}, \nabla_i\right) \qquad F = \pounds_{\vec{n}} N$$

the degrees of freedom is 3 if it is satisfied two conditions:

$\boxed{\mathcal{D}(\vec{x},\vec{y}) = 0, \qquad \text{(Degeneracy condition)}}$ → Degenerate kinetic matrix

$\boxed{\mathcal{F}(\vec{x},\vec{y}) = 0, \qquad \text{(Consistency condition)}}$ → Existence secondary constraint

Degenerate Lagrangian is not a sufficient condition to remove the ghost.

Concrete examples

Quadratic case 1

Lagrangian up to quadratic order:

$$\mathcal{L}^{(\mathrm{quad})} = a_1 K + a_2 F + b_1 K_{ij} K^{ij} + b_2 K^2 + c_1 K F + c_2 F^2 + \mathcal{V}$$

Case 1: $a_1 \sim c_2$ are the functions of (t, N)

$$\boxed{\mathcal{D}(\vec{x}, \vec{y}) = 0 \Rightarrow c_2 = \frac{3}{4} \frac{c_1^2}{b_1 + 3b_2}} \qquad \boxed{\mathcal{F}(\vec{x}, \vec{y}) \equiv 0}$$

$$\mathcal{L}^{(\mathrm{quad})} = a_1 K + a_2 F + b_1 K_{ij} K^{ij} + b_2 K^2 + c_1 K F + \frac{3}{4} \frac{c_1^2}{b_1 + 3b_2} F^2 + \mathcal{V}$$

$$\mathcal{L}^{(\mathrm{quad})} = a_1 K + a_2 F - b_2 K_{ij} K^{ij} + b_2 K^2 + c_1 K F + \frac{3}{4} \frac{c_1^2}{2b_2} F^2 + \mathcal{V}$$

[Domenech, Mukohyama and etc., PRD, 2016]

Concrete examples

Quadratic case 2

Case 2: $a_1 \sim c_2$ are the functions of $(t, N, \nabla_i N)$

$$\boxed{\mathcal{D}(\vec{x}, \vec{y}) = 0 \Rightarrow c_2 = \frac{3}{4} \frac{c_1^2}{b_1 + 3b_2}}$$

$$\boxed{\mathcal{F}(\vec{x}, \vec{y}) = \partial_{y^i} \delta^3 (\vec{x} - \vec{y}) \sqrt{h(\vec{x})} \partial^{x^i} N(\vec{x})\, \mathcal{E}(\vec{x}) - (\vec{x} \leftrightarrow \vec{y}) = 0}$$

$$\begin{aligned} 0 = \mathcal{E} \quad \equiv \quad & \frac{\partial a_2}{\partial X} - \frac{3}{2} \frac{c_1}{b_1 + 3b_2} \frac{\partial a_1}{\partial X} \\ & + \left(\frac{\partial c_2}{\partial X} - \frac{3}{4} \frac{c_1}{b_1 + 3b_2} \frac{\partial c_1}{\partial X} \right) 2A \\ & + \left(\frac{\partial c_1}{\partial X} - \frac{c_1}{b_1 + 3b_2} \frac{\partial (b_1 + 3b_2)}{\partial X} \right) B \end{aligned} \qquad X \equiv \frac{1}{2} \partial_i N \partial^i N$$

Consistency condition: responding to the mixed time and spatial derivative terms

Concrete examples

Quadratic case 2

Constrained equations:

$$\begin{cases} c_2 - \frac{3}{4}\frac{c_1^2}{b_1+3b_2} = 0 \\ \frac{\partial c_2}{\partial X} - \frac{3}{4}\frac{c_1}{b_1+3b_2}\frac{\partial c_1}{\partial X} = 0 \\ \frac{\partial a_2}{\partial X} - \frac{3}{2}\frac{c_1}{b_1+3b_2}\frac{\partial a_1}{\partial X} = 0 \\ \frac{\partial c_1}{\partial X} - \frac{c_1}{b_1+3b_2}\frac{\partial (b_1+3b_2)}{\partial X} = 0 \end{cases} \Longrightarrow \begin{cases} \frac{3}{2}\frac{c_1}{b_1+3b_2} = \gamma(t,N) \\ a_2 - \gamma(t,N)\,a_1 = \alpha(t,N) \end{cases}$$

$$\boxed{\mathcal{L}^{(\mathrm{quad})} = a_1(K+\gamma F) + \alpha F + b_1\left(K_{ij}K^{ij} - \frac{1}{3}K^2\right) + \frac{1}{3}(b_1+3b_2)(K+\gamma F)^2 + \mathcal{V}}$$

Where a_1, b_1 and b_2 are the general functions of $(t, N, \partial_i N)$ while α and γ are the functions of (t, N) only.

Hamiltonian analysis

The canonical Hamiltonian

Canonical Hamiltonian:

$$H_C|_{\Gamma_P} \approx \int d^3x\,(NC + N^i\mathcal{C}_i) \simeq \int d^3x\,(NC + \Pi_I \pounds_{\vec{N}}\Phi^I)$$

$$\begin{aligned} \mathcal{C}_i \quad \equiv \quad & \pi\nabla_i N - 2\sqrt{h}\nabla_j\frac{\pi_i^j}{\sqrt{h}} + \left(\pi_j\nabla_i N^j + \sqrt{h}\nabla_j\frac{\pi_i N^j}{\sqrt{h}}\right) \\ & + p\nabla_i A + \left(p^{kl}\nabla_i B_{kl} - 2\sqrt{h}\nabla_j\left(\frac{p^{jk}}{\sqrt{h}}B_{ik}\right)\right) \end{aligned}$$

Because of spatial covariance of the theories:

$$\boxed{\int d^3x\,\xi^i\left[\mathcal{C}_i(\vec{x}), \mathcal{F}\right] \simeq \int d^3x\,\frac{\delta\mathcal{F}}{\delta f^I}\pounds_{\vec{\xi}} f^I}$$

$$\boxed{\left[\mathcal{C}_i(\vec{x}), \varphi^J(\vec{y})\right] \approx 0 \qquad \left[\mathcal{C}_i(\vec{x}), H_C\right] = 0}$$

Conclusions

- Spatially covariant gravity with velocity of the lapse function.
- Degeneracy condition and Consistency condition.
- some concrete examples.
- Non-perturbative Hamiltonian analysis and some useful formulas.

Thank you!

Kazufumi Takahashi
Rikkyo University

“Extended Cuscuton: Cosmology”

(10+5 min.)

[JGRG28 (2018) 110606]

/kʌsˈkjuːtɒn/

Extended Cuscuton: Cosmology

Kazufumi Takahashi 髙橋 一史 (JSPS fellow)

Rikkyo University 立教大学

(sequel to the talk “Extended Cuscuton: Formulation” by Aya Iyonaga)

Based on
- Aya Iyonaga, **KT**, and Tsutomu Kobayashi
  “Extended Cuscuton: Formulation” arXiv: 1809.10935
- Aya Iyonaga, **KT**, and Tsutomu Kobayashi
  “Extended Cuscuton: Cosmology” *in preparation*

➢ Nondynamical scalar field = “cuscuton”

- A theory with 2 DOFs in the unitary gauge $\phi = \phi(t)$
  - ➡ ϕ “merely follows the dynamics of the fields that it couples to. Thus we call the field *Cuscuton*” (Afshordi+ 2006)
  - *Cuscuta*: name of a parasitic plant (“ネナシカズラ”)

$$S = \int d^4x\sqrt{-g}\left[\frac{\mathcal{R}}{2\kappa^2} + \mu^2\sqrt{2|X|} - V(\phi)\right]$$

- Some characteristics of the cuscuton model:
  - ✓ Only 2 tensor DOFs propagate → “minimal” modification of GR!
  - ✓ Nontrivial effects on cosmology (Afshordi 2007)
  - ✓ Related to a low-energy limit of Hořava-Lifshitz gravity (Afshordi 2009) → quantum gravity?

- A general class of theories having only 2 DOFs in the unitary gauge (within the GLPV theory)
  - ➡ “extended cuscuton”

➤ Extended cuscuton: summary

■ Extended cuscuton

GLPV (beyond Horndeski) action in the ADM language

$$S=\int dtd^3x\,N\sqrt{\gamma}\left[A_2+A_3K+A_4\left(K^2-K_{ij}^2\right)+B_4R\;+A_5\left(K^3-3KK_{ij}^2+2K_{ij}^3\right)+B_5G^{ij}K_{ij}\,\right]$$

$$A_5=\frac{\pm N^2}{(\mu_5N+\nu_5)^2},\qquad A_4=\frac{N(\mu_4N+\nu_4)}{(\mu_5N+\nu_5)^2},\qquad A_3=\frac{2(\mu_4N+\nu_4)^2}{3(\mu_5N+\nu_5)^2},$$

$$A_2=\mu_2+\frac{\nu_2}{N}+\frac{2(\mu_4N+\nu_4)}{9N(\mu_5N+\nu_5)^2},\qquad B_4=b_0+\frac{b_1}{N},\qquad B_5=0$$

where $\mu_2,\mu_4,\mu_5,\nu_2,\nu_3,\nu_4,\nu_5,b_0$, and b_1 are arbitrary functions of t

■ $A_5=0$ case

$$A_4=-\frac{v_4N}{N+u_4},\qquad A_3=\frac{v_3}{N+u_4},\qquad A_2=u_2+\frac{v_2}{N}-\frac{3v_3^2}{8v_4N(N+u_4)},$$

$$B_4=b_0+\frac{b_1}{N},\qquad B_5=0$$

where u_2,u_4,v_2,v_3,v_4,b_0, and b_1 are arbitrary functions of t

➤ Covariantized form

■ GLPV theory written in the covariant manner:

$$S_{\rm GLPV}=\int d^4x\sqrt{-g}\left(L_2+L_3+L_4+L_5+L_4^{\rm bH}+L_5^{\rm bH}\right),$$

$$\begin{aligned}
&L_2=G_2(\phi,X),\qquad L_3=G_3(\phi,X)\Box\phi,\qquad L_4=G_4(\phi,X)\mathcal{R}+G_{4X}\left[(\Box\phi)^2-\phi_\mu^\nu\phi_\nu^\mu\right],\\
&L_5=G_5(\phi,X)\mathcal{G}^{\mu\nu}\phi_{\mu\nu}-\frac{1}{6}G_{5X}\left[(\Box\phi)^3-3(\Box\phi)\phi_\mu^\nu\phi_\nu^\mu+2\phi_\mu^\nu\phi_\nu^\lambda\phi_\lambda^\mu\right],\\
&L_4^{\rm bH}=F_4(\phi,X)\left\{-2X\left[(\Box\phi)^2-\phi_\mu^\nu\phi_\nu^\mu\right]-2\phi_\mu\phi_\nu^\mu\left(\phi^\nu\Box\phi-\phi_\lambda^\nu\phi^\lambda\right)\right\},\\
&L_5^{\rm bH}=F_5(\phi,X)\left\{-2X\left[(\Box\phi)^3-3(\Box\phi)\phi_\mu^\nu\phi_\nu^\mu+2\phi_\mu^\nu\phi_\nu^\lambda\phi_\lambda^\mu\right]\right.\\
&\qquad\left.-3\phi_\lambda\phi_\sigma^\lambda\phi^\sigma\left[(\Box\phi)^2-\phi_\mu^\nu\phi_\nu^\mu\right]+6\phi_\mu\phi_\nu^\mu\phi^\sigma\left(\phi_\sigma^\nu\Box\phi-\phi_\lambda^\nu\phi_\sigma^\lambda\right)\right\}
\end{aligned}$$

■ In the case of $A_5=0$, the extended cuscuton action can be covariantized as follows:

$$\begin{aligned}
&G_2=u_2+v_2\sqrt{2X}-4b_0''X+2b_1''(2X)^{3/2}-\frac{v_3X}{1+u_4\sqrt{2X}}\left(\frac{3v_3}{4v_4}+2u_4'\sqrt{2X}\right)+2v_3'X\log\frac{\sqrt{2X}}{1+u_4\sqrt{2X}}+2b_0''X\log X\\
&G_3=-4b_1'\sqrt{2X}-v_3\left(\frac{1}{1+u_4\sqrt{2X}}+\log\frac{\sqrt{2X}}{1+u_4\sqrt{2X}}\right)-b_0'\log X\\
&G_4=b_0+b_1\sqrt{2X}\\
&F_4=\frac{1}{4X^2}\left(-b_0+\frac{v_4}{1+u_4\sqrt{2X}}\right)\\
&G_5=F_5=0
\end{aligned}$$

The expression for the $A_5\neq0$ case is lengthy…

➢ The rest of my talk

- Stability in the presence of a matter field
- Extended cuscutons satisfying $c_{GW} = 1$
- Late-time cosmology (preliminary)

➢ Stability of cosmological solns. (1)

- Cuscuton with a matter scalar field χ in the extended cuscuton theories:

$$S = S_{\mathrm{E.C.}} + \int d^4x\sqrt{-g}P(Y) \qquad Y \equiv -\frac{1}{2}g^{\mu\nu}\partial_\mu\chi\partial_\nu\chi$$

Energy density, pressure, squared sound speed of χ:

$$\rho = 2YP_Y - P, \qquad p = P, \qquad c_s^2 \equiv \frac{dp}{d\rho} = \frac{P_Y}{P_Y + 2YP_{YY}}$$

- Linear perturbations (unitary gauge for ϕ)

$$N = 1 + \alpha, \qquad N_i = \partial_i\beta, \qquad \gamma_{ij} = a^2 e^{2\zeta}\left(\delta_{ij} + h_{ij} + \frac{1}{2}h_{ik}h_{kj} + \cdots\right)$$

$$\phi = \phi(t), \qquad \chi = \chi(t) + \delta\chi$$

We use the following (gauge-invariant) density fluctuation instead of $\delta\chi$:

$$\delta \equiv \frac{\delta\rho}{\rho} + 3\frac{\rho + p}{\rho}\zeta = \frac{\rho + p}{\rho c_s^2}\left(\frac{\dot{\delta\chi}}{\dot{\chi}} - \alpha\right) + 3\frac{\rho + p}{\rho}\zeta$$

- Scalar perturbations: α, β, and ζ are auxiliary variables

➡ δ is the only dynamical variable! ⟷ (ζ is dynamical in generic ST theories)

Stability of cosmological solns. (2)

- Quadratic action for tensor perturbations (in the Fourier space):

$$S_T^{(2)} = \int d^3x dt\, a^3 \left[\mathcal{G}_T \dot{h}_{ij}^2 - \mathcal{F}_T \frac{k^2}{a^2} h_{ij}^2\right]$$

$$\mathcal{G}_T \equiv -2(A_4 + 3HA_5), \qquad \mathcal{F}_T \equiv 2B_4$$

memo
$L_{\mathrm{E.C.}} = A_2 + A_3 K + A_4(K^2 - K_{ij}^2)$
$+B_4 R + A_5(K^3 - 3KK_{ij}^2 + 2K_{ij}^3)$

$$\Rightarrow \quad \mathcal{G}_T > 0, \qquad \mathcal{F}_T > 0$$

$$\left(c_{GW}^2 = \frac{\mathcal{F}_T}{\mathcal{G}_T}\right)$$

- Quadratic action for scalar perturbations (in the Fourier space):

$$S_S^{(2)} = \int d^3x dt\, a^3 [\mathcal{A}(t,k)\dot{\delta}^2 - \mathcal{B}(t,k)\delta^2]$$

In the large-k limit,

$$\mathcal{A} \to \frac{a^2\rho^2}{2k^2(\rho+p)\Upsilon}, \qquad \mathcal{B} \to \frac{\rho^2 c_s^2}{2(\rho+p)}$$

$$\Rightarrow \quad \rho + p > 0, \qquad c_s^2 > 0, \qquad \Upsilon > 0$$

$$\Upsilon = \frac{2\mathcal{F}_S\Theta^2 - \bar{\mathcal{G}}_T^2(\rho+p)}{2\mathcal{F}_S\Theta^2 - \mathcal{G}_T(2\bar{\mathcal{G}}_T - \mathcal{G}_T)(\rho+p)}$$

Depends not only on theory but also on the matter!

(In the Horndeski limit, $\Upsilon \to 1$)

$c_{GW} = 1$

- The almost simultaneous detection of GW170817 and GRB170817A implies

$$|c_{GW} - 1| < 10^{-15}.$$

Note that it applies to only low-redshift universe ($z < 0.01$)!

- $c_{GW} = 1$ implies

Depend on H $\quad$ $B_5 = 0$ in E.C.

$$-2(A_4 + 3HA_5) = 2B_4 + \cancel{\dot{B}_5}$$

Requiring $A_5 = 0$, the extended cuscutons have

$$B_5 = 0, \qquad A_4 = -\frac{v_4(t)N}{N + u_4(t)}, \qquad B_4 = b_0(t) + \frac{b_1(t)}{N}, \qquad A_3 = \frac{v_3(t)}{N + u_4(t)},$$

$$A_2 = u_2(t) + \frac{v_2(t)}{N} - \frac{3v_3^2(t)}{8v_4(t)N[N + u_4(t)]}$$

$$\Rightarrow \quad A_4 = -B_4 = -v_4(t)$$

memo
$L_{\mathrm{E.C.}} = A_2 + A_3 K + A_4(K^2 - K_{ij}^2)$
$+B_4 R + A_5(K^3 - 3KK_{ij}^2 + 2K_{ij}^3)$

- Covariantized form

$$L_{c_{GW}=1}^{\mathrm{E.C.}} = u_2 + v_2\sqrt{2X} - \left(2v_3' + 4v_4'' + \frac{3v_3^2}{4v_4}\right)X$$

$$+(v_3' + 2v_4'')X\log X - \left(\frac{v_3}{2} + v_4'\right)(\log X)\Box\phi + v_4\mathcal{R} \subset (\text{Horndeski class})$$

$$\boxed{\begin{aligned} u_i &= u_i(\phi) \\ v_i &= v_i(\phi) \end{aligned}}$$

➢ Late-time cosmology (preliminary)

✓Consider a dust limit $p \to 0$, $c_s \to 0$ so that $\dot{\rho} + 3H\rho = 0$
✓For simplicity, focus on Horndeski theories

■Evolution equation for δ:

$$\ddot{\delta} + \left[2H + \frac{3\rho(\dot{\mathcal{G}}_T + H\mathcal{G}_T)}{\mathcal{G}_T\left(\frac{2k^2}{a^2}\mathcal{G}_T + 3\rho\right)}\right]\dot{\delta} - 4\pi G_{\rm eff}\rho\delta = 0,$$

$$4\pi G_{\rm eff} = \frac{2\mathcal{G}_T^2\left[2(\dot{\mathcal{G}}_T + H\mathcal{G}_T)^2 - \mathcal{F}_T(\rho + 2\dot{\Theta} + 2H\Theta)\right] - \frac{3a^2}{k^2}\mathcal{F}_T\rho[\mathcal{G}_T(\rho + 2\dot{\Theta}) - 2\dot{\mathcal{G}}_T\Theta]}{\mathcal{G}_T\left(2\mathcal{G}_T + \frac{3a^2\rho}{k^2}\right)\left\{2(2\mathcal{F}_S\Theta^2 - \mathcal{G}_T^2\rho) - \frac{3a^2\rho}{k^2}[\mathcal{G}_T(\rho + 2\dot{\Theta}) - 2\dot{\mathcal{G}}_T\Theta]\right\}}$$

■Poisson equation for $\Psi \equiv \alpha + \dot{\beta}$:

$$-\frac{k^2}{a^2}\Psi = 4\pi G_{\rm eff}\rho\delta + \frac{3\rho(\dot{\mathcal{G}}_T + H\mathcal{G}_T)}{\mathcal{G}_T\left(\frac{2k^2}{a^2}\mathcal{G}_T + 3\rho\right)}\dot{\delta}$$

✓The above expressions can be obtained without quasi-static approximation!
… Specific models are to be investigated

➢ Conclusions

■Extended cuscuton: A general class of scalar-tensor theories having only 2 DOFs in the unitary gauge

■Stability conditions for cosmological perturbations have been obtained

■Extended cuscuton with $c_{GW} = 1$:

$$L^{\rm E.C.}_{c_{GW}=1} = u_2 + v_2\sqrt{2X} - \left(2v_3' + 4v_4'' + \frac{3v_3^2}{4v_4}\right)X \qquad \boxed{\begin{aligned} u_i &= u_i(\phi) \\ v_i &= v_i(\phi)\end{aligned}}$$
$$+(v_3' + 2v_4'')X\log X - \left(\frac{v_3}{2} + v_4'\right)(\log X)\Box\phi + v_4\mathcal{R} \subset (\text{Horndeski class})$$

■The evolution Eq. for δ and the Poisson Eq. are obtained without resorting to the quasi-static approximation

■Cosmology in specific theories is to be investigated

Mai Yashiki
Yamaguchi Univ.

“Cosmological viability of the unified models of inflation and dark energy in f(R) gravity”
(10+5 min.)

[JGRG28 (2018) 110607]

Cosmological viability of the unified models of inflation and dark energy in f(R) gravity

Mai Yashiki, Nobuyuki Sakai
Yamaguchi Univ.

JGRG28 @ Rikkyo Univ., 2018. 11. 6

Introduction

- $f(R)$ gravity is one of the modified gravity theories

action: $S = \frac{1}{2\kappa^2}\int d^4x\sqrt{-g}\, f(R)$ non-linear function of R

- $f(R)$ models can explain inflation / late-time acceleration
  - Starobinsky inflation model : $f(R) = R + \alpha R^2$ $(\alpha > 0)$ Starobinsky (1980) Tomita&Nariai (1971)
  - $f(R)$ DE model : $f(R) = R - \beta R^m$ etc. $(\beta > 0, 0 < m < 1)$ Amendola+ (2007) Li+ (2007)

Introduction

- $f(R)$ gravity is one of the modified gravity

action: $S = \frac{1}{2\kappa^2}\int d^4x\sqrt{-g}\,f(R)$ non-linear function of R

- $f(R)$ models can explain inflation / late-time acceleration

— Starobinsky inflation model : $f(R) = R + \alpha R^2$ $(\alpha > 0)$ Starobinsky (1980) Tomita&Nariai (1971)

— $f(R)$ DE model : $f(R) = R - \beta R^m$ etc. $(\beta > 0, 0 < m < 1)$ Amendola+ (2007) Li+ (2007)

one $f(R)$ model may explain both inflation and DE

Purpose

- Verification of the cosmological evolution from radiation era to the present

Unified model : $f(R) = R + \alpha R^n - \beta R^{2-n}$ Artymowski & Lalak (2014)

generalized $\Rightarrow$ $\boldsymbol{f(R) = R + \alpha R^n - \beta R^m}$

$(n > 1, 0 < m < 1, \alpha \gg 1, 0 < \beta \ll 1)$

Constrain the model parameters from…

- existence conditions
- observational constraint on EoS

$f(R) = R + \alpha R^n - \beta R^m$ model

This model can be approximated during/after inflation

$(n > 1, 0 < m < 1, \alpha \gg 1, 0 < \beta \ll 1)$

- **during** inflation

  R is sufficiently large $\Rightarrow$ α term $\gg$ β term

  $\boxed{f(R) \sim R + \alpha R^n}$ $\Rightarrow$ generalized Starobinsky inflation model

  From Planck result, we constrain the parameter n :

  $$1.965 < n < 2.015$$ MY (2017)

$f(R) = R + \alpha R^n - \beta R^m$ model

This model can be approximated during/after inflation

$(n > 1, 0 < m < 1, \alpha \gg 1, 0 < \beta \ll 1)$

- **after** inflation

  R is sufficiently small $\Rightarrow$ α term $\ll$ β term

  $\boxed{f(R) \sim R - \beta R^m}$ $\Rightarrow$ Amendola+, Li+ model

  This model satisfies the conditions to be a viable DE model

  (Amendola & Tsujikawa, 2010)

$f(R) = R + \alpha R^n - \beta R^m$ model

This model can be approximated during/after inflation

$(n > 1, 0 < m < 1, \alpha \gg 1, 0 < \beta \ll 1)$

- **after** inflation

  R is sufficiently small $\Rightarrow$ α term $\ll$ β term

  $\boxed{f(R) \sim R - \beta R^m}$ $\Rightarrow$ Amendola+, Li+ model

  This model satisfies the conditions to be a viable DE model

  (Amendola & Tsujikawa, 2010)

Before the unified model,
we consider the cosmological viability in this DE model

Why consider the cosmological evolution?

- existence conditions

  Amendola+ (2007)

  — radiation, matter era and late-time exist

  $f(R) = R - \beta R^m$ model satisfies for $0 < m \leq \frac{2}{3}$

Theses conditions are not sufficient conditions

e.g.) matter era might be too short in some models

check the time evolution of density parameters

- late-time

  equation of state deviates from $w = -1$ in $f(R)$ gravity

  check the time evolution of EoS of DE (w_{DE})

How to calculate

- Friedmann eq. in $f(R)$ gravity

$$\Rightarrow \qquad 1 = \underbrace{-\frac{\dot{F}}{HF}}_{y_1} + \underbrace{\frac{FR-f}{6FH^2}}_{y_2} + \underbrace{\frac{\rho_{rad}}{3FH^2}}_{y_4} + \underbrace{\frac{\rho_m}{3FH^2}}_{y_5}$$

Amendola+ (2007)

We introduce the variables : $y_1 - y_5$, $\quad y_3 = \frac{2f-FR}{6FH^2} - \Omega_{\rm m}$

- auxiliary variable : $X \equiv \frac{R}{6H^2} = 2y_2 + y_3 + \frac{y_5}{2}$

- $\Omega_{\rm m} = y_5, \quad \Omega_{\rm DE} = y_1 + y_2, \quad \Omega_{\rm rad} = y_4$
- $w_{\rm DE} = \frac{1-y_4-2X}{3(y_1+y_2)}$

Evolution equation

$$\frac{dy_1}{dN} = y_1 + y_1^2 + (2-y_1)(X-2) + 4y_4 + 3y_5$$

$$\frac{dy_2}{dN} = y_2(4+y_1) - X(y_1+2y_2)$$

$$\frac{dy_3}{dN} = X\left(-\frac{y_1}{M} + 2y_1 - 2y_3 + 4\right) - 2y_2(y_1+4) - \frac{y_5}{2}(y_1+1)$$

$$\frac{dy_4}{dN} = y_4(y_1 - 2X)$$

$$\frac{dy_5}{dN} = y_5(1 + y_1 - 2X) \qquad , N = \ln a$$

✓ model dependence appears in $M \equiv \frac{Rf_{RR}}{f_R} \quad \left(f_R \equiv \frac{df}{dR}, f_{RR} \equiv \frac{d^2f}{dR^2}\right)$

In $f(R) = R - \beta R^m$ model, $\boxed{M = \frac{y_2}{X} m}$

We choose the initial condition to correspond to the observational values $\Omega_{\rm m0}, \Omega_{\rm DE0}$

density parameters : Ω

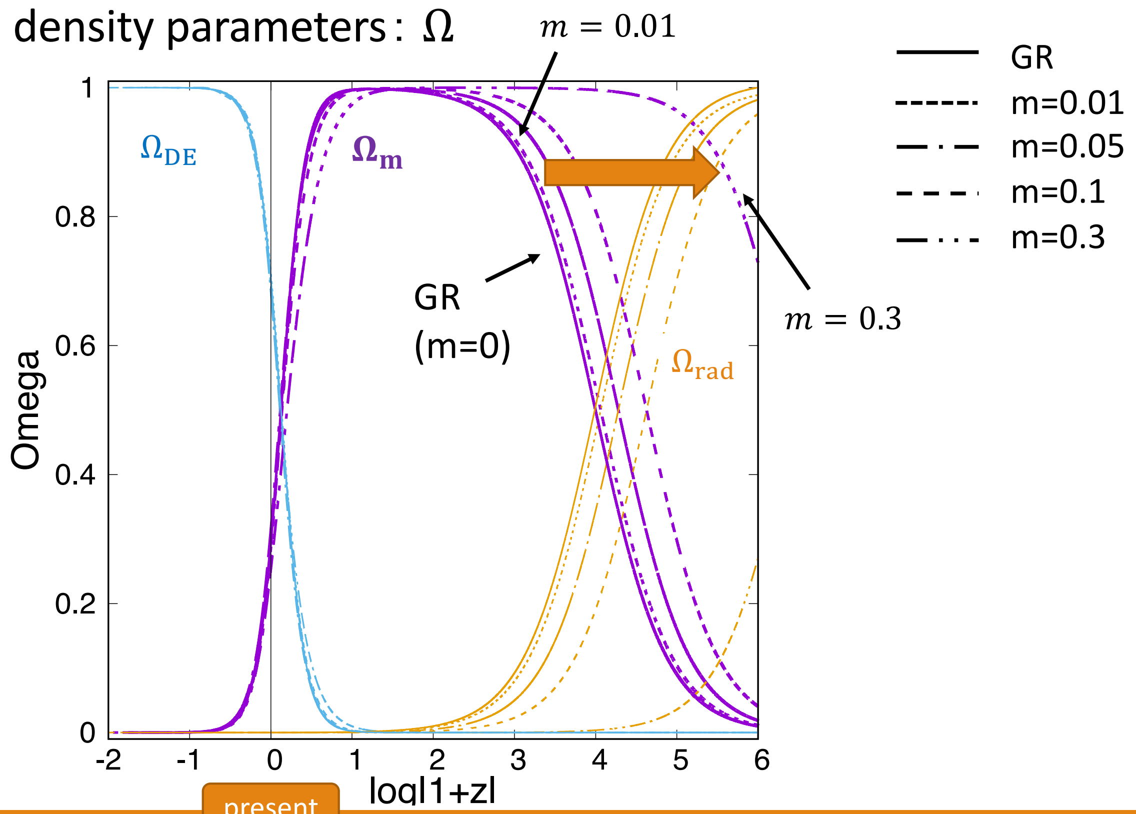

EoS of DE : $w_{\rm DE} \equiv \frac{P_{\rm DE}}{\rho_{\rm DE}}$

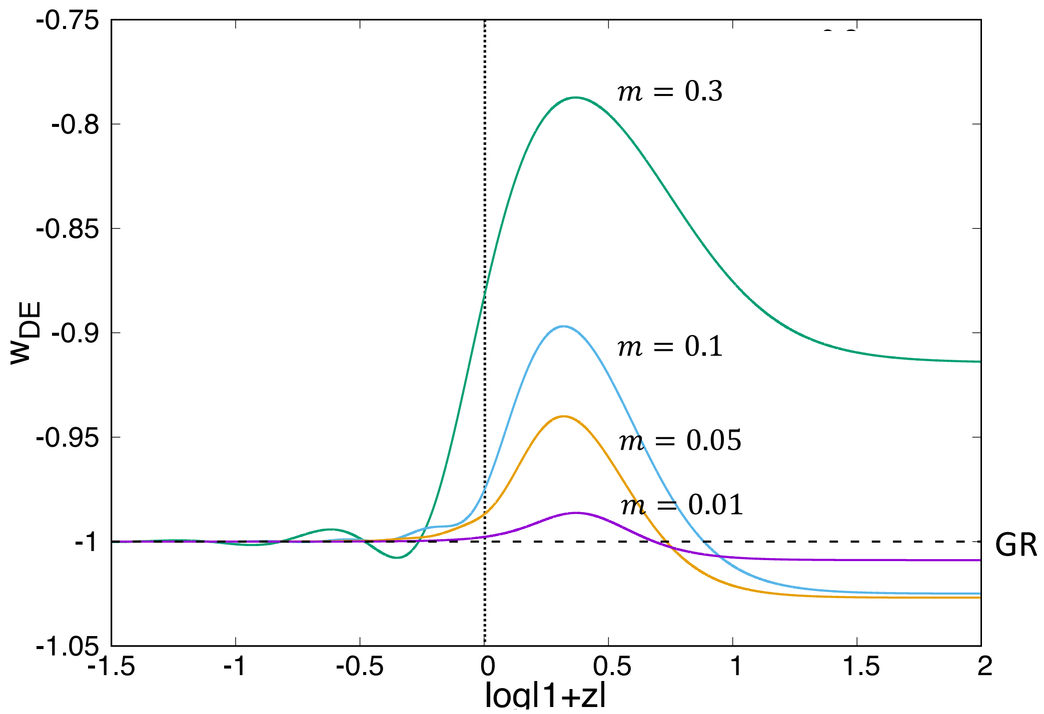

Constraint on time-varying w_{DE}

- If $w_{\mathrm{DE}} \neq -1$,

  time-varying EoS : $w(a)$

Taylor expansion @ z=0

$$w(a) = w_0 + (1-a)w_a + \cdots$$

a : scale factor

w_0 : the present value

c.f.) GR : $w_0 = -1,\ w_a = 0$

※ higher terms are not so relevant in fitting the data (Planck(2018))

- Constraints from Planck with other observational data (2018)

$$w_0 = -0.961 \pm 0.077$$

$$w_a = -0.28^{+0.31}_{-0.27}$$

Restrict the power m

Comparison with the observation

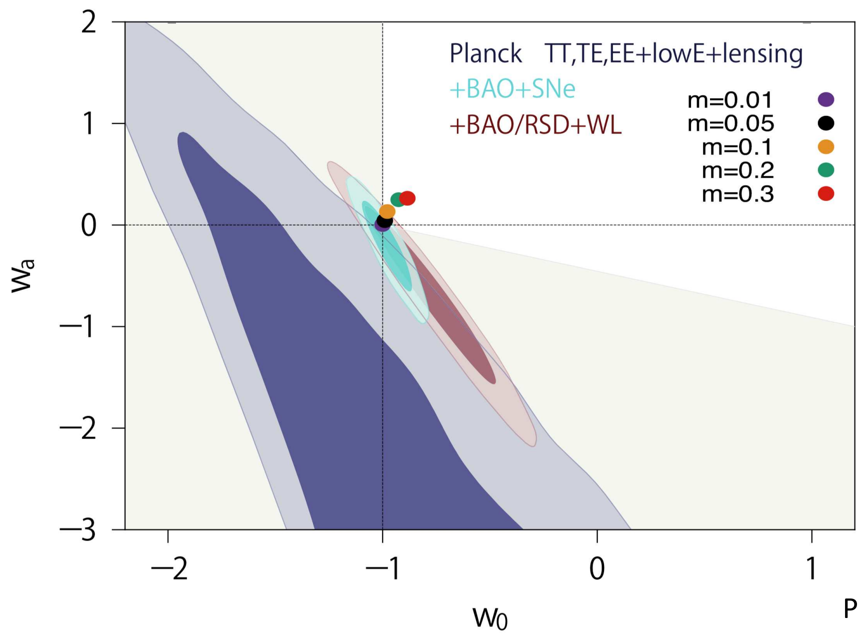

Planck (2018)

Comparison with the observation

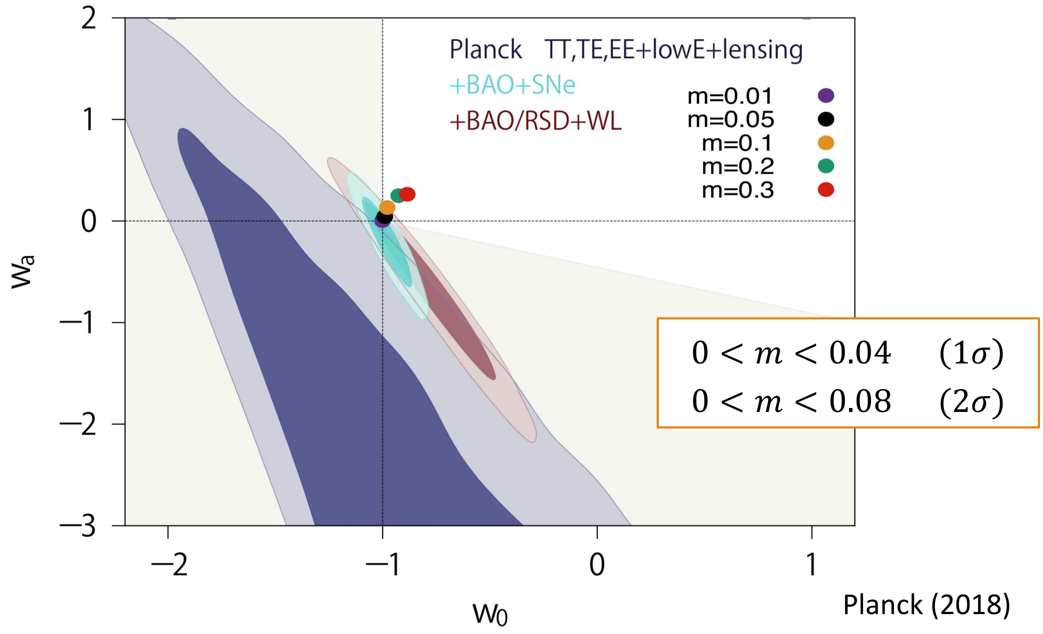

Planck (2018)

Summary / Future work

In $f(R) = R - \beta R^m$ model,

- matter-dominated era lasts longer than GR
- comparison with the observational constraint for time-varying $w_{\rm DE}$

  $\Rightarrow \quad 0 < m < 0.04 \quad (1\sigma)$ CMB+SNe+BAO

We ignore αR^n term after inflation $\Rightarrow$ Is this OK?

- a weak curvature singularity arises in f(R) DE model (Appleby+, 2009)
  - R diverges temporarily
- considering the local gravity constraints

Invited lecture 14:00–14:45

[Chair: Tetsuya Shiromizu]

JosÃľ MartÃŋn Senovilla

Department of theoretical physics and history of science, University of the Basque Country UPV/EHU

“Multiple Killing Horizons”

(40+10 min.)

[JGRG28 (2018) 110610]

Multiple Killing Horizons

José M M Senovilla

Department of Theoretical Physics and History of Science
University of the Basque Country UPV/EHU, Bilbao, Spain

Work in collaboration with Marc Mars and Tim-Torben Paetz

The 28th Workshop on General Relativity and Gravitation in Japan - JGRG28, 6th November 2018

Outline

Introduction: Killing horizons

Informal description of a Killing horizon.

Null hypersurface $\mathcal{H}_\xi$ where a Killing vector field ξ becomes non-zero null and tangent.

Introduction: Killing horizons

Informal description of a Killing horizon.

Null hypersurface $\mathcal{H}_\xi$ where a Killing vector field ξ becomes non-zero null and tangent.

$\xi^\mu \xi_\mu$ can

1. have a simple zero on $\mathcal{H}_\xi$ ($\Longrightarrow$ "ξ changes causal character")
2. have a double zero on $\mathcal{H}_\xi$ ($\Longrightarrow$ "degenerate horizon")
3. be zero around $\mathcal{H}_\xi$ (ξ is a null Killing vector)

Introduction: Killing horizons

Informal description of a Killing horizon.

Null hypersurface $\mathcal{H}_\xi$ where a Killing vector field ξ becomes non-zero null and tangent.

$\xi^\mu \xi_\mu$ can

1. have a simple zero on $\mathcal{H}_\xi$ ($\Longrightarrow$ "ξ changes causal character")
2. have a double zero on $\mathcal{H}_\xi$ ($\Longrightarrow$ "degenerate horizon")
3. be zero around $\mathcal{H}_\xi$ (ξ is a null Killing vector)

The fixed points of ξ are not part of the Killing horizon

Introduction: a Killing Horizon in Minkowski

$$ds^2 = -dt^2 + dx^2 + dy^2$$

Introduction: a Killing Horizon in Minkowski

$$ds^2 = -dt^2 + dx^2 + dy^2$$

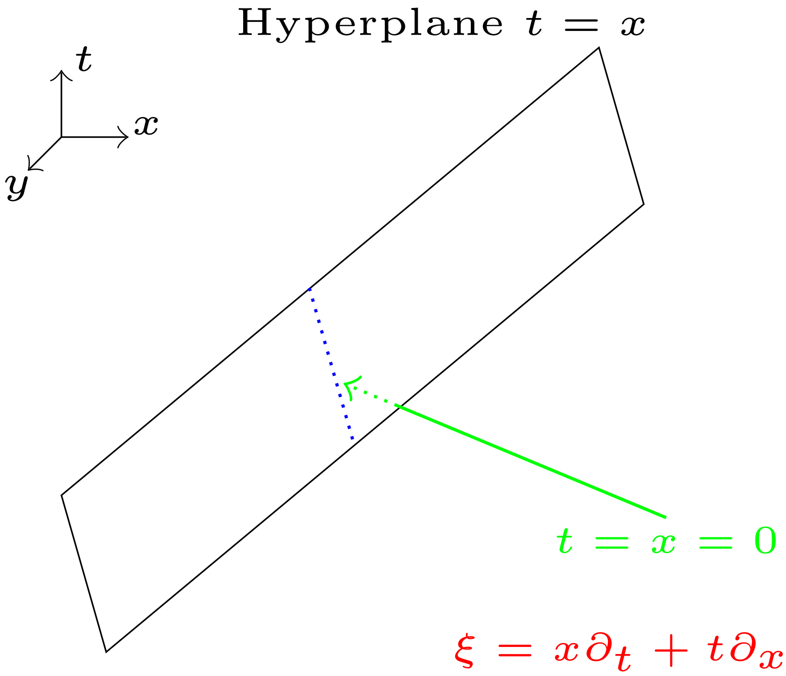

Introduction: a KH in Minkowski

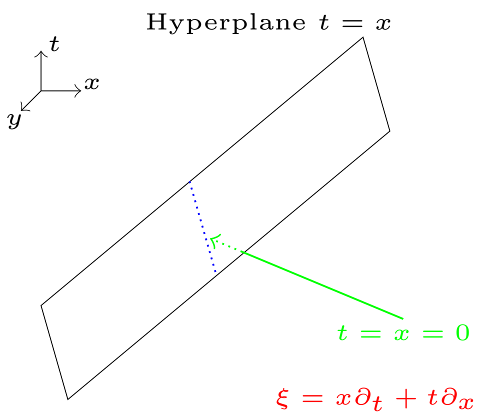

- Notice that the Killing Horizon is given by $\mathcal{H}_\xi = \{t = x > 0\} \cup \{t = x < 0\}$

Definition (Killing horizon)

A smooth null hypersurface $\mathcal{H}_\xi$ is a Killing horizon of a Killing ξ if and only if ξ is null but nowhere zero on $\mathcal{H}_\xi$ and tangent to $\mathcal{H}_\xi$. Killing horizons may have several connected components, but we always require that the interior of its closure be a smooth <u>connected</u> hypersurface.

Introduction: a KH in Minkowski

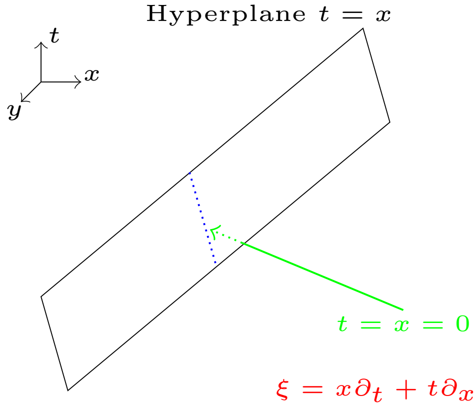

- Notice that the Killing Horizon is given by $\mathcal{H}_\xi = \{t = x > 0\} \cup \{t = x < 0\}$
- That is, the points where $\xi = 0$ do not belong to $\mathcal{H}_\xi$.

Definition (Killing horizon)

A smooth null hypersurface $\mathcal{H}_\xi$ is a Killing horizon of a Killing ξ if and only if ξ is null but nowhere zero on $\mathcal{H}_\xi$ and tangent to $\mathcal{H}_\xi$. Killing horizons may have several connected components, but we always require that the interior of its closure be a smooth <u>connected</u> hypersurface.

Introduction: a KH in Minkowski

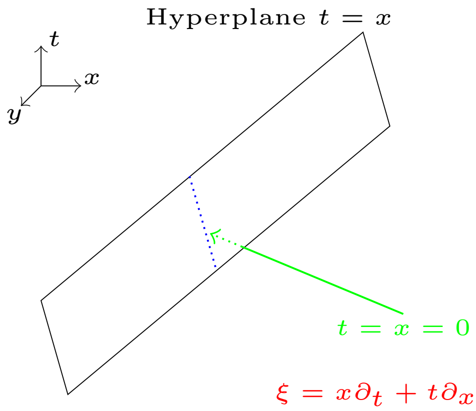

- Notice that the Killing Horizon is given by $\mathcal{H}_\xi = \{t = x > 0\} \cup \{t = x < 0\}$
- That is, the points where $\xi = 0$ do not belong to $\mathcal{H}_\xi$.
- Thus, Killing horizons can have several connected components *as long as they are linked by a set of fixed points of* ξ.

Definition (Killing horizon)

A smooth null hypersurface $\mathcal{H}_\xi$ is a Killing horizon of a Killing ξ if and only if ξ is null but nowhere zero on $\mathcal{H}_\xi$ and tangent to $\mathcal{H}_\xi$. Killing horizons may have several connected components, but we always require that the interior of its closure be a smooth <u>connected</u> hypersurface.

Introduction: another KH in Minkowski

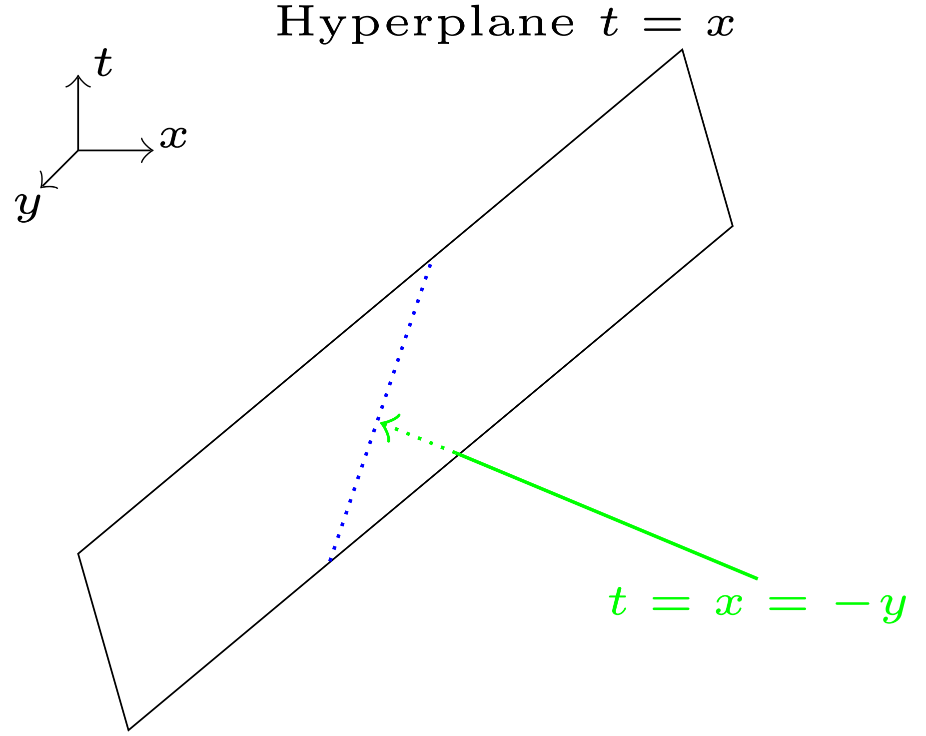

$$\tilde{\xi} = (x + y)\partial_t + (t + y)\partial_x + (t - x)\partial_y$$

Introduction: same hyperplane!

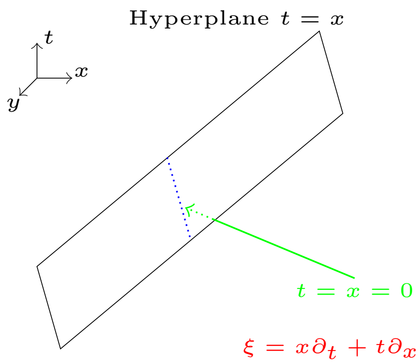

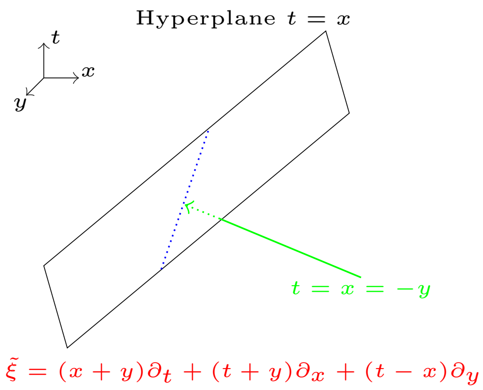

- The Killings ξ and $\tilde{\xi}$ are linearly independent

Introduction: same hyperplane!

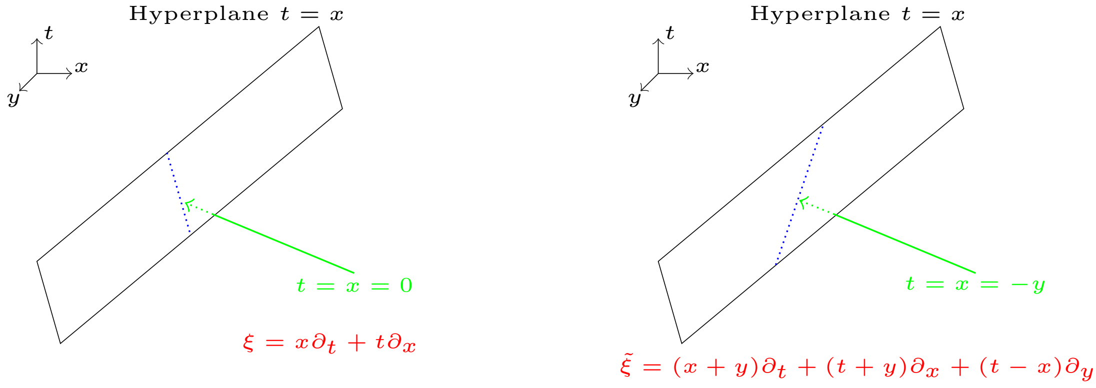

- The Killings ξ and $\tilde{\xi}$ are linearly independent
- and the set of fixed points of the respective Killings are different

Introduction: same hyperplane!

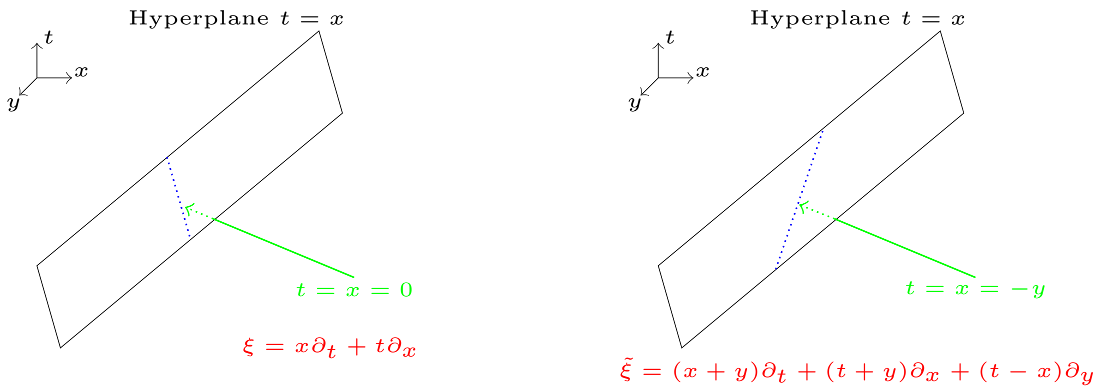

- The Killings ξ and $\tilde{\xi}$ are linearly independent
- and the set of fixed points of the respective Killings are different

- However, **the null hyperplane** $\{t = x\} = \overline{\mathcal{H}_\xi} = \overline{\mathcal{H}_{\tilde{\xi}}}$ **is the same**

Multiple Killing Horizons

Definition (Multiple Killing horizon (MKH))

A null hypersurface $\mathcal{H}$ is a multiple Killing horizon of order m if the spacetime admits Killing horizons $\mathcal{H}_{\xi_i}$, $i \in \{1, \dots, m\}$ with $m \geq 2$, associated to linearly independent Killing vectors ξ_i satisfying

$$\overline{\mathcal{H}} = \overline{\mathcal{H}_{\xi_1}} = \cdots = \overline{\mathcal{H}_{\xi_m}}.$$

Multiple Killing Horizons

Definition (Multiple Killing horizon (MKH))

A null hypersurface $\mathcal{H}$ is a multiple Killing horizon of order m if the spacetime admits Killing horizons $\mathcal{H}_{\xi_i}$, $i \in \{1, \dots, m\}$ with $m \geq 2$, associated to linearly independent Killing vectors ξ_i satisfying

$$\overline{\mathcal{H}} = \overline{\mathcal{H}_{\xi_1}} = \cdots = \overline{\mathcal{H}_{\xi_m}}.$$

$\{t = x\}$ in Minkowski is a Multiple Killing Horizon

Multiple Killing Horizons

Definition (Multiple Killing horizon (MKH))

A null hypersurface $\mathcal{H}$ is a multiple Killing horizon of order m if the spacetime admits Killing horizons $\mathcal{H}_{\xi_i}$, $i \in \{1, \ldots, m\}$ with $m \geq 2$, associated to linearly independent Killing vectors ξ_i satisfying

$$\overline{\mathcal{H}} = \overline{\mathcal{H}_{\xi_1}} = \cdots = \overline{\mathcal{H}_{\xi_m}}.$$

$\{t = x\}$ in Minkowski is a Multiple Killing Horizon

Our aim is to study the properties of MKHs, and their physical relevance.

Surface gravities

- Recall: For a Killing horizon $\mathcal{H}_\xi$ of ξ, its surface gravity κ_ξ is defined as

$$\kappa_\xi : \mathcal{H}_\xi \to \mathbb{R} \qquad\qquad \nabla_\xi \xi \stackrel{\mathcal{H}_\xi}{=} \kappa_\xi \xi.$$

Surface gravities

- Recall: For a Killing horizon $\mathcal{H}_\xi$ of ξ, its surface gravity κ_ξ is defined as

$$\kappa_\xi : \mathcal{H}_\xi \to \mathbb{R} \qquad \nabla_\xi \xi \overset{\mathcal{H}_\xi}{=} \kappa_\xi \xi.$$

- In general, this is a function which, as a consequence of the identity

$$2\kappa_\xi^2 \overset{\mathcal{H}_\xi}{=} -\nabla_\mu \xi_\nu \nabla^\mu \xi^\nu,$$

actually extends to a continuous function on the entire $\overline{\mathcal{H}_\xi}$.

Surface gravities

- Recall: For a Killing horizon $\mathcal{H}_\xi$ of ξ, its surface gravity κ_ξ is defined as

$$\kappa_\xi : \mathcal{H}_\xi \to \mathbb{R} \qquad \nabla_\xi \xi \overset{\mathcal{H}_\xi}{=} \kappa_\xi \xi.$$

- In general, this is a function which, as a consequence of the identity

$$2\kappa_\xi^2 \overset{\mathcal{H}_\xi}{=} -\nabla_\mu \xi_\nu \nabla^\mu \xi^\nu,$$

actually extends to a continuous function on the entire $\overline{\mathcal{H}_\xi}$.

- Recall also: $\mathcal{H}_\xi$ degenerate $\iff$ $\kappa_\xi \overset{\mathcal{H}_\xi}{\equiv} 0$

Surface gravities

- Recall: For a Killing horizon $\mathcal{H}_\xi$ of ξ, its surface gravity κ_ξ is defined as

$$\kappa_\xi : \mathcal{H}_\xi \to \mathbb{R} \qquad \nabla_\xi \xi \overset{\mathcal{H}_\xi}{=} \kappa_\xi \xi.$$

- In general, this is a function which, as a consequence of the identity

$$2\kappa_\xi^2 \overset{\mathcal{H}_\xi}{=} -\nabla_\mu \xi_\nu \nabla^\mu \xi^\nu,$$

actually extends to a continuous function on the entire $\overline{\mathcal{H}_\xi}$.

- Recall also: $\mathcal{H}_\xi$ degenerate $\iff$ $\kappa_\xi \overset{\mathcal{H}_\xi}{\equiv} 0$

Theorem

All surface gravities of a multiple Killing horizon $\mathcal{H}$ are necessarily constant on the entire $\mathcal{H}$.

Surface gravities $\longrightarrow$ many temperatures?

- Note that, *locally*, any black-hole horizon looks like the flat spacetime $\{t = x\}$ horizon shown (equivalence principle!).

Surface gravities $\longrightarrow$ many temperatures?

- Note that, *locally*, any black-hole horizon looks like the flat spacetime $\{t = x\}$ horizon shown (equivalence principle!).
- Constancy of the surface gravity is understood as the zero-th law of horizon thermodynamics.

Surface gravities $\longrightarrow$ many temperatures?

- Note that, *locally*, any black-hole horizon looks like the flat spacetime $\{t = x\}$ horizon shown (equivalence principle!).
- Constancy of the surface gravity is understood as the zero-th law of horizon thermodynamics.

- The Hawking quantum emission process, as well as the Unruh effect for accelerated observers, leads unequivocally to consider the surface gravity of a Killing horizon as its Temperature.

Surface gravities $\longrightarrow$ many temperatures?

- Note that, *locally*, any black-hole horizon looks like the flat spacetime $\{t = x\}$ horizon shown (equivalence principle!).
- Constancy of the surface gravity is understood as the zero-th law of horizon thermodynamics.
- The Hawking quantum emission process, as well as the Unruh effect for accelerated observers, leads unequivocally to consider the surface gravity of a Killing horizon as its Temperature.
- To a MKH we can ascribe different surface gravities (temperatures), and thus an immediate question arises: **what is the physical meaning of this?**

Surface gravities $\longrightarrow$ many temperatures?

- Note that, *locally*, any black-hole horizon looks like the flat spacetime $\{t = x\}$ horizon shown (equivalence principle!).
- Constancy of the surface gravity is understood as the zero-th law of horizon thermodynamics.
- The Hawking quantum emission process, as well as the Unruh effect for accelerated observers, leads unequivocally to consider the surface gravity of a Killing horizon as its Temperature.
- To a MKH we can ascribe different surface gravities (temperatures), and thus an immediate question arises: **what is the physical meaning of this?**

- We are going to address this problem. To that end, we need to understand the mathematical structure of the set of Killing vectors attached to the MKH.

The Killing $\zeta := \tilde{\xi} - \xi$

One can take linear combinations of the Killings providing new ones which are also null on the null hypersurface $t = x$.

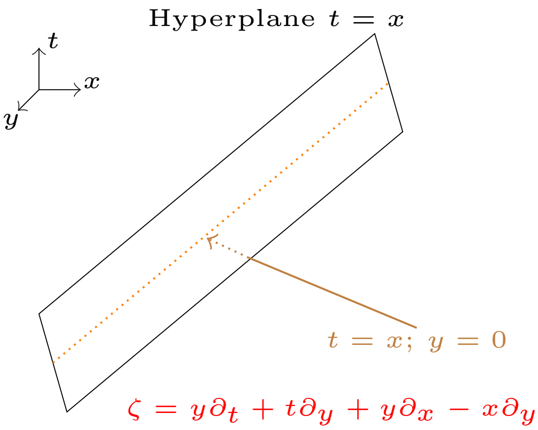

The Killing $\zeta := \tilde{\xi} - \xi$

One can take linear combinations of the Killings providing new ones which are also null on the null hypersurface $t = x$.

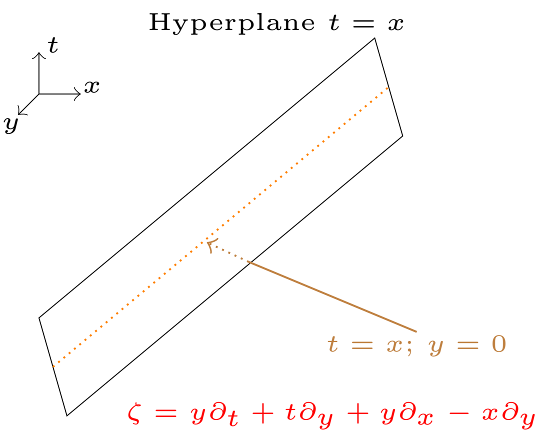

In simpler words, the set of all Killing vectors sharing (the appropriate subset of) $\mathcal{H}$ as Killing horizon is a **vector space**.

The Lie algebra of Multiple Killing Horizons

- We define:

  $\mathcal{A}_{\mathcal{H}} := \{\xi \text{ Killing with a KH } \mathcal{H}_\xi \text{ satisfying } \overline{\mathcal{H}_\xi} = \overline{\mathcal{H}}\} \cup \{\xi \equiv 0\}$

The Lie algebra of Multiple Killing Horizons

- We define:

  $\mathcal{A}_{\mathcal{H}} := \{\xi \text{ Killing with a KH } \mathcal{H}_\xi \text{ satisfying } \overline{\mathcal{H}_\xi} = \overline{\mathcal{H}}\} \cup \{\xi \equiv 0\}$

- We have seen that $\mathcal{A}_{\mathcal{H}}$ is a vector space. Moreover:

The Lie algebra of Multiple Killing Horizons

- We define:

$$\mathcal{A}_{\mathcal{H}} := \{\xi \text{ Killing with a KH } \mathcal{H}_\xi \text{ satisfying } \overline{\mathcal{H}_\xi} = \overline{\mathcal{H}}\} \cup \{\xi \equiv 0\}$$

- We have seen that $\mathcal{A}_{\mathcal{H}}$ is a vector space. Moreover:

Theorem

$\mathcal{A}_{\mathcal{H}}$ is a Lie algebra

The Lie algebra of Multiple Killing Horizons

- We define:

$$\mathcal{A}_{\mathcal{H}} := \{\xi \text{ Killing with a KH } \mathcal{H}_\xi \text{ satisfying } \overline{\mathcal{H}_\xi} = \overline{\mathcal{H}}\} \cup \{\xi \equiv 0\}$$

- We have seen that $\mathcal{A}_{\mathcal{H}}$ is a vector space. Moreover:

Theorem

$\mathcal{A}_{\mathcal{H}}$ is a Lie algebra

- $\mathcal{A}_{\mathcal{H}}$ is called the **Lie algebra of the MKH** $\mathcal{H}$

The Lie algebra of Multiple Killing Horizons

- We define:

$$\mathcal{A}_{\mathcal{H}} := \{\xi \text{ Killing with a KH } \mathcal{H}_\xi \text{ satisfying } \overline{\mathcal{H}_\xi} = \overline{\mathcal{H}}\} \cup \{\xi \equiv 0\}$$

- We have seen that $\mathcal{A}_{\mathcal{H}}$ is a vector space. Moreover:

Theorem

$\mathcal{A}_{\mathcal{H}}$ is a Lie algebra

- $\mathcal{A}_{\mathcal{H}}$ is called the **Lie algebra of the MKH** $\mathcal{H}$
- Observe that dim $\mathcal{A}_{\mathcal{H}}$ = order of $\mathcal{H}$ (also called multiplicity).

Structure of the Lie algebra of $\mathcal{H}$

The structure of the Lie algebra $\mathcal{A}_{\mathcal{H}}$ turns out to be very simple:

Theorem (Mars, Paetz, S.)

Let $\mathcal{H}$ be a multiple Killing horizon of order m.

- *$\mathcal{A}_{\mathcal{H}}$ always contains an Abelian sub-algebra $\mathcal{A}^{deg}_{\mathcal{H}}$ of dimension at least $m-1$.*
- *For any non-trivial $\eta \in \mathcal{A}^{deg}_{\mathcal{H}}$, the corresponding surface gravity κ_η vanishes (i.e. $\mathcal{H}$ is degenerate with respect to all $\eta \in \mathcal{A}^{deg}_{\mathcal{H}}$).*
- *If $\mathcal{A}^{deg}_{\mathcal{H}}$ has dimension $m-1$, any element of $\xi \in \mathcal{A}_{\mathcal{H}} \setminus \mathcal{A}^{deg}_{\mathcal{H}}$ has $\kappa_\xi \neq 0$ and satisfies*

$$[\xi, \eta] = -\kappa_\xi \eta, \qquad \forall \eta \in \mathcal{A}^{deg}_{\mathcal{H}}.$$

Structure of the Lie algebra of $\mathcal{H}$

The structure of the Lie algebra $\mathcal{A}_{\mathcal{H}}$ turns out to be very simple:

Theorem (Mars, Paetz, S.)

Let $\mathcal{H}$ be a multiple Killing horizon of order m.

- *$\mathcal{A}_{\mathcal{H}}$ always contains an Abelian sub-algebra $\mathcal{A}_{\mathcal{H}}^{deg}$ of dimension at least $m-1$.*
- *For any non-trivial $\eta \in \mathcal{A}_{\mathcal{H}}^{deg}$, the corresponding surface gravity κ_η vanishes (i.e. $\mathcal{H}$ is degenerate with respect to all $\eta \in \mathcal{A}_{\mathcal{H}}^{deg}$).*
- *If $\mathcal{A}_{\mathcal{H}}^{deg}$ has dimension $m-1$, any element of $\xi \in \mathcal{A}_{\mathcal{H}} \setminus \mathcal{A}_{\mathcal{H}}^{deg}$ has $\kappa_\xi \neq 0$ and satisfies*

$$[\xi, \eta] = -\kappa_\xi \eta, \qquad \forall \eta \in \mathcal{A}_{\mathcal{H}}^{deg}.$$

These are spacetime properties providing a necessary condition for the existence of a MKH: the Killing algebra must contain an appropriate sub-algebra with the required structure constants

MKHs types: Fully degenerate MKHs

- The previous theorem implies that there are two distinct classes of Multiple Killing Horizons:

MKHs types: Fully degenerate MKHs

- The previous theorem implies that there are two distinct classes of Multiple Killing Horizons:

Definition (Fully degenerate MKH)

A multiple Killing horizon $\mathcal{H}$ is said to be fully degenerate if $\mathcal{A}_{\mathcal{H}} = \mathcal{A}^{deg}_{\mathcal{H}}$ and non-fully degenerate otherwise.

MKHs types: Fully degenerate MKHs

- The previous theorem implies that there are two distinct classes of Multiple Killing Horizons:

Definition (Fully degenerate MKH)

A multiple Killing horizon $\mathcal{H}$ is said to be fully degenerate if $\mathcal{A}_{\mathcal{H}} = \mathcal{A}^{deg}_{\mathcal{H}}$ and non-fully degenerate otherwise.

- Hence, non-fully degenerate MKHs have a unique non-zero surface gravity —up to normalization, of course.

MKHs types: Fully degenerate MKHs

- The previous theorem implies that there are two distinct classes of Multiple Killing Horizons:

Definition (Fully degenerate MKH)

A multiple Killing horizon $\mathcal{H}$ is said to be fully degenerate if $\mathcal{A}_{\mathcal{H}} = \mathcal{A}_{\mathcal{H}}^{deg}$ and non-fully degenerate otherwise.

- Hence, non-fully degenerate MKHs have a unique non-zero surface gravity —up to normalization, of course.

Important result

To any MKH one can attach, at most, one single non-zero temperature.

Maximal order of MKHs

Let n be the spacetime dimension

Corollary

The maximum possible dimension of $\mathcal{A}_{\mathcal{H}}^{deg}$ *is* $n-1$. *Consequently, the maximum possible order of* $\mathcal{H}$ *is* $n-1$ *for fully degenerate* $\mathcal{H}$ *and* n *for non-fully degenerate* $\mathcal{H}$.

Non-fully degenerate MKHs of maximal order

- The maximal multiplicity $m = n$ can be attained.

Non-fully degenerate MKHs of maximal order

- The maximal multiplicity $m = n$ can be attained.

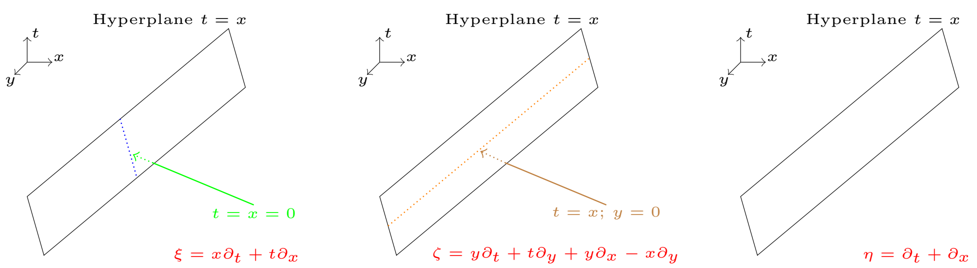

Non-fully degenerate MKHs of maximal order

- The maximal multiplicity $m = n$ can be attained.

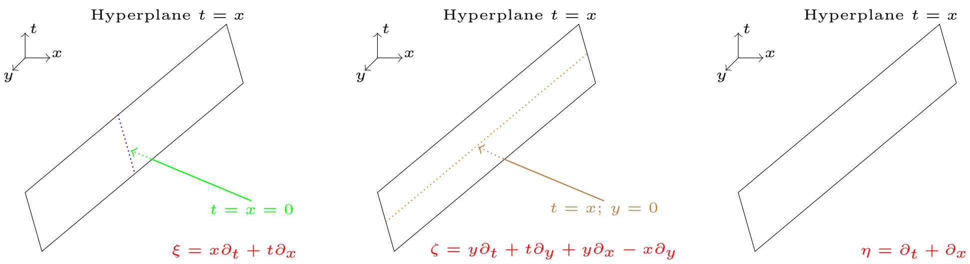

- All maximally symmetric spacetimes have a MKH of maximal order passing through any of its points.

Non-fully degenerate MKHs of maximal order

- The maximal multiplicity $m = n$ can be attained.

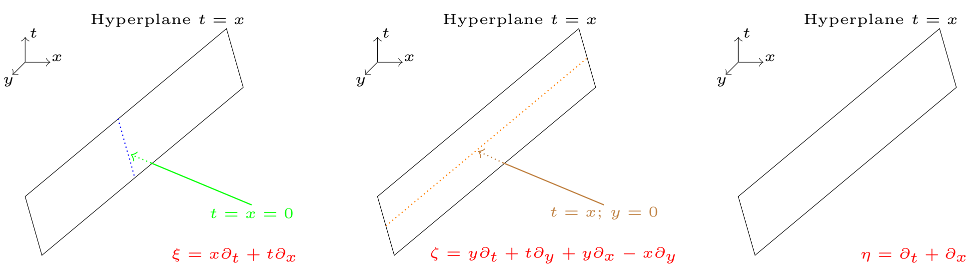

- All maximally symmetric spacetimes have a MKH of maximal order passing through any of its points.
- MKHs in Minkowski, de Sitter or anti-de Sitter spaces have been completely classified.

Reminder: Bifurcate horizons

Recall: A bifurcate Killing horizon of a Killing ξ is the set of points along all null geodesics orthogonal to a co-dimension two spacelike submanifold S of fixed points of ξ: $\xi|_S = 0$.

Reminder: Bifurcate horizons

Recall: A bifurcate Killing horizon of a Killing ξ is the set of points along all null geodesics orthogonal to a co-dimension two spacelike submanifold S of fixed points of ξ: $\xi|_S = 0$.

- This is a pair of Killing horizons $\mathcal{H}_1^+ \cup \mathcal{H}_1^-$ and $\mathcal{H}_2^+ \cup \mathcal{H}_2^-$ of ξ, each one with two connected components $\mathcal{H}_1^\pm$, $\mathcal{H}_2^\pm$,
- together with the intersection of their closures $\overline{\mathcal{H}_1^+ \cup \mathcal{H}_1^-} \bigcap \overline{\mathcal{H}_2^+ \cup \mathcal{H}_2^-} = S$,
- S spacelike codimension-two surface where $\xi|_S = 0$.

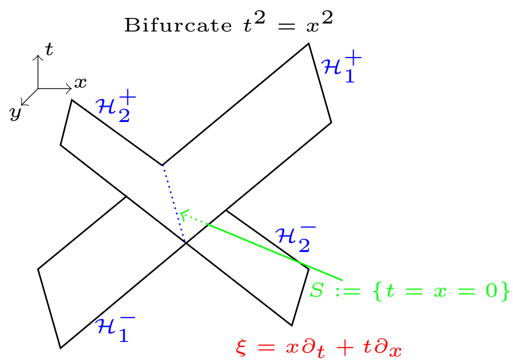

Non-fully degenerate MKHs are Bifurcate horizons

- On a MKH $\mathcal{H} \supset \mathcal{H}_\xi$ let $\tau : \mathcal{H}_\xi \to \mathbb{R}$ be defined by $\xi(\tau) = 1$.

Non-fully degenerate MKHs are Bifurcate horizons

- On a MKH $\mathcal{H} \supset \mathcal{H}_\xi$ let $\tau : \mathcal{H}_\xi \to \mathbb{R}$ be defined by $\xi(\tau) = 1$.
- $\forall \eta \in \mathcal{A}^{deg}_{\mathcal{H}}, \quad \eta \overset{\mathcal{H}_\xi}{=} f_\eta \, e^{-\kappa_\xi \tau} \xi, \qquad \xi(f_\eta) = 0,$

Non-fully degenerate MKHs are Bifurcate horizons

- On a MKH $\mathcal{H} \supset \mathcal{H}_\xi$ let $\tau : \mathcal{H}_\xi \to \mathbb{R}$ be defined by $\xi(\tau) = 1$.
- $\forall \eta \in \mathcal{A}^{deg}_{\mathcal{H}}, \quad \eta \overset{\mathcal{H}_\xi}{=} f_\eta \, e^{-\kappa_\xi \tau} \xi, \qquad \xi(f_\eta) = 0,$
- (Freedom: $\tau \to \tau + \tau_0, \quad \xi(\tau_0) = 0 \implies f_\eta \to f_\eta e^{\kappa_\xi \tau_0}$)

Non-fully degenerate MKHs are Bifurcate horizons

- On a MKH $\mathcal{H} \supset \mathcal{H}_\xi$ let $\tau : \mathcal{H}_\xi \to \mathbb{R}$ be defined by $\xi(\tau) = 1$.
- $\forall \eta \in \mathcal{A}^{deg}_{\mathcal{H}}, \quad \eta \overset{\mathcal{H}_\xi}{=} f_\eta \, e^{-\kappa_\xi \tau} \xi, \qquad \xi(f_\eta) = 0,$
- (Freedom: $\tau \to \tau + \tau_0, \quad \xi(\tau_0) = 0 \implies f_\eta \to f_\eta e^{\kappa_\xi \tau_0}$)
- $\kappa_\eta = 0 \implies \eta$ is affinely parametrized on $\mathcal{H}_\eta \subset \mathcal{H}$.

Non-fully degenerate MKHs are Bifurcate horizons

- On a MKH $\mathcal{H} \supset \mathcal{H}_\xi$ let $\tau : \mathcal{H}_\xi \to \mathbb{R}$ be defined by $\xi(\tau) = 1$.
- $\forall \eta \in \mathcal{A}^{deg}_{\mathcal{H}}, \quad \eta \overset{\mathcal{H}_\xi}{=} f_\eta \, e^{-\kappa_\xi \tau} \xi, \qquad \xi(f_\eta) = 0,$
- (Freedom: $\tau \to \tau + \tau_0, \quad \xi(\tau_0) = 0 \implies f_\eta \to f_\eta e^{\kappa_\xi \tau_0}$)
- $\kappa_\eta = 0 \implies \eta$ is affinely parametrized on $\mathcal{H}_\eta \subset \mathcal{H}$.
- Thus, affine parameter λ along the null geodesics on $\mathcal{H}_\eta \cap \mathcal{H}_\xi$ is
$$\lambda = \frac{1}{\kappa_\xi f_\eta} e^{\kappa_\xi \tau} \qquad (\kappa_\xi \neq 0)$$

Non-fully degenerate MKHs are Bifurcate horizons

- On a MKH $\mathcal{H} \supset \mathcal{H}_\xi$ let $\tau : \mathcal{H}_\xi \to \mathbb{R}$ be defined by $\xi(\tau) = 1$.
- $\forall \eta \in \mathcal{A}^{deg}_{\mathcal{H}}, \quad \eta \overset{\mathcal{H}_\xi}{=} f_\eta \, e^{-\kappa_\xi \tau} \xi, \qquad \xi(f_\eta) = 0,$
- (Freedom: $\tau \to \tau + \tau_0, \quad \xi(\tau_0) = 0 \implies f_\eta \to f_\eta e^{\kappa_\xi \tau_0}$)
- $\kappa_\eta = 0 \implies \eta$ is affinely parametrized on $\mathcal{H}_\eta \subset \mathcal{H}$.
- Thus, affine parameter λ along the null geodesics on $\mathcal{H}_\eta \cap \mathcal{H}_\xi$ is
$$\lambda = \frac{1}{\kappa_\xi f_\eta} e^{\kappa_\xi \tau} \qquad (\kappa_\xi \neq 0)$$

- $\implies$ integral curves of ξ in $\mathcal{H}_\xi \cap \mathcal{H}_\eta$ are <u>incomplete geodesics</u>

Non-fully degenerate MKHs are Bifurcate horizons

- On a MKH $\mathcal{H} \supset \mathcal{H}_\xi$ let $\tau : \mathcal{H}_\xi \to \mathbb{R}$ be defined by $\xi(\tau) = 1$.
- $\forall \eta \in \mathcal{A}^{deg}_{\mathcal{H}}$, $\quad \eta \overset{\mathcal{H}_\xi}{=} f_\eta \, e^{-\kappa_\xi \tau} \xi, \qquad \xi(f_\eta) = 0,$
- (Freedom: $\tau \to \tau + \tau_0, \quad \xi(\tau_0) = 0 \implies f_\eta \to f_\eta e^{\kappa_\xi \tau_0}$)
- $\kappa_\eta = 0 \implies \eta$ is affinely parametrized on $\mathcal{H}_\eta \subset \mathcal{H}$.
- Thus, affine parameter λ along the null geodesics on $\mathcal{H}_\eta \cap \mathcal{H}_\xi$ is
$$\lambda = \frac{1}{\kappa_\xi f_\eta} e^{\kappa_\xi \tau} \qquad (\kappa_\xi \neq 0)$$
- $\implies$ integral curves of ξ in $\mathcal{H}_\xi \cap \mathcal{H}_\eta$ are incomplete geodesics
- integral curves of η are longer geodesics and ξ vanishes along them on a co-dimension two submanifold $S \subset \overline{\mathcal{H}}$.

Non-fully degenerate MKHs are Bifurcate horizons

- On a MKH $\mathcal{H} \supset \mathcal{H}_\xi$ let $\tau : \mathcal{H}_\xi \to \mathbb{R}$ be defined by $\xi(\tau) = 1$.
- $\forall \eta \in \mathcal{A}^{deg}_{\mathcal{H}}$, $\quad \eta \overset{\mathcal{H}_\xi}{=} f_\eta \, e^{-\kappa_\xi \tau} \xi, \qquad \xi(f_\eta) = 0,$
- (Freedom: $\tau \to \tau + \tau_0, \quad \xi(\tau_0) = 0 \implies f_\eta \to f_\eta e^{\kappa_\xi \tau_0}$)
- $\kappa_\eta = 0 \implies \eta$ is affinely parametrized on $\mathcal{H}_\eta \subset \mathcal{H}$.
- Thus, affine parameter λ along the null geodesics on $\mathcal{H}_\eta \cap \mathcal{H}_\xi$ is
$$\lambda = \frac{1}{\kappa_\xi f_\eta} e^{\kappa_\xi \tau} \qquad (\kappa_\xi \neq 0)$$
- $\implies$ integral curves of ξ in $\mathcal{H}_\xi \cap \mathcal{H}_\eta$ are incomplete geodesics
- integral curves of η are longer geodesics and ξ vanishes along them on a co-dimension two submanifold $S \subset \overline{\mathcal{H}}$.
- $\implies$ non-fully degenerate MKHs can be seen as a branch of appropriate bifurcate Killing horizons with ξ as the bifurcate Killing vector field

Example 1: Nariai's spacetime

- The Nariai spacetime is the direct product $\mathrm{d}\mathbb{S}_2 \times \mathbb{S}^{n-2}$:

$$g_{Nar} = -dt^2 + \cosh^2(\varkappa t) dx^2 + \frac{1}{\varkappa^2} d\Omega^{n-2}$$

Example 1: Nariai's spacetime

- The Nariai spacetime is the direct product $\mathrm{d}\mathbb{S}_2 \times \mathbb{S}^{n-2}$:

$$g_{Nar} = -dt^2 + \cosh^2(\varkappa t) dx^2 + \frac{1}{\varkappa^2} d\Omega^{n-2}$$

- This is a Λ-vacuum solution with $\Lambda = 3(n-3)\varkappa^2/(n-1)$

Example 1: Nariai's spacetime

- The Nariai spacetime is the direct product $d\mathbb{S}_2 \times \mathbb{S}^{n-2}$:

$$g_{Nar} = -dt^2 + \cosh^2(\varkappa t)dx^2 + \frac{1}{\varkappa^2}d\Omega^{n-2}$$

- This is a Λ-vacuum solution with $\Lambda = 3(n-3)\varkappa^2/(n-1)$
- $\mathcal{H} := \{\tanh(\varkappa t) - \sin(\varkappa x) = 0\} \supset \{t = x = 0\}$

Example 1: Nariai's spacetime

- The Nariai spacetime is the direct product $d\mathbb{S}_2 \times \mathbb{S}^{n-2}$:

$$g_{Nar} = -dt^2 + \cosh^2(\varkappa t)dx^2 + \frac{1}{\varkappa^2}d\Omega^{n-2}$$

- This is a Λ-vacuum solution with $\Lambda = 3(n-3)\varkappa^2/(n-1)$
- $\mathcal{H} := \{\tanh(\varkappa t) - \sin(\varkappa x) = 0\} \supset \{t = x = 0\}$
- Topologically $\mathcal{H} \simeq \mathbb{R} \times \mathbb{S}^{n-2}$.

Example 1: Nariai's spacetime

- The Nariai spacetime is the direct product $d\mathbb{S}_2 \times \mathbb{S}^{n-2}$:

$$g_{Nar} = -dt^2 + \cosh^2(\varkappa t)dx^2 + \frac{1}{\varkappa^2}d\Omega^{n-2}$$

- This is a Λ-vacuum solution with $\Lambda = 3(n-3)\varkappa^2/(n-1)$
- $\mathcal{H} := \{\tanh(\varkappa t) - \sin(\varkappa x) = 0\} \supset \{t = x = 0\}$
- Topologically $\mathcal{H} \simeq \mathbb{R} \times \mathbb{S}^{n-2}$.
- $\mathcal{H}$ is a double Killing horizon, a basis of $\mathcal{A}_{\mathcal{H}}$ given by

$$\xi := \sin(\varkappa x)\partial_t + \cos(\varkappa x)\tanh(\varkappa t)\partial_x,$$
$$\eta := \cos(\varkappa x)\partial_t + [1 - \sin(\varkappa x)\tanh(\varkappa t)]\,\partial_x$$

Example 1: Nariai's spacetime

- The Nariai spacetime is the direct product $d\mathbb{S}_2 \times \mathbb{S}^{n-2}$:

$$g_{Nar} = -dt^2 + \cosh^2(\varkappa t)dx^2 + \frac{1}{\varkappa^2}d\Omega^{n-2}$$

- This is a Λ-vacuum solution with $\Lambda = 3(n-3)\varkappa^2/(n-1)$
- $\mathcal{H} := \{\tanh(\varkappa t) - \sin(\varkappa x) = 0\} \supset \{t = x = 0\}$
- Topologically $\mathcal{H} \simeq \mathbb{R} \times \mathbb{S}^{n-2}$.
- $\mathcal{H}$ is a double Killing horizon, a basis of $\mathcal{A}_{\mathcal{H}}$ given by

$$\xi := \sin(\varkappa x)\partial_t + \cos(\varkappa x)\tanh(\varkappa t)\partial_x,$$
$$\eta := \cos(\varkappa x)\partial_t + [1 - \sin(\varkappa x)\tanh(\varkappa t)]\,\partial_x$$

- A direct calculation gives $[\xi, \eta] = -\varkappa\eta$ and thus the non-vanishing surface gravity of $\mathcal{H}$ is $\kappa_\xi = -\varkappa$.

Example 1: Nariai's spacetime

- The Nariai spacetime is the direct product $d\mathbb{S}_2 \times \mathbb{S}^{n-2}$:

$$g_{Nar} = -dt^2 + \cosh^2(\varkappa t)dx^2 + \frac{1}{\varkappa^2}d\Omega^{n-2}$$

- This is a Λ-vacuum solution with $\Lambda = 3(n-3)\varkappa^2/(n-1)$
- $\mathcal{H} := \{\tanh(\varkappa t) - \sin(\varkappa x) = 0\} \supset \{t = x = 0\}$
- Topologically $\mathcal{H} \simeq \mathbb{R} \times \mathbb{S}^{n-2}$.
- $\mathcal{H}$ is a double Killing horizon, a basis of $\mathcal{A}_{\mathcal{H}}$ given by

$$\xi := \sin(\varkappa x)\partial_t + \cos(\varkappa x)\tanh(\varkappa t)\partial_x,$$
$$\eta := \cos(\varkappa x)\partial_t + [1 - \sin(\varkappa x)\tanh(\varkappa t)]\,\partial_x$$

- A direct calculation gives $[\xi, \eta] = -\varkappa\eta$ and thus the non-vanishing surface gravity of $\mathcal{H}$ is $\kappa_\xi = -\varkappa$.
- Observe that this is **bifurcate** with $\xi|_{t=x=0} = 0$.

Example 1: Nariai's spacetime

- The Nariai spacetime is the direct product $d\mathbb{S}_2 \times \mathbb{S}^{n-2}$:

$$g_{Nar} = -dt^2 + \cosh^2(\varkappa t)dx^2 + \frac{1}{\varkappa^2}d\Omega^{n-2}$$

- This is a Λ-vacuum solution with $\Lambda = 3(n-3)\varkappa^2/(n-1)$
- $\mathcal{H} := \{\tanh(\varkappa t) - \sin(\varkappa x) = 0\} \supset \{t = x = 0\}$
- Topologically $\mathcal{H} \simeq \mathbb{R} \times \mathbb{S}^{n-2}$.
- $\mathcal{H}$ is a double Killing horizon, a basis of $\mathcal{A}_{\mathcal{H}}$ given by

$$\xi := \sin(\varkappa x)\partial_t + \cos(\varkappa x)\tanh(\varkappa t)\partial_x,$$
$$\eta := \cos(\varkappa x)\partial_t + [1 - \sin(\varkappa x)\tanh(\varkappa t)]\,\partial_x$$

- A direct calculation gives $[\xi, \eta] = -\varkappa\eta$ and thus the non-vanishing surface gravity of $\mathcal{H}$ is $\kappa_\xi = -\varkappa$.
- Observe that this is **bifurcate** with $\xi|_{t=x=0} = 0$.
- Similar direct (or warped) products of either (A)$d\mathbb{S}_k$ with $\mathbb{S}^{n-k}$ provide many examples of MKHs.

Example 2: Plane waves

- General plane-wave spacetime in arbitrary dimension n

$$g_{PW} = 2dudv + M_{AB}(u)x^A x^B du^2 + \delta_{AB}dx^A dx^B$$

Example 2: Plane waves

- General plane-wave spacetime in arbitrary dimension n

$$g_{PW} = 2dudv + M_{AB}(u)x^A x^B du^2 + \delta_{AB}dx^A dx^B$$

- Ricci flat if $\delta^{AB}M_{AB} = 0$; Einstein-Maxwell solutions if $M_{AB} = \Psi(u)\delta_{AB}$.

Example 2: Plane waves

- General plane-wave spacetime in arbitrary dimension n

$$g_{PW} = 2dudv + M_{AB}(u)x^A x^B du^2 + \delta_{AB} dx^A dx^B$$

- Ricci flat if $\delta^{AB} M_{AB} = 0$; Einstein-Maxwell solutions if $M_{AB} = \Psi(u)\delta_{AB}$.
- Every $\mathcal{H} := \{u = u_0\}$ is a fully degenerate MKH of maximal order $n-1$.

Example 2: Plane waves

- General plane-wave spacetime in arbitrary dimension n

$$g_{PW} = 2dudv + M_{AB}(u)x^A x^B du^2 + \delta_{AB} dx^A dx^B$$

- Ricci flat if $\delta^{AB} M_{AB} = 0$; Einstein-Maxwell solutions if $M_{AB} = \Psi(u)\delta_{AB}$.
- Every $\mathcal{H} := \{u = u_0\}$ is a fully degenerate MKH of maximal order $n-1$.

- The Killing vectors generating $\mathcal{A}_{\mathcal{H}} = \mathcal{A}_{\mathcal{H}}^{deg}$ are given by

$$\eta = (b - \dot{c}_A(u)x^A)\partial_v + c^A(u)\partial_A, \quad \ddot{c}_A = M_{AB}(u)c^B, \quad c_A(u_0) = 0$$

Example 2: Plane waves

- General plane-wave spacetime in arbitrary dimension n

$$g_{PW} = 2dudv + M_{AB}(u)x^A x^B du^2 + \delta_{AB} dx^A dx^B$$

- Ricci flat if $\delta^{AB} M_{AB} = 0$; Einstein-Maxwell solutions if $M_{AB} = \Psi(u)\delta_{AB}$.
- Every $\mathcal{H} := \{u = u_0\}$ is a fully degenerate MKH of maximal order $n-1$.
- The Killing vectors generating $\mathcal{A}_{\mathcal{H}} = \mathcal{A}^{deg}_{\mathcal{H}}$ are given by

$$\eta = (b - \dot{c}_A(u)x^A)\partial_v + c^A(u)\partial_A, \quad \ddot{c}_A = M_{AB}(u)c^B, \quad c_A(u_0) = 0$$

Fully degenerate MKHs of any order m

Fully degenerate MKHs of any order $m \in \{2, \cdots, n-1\}$ can also be built explicitly.

When and how are Killing horizons multiple?

- Which equations need to be satisfied so that a Killing horizon $\mathcal{H}$ is multiple?

When and how are Killing horizons multiple?

- Which equations need to be satisfied so that a Killing horizon $\mathcal{H}$ is multiple?
- Under which conditions are these equations sufficient?

When and how are Killing horizons multiple?

- Which equations need to be satisfied so that a Killing horizon $\mathcal{H}$ is multiple?
- Under which conditions are these equations sufficient?

- Fix a Killing generator ξ on $\mathcal{H}$. We already know that

$$\forall \eta \in \mathcal{A}^{deg}_{\mathcal{H}}, \quad \eta \stackrel{\mathcal{H}_\xi}{=} f_\eta \, e^{-\kappa_\xi \tau} \xi, \qquad \xi(f_\eta) = 0,$$

When and how are Killing horizons multiple?

- Which equations need to be satisfied so that a Killing horizon $\mathcal{H}$ is multiple?
- Under which conditions are these equations sufficient?
- Fix a Killing generator ξ on $\mathcal{H}$. We already know that

$$\forall \eta \in \mathcal{A}^{deg}_{\mathcal{H}}, \qquad \eta \overset{\mathcal{H}_\xi}{=} f_\eta \, e^{-\kappa_\xi \tau} \xi, \qquad \xi(f_\eta) = 0,$$

- It is very simple to show that f_η is fully determined by $f := f_\eta e^{-\kappa_\xi \tau}|_{S_0}$, where S_0 is any spacelike cross section of $\mathcal{H}_\xi$.

When and how are Killing horizons multiple?

- Which equations need to be satisfied so that a Killing horizon $\mathcal{H}$ is multiple?
- Under which conditions are these equations sufficient?
- Fix a Killing generator ξ on $\mathcal{H}$. We already know that

$$\forall \eta \in \mathcal{A}^{deg}_{\mathcal{H}}, \qquad \eta \overset{\mathcal{H}_\xi}{=} f_\eta \, e^{-\kappa_\xi \tau} \xi, \qquad \xi(f_\eta) = 0,$$

- It is very simple to show that f_η is fully determined by $f := f_\eta e^{-\kappa_\xi \tau}|_{S_0}$, where S_0 is any spacelike cross section of $\mathcal{H}_\xi$.
- Our approach: **find equations for $f : S_0 \to \mathbb{R}$**

A little Killing Horizon geometry

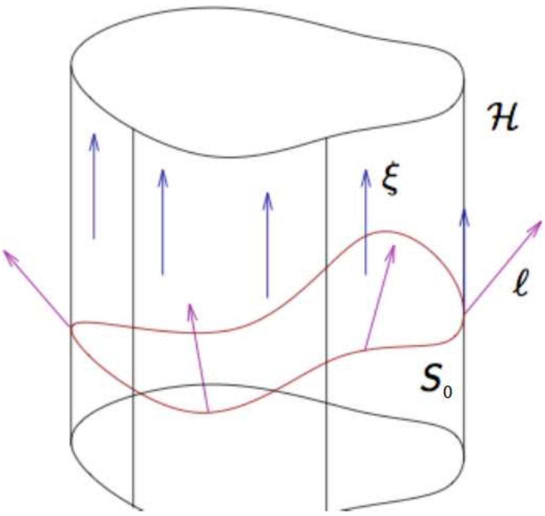

Geometry of cross sections of Killing horizons:

- $\{e_A\}$ basis of tangent vector fields on S_0
- Induced metric γ_{AB}: all cross sections are isometric.
- Associated covariant derivative: D
- K_{AB}: unique 2nd fundamental form of S_0

$$D_{e_A} e_B - \nabla_{e_A} e_B = K_{AB}\, \xi$$

- Torsion one-form s_A:

$$e^\rho_A \nabla_\rho \xi^\mu = -s_A \xi^\mu + K_A{}^B e^\mu_B$$

- $R_{AB} := R_{\mu\nu}|_{S_0} e^\mu_A e^\nu_B$: ambient Ricci tensor along S on S.
- r_{AB}: Ricci tensor of (S_0, γ).

The master equation

Theorem (Master equation)

Let $\mathcal{H}$ be a multiple Killing horizon and pick up (a non-trivial) $\xi \in \mathcal{A}_{\mathcal{H}}$ with surface gravity κ_ξ

Select a cross section S_0 of $\mathcal{H}$ and define $S_\xi := S_0 \cap \mathcal{H}_\xi$.

Then, for any $\eta \in \mathcal{A}^{deg}_{\mathcal{H}}$ the function $f : S_\xi \to \mathbb{R}$ such that $\eta \overset{S_\xi}{=} f\xi$ satisfies the following master equation:

$$D_A D_B f - 2 s_{(A} D_{B)} f + \left(\frac{1}{2} R_{AB} - \frac{1}{2} r_{AB} + s_A s_B - D_{(A} s_{B)} \right) f = 0.$$

The master equation

Theorem (Master equation)

Let $\mathcal{H}$ be a multiple Killing horizon and pick up (a non-trivial) $\xi \in \mathcal{A}_{\mathcal{H}}$ with surface gravity κ_ξ

Select a cross section S_0 of $\mathcal{H}$ and define $S_\xi := S_0 \cap \mathcal{H}_\xi$.

Then, for any $\eta \in \mathcal{A}^{deg}_{\mathcal{H}}$ the function $f : S_\xi \to \mathbb{R}$ such that $\eta \stackrel{S_\xi}{=} f\xi$ satisfies the following master equation:

$$D_A D_B f - 2 s_{(A} D_{B)} f + \left(\frac{1}{2} R_{AB} - \frac{1}{2} r_{AB} + s_A s_B - D_{(A} s_{B)} \right) f = 0.$$

- At most one can prescribe freely $f|_p$ and $df|_p$ at $p \in S_\xi$. Since dimension of S_ξ is $n-2$, maximal number of solutions is $n-1$.

The master equation

Theorem (Master equation)

Let $\mathcal{H}$ be a multiple Killing horizon and pick up (a non-trivial) $\xi \in \mathcal{A}_{\mathcal{H}}$ with surface gravity κ_ξ

Select a cross section S_0 of $\mathcal{H}$ and define $S_\xi := S_0 \cap \mathcal{H}_\xi$.

Then, for any $\eta \in \mathcal{A}^{deg}_{\mathcal{H}}$ the function $f : S_\xi \to \mathbb{R}$ such that $\eta \stackrel{S_\xi}{=} f\xi$ satisfies the following master equation:

$$D_A D_B f - 2 s_{(A} D_{B)} f + \left(\frac{1}{2} R_{AB} - \frac{1}{2} r_{AB} + s_A s_B - D_{(A} s_{B)} \right) f = 0.$$

- At most one can prescribe freely $f|_p$ and $df|_p$ at $p \in S_\xi$. Since dimension of S_ξ is $n-2$, maximal number of solutions is $n-1$.
- How does this fit with the fact that dim$\mathcal{A}_{\mathcal{H}} = n-1$ for fully degenerate $\mathcal{H}$?

A reformulation of the master equation

- For any Killing horizon $\mathcal{H}_\xi$ (not necessarily part of a MKH)

$$\xi_\rho R^\rho{}_{\mu\nu\lambda} e^\mu_A e^\nu_B \ell^\lambda \stackrel{\mathcal{H}_\xi}{=} D_A s_B - s_A s_B + \kappa_\xi K_{AB}$$

where ℓ is the unique null vector field transverse to $\mathcal{H}_\xi$ normalized to $\xi_\mu \ell^\mu = -1$.

A reformulation of the master equation

- For any Killing horizon $\mathcal{H}_\xi$ (not necessarily part of a MKH)

$$\xi_\rho R^\rho{}_{\mu\nu\lambda} e^\mu_A e^\nu_B \ell^\lambda \stackrel{\mathcal{H}_\xi}{=} D_A s_B - s_A s_B + \kappa_\xi K_{AB}$$

where ℓ is the unique null vector field transverse to $\mathcal{H}_\xi$ normalized to $\xi_\mu \ell^\mu = -1$.

- Using also here the Gauss equation for S_0, the master equation can be rewritten in the following simpler form

$$\boxed{D_A D_B f - s_A D_B f - s_B D_A f + \kappa_\xi K_{AB} f = 0.}$$

A reformulation of the master equation

- For any Killing horizon $\mathcal{H}_\xi$ (not necessarily part of a MKH)

$$\xi_\rho R^\rho{}_{\mu\nu\lambda} e^\mu_A e^\nu_B \ell^\lambda \stackrel{\mathcal{H}_\xi}{=} D_A s_B - s_A s_B + \kappa_\xi K_{AB}$$

where ℓ is the unique null vector field transverse to $\mathcal{H}_\xi$ normalized to $\xi_\mu \ell^\mu = -1$.

- Using also here the Gauss equation for S_0, the master equation can be rewritten in the following simpler form

$$\boxed{D_A D_B f - s_A D_B f - s_B D_A f + \kappa_\xi K_{AB} f = 0.}$$

- Now, if $\mathcal{H}$ is fully degenerate, then in particular $\kappa_\xi = 0$ and f =const. is a solution of the master equation which leads to the original Killing ξ itself

A reformulation of the master equation

- For any Killing horizon $\mathcal{H}_\xi$ (not necessarily part of a MKH)

$$\xi_\rho R^\rho{}_{\mu\nu\lambda} e^\mu_A e^\nu_B \ell^\lambda \stackrel{\mathcal{H}_\xi}{=} D_A s_B - s_A s_B + \kappa_\xi K_{AB}$$

where ℓ is the unique null vector field transverse to $\mathcal{H}_\xi$ normalized to $\xi_\mu \ell^\mu = -1$.

- Using also here the Gauss equation for S_0, the master equation can be rewritten in the following simpler form

$$\boxed{D_A D_B f - s_A D_B f - s_B D_A f + \kappa_\xi K_{AB} f = 0.}$$

- Now, if $\mathcal{H}$ is fully degenerate, then in particular $\kappa_\xi = 0$ and f =const. is a solution of the master equation which leads to the original Killing ξ itself

- Hence, there are at most $n-1$ independent Killings in $\mathcal{A}_{\mathcal{H}}$ in this case.

Full integrability

- Under which conditions the maximal number of solutions is achieved?

Full integrability

- Under which conditions the maximal number of solutions is achieved?
- An analysis of the integrability conditions, requiring them to be identically satisfied, leads to

Full integrability

- Under which conditions the maximal number of solutions is achieved?
- An analysis of the integrability conditions, requiring them to be identically satisfied, leads to

Theorem

The master equation admits a maximal number of solutions (i.e. $n-1$ solutions) if and only if

Full integrability

- Under which conditions the maximal number of solutions is achieved?
- An analysis of the integrability conditions, requiring them to be identically satisfied, leads to

Theorem

The master equation admits a maximal number of solutions (i.e. $n-1$ solutions) if and only if

- s_A *is closed:* $D_A s_B - D_B s_A = 0$*;*

Full integrability

- Under which conditions the maximal number of solutions is achieved?
- An analysis of the integrability conditions, requiring them to be identically satisfied, leads to

Theorem

The master equation admits a maximal number of solutions (i.e. $n-1$ solutions) if and only if

- s_A *is closed:* $D_A s_B - D_B s_A = 0$;
- (S, γ) *is maximally symmetric (ergo, it has constant curvature* q*)*

Full integrability

- Under which conditions the maximal number of solutions is achieved?
- An analysis of the integrability conditions, requiring them to be identically satisfied, leads to

Theorem

The master equation admits a maximal number of solutions (i.e. $n-1$ solutions) if and only if

- s_A *is closed:* $D_A s_B - D_B s_A = 0$;
- (S, γ) *is maximally symmetric (ergo, it has constant curvature* q*)*

- $R_{AB} = (n-1) q \gamma_{AB}$.

Sufficiency of the master equation?

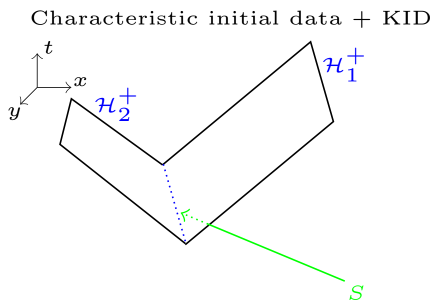

- In general, the master equation gives necessary conditions for MKH. Under which assumptions it is also sufficient?

Sufficiency of the master equation?

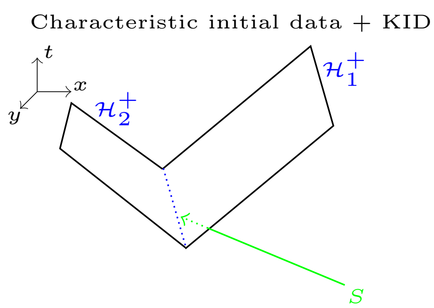

- In general, the master equation gives necessary conditions for MKH. Under which assumptions it is also sufficient?
- By using the characteristic initial-value problem [Rendall 1990] together with results on the required initial data for Killing vectors [Chruściel & Paetz, 2013], one can derive satisfactory sufficiency results.

Sufficiency of the master equation?

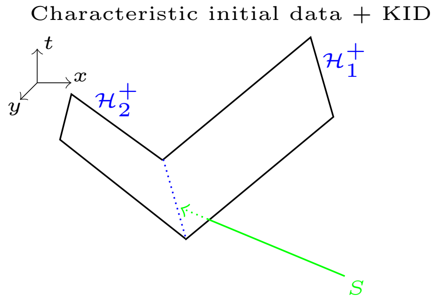

- In general, the master equation gives necessary conditions for MKH. Under which assumptions it is also sufficient?
- By using the characteristic initial-value problem [Rendall 1990] together with results on the required initial data for Killing vectors [Chruściel & Paetz, 2013], one can derive satisfactory sufficiency results.
- To deal with the case of non-fully degenerate MKHs, we also assume that the initial data give rise to a bifurcate Killing horizon (on the initial characteristic hypersurfaces).

Sufficiency of the master equation?

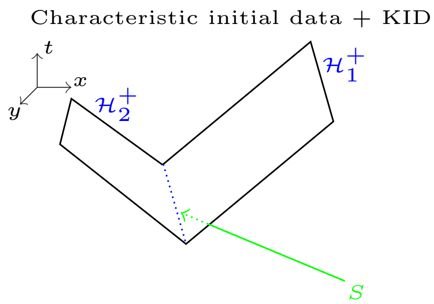

- In general, the master equation gives necessary conditions for MKH. Under which assumptions it is also sufficient?
- By using the characteristic initial-value problem [Rendall 1990] together with results on the required initial data for Killing vectors [Chruściel & Paetz, 2013], one can derive satisfactory sufficiency results.
- To deal with the case of non-fully degenerate MKHs, we also assume that the initial data give rise to a bifurcate Killing horizon (on the initial characteristic hypersurfaces).
- And we consider the master equation on the bifurcation surface S

Sufficiency of the master equation?

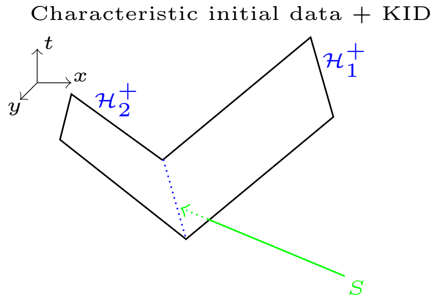

- In general, the master equation gives necessary conditions for MKH. Under which assumptions it is also sufficient?
- By using the characteristic initial-value problem [Rendall 1990] together with results on the required initial data for Killing vectors [Chruściel & Paetz, 2013], one can derive satisfactory sufficiency results.
- To deal with the case of non-fully degenerate MKHs, we also assume that the initial data give rise to a bifurcate Killing horizon (on the initial characteristic hypersurfaces).
- And we consider the master equation on the bifurcation surface S
- Of course, for the initial-value problem we need fixed field equations. Simplest situation: Λ-vacuum spacetimes.

Sufficiency of the master equation

Theorem

Let the spacetime solve the Λ-vacuum field equations and admit a bifurcate Killing horizon $\{\mathcal{H}_1^{\pm}, \mathcal{H}_2^{\pm}, S\}$.

Select k a non-vanishing future null generator of $\mathcal{H}_1^+ \cup S \cup \mathcal{H}_1^-$, and define the torsion one-form on S by $e_A^{\rho} \nabla_{\rho} k^{\mu} = \varsigma_A k^{\mu}$.

Then $\mathcal{H}_1^+ \cup S \cup \mathcal{H}_1^-$ is a MKH of order m if and only if the linear PDE (master equation on S):

$$D_A D_B f - 2\varsigma_{(A} D_{B)} f + \left(\frac{\Lambda}{n-2} \gamma_{AB} - \frac{r_{AB}}{2} + \varsigma_A \varsigma_B - D_{(A} \varsigma_{B)} \right) f = 0$$

admits $m-1$ independent solutions.

Reminder: Near Horizon Geometries

- All degenerate Killing horizons give rise to a related "near horizon geometry".

Reminder: Near Horizon Geometries

- All degenerate Killing horizons give rise to a related "near horizon geometry".
- Construction based on a limiting procedure (details: [Kunduri, Lucietti, Living Reviews Relativity (2013)] by using Gaussian null coordinates $\{u, v, x^A\}$ associated to the degenerate Killing horizon $\mathcal{H} : \{u = 0\}$, with Killing generator ∂_v:

$$g = 2dudv + 4uw_A(u,x)dx^A + u^2\Xi(u,x)dv^2 + \sigma_{AB}(u,x)dx^A dx^B,$$

Reminder: Near Horizon Geometries

- All degenerate Killing horizons give rise to a related "near horizon geometry".
- Construction based on a limiting procedure (details: [Kunduri, Lucietti, Living Reviews Relativity (2013)] by using Gaussian null coordinates $\{u, v, x^A\}$ associated to the degenerate Killing horizon $\mathcal{H} : \{u = 0\}$, with Killing generator ∂_v:

$$g = 2dudv + 4uw_A(u,x)dx^A + u^2\Xi(u,x)dv^2 + \sigma_{AB}(u,x)dx^A dx^B,$$

- Replacing $u \to u\lambda$, $v \to \lambda^{-1}v$ and taking the limit $\lambda \to 0$ yields its Near Horizon Geometry spacetime:

$$g_{\text{NHG}} = 2dudv + 4us_A(x)dx^A + u^2h(x)dv^2 + \gamma_{AB}(x)dx^A dx^B$$

with $h(x) := \Xi|_{u=0}$, $s_A := w_A|_{u=0}$, $\quad \gamma_{AB} := \sigma_{AB}|_{u=0}$.

Reminder: Near Horizon Geometries

- All degenerate Killing horizons give rise to a related "near horizon geometry".
- Construction based on a limiting procedure (details: [Kunduri, Lucietti, Living Reviews Relativity (2013)] by using Gaussian null coordinates $\{u, v, x^A\}$ associated to the degenerate Killing horizon $\mathcal{H} : \{u = 0\}$, with Killing generator ∂_v:

$$g = 2dudv + 4uw_A(u,x)dx^A + u^2\Xi(u,x)dv^2 + \sigma_{AB}(u,x)dx^A dx^B,$$

- Replacing $u \to u\lambda$, $v \to \lambda^{-1}v$ and taking the limit $\lambda \to 0$ yields its Near Horizon Geometry spacetime:

$$g_{\text{NHG}} = 2dudv + 4us_A(x)dx^A + u^2h(x)dv^2 + \gamma_{AB}(x)dx^A dx^B$$

with $h(x) := \Xi|_{u=0}$, $s_A := w_A|_{u=0}$, $\quad \gamma_{AB} := \sigma_{AB}|_{u=0}$.

- This is the "focused" geometry near the original horizon.

Near Horizon Geometries

- The near horizon geometry can be defined in an intrinsic manner, using geometrical objects.

Near Horizon Geometries

- The near horizon geometry can be defined in an intrinsic manner, using geometrical objects.
- Choose any co-dimension two submanifold $S_0 \subset \mathcal{H}$ of the original degenerate horizon. Then

Near Horizon Geometries

- The near horizon geometry can be defined in an intrinsic manner, using geometrical objects.
- Choose any co-dimension two submanifold $S_0 \subset \mathcal{H}$ of the original degenerate horizon. Then
  1. γ_{AB} is the first fundamental form on S_0

Near Horizon Geometries

- The near horizon geometry can be defined in an intrinsic manner, using geometrical objects.
- Choose any co-dimension two submanifold $S_0 \subset \mathcal{H}$ of the original degenerate horizon. Then
  1. γ_{AB} is the first fundamental form on S_0

  2. s_A is the *torsion one-form* on S_0 (relative to ∂_v)

Near Horizon Geometries

- The near horizon geometry can be defined in an intrinsic manner, using geometrical objects.
- Choose any co-dimension two submanifold $S_0 \subset \mathcal{H}$ of the original degenerate horizon. Then
  1. γ_{AB} is the first fundamental form on S_0
  2. s_A is the *torsion one-form* on S_0 (relative to ∂_v)
  3. $h = 2s^A s_A - D_A s^A + \frac{1}{2}R|_{S_0} - \frac{1}{2}\gamma^{AB}R_{AB}$

Near Horizon Geometries

- The near horizon geometry can be defined in an intrinsic manner, using geometrical objects.
- Choose any co-dimension two submanifold $S_0 \subset \mathcal{H}$ of the original degenerate horizon. Then
  1. γ_{AB} is the first fundamental form on S_0
  2. s_A is the *torsion one-form* on S_0 (relative to ∂_v)
  3. $h = 2s^A s_A - D_A s^A + \frac{1}{2}R|_{S_0} - \frac{1}{2}\gamma^{AB}R_{AB}$

- $g_{\mathsf{NHG}} = 2dudv + 4us_A(x)dx^A + u^2 h(x)dv^2 + \gamma_{AB}(x)dx^A dx^B$

Near Horizon Geometries

- The near horizon geometry can be defined in an intrinsic manner, using geometrical objects.
- Choose any co-dimension two submanifold $S_0 \subset \mathcal{H}$ of the original degenerate horizon. Then
  1. γ_{AB} is the first fundamental form on S_0
  2. s_A is the *torsion one-form* on S_0 (relative to ∂_v)
  3. $h = 2s^A s_A - D_A s^A + \frac{1}{2} R|_{S_0} - \frac{1}{2}\gamma^{AB} R_{AB}$
- $g_{\mathsf{NHG}} = 2dudv + 4us_A(x)dx^A + u^2 h(x)dv^2 + \gamma_{AB}(x)dx^A dx^B$
- In either case, intrinsic or with Gaussian null coordinates, the metric g_{NHG} is only given on a connected part of the MKH without fixed points of the degenerate Killing

All Near Horizon Geometries have MKHs

- $g_{\mathsf{NHG}} = 2dudv + 4us_A(x)dx^A + u^2 h(x)dv^2 + \gamma_{AB}(x)dx^A dx^B$

All Near Horizon Geometries have MKHs

- $g_{\text{NHG}} = 2dudv + 4us_A(x)dx^A + u^2h(x)dv^2 + \gamma_{AB}(x)dx^Adx^B$
- $\mathcal{H}_\eta := \{u = 0\}$ is a degenerate Killing horizon of g_{NHG} for the Killing $\eta = \partial_v$ (as $\eta_\mu\eta^\mu = u^2h$, a double zero at $u = 0$).

All Near Horizon Geometries have MKHs

- $g_{\text{NHG}} = 2dudv + 4us_A(x)dx^A + u^2h(x)dv^2 + \gamma_{AB}(x)dx^Adx^B$
- $\mathcal{H}_\eta := \{u = 0\}$ is a degenerate Killing horizon of g_{NHG} for the Killing $\eta = \partial_v$ (as $\eta_\mu\eta^\mu = u^2h$, a double zero at $u = 0$).
- One can check that the Near Horizon Geometry of g_{NHG} with respect to η is itself —so the process cannot be iterated.

All Near Horizon Geometries have MKHs

- $g_{\mathsf{NHG}} = 2dudv + 4us_A(x)dx^A + u^2h(x)dv^2 + \gamma_{AB}(x)dx^Adx^B$
- $\mathcal{H}_\eta := \{u = 0\}$ is a degenerate Killing horizon of g_{NHG} for the Killing $\eta = \partial_v$ (as $\eta_\mu\eta^\mu = u^2h$, a double zero at $u = 0$).
- One can check that the Near Horizon Geometry of g_{NHG} with respect to η is itself —so the process cannot be iterated.

General property [Pawlowski, Lewandowski, Jezierski, 2004]

$\xi = v\partial_v - u\partial_u$ is another Killing vector of the metric g_{NHG}.

All Near Horizon Geometries have MKHs

- $g_{\mathsf{NHG}} = 2dudv + 4us_A(x)dx^A + u^2h(x)dv^2 + \gamma_{AB}(x)dx^Adx^B$
- $\mathcal{H}_\eta := \{u = 0\}$ is a degenerate Killing horizon of g_{NHG} for the Killing $\eta = \partial_v$ (as $\eta_\mu\eta^\mu = u^2h$, a double zero at $u = 0$).
- One can check that the Near Horizon Geometry of g_{NHG} with respect to η is itself —so the process cannot be iterated.

General property [Pawlowski, Lewandowski, Jezierski, 2004]

$\xi = v\partial_v - u\partial_u$ is another Killing vector of the metric g_{NHG}.

- ξ is null and tangent to $\mathcal{H}_\eta \setminus \{u = v = 0\}$, so that $\xi \in \mathcal{A}_{\mathcal{H}_\eta}$

All Near Horizon Geometries have MKHs

- $g_{\text{NHG}} = 2dudv + 4us_A(x)dx^A + u^2h(x)dv^2 + \gamma_{AB}(x)dx^Adx^B$
- $\mathcal{H}_\eta := \{u = 0\}$ is a degenerate Killing horizon of g_{NHG} for the Killing $\eta = \partial_v$ (as $\eta_\mu \eta^\mu = u^2 h$, a double zero at $u = 0$).
- One can check that the Near Horizon Geometry of g_{NHG} with respect to η is itself —so the process cannot be iterated.

General property [Pawlowski, Lewandowski, Jezierski, 2004]

$\xi = v\partial_v - u\partial_u$ is another Killing vector of the metric g_{NHG}.

- ξ is null and tangent to $\mathcal{H}_\eta \setminus \{u = v = 0\}$, so that $\xi \in \mathcal{A}_{\mathcal{H}_\eta}$
- Obviously $[\xi, \eta] = -\eta$ so that $\kappa_\xi = -1 \neq 0$

All Near Horizon Geometries have MKHs

- $g_{\text{NHG}} = 2dudv + 4us_A(x)dx^A + u^2h(x)dv^2 + \gamma_{AB}(x)dx^Adx^B$
- $\mathcal{H}_\eta := \{u = 0\}$ is a degenerate Killing horizon of g_{NHG} for the Killing $\eta = \partial_v$ (as $\eta_\mu \eta^\mu = u^2 h$, a double zero at $u = 0$).
- One can check that the Near Horizon Geometry of g_{NHG} with respect to η is itself —so the process cannot be iterated.

General property [Pawlowski, Lewandowski, Jezierski, 2004]

$\xi = v\partial_v - u\partial_u$ is another Killing vector of the metric g_{NHG}.

- ξ is null and tangent to $\mathcal{H}_\eta \setminus \{u = v = 0\}$, so that $\xi \in \mathcal{A}_{\mathcal{H}_\eta}$
- Obviously $[\xi, \eta] = -\eta$ so that $\kappa_\xi = -1 \neq 0$

- Therefore, $\mathcal{H}_\eta$ is a non-fully degenerate MKH.

All Near Horizon Geometries have MKHs

- $g_{\mathsf{NHG}} = 2dudv + 4us_A(x)dx^A + u^2h(x)dv^2 + \gamma_{AB}(x)dx^Adx^B$
- $\mathcal{H}_\eta := \{u = 0\}$ is a degenerate Killing horizon of g_{NHG} for the Killing $\eta = \partial_v$ (as $\eta_\mu\eta^\mu = u^2h$, a double zero at $u = 0$).
- One can check that the Near Horizon Geometry of g_{NHG} with respect to η is itself —so the process cannot be iterated.

General property [Pawlowski, Lewandowski, Jezierski, 2004]

$\xi = v\partial_v - u\partial_u$ is another Killing vector of the metric g_{NHG}.

- ξ is null and tangent to $\mathcal{H}_\eta \setminus \{u = v = 0\}$, so that $\xi \in \mathcal{A}_{\mathcal{H}_\eta}$
- Obviously $[\xi, \eta] = -\eta$ so that $\kappa_\xi = -1 \neq 0$
- Therefore, $\mathcal{H}_\eta$ is a non-fully degenerate MKH.
- Actually, any cut $S_{v_0} := \{u = 0, v = v_0\} \subset \mathcal{H}_\eta$ is the bifurcation surface with respect to the Killing

$$\xi - v_0\eta = (v - v_0)\partial_v - u\partial_u$$

of a bifurcate Killing horizon with a multiple branch.

MKHs in Near Horizon Geometries

In conclusion, every Near Horizon Geometry possesses a non-fully degenerate Multiple Killing Horizon

MKHs in Near Horizon Geometries

In conclusion, every Near Horizon Geometry possesses a non-fully degenerate Multiple Killing Horizon

The near horizon geometry limit increases, or keeps, the order of the Killing horizon.

MKHs in Near Horizon Geometries

In conclusion, every Near Horizon Geometry possesses a non-fully degenerate Multiple Killing Horizon

The near horizon geometry limit increases, or keeps, the order of the Killing horizon.

Theorem

Let $\mathcal{H}$ be a degenerate Killing horizon, possibly multiple, of order $m \geq 1$ and let g_{NHG} be the near-horizon metric of a degenerate Killing vector of $\mathcal{H}$. Then

(i) *If $\mathcal{H}$ is fully degenerate, g_{NHG} admits a multiple Killing horizon of order at least $m+1$.*

(ii) *If $\mathcal{H}$ is non-fully degenerate (so that $m \geq 2$), then g_{NHG} has a multiple Killing horizon of order at least m.*

Conversely: MKHs lead to a unique NHG

- Given that any MKH has a non-empty $\mathcal{A}_{\mathcal{H}}^{deg}$, MKHs always have associated Near Horizon Geometries

Conversely: MKHs lead to a unique NHG

- Given that any MKH has a non-empty $\mathcal{A}_{\mathcal{H}}^{deg}$, MKHs always have associated Near Horizon Geometries
- However, if dim $\mathcal{A}_{\mathcal{H}}^{deg} \geq 2$, then one can construct the near-horizon limit for more than one (independent) degenerate Killing.

Conversely: MKHs lead to a unique NHG

- Given that any MKH has a non-empty $\mathcal{A}^{deg}_{\mathcal{H}}$, MKHs always have associated Near Horizon Geometries
- However, if dim $\mathcal{A}^{deg}_{\mathcal{H}} \geq 2$, then one can construct the near-horizon limit for more than one (independent) degenerate Killing.
- Does this lead to various, inequivalent, Near Horizon Geometries for such a given MKH?

Conversely: MKHs lead to a unique NHG

- Given that any MKH has a non-empty $\mathcal{A}^{deg}_{\mathcal{H}}$, MKHs always have associated Near Horizon Geometries
- However, if dim $\mathcal{A}^{deg}_{\mathcal{H}} \geq 2$, then one can construct the near-horizon limit for more than one (independent) degenerate Killing.
- Does this lead to various, inequivalent, Near Horizon Geometries for such a given MKH?

Theorem

Let $\mathcal{H}$ be a Multiple Killing Horizon either of order $m \geq 3$ or fully degenerate. Then, the near horizon geometries with respect to the elements of $\mathcal{A}^{deg}_{\mathcal{H}}$ (and away from their fixed points) are all isometric to each other.

Non-fully degenerate MKHs are NHGs locally

- We know that

Non-fully degenerate MKHs are NHGs locally

- We know that
  - Every Near Horizon Geometry contains a non-fully degenerate Multiple Killing Horizon

Non-fully degenerate MKHs are NHGs locally

- We know that
  - Every Near Horizon Geometry contains a non-fully degenerate Multiple Killing Horizon
  - Any Multiple Killing Horizon has associated a unique Near Horizon Geometry

Non-fully degenerate MKHs are NHGs locally

- We know that
  - Every Near Horizon Geometry contains a non-fully degenerate Multiple Killing Horizon
  - Any Multiple Killing Horizon has associated a unique Near Horizon Geometry
- Are these two concepts, NHG and non-degenrate MKH, “equivalent” in any sense?

Non-fully degenerate MKHs <u>are</u> NHGs locally

- We know that
  - Every Near Horizon Geometry contains a non-fully degenerate Multiple Killing Horizon
  - Any Multiple Killing Horizon has associated a unique Near Horizon Geometry
- Are these two concepts, NHG and non-degenrate MKH, "equivalent" in any sense?

Theorem (Ongoing work)

Any spacetime with a non-fully degenerate MKH $\mathcal{H}$ is <u>locally</u> isometric to the unique near horizon geometry relative to $\mathcal{H}$.

Non-fully degenerate MKHs <u>are</u> NHGs locally

- We know that
  - Every Near Horizon Geometry contains a non-fully degenerate Multiple Killing Horizon
  - Any Multiple Killing Horizon has associated a unique Near Horizon Geometry
- Are these two concepts, NHG and non-degenrate MKH, "equivalent" in any sense?

Theorem (Ongoing work)

Any spacetime with a non-fully degenerate MKH $\mathcal{H}$ is <u>locally</u> isometric to the unique near horizon geometry relative to $\mathcal{H}$.

- This provides a classification of NHGs, with explicit local expressions

Non-fully degenerate MKHs are NHGs locally

- We know that
  - Every Near Horizon Geometry contains a non-fully degenerate Multiple Killing Horizon
  - Any Multiple Killing Horizon has associated a unique Near Horizon Geometry
- Are these two concepts, NHG and non-degenrate MKH, "equivalent" in any sense?

Theorem (Ongoing work)

Any spacetime with a non-fully degenerate MKH $\mathcal{H}$ is locally isometric to the unique near horizon geometry relative to $\mathcal{H}$.

- This provides a classification of NHGs, with explicit local expressions
- More importantly, it allows for an improved definition of Near Horizon Geometries, incorporating fixed points into the picture, and thus providing *global* definitions and results

Explicit general form of NHGs

- Let the non-fully degenerate MKH generating the sought NHG be of order $m := 2 + p$, with $p \in \{0, 1, \ldots, n-2\}$

Explicit general form of NHGs

- Let the non-fully degenerate MKH generating the sought NHG be of order $m := 2 + p$, with $p \in \{0, 1, \ldots, n-2\}$
- Any cross-section $S_0 \in \mathcal{H}$ is a warped product $S_0 = V \times_\Omega \Sigma$ with p-dimensional maximally symmetric fibers. Thus, the metric γ_{AB} on S_0 decomposes as

$$\gamma = \hat{\gamma} + \Omega^2 g_\varepsilon, \qquad \Omega : V \to \mathbb{R} \setminus \{0\}$$

with g_ε the metric of constant curvature ε

Explicit general form of NHGs

- Let the non-fully degenerate MKH generating the sought NHG be of order $m := 2 + p$, with $p \in \{0, 1, \ldots, n-2\}$
- Any cross-section $S_0 \in \mathcal{H}$ is a warped product $S_0 = V \times_\Omega \Sigma$ with p-dimensional maximally symmetric fibers. Thus, the metric γ_{AB} on S_0 decomposes as

$$\gamma = \hat{\gamma} + \Omega^2 g_\varepsilon, \qquad \Omega : V \to \mathbb{R} \setminus \{0\}$$

with g_ε the metric of constant curvature ε
- p linearly independent hypersurface-orthogonal Killing vectors $\varsigma_a = \frac{1}{Z} df_a$ of (Σ, g_ε) provide the p non-constant solutions $\{f_a\}$ of the master equation.

Explicit general form of NHGs

- Let the non-fully degenerate MKH generating the sought NHG be of order $m := 2 + p$, with $p \in \{0, 1, \ldots, n-2\}$
- Any cross-section $S_0 \in \mathcal{H}$ is a warped product $S_0 = V \times_\Omega \Sigma$ with p-dimensional maximally symmetric fibers. Thus, the metric γ_{AB} on S_0 decomposes as

$$\gamma = \hat{\gamma} + \Omega^2 g_\varepsilon, \qquad \Omega : V \to \mathbb{R} \setminus \{0\}$$

  with g_ε the metric of constant curvature ε
- p linearly independent hypersurface-orthogonal Killing vectors $\varsigma_a = \frac{1}{Z} df_a$ of (Σ, g_ε) provide the p non-constant solutions $\{f_a\}$ of the master equation.
- Then, $s_A = D_A Z/(2Z)$, and h either vanishes or $h = Z$

Explicit general form of NHGs

- Let the non-fully degenerate MKH generating the sought NHG be of order $m := 2 + p$, with $p \in \{0, 1, \ldots, n-2\}$
- Any cross-section $S_0 \in \mathcal{H}$ is a warped product $S_0 = V \times_\Omega \Sigma$ with p-dimensional maximally symmetric fibers. Thus, the metric γ_{AB} on S_0 decomposes as

$$\gamma = \hat{\gamma} + \Omega^2 g_\varepsilon, \qquad \Omega : V \to \mathbb{R} \setminus \{0\}$$

  with g_ε the metric of constant curvature ε
- p linearly independent hypersurface-orthogonal Killing vectors $\varsigma_a = \frac{1}{Z} df_a$ of (Σ, g_ε) provide the p non-constant solutions $\{f_a\}$ of the master equation.
- Then, $s_A = D_A Z/(2Z)$, and h either vanishes or $h = Z$
- Z has a fully explicit expression in terms of $\{f_a\}$, ε and some free constants

Explicit general form of NHGs

- Let the non-fully degenerate MKH generating the sought NHG be of order $m := 2 + p$, with $p \in \{0, 1, \ldots, n-2\}$
- Any cross-section $S_0 \in \mathcal{H}$ is a warped product $S_0 = V \times_\Omega \Sigma$ with p-dimensional maximally symmetric fibers. Thus, the metric γ_{AB} on S_0 decomposes as

$$\gamma = \hat{\gamma} + \Omega^2 g_\varepsilon, \qquad \Omega : V \to \mathbb{R} \setminus \{0\}$$

  with g_ε the metric of constant curvature ε
- p linearly independent hypersurface-orthogonal Killing vectors $\varsigma_a = \frac{1}{Z} df_a$ of (Σ, g_ε) provide the p non-constant solutions $\{f_a\}$ of the master equation.
- Then, $s_A = D_A Z/(2Z)$, and h either vanishes or $h = Z$
- Z has a fully explicit expression in terms of $\{f_a\}$, ε and some free constants
- A basis of $\mathcal{A}_\mathcal{H}$ is

$$v\partial_v - u\partial_u, \quad \partial_v, \quad f_a \partial_v + \frac{u^2}{2} \Delta f_a \partial_u - u \,\mathrm{grad} f_a$$

Conclusions and outlook

- MKHs are very interesting geometrical objects that can provide useful insights into the classification and properties of black holes and other black objects in higher dimensions

Conclusions and outlook

- MKHs are very interesting geometrical objects that can provide useful insights into the classification and properties of black holes and other black objects in higher dimensions
- Study of non-fully degenerate MKHs leads to a better understanding of NHGs —and permits to classify them

Conclusions and outlook

- MKHs are very interesting geometrical objects that can provide useful insights into the classification and properties of black holes and other black objects in higher dimensions
- Study of non-fully degenerate MKHs leads to a better understanding of NHGs —and permits to classify them
- Characterization of NHGs: those spacetimes with a non-fully degenerate MKH. Thus, one has a criterion to decide if a given spacetime is a NHG or not.

Conclusions and outlook

- MKHs are very interesting geometrical objects that can provide useful insights into the classification and properties of black holes and other black objects in higher dimensions
- Study of non-fully degenerate MKHs leads to a better understanding of NHGs —and permits to classify them
- Characterization of NHGs: those spacetimes with a non-fully degenerate MKH. Thus, one has a criterion to decide if a given spacetime is a NHG or not.
- Improved (global) definition of NHG, including bifurcation surfaces and other fixed-point sets.

Conclusions and outlook

- MKHs are very interesting geometrical objects that can provide useful insights into the classification and properties of black holes and other black objects in higher dimensions
- Study of non-fully degenerate MKHs leads to a better understanding of NHGs —and permits to classify them
- Characterization of NHGs: those spacetimes with a non-fully degenerate MKH. Thus, one has a criterion to decide if a given spacetime is a NHG or not.
- Improved (global) definition of NHG, including bifurcation surfaces and other fixed-point sets.
- Topology of cross sections

Conclusions and outlook

- MKHs are very interesting geometrical objects that can provide useful insights into the classification and properties of black holes and other black objects in higher dimensions
- Study of non-fully degenerate MKHs leads to a better understanding of NHGs —and permits to classify them
- Characterization of NHGs: those spacetimes with a non-fully degenerate MKH. Thus, one has a criterion to decide if a given spacetime is a NHG or not.
- Improved (global) definition of NHG, including bifurcation surfaces and other fixed-point sets.
- Topology of cross sections
- Fully degenerate MKHs are special and must be studied in deep.

Conclusions and outlook

- MKHs are very interesting geometrical objects that can provide useful insights into the classification and properties of black holes and other black objects in higher dimensions
- Study of non-fully degenerate MKHs leads to a better understanding of NHGs —and permits to classify them
- Characterization of NHGs: those spacetimes with a non-fully degenerate MKH. Thus, one has a criterion to decide if a given spacetime is a NHG or not.
- Improved (global) definition of NHG, including bifurcation surfaces and other fixed-point sets.
- Topology of cross sections
- Fully degenerate MKHs are special and must be studied in deep.

- For maximal order, plane waves arise, thus they are related to Penrose limits. But little is known hitherto for smaller orders

Thank you for your attention!

ご清聴ありがとうございました

References

- Multiple Killing Horizons, Mars M., Paetz, T.-T, and Senovilla J.M.M. 2018 *Class. Quantum Grav.* **35** 155015.
- Multiple Killing Horizons and Near Horizon Geometries, Mars M., Paetz, T.-T, and Senovilla J.M.M. 2018 arXiv:1807.02679
- Multiple Killing Horizons in Λ-vacuum spacetimes: the initial value formulation, Mars M., Paetz, T.-T, and Senovilla J.M.M. 2018

Session S2P1 14:45–15:45

[Chair: Tetsuya Shiromizu]

Hayato Motohashi

Yukawa Institute for Theoretical Physics, Kyoto University

“Shape dependence of spontaneous scalarization”

(10+5 min.)

[JGRG28 (2018) 110611]

Shape dependence of spontaneous scalarization

Hayato Motohashi
Center for Gravitational Physics
Yukawa Institute for Theoretical Physics

HM & Mukohyama, arXiv:1810.12691

2018.11.05 – 09 JGRG28 at Rikkyo University

YITP YUKAWA INSTITUTE FOR THEORETICAL PHYSICS | CGP Center for Gravitational Physics Yukawa Institute for Theoretical Physics | Gravitational Wave Physics and Astronomy Genesis | 科研費 KAKENHI

Spontaneous scalarization (SS)

Damour, Esposito-Farese (1993)

$$S = \int d^4x\sqrt{-g}\left(\frac{R}{16\pi G} - \frac{1}{2}\partial_\mu\phi\partial^\mu\phi\right) + S_m(\tilde{g}_{\mu\nu}, \psi)$$

$$\tilde{g}_{\mu\nu} = \Omega^2(\phi)g_{\mu\nu}$$ Nonminimal coupling to matter

---

cf. Many variations have been considered recently, including

- Massive scalar field   Chen et al. 1508.01384, Ramazanolu, Pretorius, 1601.07475
- Coupling via disformally transformed metric   Minamitsuji, Silva, 1604.07742
- Coupling to Gauss-Bonnet term   Doneva, Yazadjiev, 1711.01187, Silva et al. 1711.02080, Antoniou et al. 1711.03390
- Coupling to Chern-Simons term   Brihaye et al. 1810.09560
- Coupling to Maxwell invariant   Herdeiro et al. 1806.05190

Spontaneous scalarization (SS)

Damour, Esposito-Farese (1993)

$$S = \int d^4x\sqrt{-g}\left(\frac{R}{16\pi G} - \frac{1}{2}\partial_\mu\phi\partial^\mu\phi\right) + S_m(\tilde{g}_{\mu\nu}, \psi)$$

$\tilde{g}_{\mu\nu} = \Omega^2(\phi)g_{\mu\nu}$ Nonminimal coupling to matter

Background

$$G^{\mu\nu} = 8\pi G\left(\Omega^2 T^{\mu\nu} + T^{(\phi)\mu\nu}\right)$$
$$\Box\phi = V_{,\phi} - \Omega^3\Omega_{,\phi}\tilde{T}$$

Ansatz: $\Omega(\phi_0) = 1$ and $\Omega_{,\phi}(\phi_0) = 0$

Solution: GR metric & $\phi = \phi_0 = \text{const.}$

Spontaneous scalarization (SS)

Linear perturbation $\phi = \phi_0 + \delta\phi$

- Einstein eq is unchanged from GR at linear order
- Klein-Gordon eq is given by

$$\Box\delta\phi = m_{\text{eff}}^2\delta\phi$$

Effective mass

$$m_{\text{eff}}^2(\phi) \equiv -\Omega_{,\phi\phi}(\phi_0)T \equiv -\frac{\hat{\beta}_0}{3M_{Pl}^2}T \sim \frac{\hat{\beta}_0}{3M_{Pl}^2}\rho$$

Tachyonic instability of $\delta\phi$

$\Leftrightarrow$ SS: local modification of gravity

Stability analysis

$\Longrightarrow$ Schrödinger problem

Schrödinger problem

1D (3D Planar sym.): $\psi = \psi(z)$

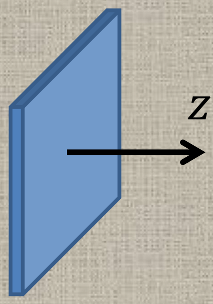

$$\left(-\frac{d^2}{dz^2} + U\right)\psi = E\psi$$

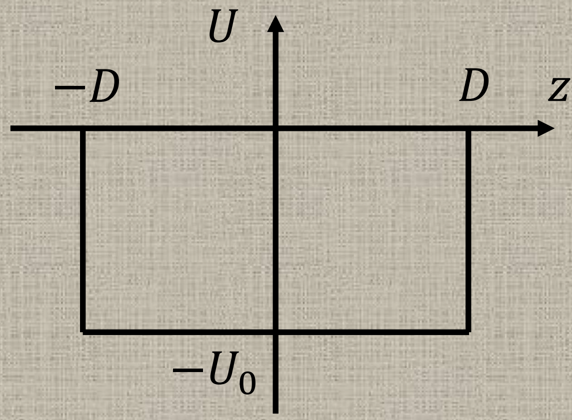

Solution: $\psi(z) \sim \sin + \cos$

Odd Even

Critical value $U_{0,c} = 0$

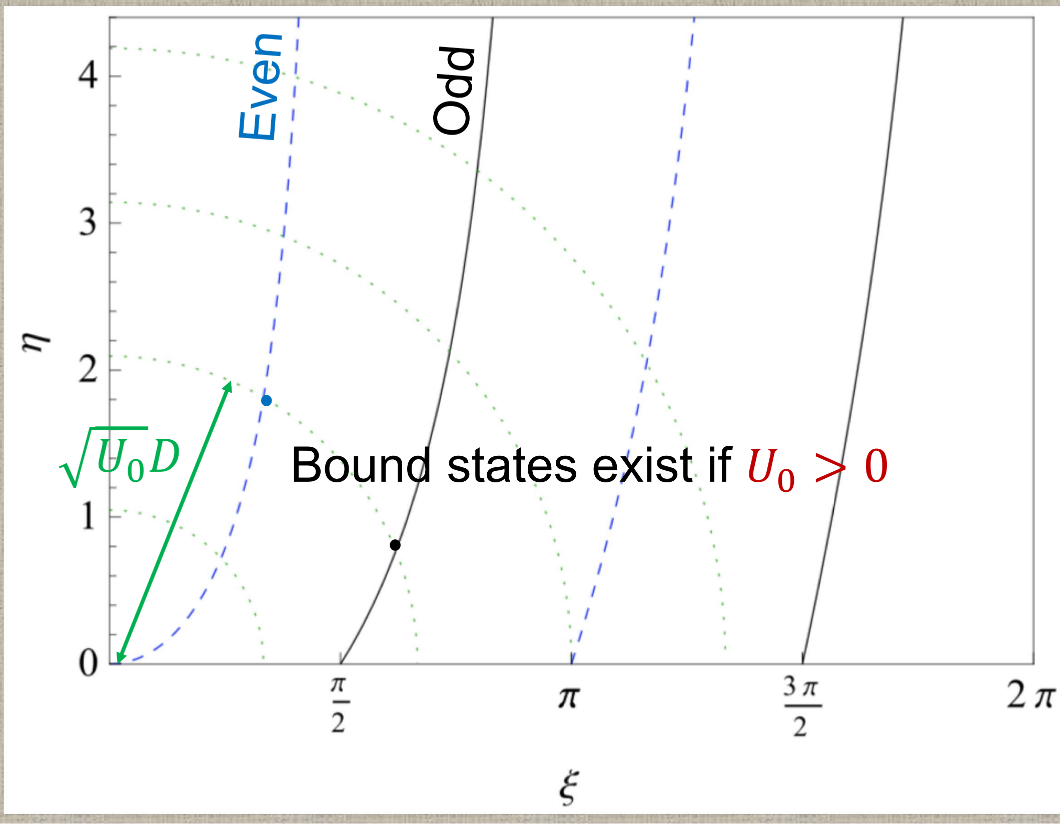

Schrödinger problem

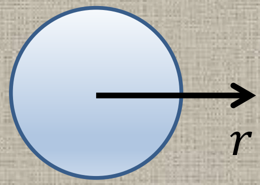

Spherically sym:

$$\Psi = \sum_{\ell,m} \frac{\psi_\ell(r)}{r} Y_{\ell m}(\theta, \varphi)$$

$\ell = 0$ mode

$$\left(-\frac{d^2}{dr^2} + U\right)\psi_0 = E\psi_0$$

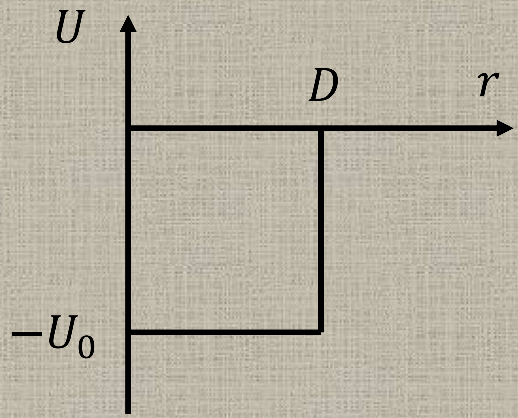

Solution: $\psi_0(r) \sim \sin + \cancel{\cos}$
Odd ~~Even~~

Regularity of $\Psi(0)$

$\Longrightarrow \psi_0(0) = 0$: Odd-parity solution only

Critical value $U_{0,c} = \pi^2/(4D^2)$

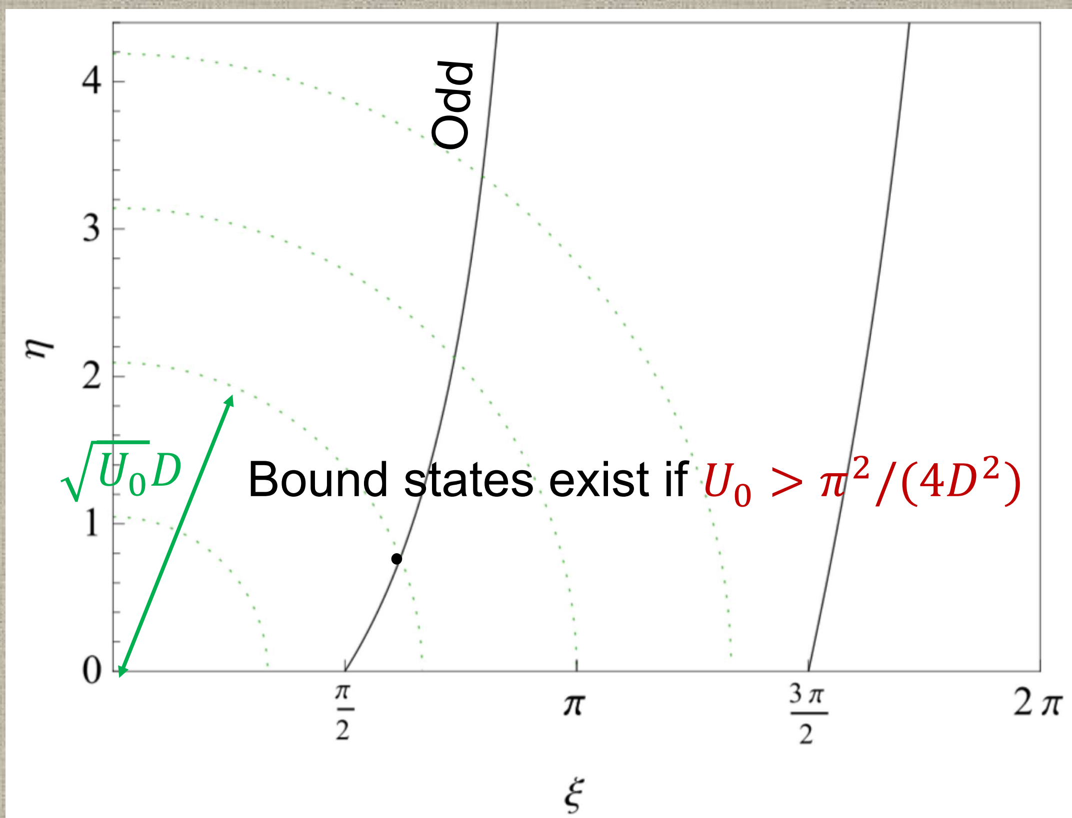

Critical values

	$U_{0,c}$	
Spherically sym.	$\frac{\pi^2}{4D^2}$	
Planar sym.	0	

Spontaneous scalarization (SS)

(1) Spherically sym. [Well-studied] Harada, gr-qc/9706014

SS occurs when $\hat{\beta}_0 < \hat{\beta}_{0,c} < 0$

(⟺ Tachyon mass is sufficiently large)

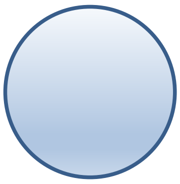

To be a realistic model, it is important to study other configuration. As an extreme case we consider…

(2) Planar sym. [New] HM, Mukohyama, 1810.12691

Using the analogy, we expect that $\hat{\beta}_{0,c} = 0$

Sensitive shape dependence of SS

Spherically symmetric $\rho(r)$

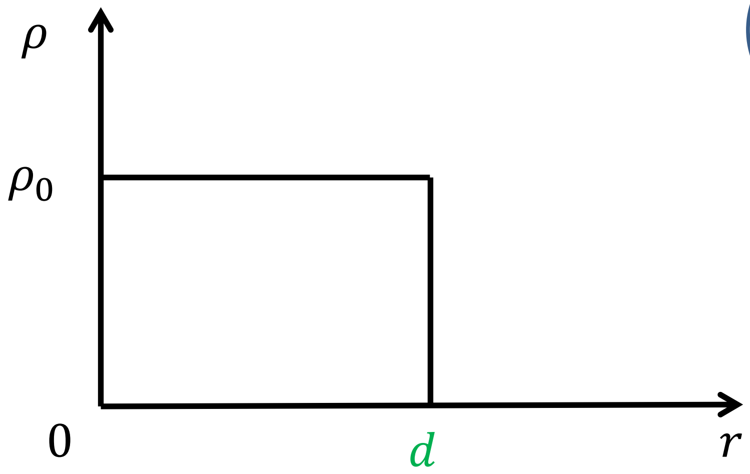

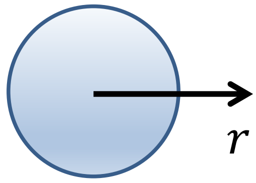

Metric = Internal & external Schwarzschild solution

$$ds^2 = -A(r)dt^2 + \frac{dr^2}{B(r)} + r^2 d\Omega^2$$

Pressure $P(r)$ = Exact solution for TOV equation

Spherically symmetric $\rho(r)$

Perturbation $\phi = \phi_0 + \delta\phi$

$$\Box\delta\phi \simeq \frac{\hat{\beta}_0 \rho}{3M_{Pl}^2}\delta\phi$$

- Spherical harmonics decomposition
- Focus on $\ell = 0$ mode
- Fourier decomposition

$$\delta\phi \sim \frac{e^{-i\omega\hat{t}}}{r}\psi(\hat{r}_*)$$

$dr/dr_* = \sqrt{AB}$
$\hat{t}, \hat{r}_*, \hat{d}$: dimensionless variables normalized by Jeans scale $L \equiv (8\pi G\rho_0/3)^{-1/2}$

EOM: Schrödinger eq

$$\left(-\frac{d^2}{d\hat{r}_*^2} + U(\hat{r}_*)\right)\psi = \omega^2\psi$$

Effective potential

Large $-\hat{\beta}_0$: Deep well
Large $\hat{d}$: Wide well

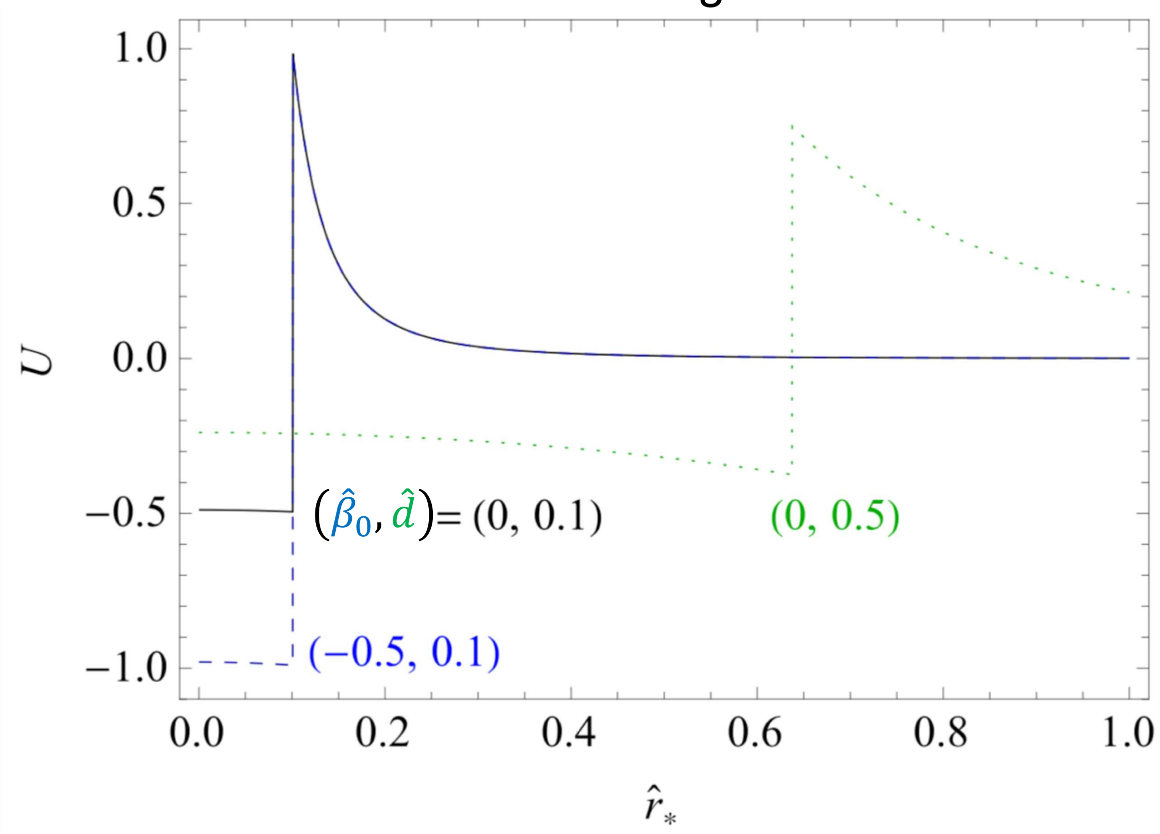

Spherically symmetric $\rho(r)$

$$\delta\phi \sim \frac{e^{-i\omega\hat{t}}}{r}\psi(\hat{r}_*)$$
$$\left(-\frac{d^2}{d\hat{r}_*^2} + U(\hat{r}_*)\right)\psi = \omega^2\psi$$

Boundary condition $\psi(0) = 0$ (Regularity of $\delta\phi(0)$)

SS
$\Leftrightarrow$ $\delta\phi$: Tachyonic instability
$\Leftrightarrow$ ψ: $\exists$ Bound state with $\omega^2 < 0$

Critical value $-\hat{\beta}_{0,c} \approx 2\hat{d}^{-2}$

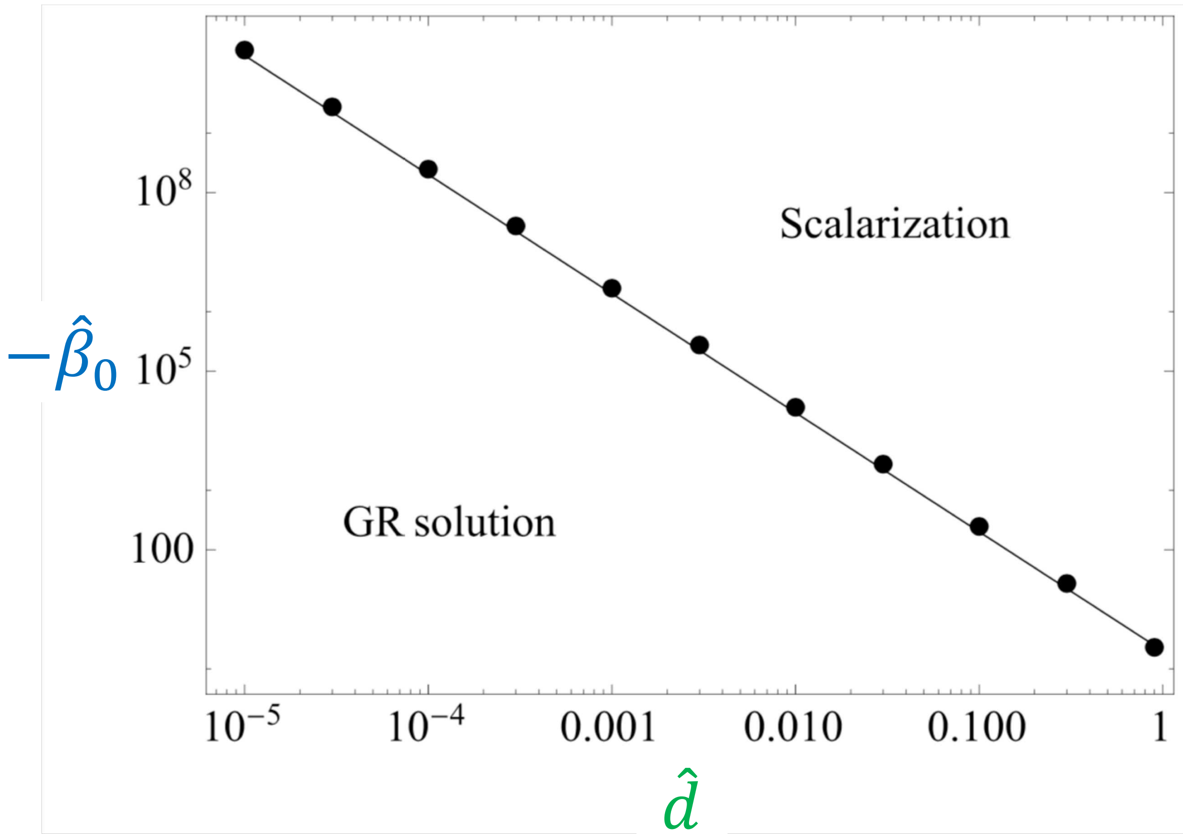

Critical values

	$U_{0,c}$	$-\hat{\beta}_{0,c}$
Spherically sym.	$\frac{\pi^2}{4D^2}$	$\frac{2}{\hat{d}^2}$
Planar sym.	0	

Planar symmetric $\rho(z)$

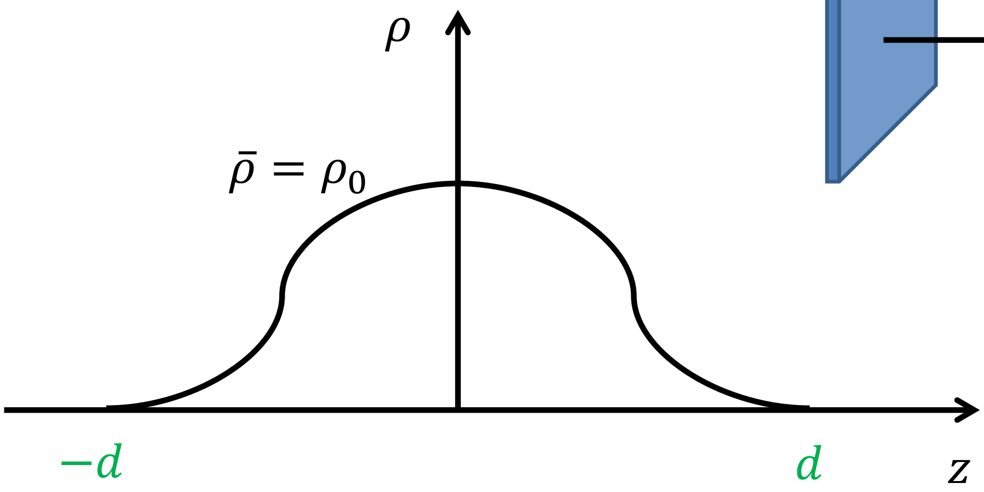

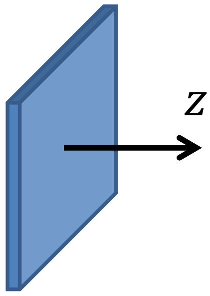

Consider general planar sym. $\rho(z)$ and pressure satisfying a kind of energy condition.

Metric

Bonjour, Charmousis, Gregory, gr-qc/9902081

$$ds^2 = -a^2(z)dt^2 + e^{2Ht}a^2(z)(dx^2 + dy^2) + dz^2$$

Follow the process similar to the spherical case.

Effective potential

Large $-\hat{\beta}_0$: Deep well

Large $\hat{d}$: Wide well

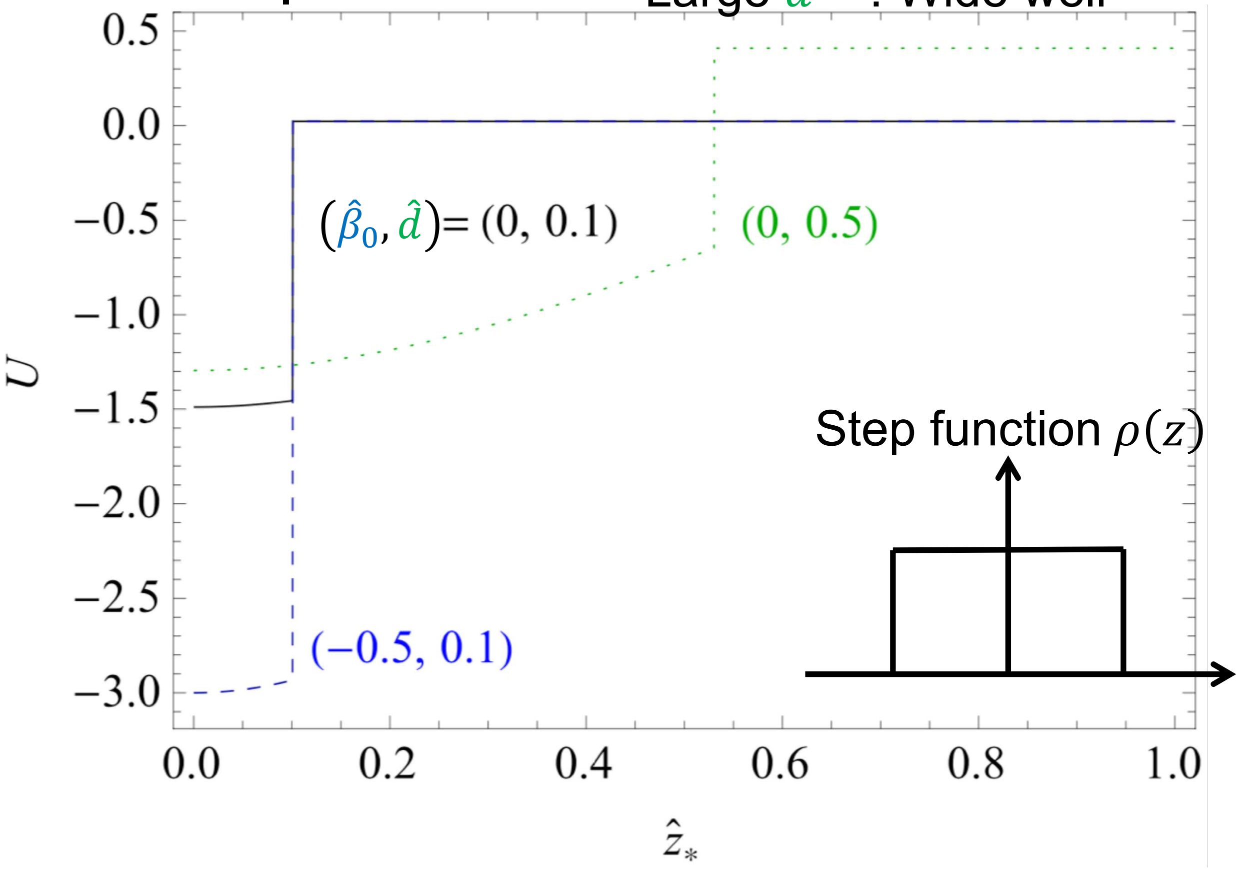

Critical value $\hat{\beta}_{0,c} = 0$

- ✓ Analytically proved for general $\rho(z)$
- ✓ Numerically confirmed for step function $\rho(z)$

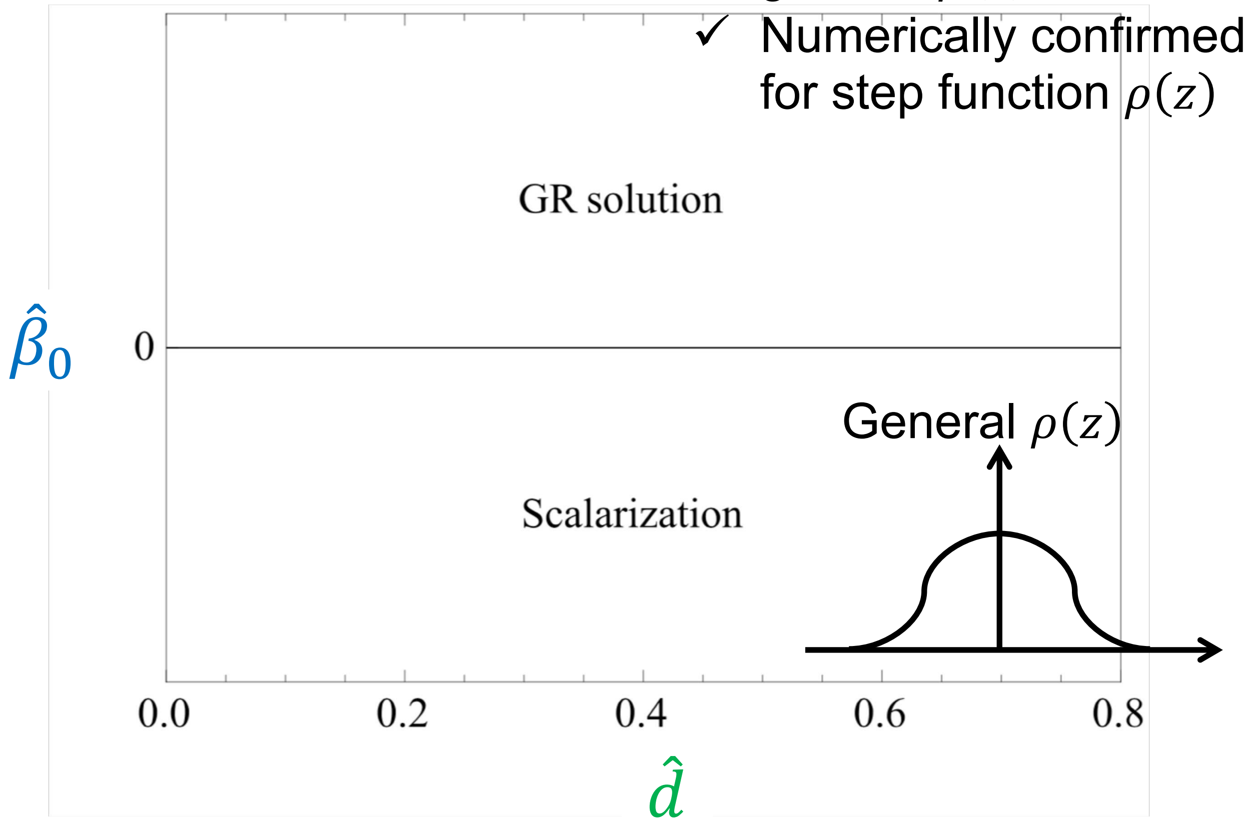

Critical values

	$U_{0,c}$	$-\hat{\beta}_{0,c}$
Spherically sym.	$\frac{\pi^2}{4D^2}$	$\frac{2}{\hat{d}^2}$
Planar sym.	0	0

Summary

Spherically sym.

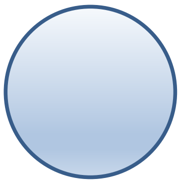

Planar sym.

SS occurs much more easily.

- Possible application: Constraints from planar sym. objects such as domain wall, accretion disk, galactic disk etc.
- Similar analysis for other configurations.

Masato Minamitsuji
Center for Astrophysics and Gravitation (CENTRA), University of Lisbon

“Scalarized Black Holes in the presence of the Coupling to Gauss-Bonnet Gravity”

(10+5 min.)

[JGRG28 (2018) 110612]

centra

centre for astrophysics and gravitation

FCT

Fundação para a Ciência e a Tecnologia

MINISTÉRIO DA CIÊNCIA, TECNOLOGIA E ENSINO SUPERIOR

Scalarized Black Holes in the Presence of the Coupling to Gauss-Bonnet Gravity

Masato Minamitsuji

with Taishi Ikeda, Work in progress

Scalar Fields

- appear ubiquitously in theoretical physics beyond general relativity (GR) and particle physics.

- provide the robust mechanisms for inflaton and dark energy, which have been tested in observations and experiments.

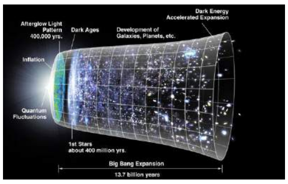

- may ``scalarize'' compact objects in strong gravity regimes, which will be a target for the future GW observations.

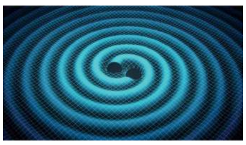

Spontaneous Scalarization

$$S=\frac{1}{2\kappa^2}\int d^4x\sqrt{-g}\left(R-\frac{1}{2}g^{\mu\nu}\partial_\mu\phi\partial_\nu\phi+\xi(\phi)R_{\rm GB}\right)+\int d^4x\sqrt{-\tilde{g}}\mathcal{L}_m\left[\tilde{g}_{\mu\nu},\Psi\right]$$

$$R_{\rm GB}:=R^2-4R^{\alpha\beta}R_{\alpha\beta}+R^{\alpha\beta\mu\nu}R_{\alpha\beta\mu\nu}\qquad \tilde{g}_{\mu\nu}=e^{2A(\phi)}g_{\mu\nu}$$

Scalar EOM: $$\Box\phi+\underbrace{\xi^{(1)}(\phi)R_{\rm GB}}_{\text{GB coupling}}+\frac{\kappa^2}{2}\underbrace{A^{(1)}(\phi)T^{\mu}{}_{\mu}}_{\text{Matter coupling}}=0$$

- GR solution at $\phi=\phi_0=const \Longleftarrow \xi^{(1)}(\phi_0)=A^{(1)}(\phi_0)=0$
- GR solution $\Longrightarrow$ solution with $\phi\neq const.$

i) $\xi(\phi)=0$: Inside a star $\quad\beta\le -4.35$ for $A(\phi)=\beta\phi^2$ Damour and Esposio-Farese (93, 96)

ii) $L_m=0$: Around a vacuum BH $\quad\xi(\phi)\propto 1-e^{-c\phi^2}$ Doneva and Yazadjiev (17)

$\xi(\phi)\propto\phi^2$ Silva, Sakstein, Gualtieri, Sotiriou, and Berti (17)

Instability of a Schwarzschild Solution

$$\xi(\phi)=\frac{\eta}{8}\phi^2+\sum_{i\ge 3}c_i\phi^i$$: Schwarzschild solution with $\phi=0$

- Perturbation $\delta\phi$: $$\Big(\Box_{\rm Sch}+\underbrace{\frac{\eta}{4}R_{\rm GB}^{\rm (Sch)}}_{>0\ (\eta>0)}\Big)\delta\phi+\mathcal{O}(\delta\phi^2)=0$$ $\quad R_{\rm GB}^{\rm (Sch)}=48M^2/r^6$

M: BH mass

$$\delta\phi(x^\mu)=\sum_{\ell,m}e^{-i\omega_{\ell m}t}\frac{\sigma_{\ell m}(r)}{r}Y_{\ell m}(\Omega)\qquad \left[-\frac{d^2}{dr_*^2}+V_{\rm eff}(r)\right]\sigma_{\ell m}(r)=\omega_{\ell m}^2\sigma_{\ell m}(r)$$

$$V_{\rm eff}=(r-2M)\left[\frac{2M}{r^7}(r^3-6M\eta)+\frac{\ell(\ell+1)}{r^3}\right]$$

$V_{\rm eff}$ for the radial mode ($l=0$) contains a negative region for $\eta/M^2>\frac{4}{3}$

$\Longrightarrow$ Gravitational spontaneous scalarization

Scalarized BHs- Test Field Analysis

- Static scalar field $\phi = \psi(r)$ on a fixed Schwarzschild BG

$$\psi'' + \frac{2(r-M)}{r(r-2M)}\psi' + \frac{48M^2}{r^5(r-2M)}\xi^{(1)}(\psi) = 0$$

$\psi(r \to 2M) = \psi_0 > 0, \ \ \psi(r \to \infty) = \psi_\infty = 0 \Longrightarrow \xi^{(1)}(\psi_0) > 0$

- Scalar charge: $\psi = \frac{Q}{r} + O\left(\frac{1}{r^2}\right)$
- Perturbation about: $\phi = \psi(r) + \delta\phi$:

$$\left(\Box_{\rm Sch} + \xi^{(2)}(\psi) R_{\rm GB}^{(\rm Sch)}\right)\delta\phi = 0$$

$$\Longrightarrow V_{\rm eff}(r) = (r-2M)\left[\frac{2M}{r^7}\left(r^3 - 24M\xi^{(2)}(\psi)\right) + \frac{\ell(\ell+1)}{r^3}\right]$$

1) $\xi(\phi) = \frac{\eta}{8}\phi^2$

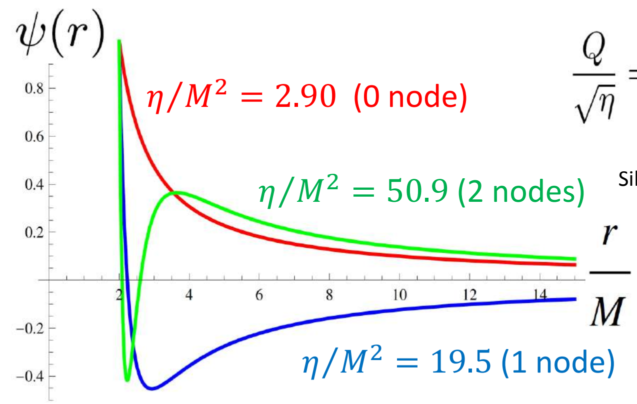

$$\frac{Q}{\sqrt{\eta}} = 0.525\psi_0, -0.250\psi_0, 0.174\psi_0$$

0 node 1 node 2 nodes

Silva, Sakstein, Gualtieri, Sotiriou, and Berti (17)

$\left(\Box_{\rm Sch} + \frac{\eta}{4}R_{\rm GB}^{(\rm Sch)}\right)\delta\phi = 0 \Longrightarrow$ All scalarized solutions $(\eta/M^2 > \frac{4}{3})$ are unstable.

Full analysis Blzquez-Salcedo, Doneva, Kunz, and Yazadjiev (18)

$\xi = \frac{\eta}{8}\phi^2$: All scalarized BH solutions are unstable against radial perturbation.

$\xi = \frac{\eta}{48}\left(1 - e^{-6\phi^2}\right)$: 0-node solutions are radially stable.

Importance of higher order terms in $\xi(\phi)$ in obtaining stable scalarized BHs

(2) $\xi = \frac{\eta}{8}\phi^2(1+\alpha\phi^2)$ $\quad \psi_0 > 0, \psi_\infty = 0 \Longrightarrow \alpha\psi_0^2 \geq -\frac{1}{2}$

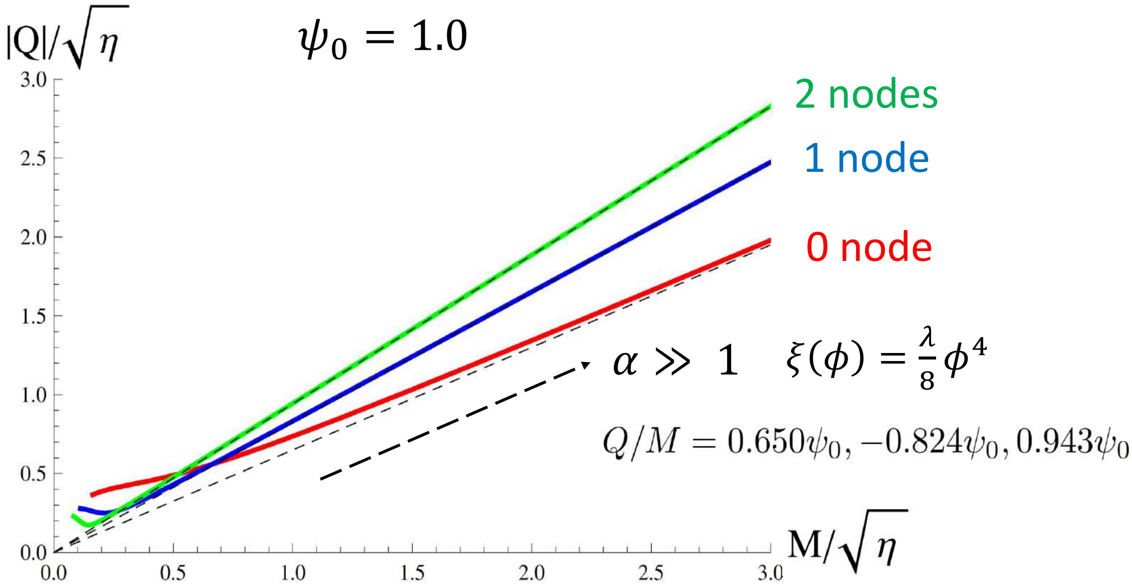

The radial perturbation ($l = 0$)

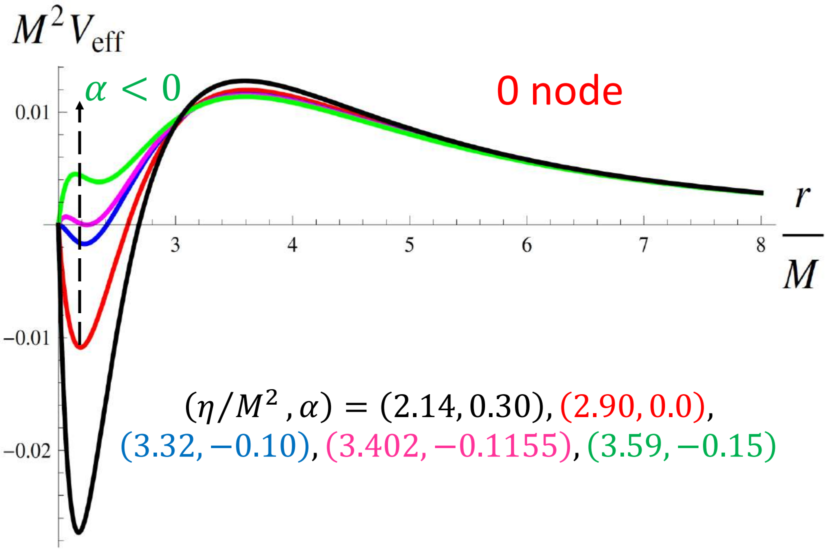

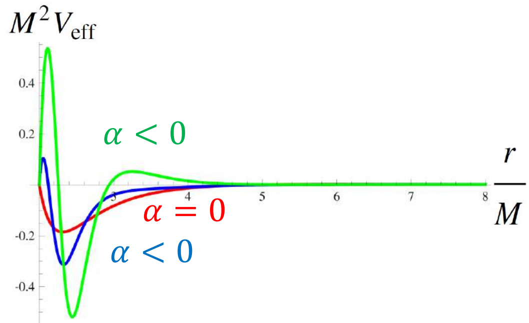

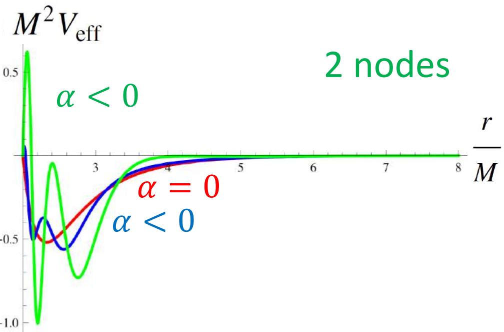

No negative region mode for 0 -node solution of $-1/2 < \alpha\psi_0^2 < -0.1155$

Scalarized BHs- Full Analysis

- Static and spherically symmetric spacetime and scalar field

$$ds^2 = -A(r)dt^2 + \frac{dr^2}{B(r)} + r^2\left(d\theta^2 + \sin^2\theta d\varphi^2\right) \qquad \phi = \psi(r)$$

- Near horizon $r \geq r_h$: $\psi = \psi_0 - \left(\frac{r_h^2 - \sqrt{r_h^4 - 96\xi^{(1)}(\psi_0)^2}}{4r_h\xi^{(1)}(\psi_0)}\right)(r - r_h) + \mathcal{O}\left((r - r_h)^2\right),$

$$r_h^4 > 96\,\xi^{(1)}(\psi_0)^2$$

- Asymptotic behavior at $r \to \infty$, ADM mass M, and Scalar charge Q

$$B = 1 - \frac{2M}{r} + \frac{Q^2}{4r^2} + \frac{MQ^2}{4r^3} + \frac{MQ}{3r^4}\left(MQ + 24\xi^{(1)}(\psi_\infty)\right) + \mathcal{O}\left(\frac{1}{r^5}\right),$$

$$\psi = \psi_\infty + \frac{Q}{r} + \frac{MQ}{r^2} + \frac{1}{r^3}\left(\frac{4M^2Q}{3} - \frac{Q^3}{24}\right) + \frac{M}{6r^4}\left(12M^2Q - Q^3 - 24M\xi^{(1)}(\psi_\infty)\right) + \mathcal{O}\left(\frac{1}{r^5}\right)$$

For $\xi(-\phi) = \xi(\phi)$ and $\psi_0 > 0,\ \psi_\infty = 0 \Longrightarrow \xi^{(1)}(\psi_0) > 0$

(1) $\xi = \frac{\eta}{8}\phi^2$: $r_h^4 > 6\eta^2\psi_0^2$

Silva, Sakstein, Gualtieri, Sotiriou, and Berti (17)

Blzquez-Salcedo, Doneva, Kunz, and Yazadjiev (18)

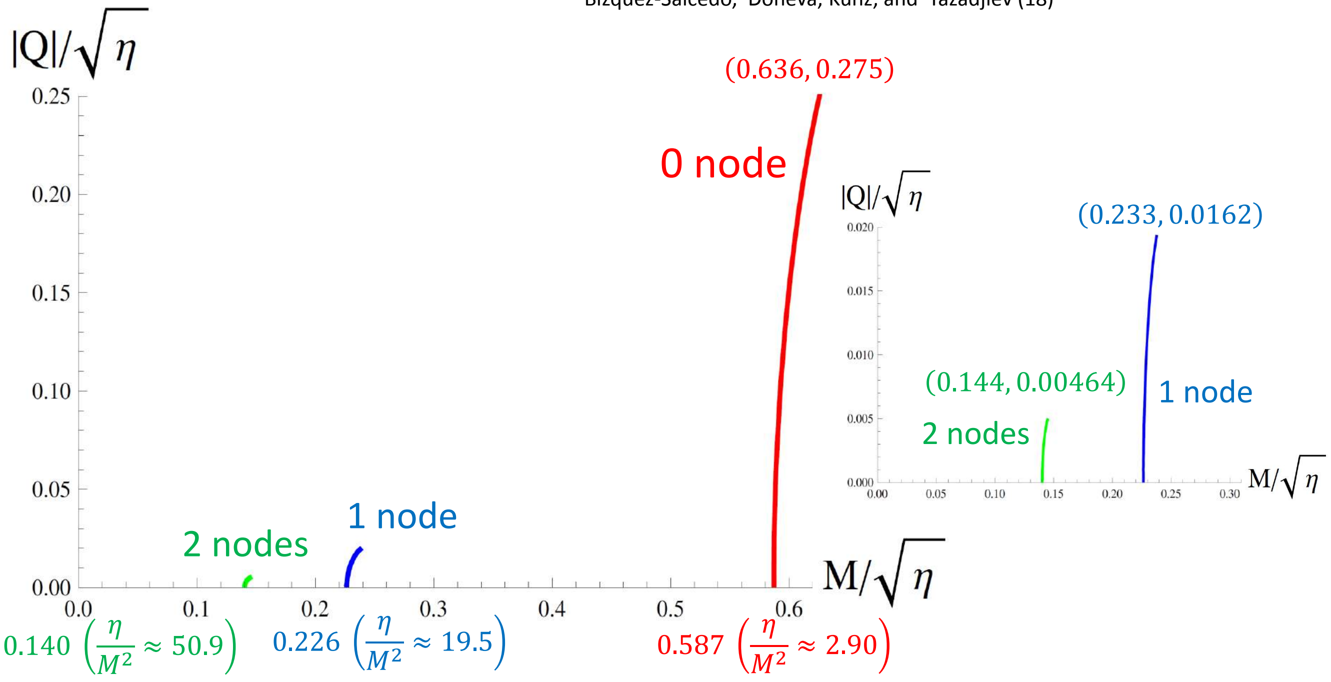

(2) $\xi = \frac{\eta}{8}\phi^2(1+\alpha\phi^2)$: $r_h^4 > 6\eta^2\psi_0^2(1+2\alpha\psi_0^2)^2$, $\alpha\psi_0^2 > -\frac{1}{2}$

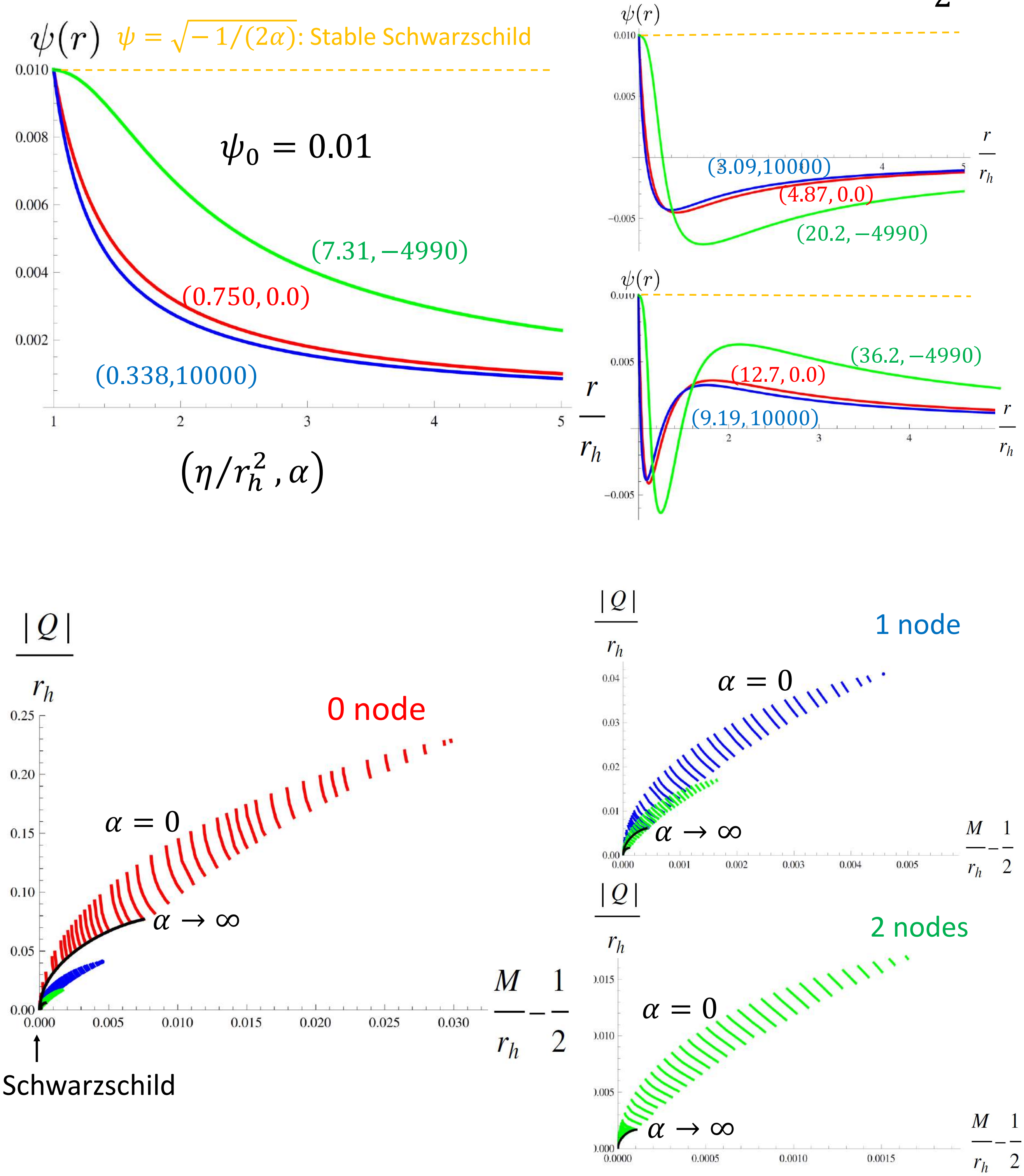

Radial perturbation

$$\tilde{A} = A(r) + \varepsilon a(t,r), \qquad \tilde{B} = B(r) + \varepsilon b(t,r), \qquad \phi = \psi(r) + \varepsilon \Phi(t,r) \qquad \varepsilon \ll 1$$

Master equation: $-\rho_1 \ddot{\Phi} + \rho_2 \Phi'' + \rho_3 \Phi' + \rho_4 \Phi = 0$

Effective Potential $\quad \Phi = e^{-i\omega t}\Phi_\omega(r) \quad \Phi_\omega = C(r)\Psi_\omega(r)$

$$\left[-\frac{d^2}{dr_*^2} + U_{\rm eff}(r)\right]\Psi_\omega(r) = \frac{\rho_1}{\rho_2}(AB)\omega^2\Psi_\omega(r)$$

$$U_{\rm eff}(r) = -AB\left\{\frac{1}{4}(\ln(AB))'' + \frac{1}{16}\left[(\ln(AB))'\right]^2 - \frac{1}{2}\left(\frac{\rho_3}{\rho_2}\right)' - \frac{\rho_3^2}{4\rho_2^2} + \frac{\rho_4}{\rho_2}\right\}$$

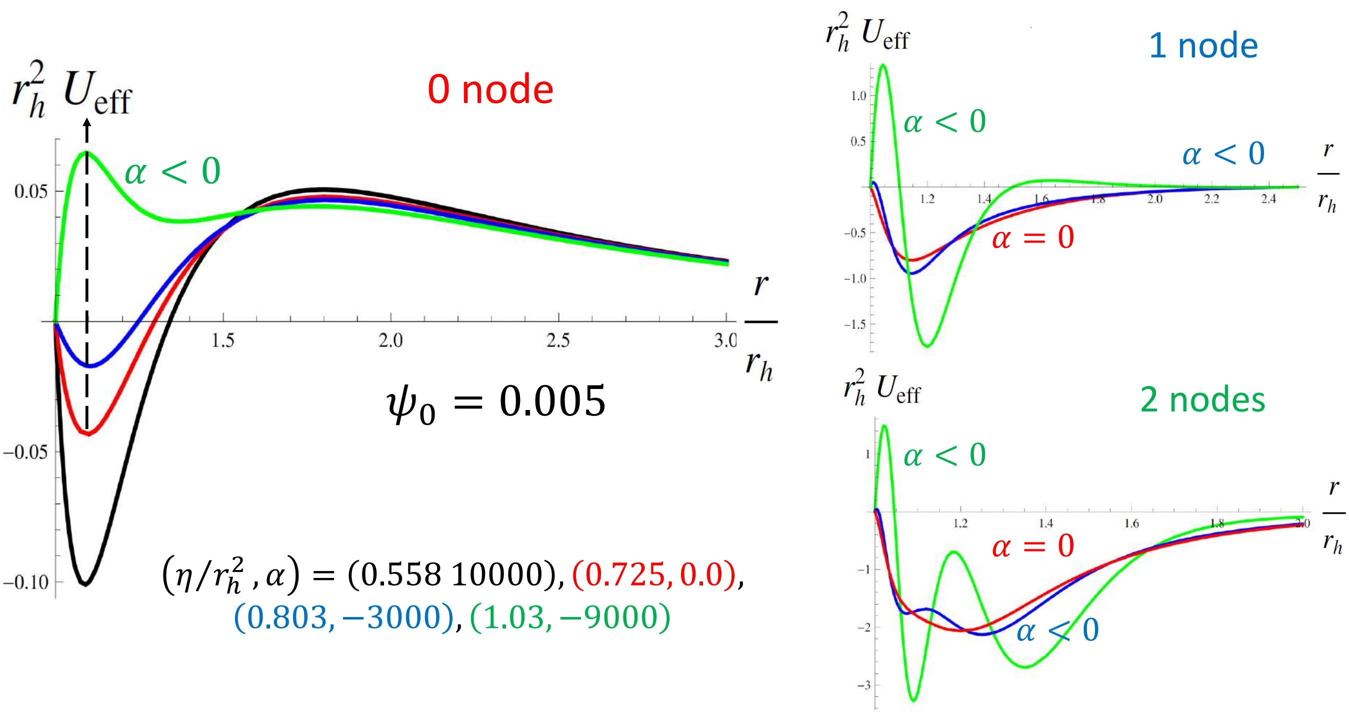

No pure imaginary mode for 0 node scalarized BH solutions of $\alpha < 0$

Summary

- We have investigated scalarized BH solutions and their radial perturbation in the presence of higher order power of the GB coupling function.

- Test field analysis on a fixed Schwarschild background povides qualitatively the same results as full analysis, due to the bound $r_h^4 > 96\,\xi^{(1)}(\psi_0)^2$.

- For $\alpha < 0$, the Schwarzschild solution with $\phi = \pm\sqrt{-1/(2\alpha)}$, and the scalarized BHs with 0 node seem to be stable against the radial perturbation.

Thank you.

Masato Nozawa
Yukawa Institute for Theoretical Physics, Kyoto University

"On the uniqueness theorems of static black holes"

(10+5 min.)

[JGRG28 (2018) 110614]

On the uniqueness theorems of static black holes

Masato Nozawa

YUKAWA INSTITUTE FOR THEORETICAL PHYSICS

Ref: CQG 35 175009 (2018) [arXiv:1805.11385]
w/ T.Shiromizu, K.Izumi, S.Yamada

No hair conjecture

black hole formation

⇒ higher multipole moments (l≧2) carried by gravitational waves

⇒ stationary states characterized by mass (l=0) & angular momentum (l=1)

- *no hair conjecture*   *Ruffini & Wheeler 1971*

  stationary black holes admit only small set of parameters

- *uniqueness theorems*   *Israel 1967, Carter 1972, Robinson 1975, Mazur 1982....*

  stationary & vacuum black holes are exhausted by Kerr family

Static uniqueness

Theorem:

Consider a static vacuum black hole in the asymptotically flat spacetimes. If the horizon is nondegenerate and connected, the spacetime is isometric to the Schwarzschild solution.

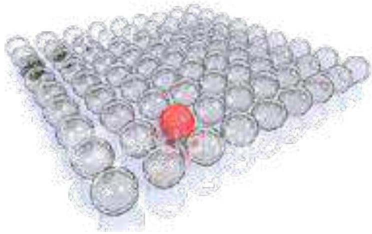

- *Israel 1967*

  1 dimensional divergence equation (assumption: S^2 horizon)

- *Robinson 1977*

  3 dimensional divergence equation

- *Bunting & Maswood-ul-Alam 1987*

  positive mass theorem

Robinson's proof

Robinson's idea: 2-parameter divergence equations *Robinson 1977*

$$\mathrm{div}J = |\text{deviation from spherical symmetry}|^2 \geq 0$$

Integrate over hypersurface Σ and use Stokes' theorem

$$0= \int_{S^\infty} J_i \mathrm{d}S^i - \int_B J_i \mathrm{d}S^i = \int_\Sigma \mathrm{div}J \mathrm{d}\Sigma \geq 0$$

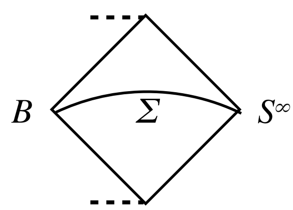

S^∞: surface at infinity, B: horizon cross-section

By adjusting 2 parameters in J^i , one can set the surface integral to vanish

$\Rightarrow$ div$J$=0

$\Rightarrow$ deviation from spherical symmetry vanishes

$\Rightarrow$ spherical symmetry (Schwarzschild)

Robinson's current

"Miraculous identity"

(no systematic derivation available)

$$\boxed{D_iJ^i = \frac{1}{4}\rho^2 f_1^R(V)V^4 C_{ijk}C^{ijk} + \frac{3f_1^R(V)}{\rho^2}\left|\frac{D_i\rho}{\rho} - \frac{4V}{1-V^2}D_iV\right|^2 ,}$$

$$J^i = -2f_1^R(V)\frac{D^i\rho}{\rho^3} + \frac{f_2^R(V)}{\rho^2}D^iV$$

$$f_1^R(V) = \frac{c_1V^2+c_2}{V(1-V^2)^3}\,, \qquad f_2^R(V) = -\frac{2c_1}{(1-V^2)^3} + \frac{6(c_1V^2+c_2)}{(1-V^2)^4}\,.$$

$C_{ijk} = 2D_{[i}({}^{(3)}R_{j]k} - ({}^{(3)}R/4)g_{j]k})$:Cotton tensor

Motivations

Extend Robinson's proof into several directions

- **How to derive equations of divergence type** (div$J$=$S\geqq 0$)**?**

  unknown for nonvacuum/non-asymptotically flat

  what is the physical/geometric meaning of the current?

- **Possible to prove w/o using Smarr's formula?**

  $M = \frac{\kappa}{4\pi}A_H$ $\quad$ M: ADM mass, A_H: horizon area, κ: surface gravity

  no analogous formula in *asymptotically AdS* case

- **Possible to extend into nonvacuum/ higher dimensions?**

  Robinson's equation involves Cotton tensor (intrinsic to 3 spatial dim)

  proofs thus far utilized nonlinear sigma-model property

- **Related to the proof based on the positive mass theorem?**

Vacuum static spacetime

static spacetime (invariant under $t \to -t$)

$$ds^2 = -V^2(x)dt^2 + g_{ij}(x)dx^i dx^j\,,$$

g_{ij} : metric of a spatial slice Σ={t=constant}

- event horizon at V=0 where static Killing vector $\partial/\partial t$ becomes null
- vacuum Einstein's equations $R_{\mu\nu} = 0$ decompose into

$$\boxed{D^2V = 0\,, \quad {}^{(3)}R_{ij} = \frac{1}{V}D_iD_jV\,,} \longrightarrow$$

our aim: uniqueness of solutions to the boundary value problem

D_i :covariant derivative for g_{ij}

notation: $D^2V = D_iD^iV$

$(DV)^2 = |D_iV|^2 = D_iVD^iV\,.$

Local foliations

Locally foliate Σ by S_V={V= constant} as $\Sigma = \mathbb{R}\times\mathcal{S}_V$ $\quad$ V ~radial coordinate

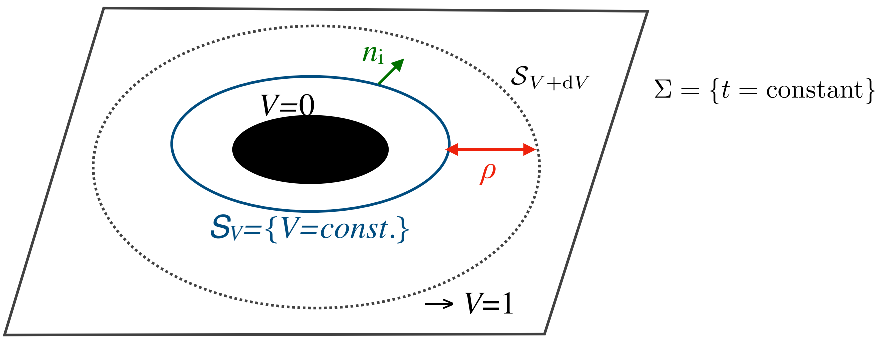

$n_i = \rho D_iV\,,$: unit normal to S_V

$\rho \equiv (D^iVD_iV)^{-1/2}$: lapse function

$$g_{ij}dx^idx^j = \rho^2 dV^2 + h_{ij}dx^idx^j$$

$h_{ij} = g_{ij} - n_in_j$: 1st fundamental form on S_V

$k_{ij} = h_i{}^kD_kn_j$: 2nd fundamental form on S_V in Σ

$k = h^{ij}k_{ij}$: mean curvature $\quad \sigma_{ij} = k_{ij} - \frac{1}{2}kh_{ij}$: shear

vacuum Einstein's eqs:

$$n^iD_i\rho = \rho k\,,$$

$${}^{(2)}R = \frac{2k}{V\rho} + k^2 - k_{ij}k^{ij}\,.$$

Boundary conditions

(1) Infinity : asymptotically flat

$$V \sim 1 - \frac{M}{r}\,, \qquad g_{ij} \sim \left(1 + \frac{2M}{r}\right)\delta_{ij}\,,$$ M>0: ADM mass

$$\longrightarrow \quad k \sim \frac{2}{r}\,, \qquad \rho \sim \frac{r^2}{M}\,,$$

(2) Horizon : regular surface

$$\mathcal{K} \equiv R_{\mu\nu\rho\sigma}R^{\mu\nu\rho\sigma} = \frac{8}{V^2\rho^2}\left[k_{ij}k^{ij} + k^2 + \frac{2}{\rho^2}(\mathcal{D}\rho)^2\right]\,,$$

$\mathcal{K}$ must be finite at the horizon (V=0) $\quad \mathcal{D}_i = h_i{}^j D_j$:covariant derivative for h_{ij}

$$\begin{cases} k_{ij}|_{V=0} = 0\,, & \text{: horizon is totally geodesic} \\ \mathcal{D}_i\rho|_{V=0} = 0\,. & \longrightarrow \; 0 < \rho_0 \equiv \rho|_{V=0} < \infty \quad \text{(0th law of thermodynamics)} \end{cases}$$

ρ_0: inverse of surface gravity

Deviation from spherical symmetry

deviation from spherical symmetry is encoded in

Nozawa-Shiromizu-Izumi-Yamada 2018

$$H_{ij} \equiv D_iD_jV - \frac{2V}{\rho^2(1-V^2)}g_{ij} + \frac{6V}{1-V^2}D_iVD_jV\,,$$

2+1 decomposition $\quad H_{ij} = \rho^{-1}\underbrace{\sigma_{ij}}_{=0} - 2\rho^{-2}n_{(i}\underbrace{\mathcal{D}_{j)}\rho}_{=0} + \frac{1}{2\rho}\underbrace{\left(k - \frac{4V}{\rho(1-V^2)}\right)}_{=0}(h_{ij} - 2n_in_j)\,.$

$$k = \frac{4V}{\rho(1-V^2)},\ \partial_V\rho = \rho^2 k,\ \mathcal{D}_i\rho = 0 \longrightarrow \rho(V) = 4M/(1-V^2)^2$$

$$\sigma_{ij} = 0 \longrightarrow k_{ij} = \frac{1}{2\rho}\partial_V h_{ij} = \frac{1}{2}kh_{ij} \longrightarrow h_{ij} = M\rho(V)\hat{h}_{ij}(x^k) \longrightarrow \hat{R} = 2$$

V-independent metric $\qquad \hat{h}_{ij}$: unit sphere

H_{ij}=0 ⇔ spherical symmetry (Schwarzschild)

Remark: Robinson's proof shows the conformal flatness of Σ

Cotton tensor: $\quad C_{ijk} = \frac{2}{V^2}(2H_{k[i}D_{j]}V + \rho^{-2}H_{[i}g_{j]k})\,. \quad H_{ij}D^jV = -\rho^{-2}H_i\,,$

H_{ij} is more fundamental and well-defined also in higher dimensions

we wish to find a divergence equations of the form $\quad D_iJ^i \sim |H_{ij}|^2 + |H_i|^2$

Derivation of divergence equation

Separable ansatz

$$J^i = f_1(V)g_1(\rho)D^i\rho + f_2(V)g_2(\rho)D^iV\,,$$

$$H_{ij} \equiv D_iD_jV - \frac{2V}{\rho^2(1-V^2)}g_{ij} + \frac{6V}{1-V^2}D_iVD_jV\,,$$
$$H_i \equiv \frac{D_i\rho}{\rho} - \frac{4V}{1-V^2}D_iV\,.$$

$$\rightarrow \quad D_iJ^i = f_1(V)\rho^3g_1(\rho)\left[-|H_{ij}|^2 + \frac{|H_i|^2}{\rho^2}\left(3+\frac{\rho g_1'(\rho)}{g_1(\rho)}\right)\right] + \boxed{H_iD^iVS_1 + S_2\,,}$$

$$D^2V = 0\,, \quad {}^{(3)}R_{ij} = \frac{1}{V}D_iD_jV\,,$$

terms of no definite sign

$\Rightarrow$ we require $S_1 = S_2 = 0$

$$S_2 = \frac{4V}{(1-V^2)\rho^2}S_1 + \frac{V^2f_1(V)g_2(\rho)}{(1-V^2)^2\rho^2}\left[\frac{(1-V^2)^2f_2'(V)}{V^2f_1(V)} - \frac{8\rho g_1(\rho)}{g_2(\rho)}\left(3+\frac{2\rho g_1'(\rho)}{g_1(\rho)}\right)\right].$$

$$S_1 = \frac{\rho g_1(\rho)Vf_1(V)}{1-V^2}\left[\frac{1-V^2}{V}\left(\frac{1}{V}+\frac{f_1'(V)}{f_1(V)}\right) + 12 + \frac{8\rho g_1'(\rho)}{g_1(\rho)} + \boxed{\frac{1-V^2}{V}\frac{f_2(V)}{f_1(V)}\frac{g_2'(\rho)}{g_1(\rho)}}\right],$$

$\rightarrow$ (i) $g_2'(\rho) \propto g_1(\rho)$

(ii) $f_2(V) \propto \frac{V}{1-V^2}f_1(V)$

either choice gives the same final result

$$g_1(\rho) = -c\rho^{-(c+1)}\,, \qquad f_1(V) = \frac{(1-V^2)^{1-2c}}{V}\left[a + b(1-V^2)\right],$$
$$g_2(\rho) = \rho^{-c}\,, \qquad f_2(V) = \frac{2}{(1-V^2)^{2c}}\left[a(2c-1) + 2bc(1-V^2)\right],$$

a,b,c :integration constants

Divergence formula

$$D_iJ^i = S\,, \qquad S \equiv \frac{cf_1(V)}{2\rho^c}\left[\left|2\rho^2D_{[i}VH_{j]k} - H_{[i}g_{j]k}\right|^2 + (2c-1)\left|H_i\right|^2\right].$$

$$g_1(\rho) = -c\rho^{-(c+1)}\,, \qquad f_1(V) = \frac{(1-V^2)^{1-2c}}{V}\left[a + b(1-V^2)\right], \qquad H_{ij}D^jV = -\rho^{-2}H_i\,,$$
$$g_2(\rho) = \rho^{-c}\,, \qquad f_2(V) = \frac{2}{(1-V^2)^{2c}}\left[a(2c-1) + 2bc(1-V^2)\right],$$

$$S \geq 0 \quad \longleftrightarrow \quad a \geq 0\,, \quad a+b \geq 0\,. \quad c \geq \frac{1}{2}\,.$$

- 3 parameter family of divergence equation

  $c=2$:Robinson's identity is recovered

- $S=0 \Leftrightarrow$ spherical symmetry

- beyond the separable ansatz, the current involves two arbitrary functions

Uniqueness proof

Inequality for surface integral $\qquad D_i J^i = S \geq 0 \quad \Leftrightarrow \quad a \geq 0\,, \quad a+b \geq 0\,. \;\; c \geq \frac{1}{2}\,.$

$$0 \leq \int_\Sigma D_i J^i \mathrm{d}\Sigma = \int_{S^\infty} J_i n^i \mathrm{d}S - \int_B J_i n^i \mathrm{d}S$$

$$= \underbrace{a}_{\geq 0}\underbrace{[A_H \rho_0^{-(1+c)} - \pi(4M)^{1-c}]}_{\geq 0} + \underbrace{(a+b)}_{\geq 0} c\rho_0^{-(1+c)} \underbrace{[\pi\chi\rho_0^2 - 2A_H]}_{\geq 0}\,.$$

insert boundary conditions:

$k \sim \frac{2}{r}\,, \quad \rho \sim \frac{r^2}{M}\,,$ infinity

$k_{ij}|_{V=0} = 0\,,$ $\mathcal{D}_i\rho|_{V=0} = 0\,.$ horizon

$A_H = \int_B \mathrm{d}S$: area of horizon

$\chi = \frac{1}{4\pi}\int_B {}^{(2)}R\mathrm{d}S$: Euler characteristic of horizon

$$\longrightarrow \quad \pi\left(\frac{4M}{\rho_0}\right)^{1-c} \leq \frac{A_H}{\rho_0^2} \leq \frac{\pi}{2}\chi$$

set c=1: $\pi \leq A_H\rho_0^{-2} \leq \frac{\pi}{2}\chi$ $\quad \Rightarrow \chi \geqq 2 \Rightarrow \chi = 2$ (horizon is sphere)

set χ=2: $\pi \leq A_H\rho_0^{-2} \leq \pi$ $\quad \Rightarrow$ saturate equality

$\Rightarrow$ div$J$=0 $\Rightarrow$ S=0 spherical symmetry (QED)

Utilities

- no use of Smarr's formula

  possible to extend to the asymptotically AdS case

- $\chi \geqq 2$: **RP**^{2} (χ=1: unorientable) is explicitly ruled out

  stronger restriction than Hawking's topology theorem $\chi \geqq 0$ (Hawking, 1973)

- conservation of J^i is obvious for spherical symmetry

  $$J^i = -[(1-V^2)^2\rho]^{-c}\left[\frac{c}{V}(1-V^2)[a+b(1-V^2)]H^i + 2aD^iV\right]\,.$$

  $H_i \equiv D_i[\log\{(1-V^2)^2\rho\}]\,, \quad (1-V^2)^2\rho = 4M$ for Schwarzschild

- H_{ij}: obstruction for the existence of dilatational conformal Killing field

  $$\zeta_i \equiv (1-V^2)^{-3}D_iV\,, \qquad D_i\zeta_j + D_j\zeta_i - \frac{2}{3}D_k\zeta^k g_{ij} = \frac{2}{(1-V^2)^3}H_{ij}\,.$$

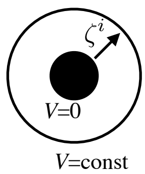

- non-vacuum cases

  Maxwell $\Rightarrow$ Reissner-Nordstrom, Maxwell-dilaton $\Rightarrow$ Gibbons-Maeda

  key: *maximum principle* can be applied to divergence type equations

Final comments

Summary

established a unified picture of static black hole uniqueness based on "divergence equation"

- simple proof, general proscription for derivation, lots of applications
- only S^2 horizon, independent of Smarr's formula, extensible to nonvacuum
- possible to combine w/ positive mass theorem (valid in higher dimensions)

Outlook

- extension to asymptotically AdS case (in progress)
- extension to stationary case (complex gen. of H_{ij} $\Leftrightarrow$ Simon tensor)
- application to static stars/modified gravity

Session S2P2 16:45–18:30

[Chair: Takeshi Chiba]

Sirachak Panpanich

Chulalongkorn University

"Fitting rotation curves of galaxies by de Rham-Gabadadze-Tolley massive gravity"

(10+5 min.)

[JGRG28 (2018) 110616]

Fitting rotation curve of galaxies by de Rham-Gabadadze-Tolley massive gravity

Sirachak Panpanich (with Piyabut Burikham)

Chulalongkorn University

November 6, 2018

ArXiv:1806.06271 [gr-qc], Phys.Rev.D98 (2018), 064008

Outline

Outline

Introduction and Motivation

Rotation curve problem

We cannot explain the flatness of rotation curves of galaxies by the Newtonian gravity.

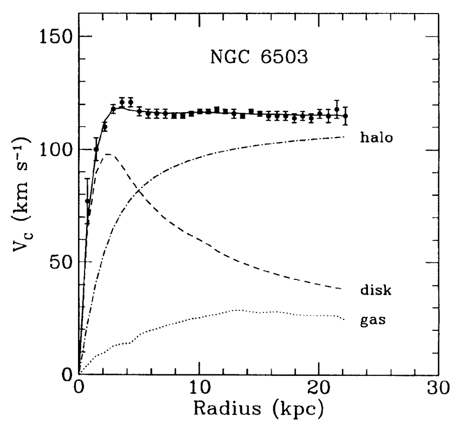

http://inspirehep.net/record/805890/files/fig1.png

There are 2 possibilities to solve this problem.

1. Dark matter + Newtonian gravity
2. Modified gravity theories
   - MOND
   - f(R) gravity
   - massive graviton

Introduction and Motivation

Recently we have a black hole solution from the dRGT massive gravity (S. Ghosh et al., 2015):

$$n(r) = f(r) = 1 - \frac{2GM}{r} - \frac{\Lambda r^2}{3} + \gamma r + \zeta\,, \tag{1}$$

and we know that a circular velocity can be obtained from the geodesic equation as (using $g_{\mu\nu} = \eta_{\mu\nu} + h_{\mu\nu}$)

$$v_c^2(r) = -\frac{1}{2} r \partial_r h_{00}\,. \tag{2}$$

Research question

Can we fit rotation curves of galaxies by the dRGT massive graviton?

Outline

Massive graviton halo

The dRGT massive gravity (C. de Rham et al., 2010)

$$S = \int d^4x\sqrt{-g}\frac{M_{\rm Pl}^2}{2}\left[R + m_g^2\mathcal{U}(g,f)\right] + S_m\,, \tag{3}$$

where m_g is a graviton mass, and the potential is defined as

$$\begin{aligned}
\mathcal{U} &\equiv \mathcal{U}_2 + \alpha_3\mathcal{U}_3 + \alpha_4\mathcal{U}_4\,,\\
\mathcal{U}_2 &\equiv [\mathcal{K}]^2 - [\mathcal{K}^2]\,,\\
\mathcal{U}_3 &\equiv [\mathcal{K}]^3 - 3[\mathcal{K}][\mathcal{K}^2] + 2[\mathcal{K}^3]\,,\\
\mathcal{U}_4 &\equiv [\mathcal{K}]^4 - 6[\mathcal{K}]^2[\mathcal{K}^2] + 3[\mathcal{K}^2]^2 + 8[\mathcal{K}][\mathcal{K}^3] - 6[\mathcal{K}^4]\,,\\
\text{and}\quad \mathcal{K}^\mu_\nu &\equiv \delta^\mu_\nu - (\sqrt{g^{-1}f})^\mu_\nu\,.
\end{aligned}$$

Variation with respect to $g^{\mu\nu}$, we find field equations as

$$G^\mu_\nu + m_g^2X^\mu_\nu = 8\pi G T^{\mu(m)}_\nu\,. \tag{4}$$

Introduction and Motivation | Circular velocity in the presence of massive graviton | Results | Summary

Massive graviton halo

The tensor X^μ_ν is given by

$$\begin{aligned}
X^\mu_\nu &= \mathcal{K}^\mu_\nu - [\mathcal{K}]\delta^\mu_\nu - \alpha\left[(\mathcal{K}^2)^\mu_\nu - [\mathcal{K}]\mathcal{K}^\mu_\nu + \frac{1}{2}\delta^\mu_\nu([\mathcal{K}]^2 - [\mathcal{K}^2])\right]\\
&+ 3\beta\left[(\mathcal{K}^3)^\mu_\nu - [\mathcal{K}](\mathcal{K}^2)^\mu_\nu + \frac{1}{2}\mathcal{K}^\mu_\nu([\mathcal{K}]^2 - [\mathcal{K}^2])\right.\\
&\left.-\frac{1}{6}\delta^\mu_\nu([\mathcal{K}]^3 - 3[\mathcal{K}][\mathcal{K}^2] + 2[\mathcal{K}^3])\right]\,,
\end{aligned} \tag{5}$$

where $\alpha_3 = \frac{\alpha-1}{3}$ and $\alpha_4 = \frac{\beta}{4} + \frac{1-\alpha}{12}$ to simplify the EOM (for $\alpha = \beta = 0$ the nonlinear interactions vanish).

We choose the fiducial metric ansatz as (D.Vegh, 2013)

$$f_{\mu\nu} = \begin{pmatrix} 0 & 0 & 0 & 0\\ 0 & 0 & 0 & 0\\ 0 & 0 & C^2 & 0\\ 0 & 0 & 0 & C^2\sin^2\theta \end{pmatrix}\,, \tag{6}$$

where C is a positive constant.

Massive graviton halo

Using the static spherically symmetric metric:

$$g_{\mu\nu} = \begin{pmatrix} -n(r) & 0 & 0 & 0 \\ 0 & f(r)^{-1} & 0 & 0 \\ 0 & 0 & r^2 & 0 \\ 0 & 0 & 0 & r^2 \sin^2\theta \end{pmatrix}, \qquad (7)$$

the field equations become

$$-\frac{1}{r^2} + \frac{f}{r^2} + \frac{f'}{r} = m_g^2 \left(\frac{3r-2C}{r} + \frac{\alpha(3r-C)(r-C)}{r^2} + \frac{3\beta(r-C)^2}{r^2} \right) - 8\pi G \rho_m(r)\,,$$
$$-\frac{1}{r^2} + \frac{f}{r^2} + \frac{fn'}{rn} = m_g^2 \left(\frac{3r-2C}{r} + \frac{\alpha(3r-C)(r-C)}{r^2} + \frac{3\beta(r-C)^2}{r^2} \right) + 8\pi G P_m(r)\,,$$
$$\frac{f'}{2r} - \frac{fn'^2}{4n^2} + \frac{f'n'}{4n} + \frac{fn'}{2rn} + \frac{fn''}{2n} = m_g^2 \left(\frac{3r-C}{r} + \frac{\alpha(3r-2C)}{r} + \frac{3\beta(r-C)}{r} \right) + 8\pi G P_m(r$$

For $T^{(m)}_{\mu\nu} = 0$, we find the BH solution.

$$n(r) = f(r) = 1 - \frac{2GM}{r} - \frac{\Lambda r^2}{3} + \gamma r + \zeta\,, \qquad (8)$$

Massive graviton halo

However, if there are massive gravitons around galaxies (assuming that the massive gravitons act as a halo), we have to find the TOV equation.

Massive graviton halo

However, if there are massive gravitons around galaxies (assuming that the massive gravitons act as a halo), we have to find the TOV equation.

Integrating the (00) component from 0 to r, we find

$$-\frac{1}{r^2}+\frac{f}{r^2}+\frac{f'}{r}=m_g^2\left(\frac{3r-2C}{r}+\frac{\alpha(3r-C)(r-C)}{r^2}+\frac{3\beta(r-C)^2}{r^2}\right)-8\pi G\rho_m(r)\,,$$

$$f(r)=1-\frac{2Gm(r)}{r}-\frac{\Lambda r^2}{3}+\gamma r+\zeta\,, \tag{9}$$

where

$$\Lambda\equiv-3m_g^2(1+\alpha+\beta)\,,\gamma\equiv-m_g^2C(1+2\alpha+3\beta)\,,\zeta\equiv m_g^2C^2(\alpha+3\beta)\,.$$

Circular velocity

Substituting $f(r)$ into the (rr) component, we find

$$\frac{d\ln n}{dr}=\frac{2Gm(r)+8\pi GP_m-\frac{2\Lambda r^3}{3}+\gamma r^2}{r(r-2Gm(r)-\frac{\Lambda r^3}{3}+\gamma r^2+\zeta r)}\,. \tag{10}$$

If $m_g=0$, i.e. $\Lambda=\gamma=\zeta=0$, we obtain the usual TOV equation.

Circular velocity

Substituting $f(r)$ into the (rr) component, we find

$$\frac{d\ln n}{dr} = \frac{2Gm(r) + 8\pi G P_m - \frac{2\Lambda r^3}{3} + \gamma r^2}{r(r - 2Gm(r) - \frac{\Lambda r^3}{3} + \gamma r^2 + \zeta r)} . \qquad (10)$$

If $m_g = 0$, i.e. $\Lambda = \gamma = \zeta = 0$, we obtain the usual TOV equation.

Since a galaxy scale is a non-relativistic scale,

- we ignore pressures of the visible matter, $P_m \approx 0$,
- and assume that gravity is weak, $n(r) \approx f(r)$.

Circular velocity

$$\therefore\ v_c(r) = \sqrt{\frac{Gm(r)}{r} - \frac{\Lambda r^2}{3} + \frac{\gamma r}{2}} . \qquad (11)$$

Circular velocity

A galaxy can be decomposed into bulge, disk, and gas:

$$\frac{Gm(r)}{r} = x\ v_{\text{bulge}}^2(r) + y\ v_{\text{disk}}^2(r) + z\ v_{\text{gas}}^2 ,$$

where x, y, z are the dimensionless mass-to-light ratio.

Set up

In this work we choose $\alpha = -3\beta$, $\beta = 1/2 + \epsilon$, then

$$\Lambda_{\rm obs} = -3m_g^2(1+\alpha+\beta) = 6m_g^2\epsilon\,,$$
$$\gamma = -m_g^2 C(1+2\alpha+3\beta) = \frac{1}{2}m_g^2 C + \mathcal{O}(\epsilon)\,,$$
$$\zeta = m_g^2 C^2(\alpha+3\beta) = 0\,.$$

$\therefore$ Λ finely tunes to the DE observed value, $\sim 10^{-52}\ \mathrm{m}^{-2}$.

Introduction and Motivation | Circular velocity in the presence of massive graviton | Results | Summary

Set up

In this work we choose $\alpha = -3\beta$, $\beta = 1/2 + \epsilon$, then

$$\Lambda_{\rm obs} = -3m_g^2(1+\alpha+\beta) = 6m_g^2\epsilon\,,$$
$$\gamma = -m_g^2 C(1+2\alpha+3\beta) = \frac{1}{2}m_g^2 C + \mathcal{O}(\epsilon)\,,$$
$$\zeta = m_g^2 C^2(\alpha+3\beta) = 0\,.$$

$\therefore$ Λ finely tunes to the DE observed value, $\sim 10^{-52}\ \mathrm{m}^{-2}$.

Circular velocity

$$v_c(r) = \sqrt{\frac{Gm(r)}{r} - \frac{\Lambda r^2}{3} + \frac{\gamma r}{2}}\,.$$

The fitting parameter is only γ, thus we obtain constraints on $m_g^2 C$ (not on m_g^2).

Outline

Milky Way

Observational data from Y. Sofue, et al., 2009

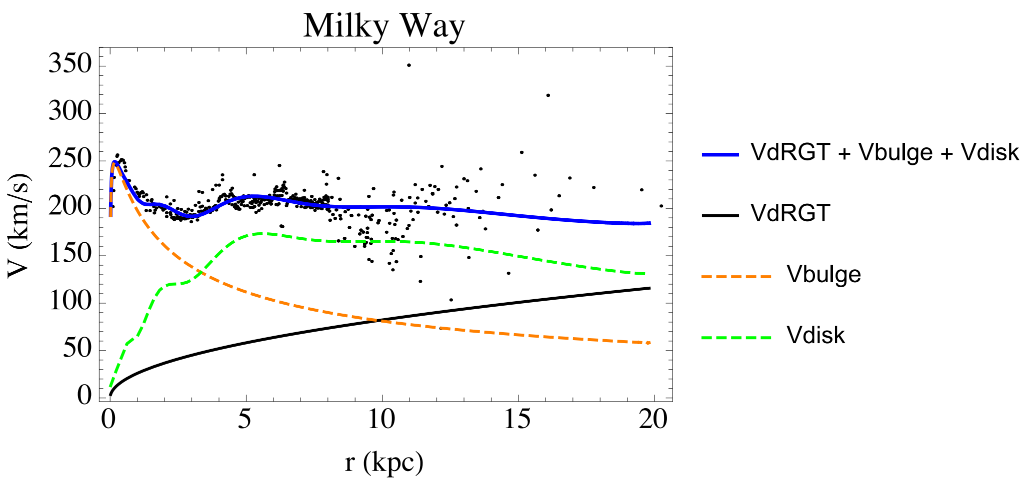

$$\gamma = 4.877 \times 10^{-28}\mathrm{m}^{-1},\ m_g = 6.163 \times 10^{-21}\mathrm{eV} \text{ where } C = 1 \text{ m}.$$

Spiral galaxies

Observational data from F. Lelli, et al., 2016 (SPARC)

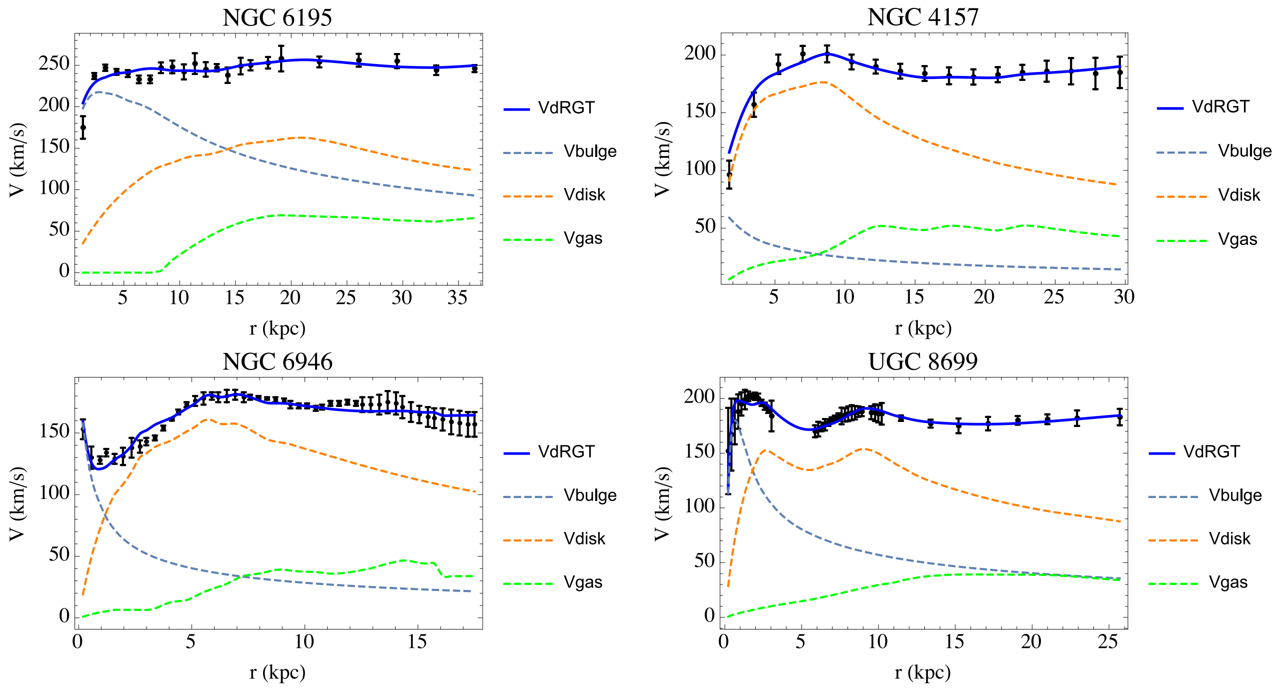

Spiral galaxies

The x, y, z are the dimensionless mass-to-light ratio.

dRGT	γ $(10^{-28}$ m$^{-1})$	x, y, z	C (m)
Milky Way	4.87739	$1^*, 1, 0$	1.00
NGC6195 (Sb)	6.74171	$0.7, 0.4427, 1$	1.39
NGC4157 (Sb)	6.43075	$0.7, 0.49216, 1$	1.32
NGC6946 (Scd)	6.14538	$0.4580, 0.6127, 1$	1.26
UGC8699 (Sab)	6.70334	$0.514856, 1.18365, 1$	1.38

Table: The γ of each spiral galaxy where C is calculated from γ and m_g (from the Milky Way). For the Milky Way, the bulge are refitted together with the γ.

Low-surface-brightness (LSB) galaxies

Observational data from W. de Blok and A. Bosma, 2002

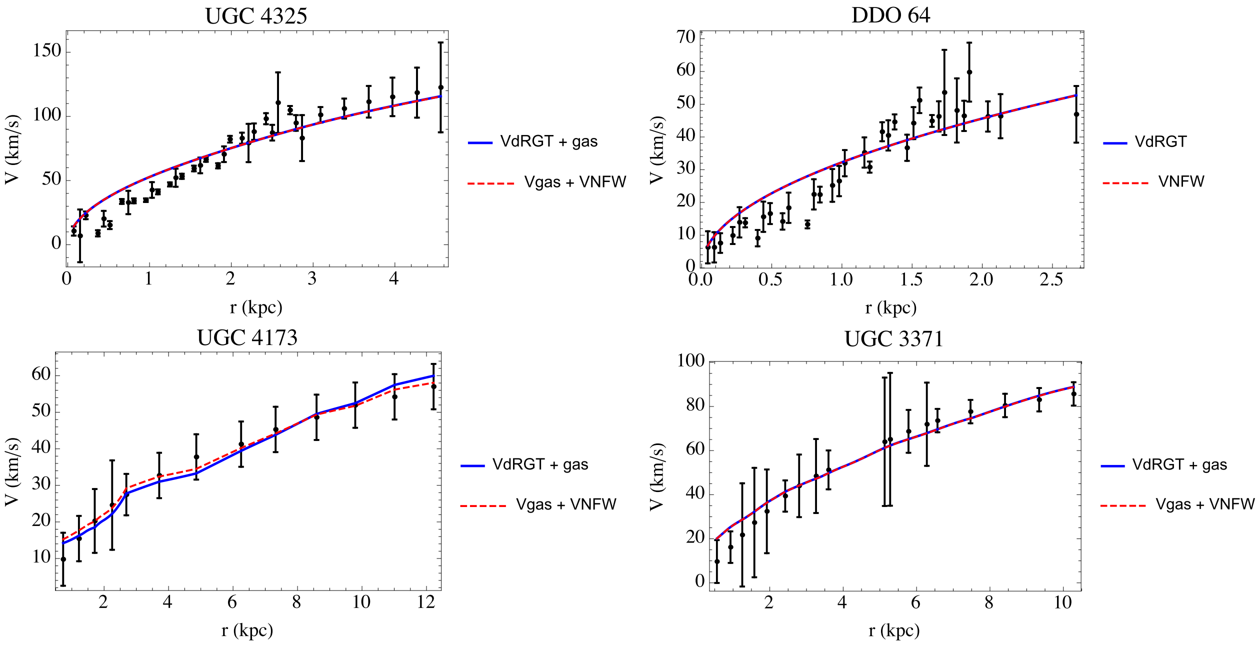

$\ast$ The dRGT yields similar effects as the NFW DM halo.

Low-surface-brightness (LSB) galaxies

Since for small galaxies ($r \to$ small),

$$\rho_{\rm NFW}(r) = \frac{\rho_i}{\frac{r}{r_s}\left(1+\frac{r}{r_s}\right)^2} \propto \frac{1}{r} \quad \to \quad v_c \propto \sqrt{r}\,.$$

Circular velocity

$$v_c(r) = \sqrt{\frac{Gm(r)}{r} - \frac{\Lambda r^2}{3} + \frac{\gamma r}{2}} \quad \to \quad v_c \propto \sqrt{r}\,.$$

$\therefore$ Both circular velocities are similar.

$\ast$ However, it is true for small galaxies or galaxies with large r_s.

Low-surface-brightness (LSB) galaxies

For these LSB galaxies we set $y = 0$, i.e. only DM and gas contribute the rotation curves.

dRGT	γ (10^{-28} m^{-1})	C m)
UGC4325	19.9956	4.11
DDO64	7.49968	1.54
UGC4173	1.5165	0.31
UGC3371	5.0024	1.03

Note that rotation speeds of the UGC4235 are faster than other LSB galaxies.

Low-surface-brightness (LSB) galaxies

However, some LSB galaxies require modification on the stellar disk.

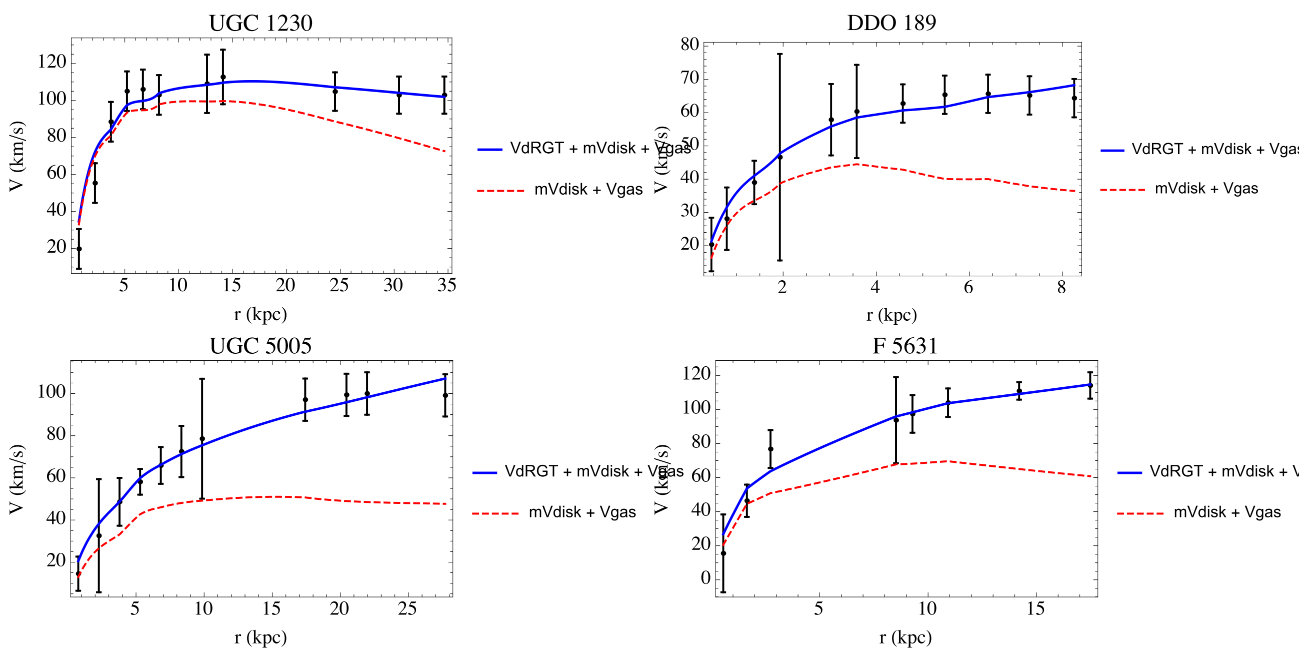

Large values of the stellar M/L ratio of the disk is required.

Low-surface-brightness (LSB) galaxies

Thus, for the last four LSB galaxies

$$v_c(r) = \sqrt{y\ v_{\rm disk}^2(r) + v_{\rm gas}^2 - \frac{\Lambda r^2}{3} + \frac{\gamma r}{2}}\,.$$

dRGT	γ (10^{-28} m^{-1})	C m)
UGC41230	$1.06442(y = 10.2822)$	0.22
DDO189	$2.90571(y = 7.03932)$	0.60
UGC5005	$2.39079(y = 2.9603)$	0.49
F5631	$3.89396(y = 6.05839)$	0.80

Large values of the stellar M/L ratio of the disk is required.

Outline

Summary

- The dRGT massive gravity contributes an increasing circular velocity ($v_c \propto \sqrt{r}$) which be able to fit most of the galactic rotation curves.

$$v_c(r) = \sqrt{\frac{Gm(r)}{r} - \frac{\Lambda r^2}{3} + \frac{\gamma r}{2}}\,.$$

- There is only one fitting parameter in the model, and the best-fit values are in the same order for all of galaxies, including cluster scale ($\gamma \sim 10^{-28}\ \mathrm{m}^{-1}$).
- However, some LSB galaxies requires large value of the stellar mass-to-light ratio of the disk.

Summary

- Since there is no direct constraint on C in the galactic scale, we can choose C to be very large to satisfy Lunar Laser Ranging experiments.

  For $C = 1 - 10^{18}\ \mathrm{m}$, we find $m_g \sim 10^{-21} - 10^{-30}\ \mathrm{eV}$.

Thank you very much for your attention.

Michele Oliosi
Yukawa Institute for Theoretical Physics, Kyoto University

“Black holes and stars in the minimal theory of massive gravity (MTMG)”

(10+5 min.)

[JGRG28 (2018) 110617]

Black holes and stars in the minimal theory of massive gravity (MTMG)

Michele Oliosi

Yukawa Institute for Theoretical Physics
Kyoto University

presentation at JGRG28, November 6, 2018

based on **arXiv:1808.01403**

with Antonio De Felice, François Larrouturou, and Shinji Mukohyama.

Outline

Introduction

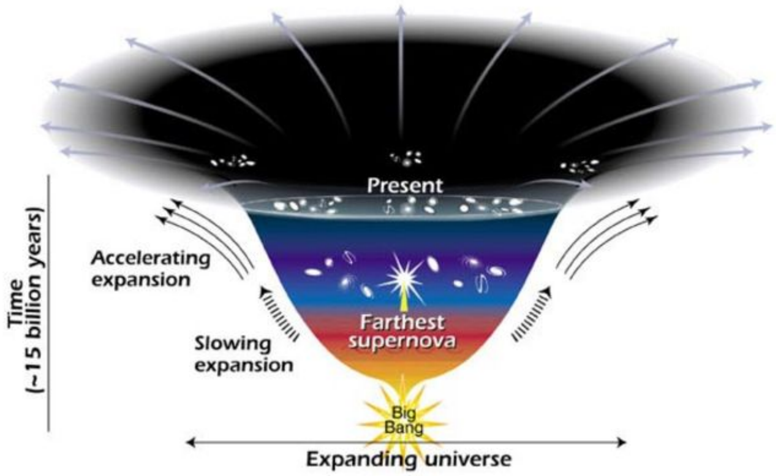

image by NASA

What is the **accelerating expansion**?

- cosmological constant?
- dark energy source?
- IR modification of GR?

$$\text{Massive gravity} \quad S_{\text{gravity}} = S_{\text{EH}} + S_{\text{mass}} \tag{1}$$

Massive gravity (MG)

- Physical metric $g_{\mu\nu}$, nondynamical reference metric $\tilde{g}_{\mu\nu}$.
- mass term $\ni \tilde{g}^{\mu\rho} g_{\rho\nu} \to$ Diffeomorphisms are broken.
- Boulware-Deser ghost-free, Lorentz invariance (LI):

  de Rham, Gabadadze, Tolley MG [de Rham et al, 2010]

$$S_{\text{mass}} = \frac{m^2 M_{\text{Pl}}^2}{2} \int d^4x \, \mathcal{U}\left[\sqrt{\tilde{g}^{\mu\rho} g_{\rho\nu}}\right] \tag{2}$$

  where $\mathcal{U}$ is a symmetric polynomial, whereas m controls the graviton mass. Propagates 5 d.o.f.

- Cosmology $\to$ look further: inhomog., bigravity, MTMG

See [Boulware, Deser, 1972], [de Rham et al, 2011], [Hassan, Rosen, 2011], [De Felice, Mukohyama, 2015]

Black holes in dRGT

Reviews: [Volkov, 2014], [Babichev, Brito, 2015]

	$\tilde{g}_{\mu\nu} \propto g_{\mu\nu}$	$\tilde{g}_{\mu\nu} \not\propto g_{\mu\nu}$	
		both diagonal	~~both diagonal~~
Static, LI	$\times$	Singularity at the horizon [Deffayet, Jacobson, 2011] Hairy BH?	(A)dS-Schwarzschild: infinite strong coupling. Hairy BH?

Different coordinates means different solutions.

~~Static~~: this is one way out, see e.g. [Rosen, 2018]

Minimal theory of massive gravity [De Felice, Mukohyama, 2015]

(Cosmological) LI violations allow for more variety

$$S_{\rm mass} = \frac{m^2 M_{\rm Pl}^2}{2} \int d^4x \, \mathcal{W} \left[\sqrt{\tilde{\gamma}^{ik}\gamma_{kj}}, \frac{\tilde{N}}{N}, K^i{}_j, \partial_t \sqrt{\tilde{\gamma}^{ik}\gamma_{kj}}, \mathcal{D}_i \right] \quad (3)$$

where the γ and $\tilde{\gamma}$ are the physical and reference 3D metrics, N and $\tilde{N}$ the physical and reference ADM lapses, and K_{ij} the extrinsic curvature.

- By a careful choice, propagates only 2 d.o.f., nonlinearly.
- There exist 2 branches of FLRW solutions: the normal branch, and the self-accelerating branch.
- Successful cosmology [De Felice, Mukohyama, 2018]

Lemma in MTMG

Ansatz: Spatially flat physical metric, FLRW reference metric.

- Both the normal and the self-accelerating branches still exist.
- Choosing the self-accelerating branch, one finds the usual Einstein equations

$$M_{\rm Pl}^2\left(G_{\mu\nu} + m^2\Lambda_{\rm eff}g_{\mu\nu}\right) = T_{\mu\nu} \tag{4}$$

  with $\Lambda_{\rm eff} = \text{cst}$.
- $\Rightarrow$ Spatially flat GR solutions are solutions in MTMG

Applications of the Lemma

1. **Painlevé-Gullstrand** forms of Schwarzschild-(Anti)de Sitter black-holes.

$$\mathrm{d}s^2 = -\mathrm{d}\tau^2 + \left(\mathrm{d}r \pm \sqrt{\frac{2M}{r} - \frac{\Lambda_{\rm eff}m^2r^2}{3}}\mathrm{d}\tau\right)^2 + r^2\mathrm{d}\Omega^2\,. \tag{5}$$

2. Spherically symmetric static matter solutions (e.g. Schwarzschild interior). Solutions are regular at the center.
3. Solutions matched to background cosmology.
4. …

Solutions are free from the strong-coupling issues that exist in dRGT

Summary

- Black holes are difficult to find in dRGT massive gravity
- They may be easier to find in other theories
- Our result: spatially flat solutions of GR are also solutions in MTMG.
- MTMG Schwarzschild black holes are free from strong couplings. There are other nice solutions.

...thank you ! ☺

Andrea Nerozzi
Instituto Superior TÃl'cnico

"Tetrad formalisms and gauge fixing for binary black hole simulations"

(10+5 min.)

[JGRG28 (2018) 110618]

Tetrad formalisms and gauge fixing for binary black hole simulations

Andrea Nerozzi

JGRG28 - Rikkyo University, Tokyo

November 6th, 2018

Tetrad approaches in numerical relativity

- Tetrad approaches have been used only in few cases in numerical relativity (see for example the work by Bardeen and Buchman).
- The Newman-Penrose formalism is used in numerical codes to extract the information about gravitational waves.
- Thinking of implementing the whole set of NP equations in a numerical code would be rather tough, however a specific gauge choice can help simplify the equations to a big extent.

Self-dual forms

The Newman-Penrose formalism can be rewritten in a much more compact way using self-dual forms. A self dual two-form is defined by the condition

$$\epsilon_{ab}{}^{cd}\,\Sigma_{cd} = -2i\Sigma_{ab}$$

Instead of tetrad vectors, an equivalent approach is to introduce the following set of three self-dual forms

$$\begin{aligned}
\Sigma_{\mu\nu} &= \ell_{[\mu} n_{\nu]} - m_{[\mu} \bar{m}_{\nu]}, \\
\Sigma^{+}_{\mu\nu} &= \ell_{[\mu} m_{\nu]}, \\
\Sigma^{-}_{\mu\nu} &= n_{[\mu} \bar{m}_{\nu]}.
\end{aligned}$$

The Σ variables satisfy contraction relations of the type

$$\Sigma_a{}^c \Sigma^+_{cb} = -\Sigma^+_{ab}.$$

Connection and Curvature

The connection is completely determined by the following three vectors:

$$\begin{aligned}
A_a &= -\frac{1}{4}\,\Sigma_a^{-\,b}\,\Sigma^{+de}\,\nabla_a\Sigma_{de} - \frac{1}{4}\,\Sigma_a^{+\,b}\,\Sigma^{-de}\,\nabla_a\Sigma_{de}, \\
B_a &= \frac{1}{4}\,\Sigma_a^{+\,b}\,\Sigma^{+de}\,\nabla_a\Sigma_{de} + \frac{1}{4}\,\Sigma_a^{-\,b}\,\Sigma^{-de}\,\nabla_a\Sigma_{de}, \\
C_a &= \frac{1}{4}\,\Sigma_a{}^b\,\Sigma^{-de}\,\nabla_b\Sigma^+_{de}.
\end{aligned}$$

While the self-dual Weyl tensor is given by

$$\begin{aligned}
C^*_{abcd} &= i\Psi_-\left[\Sigma^+_{ab}\,\Sigma^+_{cd} + \Sigma^-_{ab}\,\Sigma^-_{cd}\right] \\
&+ \frac{\Psi_+}{\sqrt{3}}\left[\Sigma_{ab}\,\Sigma_{cd} - \Sigma^+_{ab}\,\Sigma^-_{cd} - \Sigma^-_{ab}\,\Sigma^+_{cd}\right].
\end{aligned}$$

Gauge fixing

The gauge freedom corresponds to the 6 parameter Lorentz group. It is possible to fix completely this gauge freedom by imposing the following three conditions:

$$\begin{aligned}
C^{*abcd}\,\Sigma^{+}_{ab}\,\Sigma_{cd} &= 0,\\
C^{*abcd}\,\Sigma^{-}_{ab}\,\Sigma_{cd} &= 0,\\
C^{*abcd}\,\left[\Sigma^{+}_{ab}\,\Sigma^{+}_{cd} - \Sigma^{-}_{ab}\,\Sigma^{-}_{cd}\right] &= 0.
\end{aligned}$$

So that the Weyl tensor is given by

$$\begin{aligned}
C^{*}_{abcd} &= i\Psi_{-}\,\left[\Sigma^{+}_{ab}\,\Sigma^{+}_{cd} + \Sigma^{-}_{ab}\,\Sigma^{-}_{cd}\right]\\
&+ \frac{\Psi_{+}}{\sqrt{3}}\,\left[\Sigma_{ab}\,\Sigma_{cd} - \Sigma^{+}_{ab}\,\Sigma^{-}_{cd} - \Sigma^{-}_{ab}\,\Sigma^{+}_{cd}\right].
\end{aligned}$$

Different approaches to Einstein's equations

Coord. approach	Newman-Penrose	Gauged self-dual
$g_{\mu\nu}$	$\ell^{\mu}, n^{\mu}, m^{\mu}, \bar{m}^{\mu}$	$\Sigma_{\mu\nu}, \Sigma^{+}_{\mu\nu}, \Sigma^{-}_{\mu\nu}$
Γ_{abc}	$\rho, \mu, \tau, \pi, \sigma, \lambda, \nu, \kappa, \epsilon, \gamma, \beta, \alpha$	$A_{\mu}, B_{\mu}, C_{\mu}$
C_{abcd}	$\Psi_0, \Psi_1, \Psi_2, \Psi_3, \Psi_4$	Ψ_{+}, Ψ_{-}

- Ψ_{+} and Ψ_{-} are simple functions of the two curvature invariants I and J:

$$\begin{aligned}
\Psi_{+} &= -\frac{I^{\frac{1}{2}}}{2\sqrt{3}}\left(\Theta + \Theta^{-1}\right),\\
\Psi_{-} &= \frac{I^{\frac{1}{2}}}{2i}\left(\Theta - \Theta^{-1}\right),
\end{aligned}$$

- $\Theta = f(I, J)$.

Relevant equations

The relevant equations in tetrad formalisms are the Bianchi and Ricci identities.

- Bianchi identities

$$\nabla_a C^{*a}{}_{bcd} = 0.$$

- Ricci identities

$$2\nabla_{[a}\nabla_{b]}\ell_c = C_{abcd}\ell^d.$$

In order to obtain scalar relations, all the possible independent projections along the tetrad vectors are considered.

The Bianchi identities

When written as functions of the variables introduced in this approach, they give the following simple relations

$$\begin{aligned}
\nabla_a \ln\left[I^{\frac{1}{2}}(\Theta + \Theta^{-1})\right] &= -i\sqrt{3}\left(\frac{\Theta - \Theta^{-1}}{\Theta + \Theta^{-1}}\right) B_a - 3A_a, \\
\nabla_a \ln\left[I^{\frac{1}{2}}(\Theta - \Theta^{-1})\right] &= i\sqrt{3}\left(\frac{\Theta + \Theta^{-1}}{\Theta - \Theta^{-1}}\right) B_a + (2C_a - A_a).
\end{aligned}$$

It turns out that the Bianchi identities can be used as simple relations to derive the two vectors A_a and C_a once B_a is known. But what about the third vector? Is there a third potential involved?

The Petrov type D limit

In the single black hole limit ($\Theta \to 1$) the connection vectors tend to

$$\begin{aligned} A_a &= \frac{1}{6}\nabla_a \ln\, I, \\ B_a &= 0, \\ C_a &= -\frac{1}{6}\nabla_a \ln\, I - \frac{1}{2}\nabla_a \ln \Phi. \end{aligned}$$

ρ, μ, τ, π
$\lambda, \sigma, \nu, \kappa$
$\epsilon, \gamma, \beta, \alpha$

where

$$\Phi = \left(r^2 - 2Mr + a^2\right)\sin^2\theta.$$

- These values are consistent with the known expressions for the spin coefficients in Kerr.
- The value of C_a calculated in the Kerr space-time confirms that $\mathcal{S}_a = \nabla_a \ln \Phi$! (at least in this limit).

The Ricci identities

When written in function of the variables introduced in this approach:

$$\begin{aligned} \nabla_a A^a &= A_a A^a - B_a B^a - \frac{2I^{\frac{1}{2}}}{\sqrt{3}}\left(\Theta + \Theta^{-1}\right) \\ \nabla_a B^a &= -2B_a C^a + \frac{2iI^{\frac{1}{2}}}{\sqrt{3}}\left(\Theta - \Theta^{-1}\right) \\ \nabla_a C^a &= A_a A^a - B_a B^a + 2A_a C^a - \frac{4I^{\frac{1}{2}}}{\sqrt{3}}\left(\Theta + \Theta^{-1}\right) \end{aligned}$$

Given that A_a, B_a and C_a are functions of $\nabla_a I$, $\nabla_a\Theta$ and $\nabla_a\Phi$ (?) would then lead to equations for $\nabla_a\nabla^a I$, $\nabla_a\nabla^a\Theta$ and $\nabla_a\nabla^a\Phi$.

Conclusions

- A tetrad approach with this specific gauge fixing is an alternative approach to Einstein's equations worth studying further.
- It has been shown that using the self-dual approach equations become much simpler and compact.
- Connection and curvature can be expressed as functions of the two curvature invariants I and J plus a third (possibly scalar) quantity.
- The dynamics for these quantities is governed by the Ricci identities.
- Numerical implementation of these equations is the subject of future work.

Kazuma Takahashi
Osaka City University

“Imaging of gravitationally collapsing star by numerical calculation”

(10+5 min.)

[JGRG28 (2018) 110619]

Imaging of gravitationally collapsing star by numerical calculation

Kazuma Takahashi

In collaboration with Hirotaka Yoshino and Ken-ichi Nakao

from Osaka City University

Contents

Introduction

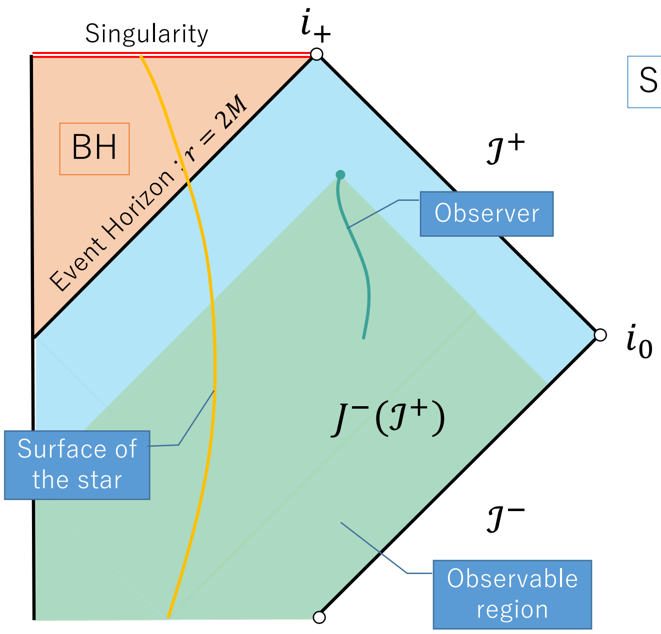

Space time of Gravitational Collapsing star

- Blue region : Causal past of future null infinity
- Orange region : Black Hole

Observers outside black holes can't get any signals from black holes.

The shadow image that we observe is not the black hole itself, but the surface of the gravitationally collapsing star.

Gravitationally Collapsing Star

Oppenheimer-Snyder Collapse

This model showed for the first time based on the General relativity scenario of the black hole formation through gravitational collapse of a dust sphere.

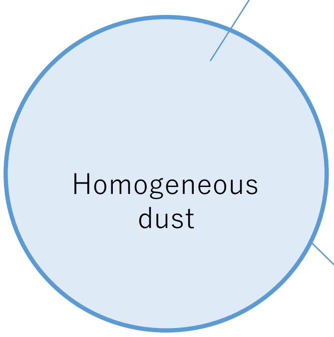

V^- : FLRW

$$ds^2 = -d\tau^2 + a^2\left(\frac{dr^2}{1-kr^2} + r^2 d\Omega^2\right)$$

V^+ : Schwarzschild

$$ds^2 = -f(R)c^2dt^2 + \frac{dR^2}{f(R)} + R^2 d\Omega^2 \qquad \left(f(R) \equiv 1 - \frac{R_g}{R}\right)$$

Matching of the metric at the surface of the dust star

Gravitationally Collapsing Star

Oppenheimer-Snyder Collapse

Matching of metric

→ the surface move along a radial timelike geodesic.

$$r = \frac{R}{2}(1 + \cos\xi)$$

$$t = 2M\log\left[\frac{\sqrt{\frac{R}{2M}-1}+\tan\left(\frac{\xi}{2}\right)}{\sqrt{\frac{R}{2M}-1}-\tan\left(\frac{\xi}{2}\right)}\right] + \sqrt{\frac{R}{2M}-1}\left(\frac{R}{2}\sin\xi + \left(2M+\frac{R}{2}\right)\xi\right)$$

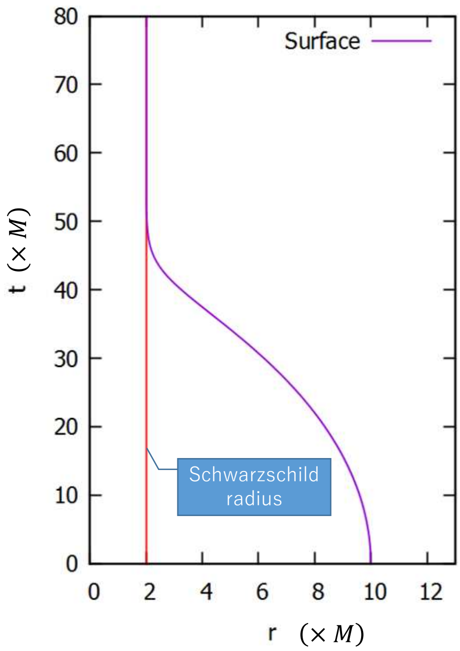

The trajectory of the timelike geodesic is right figure.

$(R = 10, M = G = 1)$

Gravitationally Collapsing Star

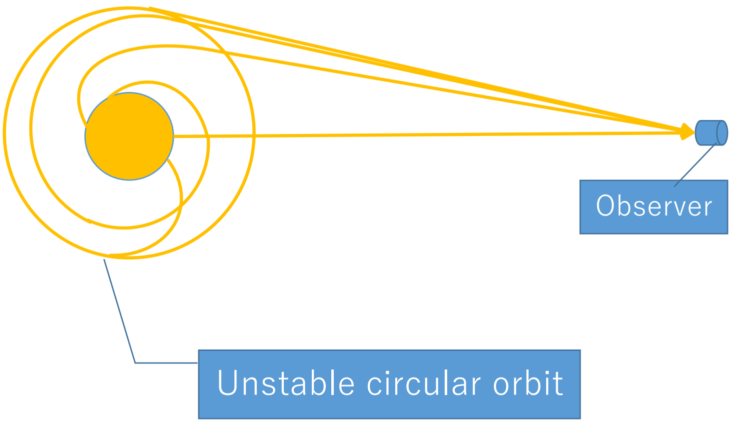

Lights emitted from the star surface is bent by gravity.

For that reason, light that reaches the observer has various trajectories.

At the late stage, lights leakage from the unstable circular orbit remains.

Gravitationally Collapsing Star

In this study,
The star surface is assumed to isotropically emit the light of the same frequency from each point .

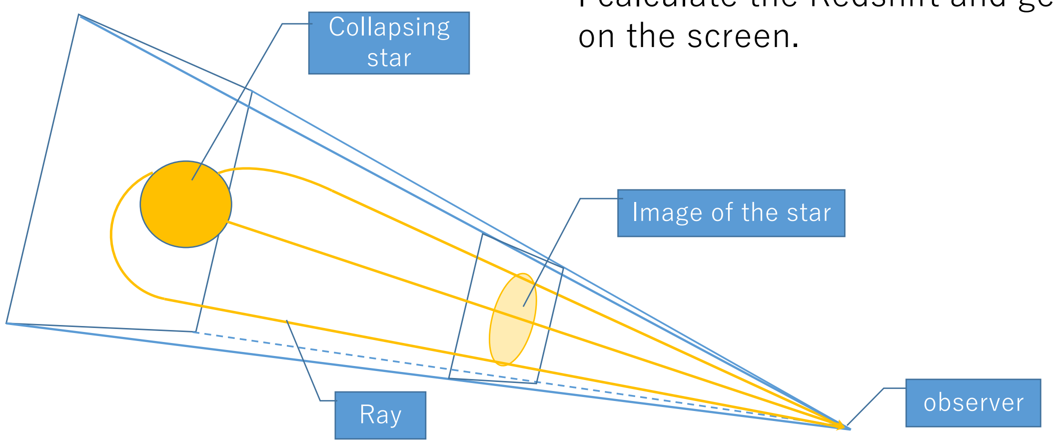

I calculate the Redshift and get the image on the screen.

Numerical Calculation-Redshift-

Setup

Photon Number : $N = 5000$
Initial radius of surface of the star : $R_s = 10M$
Location of the observer : $r_o = 50M$

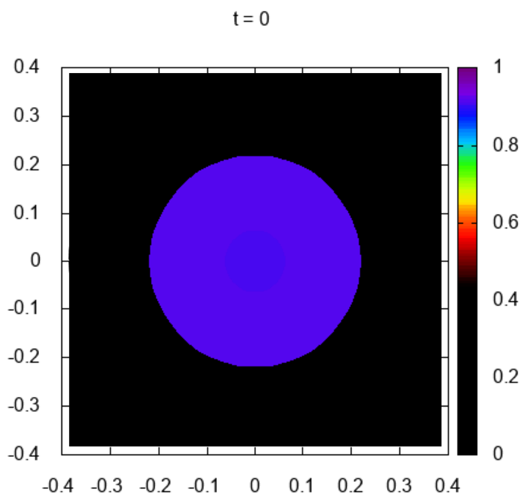

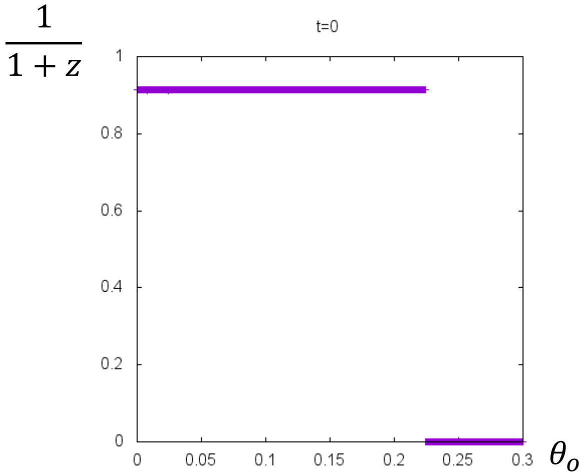

Numerical Calculation-Redshift-

Setup

Photon Number : $N = 5000$
Initial radius of surface of the star : $R_s = 10M$
Location of the observer : $r_o = 50M$

- The image size that the observer receives will become smaller with the collapse.
- At the late stage of collapse the edge of the image asymptotically approaches 3M.
- The strength of the Redshift of the limb **not** time dependent.

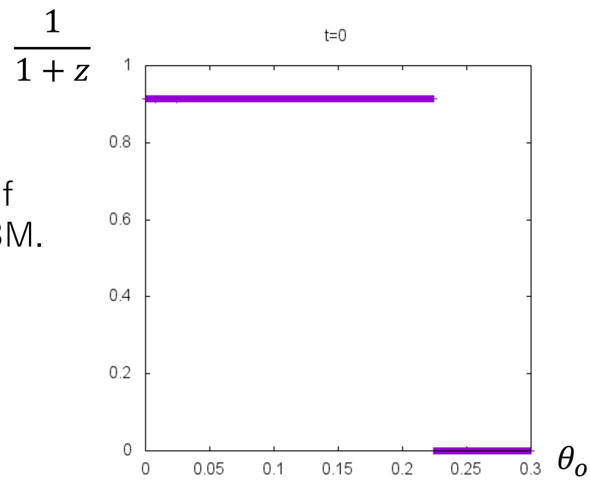

Numerical Calculation-Energy Spectrum-

We consider the Energy Spectrum of the Black body.

In this study,
The star surface is assumed to isotropically emit the light from each point .

The Energy Flux $dF_E(\tau_o)$ normalized with $F_E(0)$ is written by

$$\boxed{\frac{dF_E(\tau_o)}{F_E(0)} = \pi^{-1}\left(\frac{r_o}{R}\right)^2 \frac{f(R)}{f(r_o)}\frac{J(r_e)}{J(R)}\left(\frac{1}{1+z}\right)^4 cos\theta_o d\Omega_o} \quad \left(F_E(0) = \hbar\omega_o \pi J(R) A_{lens}\sqrt{\frac{f(R)}{f(r_o)}\frac{R^2}{r_o^2}}\right)$$

Here, we call $\frac{dF_E(\tau_o)}{d\Omega_o}$ the surface brightness.

Numerical Calculation-Energy Spectrum-

The Surface brightness

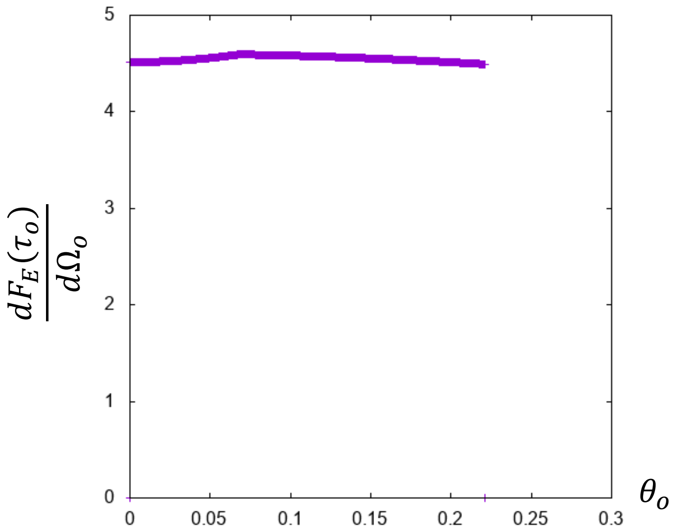

The limb of the surface brightness
is time independent as well as redshift.

Numerical Calculation-Energy Spectrum-

And the Energy Spectrum of the Blackbody Radiation is

$$T_e \frac{dF_E(\tau_o)/d\omega_o}{F_E(0)} = \frac{30}{\pi^4}\left(\frac{r_o}{R}\right)^2 \frac{f(r_o)}{f(R)} \left(\frac{\omega_o}{T_e}\right)^3 \int_0^{\theta_s(\tau_o)} \frac{sin\theta_o cos\theta_o d\theta_o}{exp[(\omega_o/T_e)(1+z)]-1}$$
$$+\frac{15}{\pi^4}\left(\frac{f(r_o)}{f(R)}\right)^2 \frac{(\omega_o/T_e)^3}{exp\left[\sqrt{\frac{f(r_o)}{f(R)}}\frac{\omega_o}{T_e}\right]-1}\left[1-\left(\frac{sin\theta_s(\tau_o)}{sin\theta_{max}(0)}\right)^2\right]$$

Numerical Calculation-Energy Spectrum-

The Spectrum of the Blackbody Radiation

Surface temperature : $T_e = 1$

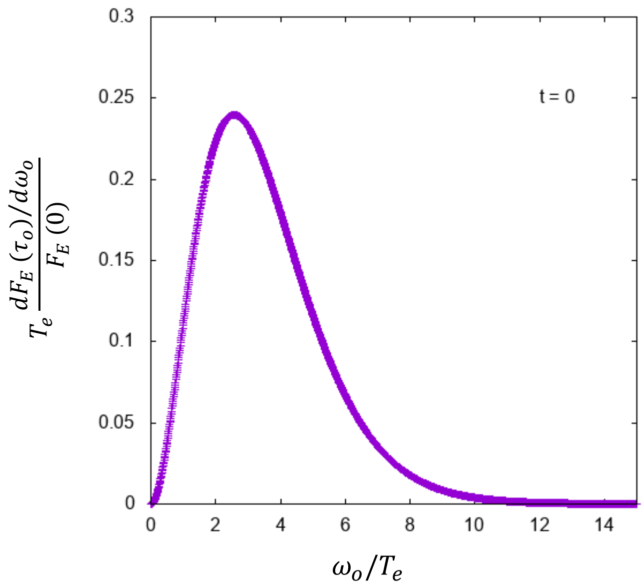

When the time evolves, the spectrum gradually gets darker.

the shape of the spectrum is maintained and the peak appears to be not moving.

Numerical Calculation-Energy Spectrum-

The Spectrum of the Blackbody Radiation

To make the behavior of the peak easy to see, normalize to the initial peak.

[Normalized to the value of peak]

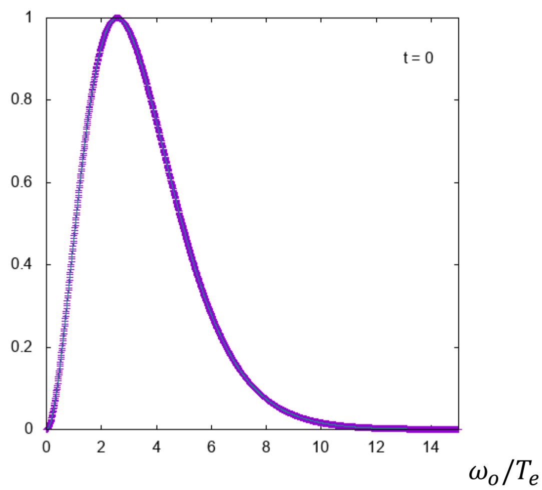

[Normalized to the value and location of peak]

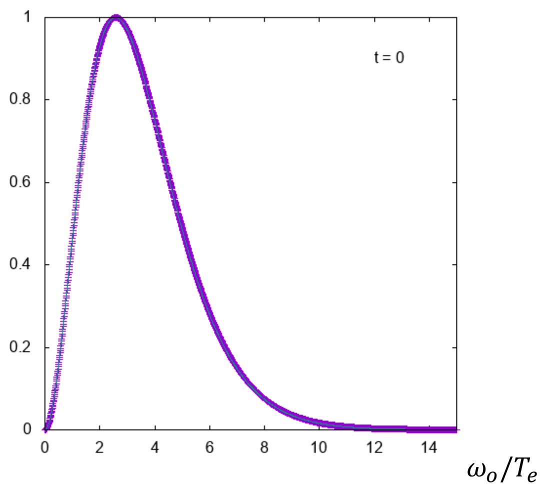

Numerical Calculation-Energy Spectrum-

The Spectrum of the Blackbody Radiation

To make the behavior of the peak easy to see, normalize to the initial peak.

[Normalized to the value of peak]

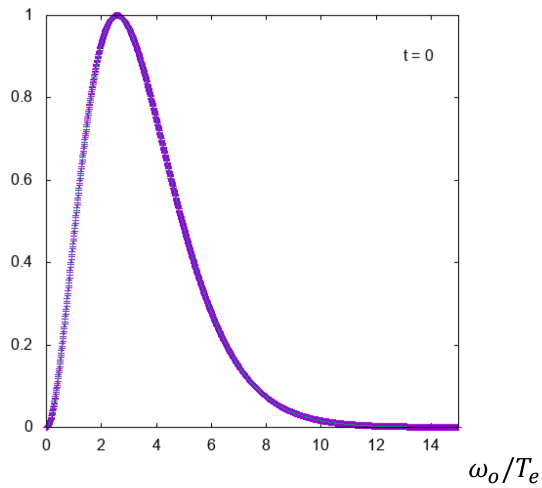

- The peak of flux slide the Red side by the Redshift.
- The peak approaches asymptotically to a certain value.
- The slide to Red side will stop at late stage.

The spectrum can't be observed due to becomes dark rather than becomes red.

Analysis of the limb

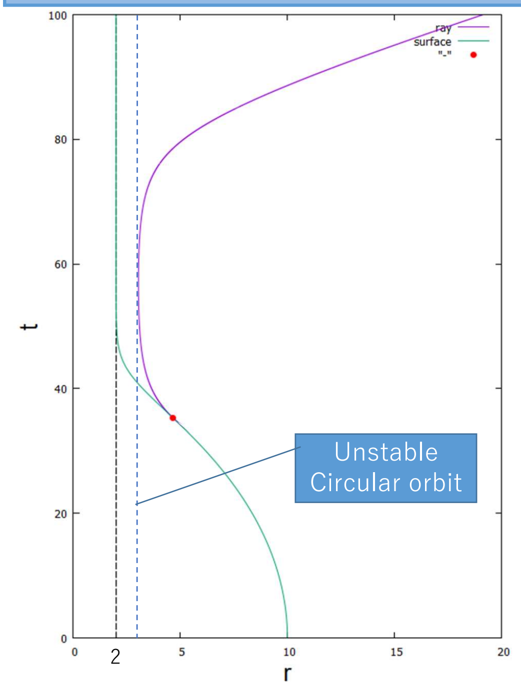

We consider the light of the limb.

The trajectory of the light of the limb which the observer receives at a certain time is as shown in this figure.

This light is emitted inward from the emission point, and it reaches the observer through 3M.

The Doppler effect working on this light is the Blueshift, not the Redshift.

Analysis of the limb

The Redshift of the limb's light can be written analytically.

When the surface's 4-velocity $u^\mu = (\dot{t}, \dot{r}, 0, 0)$, the redshift factor $1/1+z$ is

$$\boxed{\frac{1}{1+z} = \frac{f\dot{t}}{\sqrt{f(r_o)}}\ .} \qquad \left(f \equiv 1 - \frac{2M}{r}\right)$$

Here, the surface of the star follows timelike geodesics.

Therefore, when we use $\dot{t} = \sqrt{f(R_s)}/f$, the Redshift factor α becomes

$$\boxed{\frac{1}{1+z} = \frac{\sqrt{f(R_s)}}{\sqrt{f(r_o)}}\ .}$$

This form is consistent with the Gravitational potential due to the initial radius of the star.

Conclusion

- We calculated the Redshift of the light of gravitationally collapsing star receives by the observer.
  - The edge of the image is characteristic, and it is time independent for Timelike geodesics.
- We consider the energy spectrum of the Blackbody radiation.
  - When the time evolves, the spectrum gradually gets darker.
  - However, the peak of the spectrum asymptotically approaches a certain value.

Anton Khirnov
Institute of Theoretical Physics, Charles University

“Numerical evolution of axisymmetric gravitational wave collapse”
(10+5 min.)

[JGRG28 (2018) 110620]

Numerical evolution of axisymmetric gravitational wave collapse

Anton Khirnov   Tomáš Ledvinka

Institute of Theoretical Physics, Charles University
Prague, Czechia

JGRG28

Critical collapse in general relativity

- critical behaviour discovered by Choptuik in 1993 for scalar field in spherical symmetry
- take a family of initial configurations parameterized by "field strength" — weak ones disperse and strong ones collapse and form a black hole
- "critical point" at the threshold of collapse — discrete self-similarity & power-law scaling
- analogous results by Abrahams and Evans in 1993 for gravitational waves in axial symmetry ("Teukolsky waves")
- several attempts to find critical behaviour for "Brill waves", so far no reproducible success

Evolution method

- 3+1 splitting à la ADM — spacetime foliated by a sequence of spacelike surfaces labelled by the time parameter t
- evolved variables — spatial 3-metric γ_{ij} and extrinsic curvature K_{ij}
- Einstein equations split into a set of evolution equations and a set of constraints
- solve the constraints to construct initial data
- evolve $\{\gamma_{ij}, K_{ij}\}$ forward in time using the evolution equations (free evolution)
- coordinate choice — determined by the lapse α and shift β^i

Initial data

- Brill waves — a family of axially symmetric vacuum initial data at the moment of time symmetry
- parametrized by an “amplitude parameter” A
- $A = 0$ is flat space
- $|A| \to A_{\text{big}}$ is a black hole
- critical point — smallest value of A when a black hole is formed, for our initial data $A^* \approx 4.69$

Coordinate choice

- time coordinate encoded in the lapse $\alpha(t, x^i)$
- spatial coordinates determined by the shift vector $\beta^i(t, x^j)$
- $\{\alpha, \beta^i\}$ freely specifiable functions
- typically chosen dynamically as solutions to hyperbolic or elliptic equations
- common slicings
    - maximal: $K_i^i \equiv K = 0 \Rightarrow D^2\alpha - K_{ij}K^{ij}\alpha = 0$
    - 1+log: $\dot{\alpha} = -2\alpha K$

1+log slicing breakdown for near-critical Brill waves

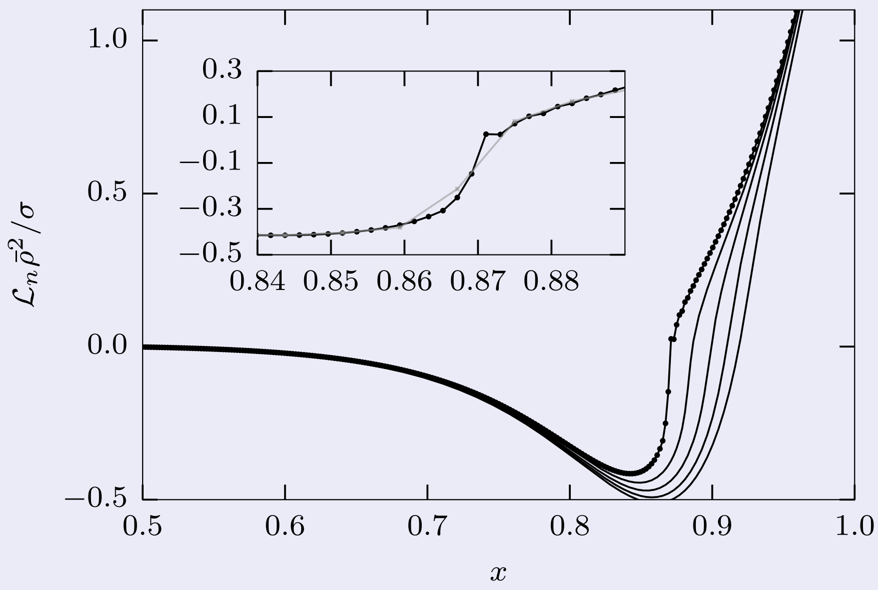

1+log slicing vs maximal slicing

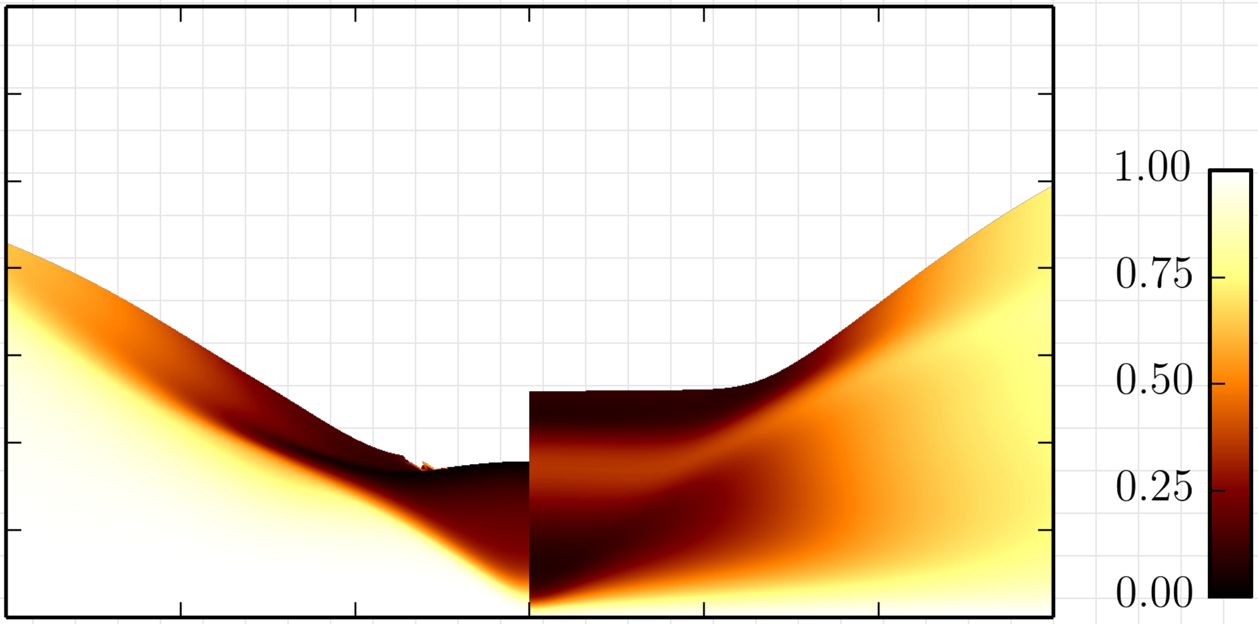

Quasi-maximal slicing I

- 1+log slicing is simple and fast, but breaks down
- maximal slicing is well-behaved, but slow and hard to implement
- try to combine them to get the best of both world
- extract just the “core / lowest-order” information from maximal slicing and plug it into 1+log

Quasi-maximal slicing II

- take the time derivative of the maximal slicing condition

$$0 = \left(\partial_t - \mathscr{L}_\beta\right)\left[D^2\alpha - K_{ij}K^{ij}\alpha\right]$$

- define a new function $W = (\partial_t - \mathscr{L}_\beta)\alpha$
- get an elliptic equation for W

$$\begin{aligned} D^2 W - K_{ij}K^{ij}W = & -2\alpha K^{ij}D_iD_j\alpha + \gamma^{ij}\left(\partial_t\Gamma^k_{ij}\right)\partial_k\alpha \\ & -\left(\gamma^{ij}D_iD_j\beta^k\right)D_k\alpha - \beta^j R^i_j D_i\alpha \\ & +\alpha\left(2\dot{K}_{ij}K^{ij} + 4\alpha K^i_j K^k_i K^j_k\right) \end{aligned}$$

- compute a low-order solution for W and add it as an extra term in 1+log slicing

$$(\partial_t - \mathscr{L}_\beta)\alpha = -2\alpha K + W$$

Invariants

- Kretschmann scalar $\mathscr{K} = R_{\mu\nu\alpha\beta}R^{\mu\nu\alpha\beta}$
- axial symmetry — angular Killing vector η^μ
- circumferential radius $\bar{\rho}^2 = \eta_\mu\eta^\mu$
- $4\bar{\rho}'^2 = \left|\nabla\rho^2\right|^2$
- dimensionless quantity $\chi = \dfrac{\bar{\rho}'^2}{\bar{\rho}^2}$
- for Schwarzschild $\chi = 1 - \dfrac{2M}{R}\sin^2\theta$

Conformal diagrams for constructed spacetimes

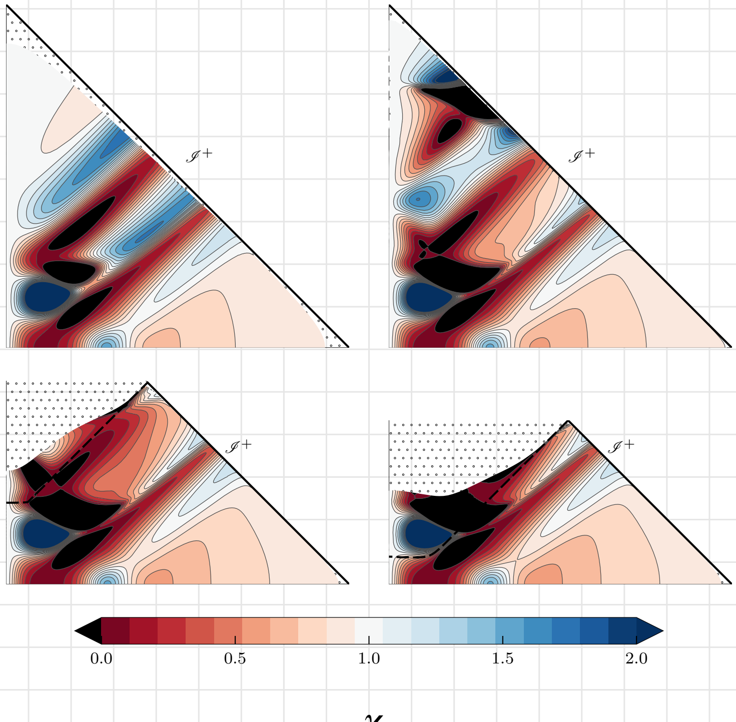

Event horizon evolution

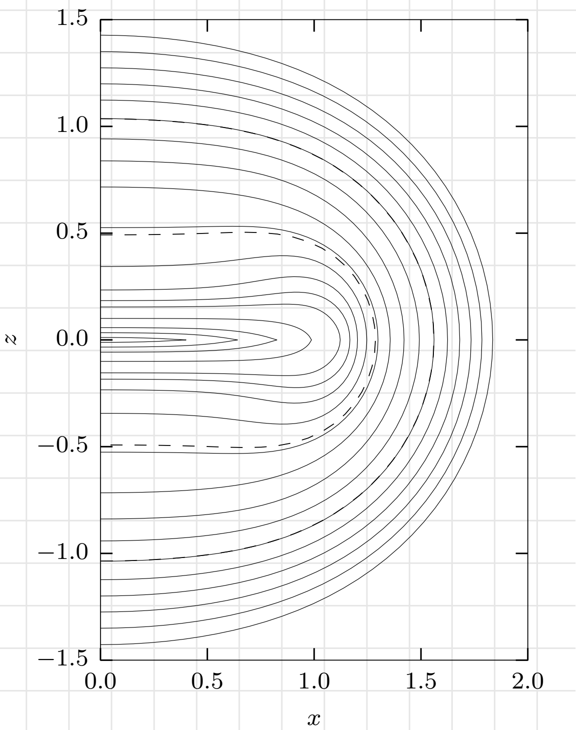

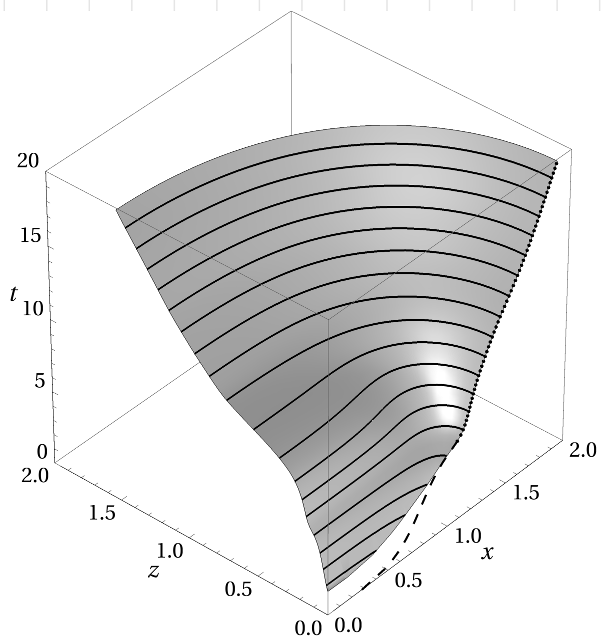

Ongoing work

- true maximal slicing — hard to integrate with mesh refinement
- other initial data families, e.g. Teukolsky waves as per Abrahams&Evans
  - no longer time-symmetric, so requires solving a set of nonlinear elliptic equations
  - preliminary results hint at non-uniqueness of the constraint solutions

Summary

- 1+log slicing is pathological for near-critical Brill waves
- we have extended it by adding a source function derived from the maximal slicing
- this "quasi-maximal" slicing allows us to get closer to the critical point
- for supercritical initial data we are able to follow the collapse as an apparent horizon forms and the geometry settles down to a Schwarzschild black hole
- we discover non-regular shape of the event horizon for weakly supercritical data

Thank you for your attention

- This work is supported by the Charles University in Prague, project GA UK No 2000314, GA UK No 1176217 and SVV-260211.
- Computational resources were provided by the CESNET LM2015042 and the CERIT Scientific Cloud LM2015085, provided under the programme 'Projects of Large Research, Development, and Innovations Infrastructures'.
- Our code is based on The Einstein Toolkit.

Muhammad Sharif
University of the Punjab

“Tilted Anisotropic Polytropes”
(10+5 min.)

[JGRG28 (2018) 110621]

Tilted Anisotropic Polytropes

Muhammad Sharif

University of the Punjab, Lahore-Pakistan

JGRG28

Rikkyo University - Tokyo, November 05-09, 2018

November 06, 2018

Mechanical Structure

- Hydrostatic Equilibrium Equation

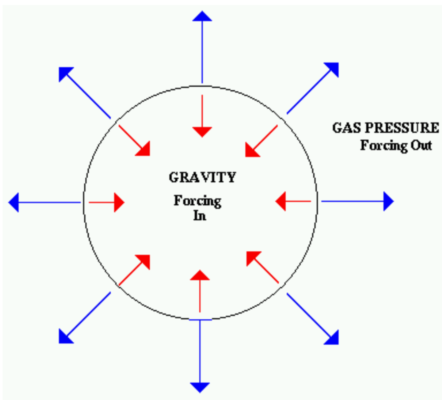

- Mass Equation

Coupling of hydrostatic equilibrium equation and mass conservation equation leads to

$$\frac{1}{r^2}\frac{d}{dr}\left(\frac{r^2}{\rho}\frac{dp}{dr}\right) = -4\pi G\rho.$$

$$\downarrow$$

The Poisson Equation

Polytropic Equation of State

A gas governed by polytropic change has an EoS

$$pV^{\gamma} = constant, \quad \gamma = 1 + \frac{1}{n}.$$

Since $\rho = m/V$, we have

$$p \propto V^{-\gamma} \propto \left(\frac{m}{\rho}\right)^{-\gamma},$$

$$p = k\rho^{\gamma} = k\rho^{1+\frac{1}{n}}.$$

A combination of the Poisson equation with polytropic EoS

$$\downarrow$$

Lane-Emden equation

Polytropes

Whether the equilibrium state is stable?

Adiabatic Index

$$\Gamma = \frac{\rho + p_r}{p_r}\frac{dp_r}{d\rho}.$$

$$\begin{array}{lcl} \text{Stable} & \rightarrow & \Gamma > \frac{4}{3}, \\ \text{Unstable} & \rightarrow & \text{otherwise.} \end{array}$$

[Heintzmann, H. and Hillebrandt, W.: Astron. Astrophys. **38**(1975)51]

Energy Conditions

For physically realistic matter, energy conditions must be imposed on the energy-momentum tensor.

- Weak Energy Condition: $\rho + p_i \geq 0, \quad \rho \geq 0,$
- Dominant Energy Condition: $\rho \pm p_i \geq 0, \quad \rho \geq 0,$
- Strong Energy Condition: $\rho + p_i \geq 0, \quad \rho + 3\hat{p} \geq 0,$

where $i = r, t$ and $\hat{p} = \frac{p_r + 2p_t}{3}$.

[Hawking, S.W. and Ellis, G.F.R.: *The Large Scale Structure of Space- time* (Cambridge Univ. Press, 1975)]

Congruence

- A congruence is a collection of curves in a region of spacetime through each point of which there passes precisely one curve, i.e., the curves never intersect with each other.
- For an observer comoving with the fluid, congruence of both the observer and the fluid remains the same.
- For an observer moving relative to the fluid, the congruence of the observer is tilted.

- A tilted congruence can be obtained by applying the Lorentz transformation to a non-tilted congruence.

The analysis of the universe with two different congruences can be completely different.

Spacetime

$$ds^2 = -e^{\mathcal{F}(t,r)}dt^2 + e^{\mathcal{G}(t,r)}dr^2 + r^2\left(d\theta^2 + \sin^2\theta d\phi^2\right).$$

Matter Distribution

$$T_{\mu\nu} = (\rho + p_t)V_\mu V_\nu + p_t g_{\mu\nu} + (p_r - p_t)S_\mu S_\nu,$$

$$V_\mu = \frac{1}{\sqrt{1-\varpi^2}}(-e^{\mathcal{F}/2}, \varpi e^{\mathcal{G}/2}, 0, 0),$$

$$S_\mu = \frac{1}{\sqrt{1-\varpi^2}}(-\varpi e^{\mathcal{F}/2}, e^{\mathcal{G}/2}, 0, 0), \quad \varpi = e^{\frac{(\mathcal{G}-\mathcal{F})}{2}}\frac{dr}{dt}.$$

Einstein field equations

$$\frac{\rho+\varpi^2p_r}{1-\varpi^2}=\frac{1}{8\pi r^2}+\frac{e^{-\mathcal{G}}}{8\pi}\left(\frac{\mathcal{G}'}{r}-\frac{1}{r^2}\right),$$
$$\frac{\varpi^2\rho+p_r}{1-\varpi^2}=-\frac{1}{8\pi r^2}+\frac{e^{-\mathcal{G}}}{8\pi}\left(\frac{\mathcal{F}'}{r}+\frac{1}{r^2}\right),$$
$$\frac{\varpi\left(\rho+p_r\right)e^{\frac{(\mathcal{F}+\mathcal{G})}{2}}}{1-\varpi^2}=-\frac{\dot{\mathcal{G}}}{8\pi r},$$
$$p_t=\frac{e^{-\mathcal{F}}}{32\pi}\left(\dot{\mathcal{G}}(\dot{\mathcal{F}}-\dot{\mathcal{G}})-2\ddot{\mathcal{G}}\right)+\frac{e^{-\mathcal{G}}}{16\pi}\left(\mathcal{F}''+\frac{\mathcal{F}'^2}{2}-\frac{\mathcal{F}'\mathcal{G}'}{2}+\frac{\mathcal{F}'}{r}-\frac{\mathcal{G}'}{r}\right).$$

Conservation Law

$$T^{\alpha}_{1;\alpha}=0,$$

$$T_1^{1'}+\frac{2}{r}(T_1^1-T_2^2)+\frac{\mathcal{F}'}{2}(T_1^1-T_0^0)-\frac{e^{-\mathcal{F}}}{r}\left(\ddot{\mathcal{G}}+\frac{\dot{\mathcal{G}}^2}{2}-\frac{\dot{\mathcal{F}}\dot{\mathcal{G}}}{2}\right)=0.$$

Slowly Evolving Approximation

- A system either does not change or alters slowly on a very long time scale compared to hydrostatic time.
- For such evolution, the radial velocity is smaller than the speed of light $(\varpi << 1)$ leading to the vanishing of the terms of order $O(\varpi^2)$.

$$\varpi^2 \approx \dot{\varpi} \approx \ddot{\mathcal{F}} \approx \ddot{\mathcal{G}} \approx \dot{\mathcal{F}}\dot{\mathcal{G}} \approx \dot{\mathcal{G}}^2 \approx 0.$$

Consequently, the field equations yield

$$8\pi\rho = \frac{1}{r^2} + e^{-\mathcal{G}}\left(\frac{\mathcal{G}'}{r} - \frac{1}{r^2}\right),$$
$$8\pi p_r = -\frac{1}{r^2} + e^{-\mathcal{G}}\left(\frac{\mathcal{F}'}{r} + \frac{1}{r^2}\right),$$
$$8\pi\varpi\left(\rho + p_r\right)e^{\frac{(\mathcal{F}+\mathcal{G})}{2}} = -\frac{\dot{\mathcal{G}}}{r},$$
$$8\pi p_t = e^{-\mathcal{G}}\left(\frac{\mathcal{F}''}{2} + \frac{\mathcal{F}'^2}{4} - \frac{\mathcal{F}'\mathcal{G}'}{4} + \frac{\mathcal{F}'}{2r} - \frac{\mathcal{G}'}{2r}\right).$$

Misner-Sharp mass

$$m=\frac{C}{2}(1-g^{\alpha\beta}C_{,\alpha}C_{,\beta}),$$

$$m(t,r)=\frac{r}{2}\left(1-e^{-\mathcal{G}}\right).$$

$$\downarrow$$

$$\frac{dm}{dr}=4\pi r^{2}\rho.$$

[Misner, C.W. and Sharp, D.H.: Phys. Rev. **136**(1964)B571]

A combination of second field equation and mass function gives

$$\mathcal{F}'=\frac{8\pi p_r r^3+2m}{r(r-2m)}.$$

Consequently,

$$p_r'+\frac{4\pi p_r r^3+m}{r(r-2m)}(\rho+p_r)-\frac{2\Delta}{r}=0.$$

where $\Delta=p_t-p_r$.

Polytropic EoS

- Case I: $p_r = k\rho_0^{1+\frac{1}{n}}, \quad \rho_0 = \rho - np_r,$
- Case II: $p_r = k\rho^{1+\frac{1}{n}}, \quad \rho_0 = \rho\left(1 - k\rho_0^{\frac{1}{n}}\right)^n.$

[Herrera, L. and Barreto, W.: Phys. Rev. D **88**(2013)084022]

- Case I

Consider dimensionless variables

$$\beta = \frac{p_{rc}}{\rho_c}, \quad t = \frac{\varrho}{\mathcal{A}}, \quad r = \frac{\varsigma}{\mathcal{A}}, \quad \mathcal{A}^2 = \frac{4\pi\rho_c}{\beta(n+1)},$$
$$\bar{\Psi}_0^n(\varrho,\varsigma) = \frac{\rho_0}{\rho_{0c}}, \quad m(t,r) = \frac{4\pi\rho_c\bar{\upsilon}(\varrho,\varsigma)}{\mathcal{A}^3}.$$

"c" indicates that values are evaluated at star's center,

$\varsigma,\ \beta,\ \bar{\upsilon},\ \bar{\Psi}_0$ are dimensionless variables and $\mathcal{A}$ is constant.

[Herrera, L. et al.: Gen. Relativ. Gravit. **46**(2014)1827]

Structure Equations

$$\left\{\varsigma^2\frac{\partial\bar{\Psi}_0}{\partial\varsigma}+\frac{2\Delta\bar{\Psi}_0^{-n}\varsigma}{\beta\rho_c(n+1)}\right\}\left(\frac{1-2\beta(n+1)\frac{\bar{\upsilon}}{\varsigma}}{1-n\beta+\beta(n+1)\bar{\Psi}_0}\right)+\beta\varsigma^3\bar{\Psi}_0^{n+1}+\bar{\upsilon}=0, \quad (1)$$

$$\frac{\partial\bar{\upsilon}}{\partial\varsigma}=\varsigma^2\bar{\Psi}_0^n(1-n\beta+n\beta\bar{\Psi}_0). \quad (2)$$

Two differential equations (non-linear)

Three unknowns, i.e., $\bar{\Psi}_0,\ \bar{\upsilon},\ \Delta$.

Conformally Flat Condition

The Weyl scalar is obtained as

$$\mathcal{C}=\frac{r^3e^{-\mathcal{G}}}{6}\left(\frac{e^{\mathcal{G}}}{r^2}+\frac{\mathcal{F}'\mathcal{G}'}{4}-\frac{1}{r^2}-\frac{\mathcal{F}'^2}{4}-\frac{\mathcal{F}''}{2}-\frac{\mathcal{G}'-\mathcal{F}'}{2r}\right).$$

From the field equations, the anisotropy parameter is found to be

$$\Delta = \frac{e^{-\mathcal{G}}}{8\pi}\left(\frac{\mathcal{F}''}{2}+\frac{\mathcal{F}'^2}{4}-\frac{\mathcal{F}'\mathcal{G}'}{4}+\frac{\mathcal{F}'}{2r}-\frac{\mathcal{G}'}{2r}-\frac{\mathcal{F}'}{r}-\frac{1}{r^2}\right) + \frac{1}{8\pi r^2}.$$

The conformally flat condition $(\mathcal{C}=0)$ yields

$$\Delta = \frac{r}{8\pi}\left(\frac{e^{-\mathcal{G}}-1}{r^2}\right)' = \frac{-r}{8\pi}\left(\frac{2m}{r^3}\right)'.$$

In terms of dimensionless parameters, this gives

$$\Delta = \rho_c\left[\frac{3\bar{\upsilon}}{\varsigma^3}-\bar{\Psi}_0^n(1-n\beta+n\beta\bar{\Psi}_0)\right].$$

Structure Equations

$$\varsigma^2\frac{\partial\bar{\Psi}_0}{\partial\varsigma}\left(\frac{1-2\beta(n+1)\frac{\bar{\upsilon}}{\varsigma}}{1-n\beta+\beta(n+1)\bar{\Psi}_0}\right)+\frac{2\bar{\Psi}_0^{-n}\varsigma}{\beta(n+1)}\left\{\frac{3\bar{\upsilon}}{\varsigma^3}-\bar{\Psi}_0^n(1-n\beta+n\beta\bar{\Psi}_0)\right\} \times\left(\frac{1-2\beta(n+1)\frac{\bar{\upsilon}}{\varsigma}}{1-n\beta+\beta(n+1)\bar{\Psi}_0}\right)+\beta\varsigma^3\bar{\Psi}_0^{n+1}+\bar{\upsilon}=0,$$

$$\frac{\partial\bar{\upsilon}}{\partial\varsigma}=\varsigma^2\bar{\Psi}_0^n(1-n\beta+n\beta\bar{\Psi}_0).$$

Now, we investigate the behavior of density, pressure, anisotropy, energy conditions and the stability.

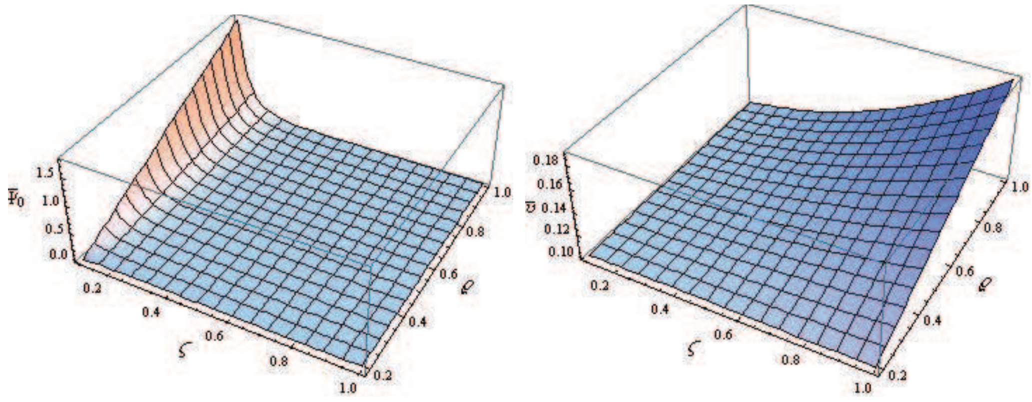

Figure 1: Plots for $\bar{\Psi}_0$ (left) and $\bar{\upsilon}$ (right) versus ς and ϱ with $\beta = 3$ and $n = 0.5$.

The dimensionless density parameter satisfies the maximality condition (maximum at the center but monotonically decreases towards the stellar surface). Mass function increases with radius.

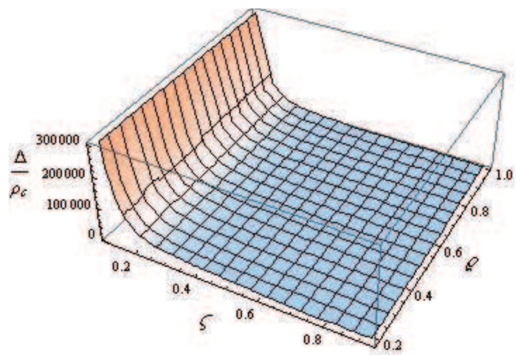

Figure 2: Plot for $\frac{\Delta}{\rho_c}$ versus ς and ϱ with $\beta = 3$ and $n = 0.5$ for case **I**.

Ratio of anisotropy to the central density has maximum values in the interior regions while smaller in the exterior.

Energy Conditions

WEC: (i) $\rho_c\bar{\Psi}_0^n(1-n\beta+n\beta\bar{\Psi}_0)\geq 0,$

(ii) $\rho_c\left(\bar{\Psi}_0^{n+1}+\frac{3\bar{\upsilon}}{\varsigma^3}\right)\geq 0,$

(iii) $\rho_c\bar{\Psi}_0^n(1-n\beta+(n+1)\beta\bar{\Psi}_0)\geq 0,$

DEC: (i) $\rho_c\bar{\Psi}_0^n(1-n\beta+(n-1)\beta\bar{\Psi}_0)\geq 0,$

(ii) $\rho_c\left\{\bar{\Psi}_0^n(2-2n\beta+(2n-1)\beta\bar{\Psi}_0)-\frac{3\bar{\upsilon}}{\varsigma^3}\right\}\geq 0,$

SEC: $\rho_c\left\{\bar{\Psi}_0^n(n\beta-1-n\beta\bar{\Psi}_0+3\beta\bar{\Psi}_0)+\frac{6\bar{\upsilon}}{\varsigma^3}\right\}\geq 0.$

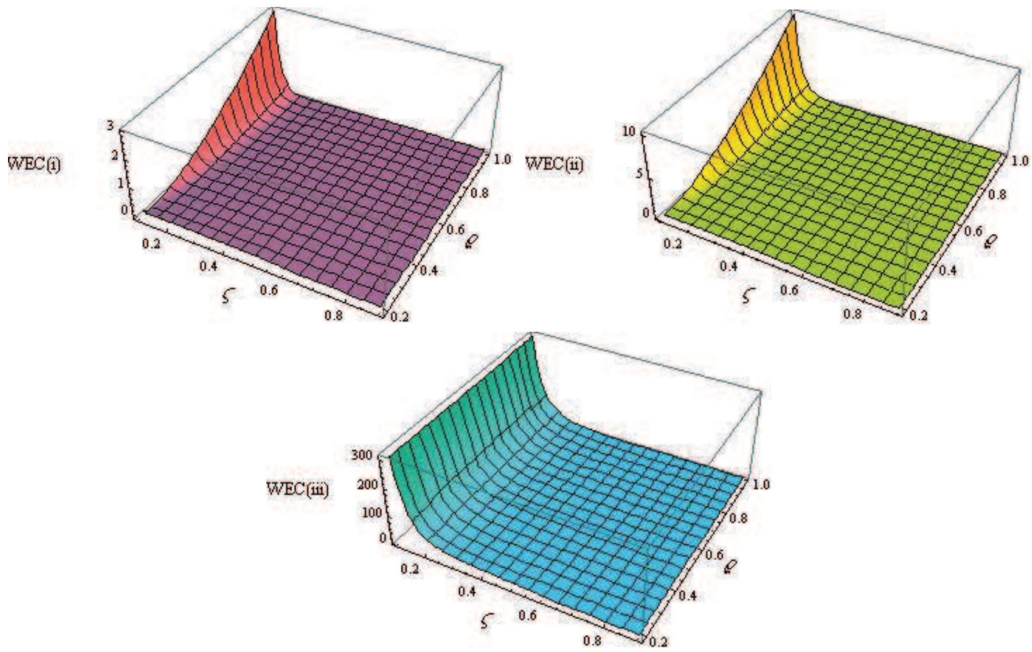

Figure 3: Plots for WEC versus ς and ϱ with $\beta=3$ and $n=0.5$ for case **I**.

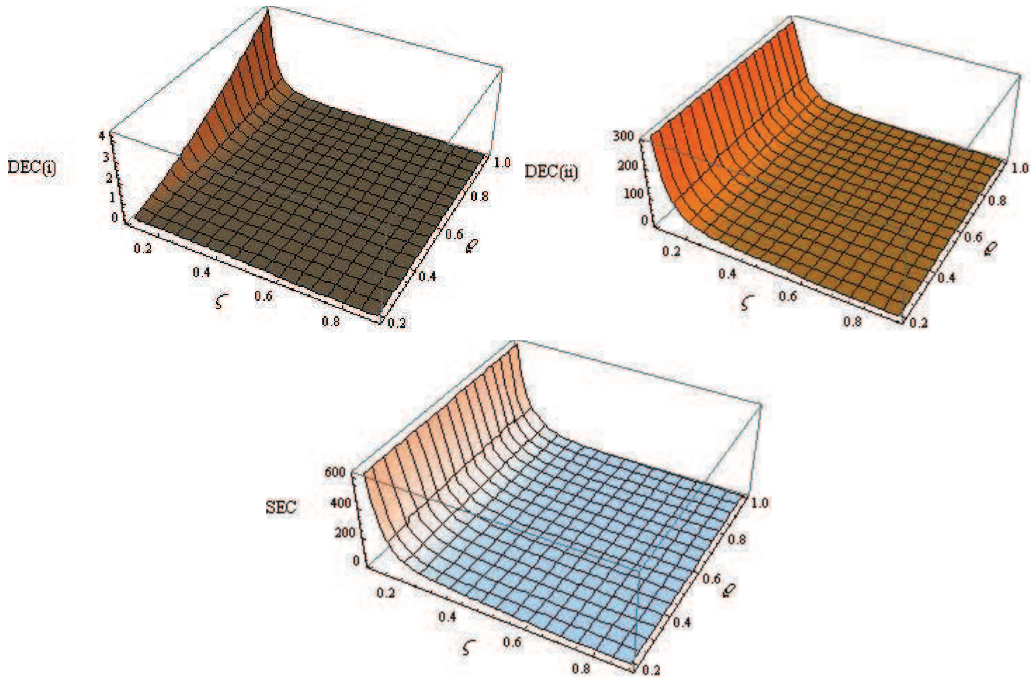

Figure 4: Plots for DEC and SEC versus ς and ϱ with $\beta = 3$ and $n = 0.5$ for case **I**.

Adiabatic Index

$$\Gamma = \frac{1 - n\beta + \beta(n+1)\Psi_0}{\Psi_0}\frac{d(\Psi_0^{n+1})}{d((1-n\beta)\Psi_0^n + n\beta\Psi_0^{n+1})} > 4/3.$$

Figure 5: Plot for Γ versus ς and ϱ with $\beta = 3$ and $n = 0.5$ for case **I**.

- Case II

$$\bar{\Psi}^n(\varrho, \varsigma) = \rho/\rho_c.$$

$$\left\{\varsigma^2 \frac{\partial \bar{\Psi}}{\partial \varsigma} + \frac{2\Delta \bar{\Psi}^{-n}\varsigma}{\beta \rho_c (n+1)}\right\} \left(\frac{1 - 2\beta(n+1)\frac{\bar{\upsilon}}{\varsigma}}{1 + \beta \bar{\Psi}}\right) + \beta \varsigma^3 \bar{\Psi}^{n+1} + \bar{\upsilon} = 0,$$

$$\frac{\partial \bar{\upsilon}}{\partial \varsigma} = \varsigma^2 \bar{\Psi}^n, \quad \Delta = \rho_c \left[\frac{3\bar{\upsilon}}{\varsigma^3} - \bar{\Psi}^n\right].$$

Structure Equations

$$\varsigma^2\frac{\partial\bar{\Psi}}{\partial\varsigma}\left(\frac{1-2\beta(n+1)\frac{\bar{\upsilon}}{\varsigma}}{1+\beta\bar{\Psi}}\right) + \frac{2\bar{\Psi}^{-n}\varsigma}{\beta(n+1)}\left\{\frac{3\bar{\upsilon}}{\varsigma^3}-\bar{\Psi}^n\right\}\left(\frac{1-2\beta(n+1)\frac{\bar{\upsilon}}{\varsigma}}{1+\beta\bar{\Psi}}\right) + \beta\varsigma^3\bar{\Psi}^{n+1}+\bar{\upsilon}=0,$$

$$\frac{\partial\bar{\upsilon}}{\partial\varsigma}=\varsigma^2\bar{\Psi}^n.$$

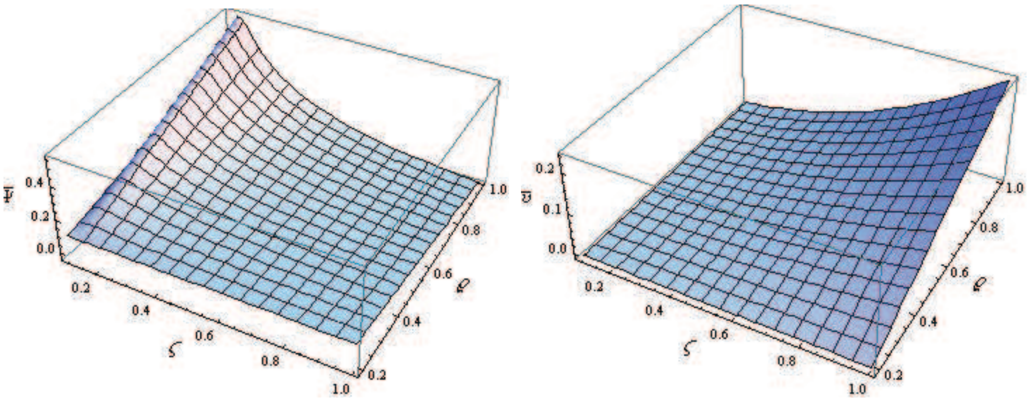

Figure 6: Plots for $\bar{\Psi}$ (left) and $\bar{\upsilon}$ (right) versus ς and ϱ with $\beta = 3$ and $n = 0.5$ for case **II**.

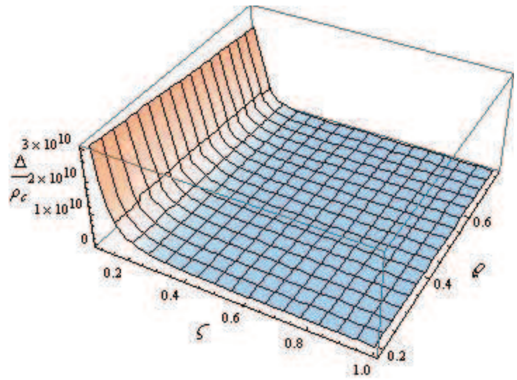

Figure 7: Plot for $\frac{\Delta}{\rho_c}$ versus ς and ϱ with $\beta=3$ and $n=0.5$ for case **II**.

Energy Conditions

WEC: (i) $\rho_c\bar{\Psi}^n\geq0,$ (ii) $\rho_c\bar{\Psi}^n(1+\beta\bar{\Psi})\geq0,$ (iii) $\rho_c\left(\beta\bar{\Psi}^{n+1}+\frac{3\bar{\upsilon}}{\varsigma^3}\right)\geq0,$

DEC: (i) $\rho_c\bar{\Psi}^n(1-\beta\bar{\Psi})\geq0,$ (ii) $\rho_c\left\{\bar{\Psi}^n(2-\beta\bar{\Psi})-\frac{3\bar{\upsilon}}{\varsigma^3}\right\}\geq0,$

SEC: $\rho_c\left\{\bar{\Psi}^n(3\beta\bar{\Psi}-2)+\frac{6\bar{\upsilon}}{\varsigma^3}\right\}\geq0.$

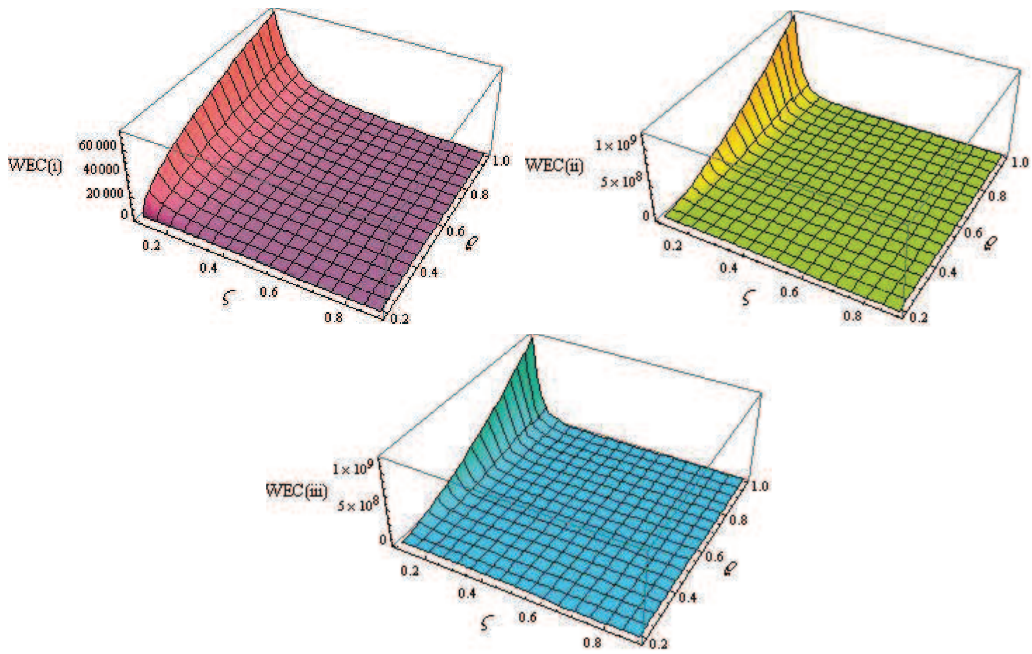

Figure 8: Plots for WEC versus ς and ϱ with $\beta = 3$ and $n = 0.5$ for case **II**.

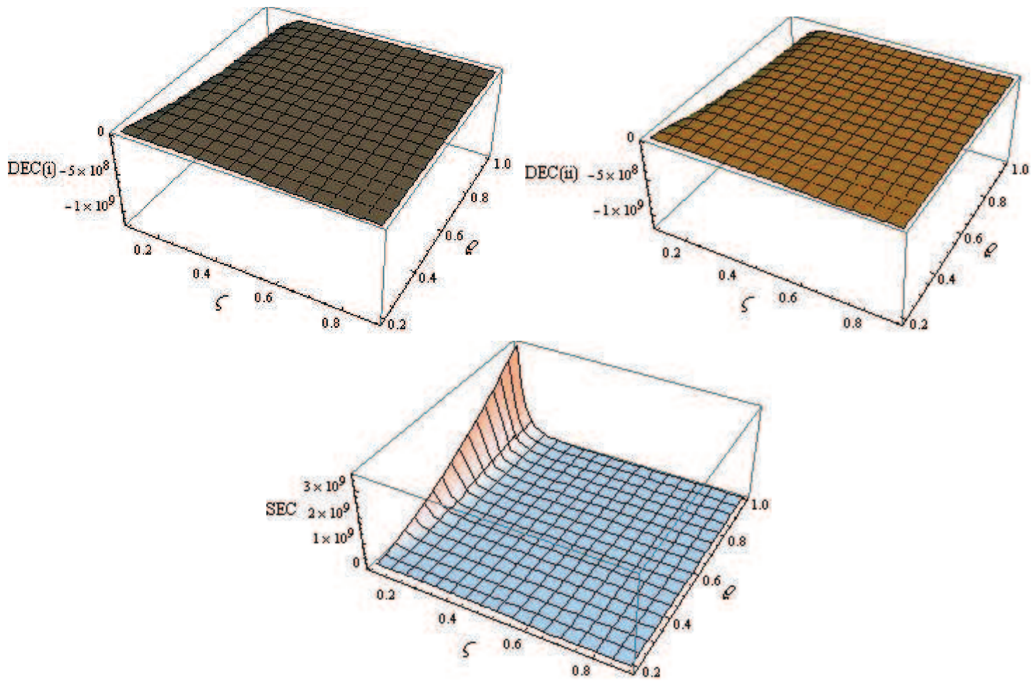

Figure 9: Plots for DEC and SEC versus ς and ϱ with $\beta = 3$ and $n = 0.5$ for case **II**.

Adiabatic Index

$$\Gamma = \frac{1+\beta\Psi}{\Psi}\frac{d(\Psi^{n+1})}{d\Psi^{n}} > 4/3.$$

Figure 10: Plot for Γ versus ς and ϱ with $\beta = 3$ and $n = 0.5$ for case **II**.

Conclusions

- Role of tilted congruence on spherical system satisfying two types of polytropic EoS under slowly evolving approximation.
- Compactness of system increases with the passage of time.
- The developed models are stable.
- All the energy conditions are satisfied for the first case only.
- Polytropic models of the first case are physically viable for tilted observer.
- Non-tilted anisotropic spherical system, these energy bounds are satisfied only for the first case. This shows that our results are consistent with non-tilted spherical system.


Thank you!